Analysis of rat brain lipids and metabolites after antidepressant drug treatment

ESTABRAQ JADDOA

April 2018

Department of Pharmacology

School of Pharmacy

De Montfort University

Leicester, LE1 9BH

United Kingdom

Analysis of rat brain lipids and metabolites after antidepressant drug treatment

ESTABRAQ JADDOA

Thesis submitted in partial fulfilment of the requirements for the degree of Doctor of Philosophy.

April 2018

Thesis conducted under the supervision of Dr. **Tyra S. C. Zetterström**, first supervisor; and Prof. Martin Elliott and Dr. Daniel Sillence second supervisors.

Department of Pharmacology

School of Pharmacy

De Montfort University

Leicester, LE1 9BH

United Kingdom

ABSTRACT

Depression is a major debilitating disorder and the key aim of the current project was to investigate some of the molecular/biochemical mechanisms of antidepressant drugs with an emphasis on the relatively unexplored role of sphingolipids. For this purpose, the current study used two antidepressant drugs: the tricyclic antidepressant desipramine, and the selective serotonin re-uptake inhibitor paroxetine. The effects of the drugs in rat brain regions implicated in depression: the prefrontal cortex (PFC), hippocampus (HP) and striatum (ST) were investigated both acutely (single administration) and chronically (daily treatment for 15 days). In Chapter Three, ^{1}H NMR spectroscopy was used to explore the metabolic response of acute and chronic administration of desipramine and paroxetine. These experiments showed significant changes in a number of water-soluble metabolites (i.e. N-acetylaspartylglutamate, glutamate, glutamine, lactate and creatine) following acute but not chronic treatment of the drugs. Sphingolipids including ceramide and its main metabolite sphingosine are key modulators of numerous cellular functions and in Chapter Four, it was shown by using liquid chromatography with mass spectrometry (LC-MS) that chronic but not acute administration of the antidepressant drugs decreased sphingosine levels in the HP and PFC but not in the ST. The effect of the drugs (e.g. paroxetine) on ceramide levels was also tested (HP only) by benzoylation of ceramide using high-performance liquid chromatography with ultraviolet detection (HPLC-UV) and in Chapter Four, it was shown that hippocampal levels of ceramide were as for sphingosine decreased by chronic paroxetine treatment. This chapter also demonstrated a highly significant correlation for the two sphingolipids in both controls and drug-treated animals. In Chapter Five , the effect of chronic paroxetine and desipramine administration was investigated on gene expression for two key enzymes of the brain sphingolipid pathway namely, acid sphingomyelinase (ASM) and acid ceramidase (AC). By using real-time quantitative polymerase chain reaction (RT-qPCR) it was shown that paroxetine and desipramine significantly reduced mRNA levels of ASM in the HP while effects in the PFC and ST did not reach significance. Similar effect was seen for desipramine but not paroxetine on mRNA levels for AC in the HP.

Recent studies indicate that ceramide modifies monoaminergic neurotransmission. In Chapter Six, the effect of carmofur, a potent inhibitor of acid ceramidase (AC) was investigated on monoamine

neurotransmitters levels and their corresponding metabolites in rat brain regions by using HPLC with electrochemical detection (HPLC-ECD). Carmofur significantly increased 5-HT and decreased its metabolite 5-hydroxyindole-3-acetic acid (5-HIAA) in tissue samples from the PFC, HP and ST. In contrast, carmofur failed to significantly alter brain levels of dopamine, noradrenaline and the dopamine metabolite 3, 4- dihydroxyphenylacetic acid (DOPAC).

In conclusion, findings of this project are supportive of a putative role for sphingolipids in the mechanism of action by antidepressant drugs. The potential clinical significance of these findings requires further studies.

ACKNOWLEDGEMENTS

First and foremost, I would like to express my deepest gratitude and appreciation to my wonderful first supervisor; Dr. Tyra S. C. Zetterström for encouraging me to complete my research under her supervision and guidance. I am deeply grateful forever for Dr. Tyra not only for her help regarding research issues but also for her boundless personal and emotional support throughout my study period.

I would also like to thank my second supervisors Prof. Martin Elliott and Dr. Daniel Sillence, also Prof. Randolph Arroo for their supportive role and advice which were offered throughout my PhD research. I am particularly grateful to the Iraqi Ministry of higher education, Iraqi Cultural Attaché in London, Baghdad University and Al-Kindy College of medicine for their encouraging and supportive roles and without their support, this work would not have been successfully completed. In addition, I would like to thank Prof. Martin Grootveld, Dr. Tiziana Sgamma, Dr. Eva Masiero, Dr. Victor Ruiz Rodado, and Dr. Fay Probert for their instrumental contributions to the success of this project. I am also grateful to De Montfort University for the 'High Flyers' scholarship, which offered the tuition fees of the last two years of my study. Special thanks also go to all my colleagues in neuropharmacology laboratory including Dr. Mathieu Di Miceli, Dr. Emmanuel Quansah and Adesina Omoloye for their support regarding the animal experiments. Special thanks also go to the B.S.U. team for their efforts in maintaining optimal conditions within the animal unit. Many thanks also go to Zahoor-Ul-haq, Dr. Jinit Masania, Unmesh Desai and Nazmin Juma for their technical assistance and for all the technicians in room 2.17 of the Hawthorn Building, including Dave Reeder, Amrat Khorana and Anita O'Donoghue for their technical help and the provision of some essential consumables and chemicals.

Most of all, I would like to thank the most precious person in my life, my lovely daughter and my beautiful princess Zahraa and my dear husband Dr. Maher Al-Khazraji for being with me always and in any time of need. I am also grateful to the rest of my family especially my dearest brother Muhammad and his nice family including his dear wife Huda AL-Jumaily, his precious daughter Zainab and his two dear sons Hashim and Haider, also the rest of my sisters and brothers, my relatives and friends in Iraq particularly my best friend Dr. Saba Jassim and her husband Dr. Ali Khaffi with whom I shared my research problems and daily concerns.

PUBLICATIONS

Author's publications:

Emmanuel Quansah, Tiziana Sgamma, **Estabraq M. J.**, Tyra S C Zetterström (2017). Chronic methylphenidate regulates genes and proteins mediating neuroplasticity in the juvenile rat brain doi:10.1016/j. neulet2017.06.012.

Estabraq M. J.; Al-Khazraji M. (2013). The role of zinc sulphate ointment 5% in preventing post haemorrhoidectomy stricture. Am. J. Pharm Tech. Res. 2013; 3(1) ISSN: 2249-3387www.ajptr.com.

Mosah H. A; **Estabraq M. J**.; Jassim H. S.; Jabbar A. M. (2013). The role of Diltiazem enriched with zinc sulphate in Anal fissure. Journal of Intercultural Ethnopharmacology. 2013; 2(3) pp.173-176(4).

Estabraq M. J. (2011). The role of Aspirin as Otoprotective Agent in Patients receiving amikacin therapy. Al-kindy College of Medicine Journal: 18109543,2011 VOL: 7, pp. 11-13, Baghdad University, Iraq.

Mosah H; **Estabraq M J**; Maher J A. (2011). Topical Diclofenac Therapy for Mordor's Disease of the Breast. Al-Kindy College of Medicine Journal; VOL: 8, No. 1, Baghdad University, Iraq.

Estabraq M. J. (2010). The influence of aminophylline and indomethacin in Glycerol induced acute renal failure in rats. Al-Kindy College of Medicine Journal ISSN: 18109543 VOL: 6, pp. 62-70, Baghdad University, Iraq.

Estabraq M. J. (2009). The effect of continuous Darkness and Continues Light on the reactivity of smooth muscles to Drugs in Rats Vas Deferens. Al-kindy College of Medicine Journal ISSN: 18109543, 2009 VOL: 5, pp. 47-51, Baghdad University, Iraq.

ABBREVIATIONS

^{1}H-MRS	Proton magnetic resonance spectroscopy
^{1}H-NMR	Proton nuclear magnetic resonance spectroscopy
AADC	Aromatic amino acid decarboxylase
AC	Acid ceramidase
ACTH	Adrenocorticotropic hormone
ASAH1	N-acylsphingosine amidohydrolase 1
cDNA	Complementary DNA
CSF	Cerebrospinal fluid
ADHD	Attention deficit hyperactivity disorder
ASM	Acid sphingomyelinase
ATP	Adenosine triphosphate
BBB	Blood brain barrier
BCAA	Branched-chain amino acid
BDNF	Brain derived neurotrophic factor
β-actin	Beta-actin
cAMP	adenosine monophosphate
CERT	Ceramide transporter
Chol	Choline
CNS	Central nervous system
COMT	Catechol-O-methyltransferase
CRF	Corticotropin-releasing factor
CRH	Corticotropin-releasing hormone
d	Doublet
DA	Dopamine
DAG	Diacylglycerol
DAT	Dopamine transporter
dd	Doublet of doublet
DG	Dentate gyrus
D_2O	Deuterium oxide
DOPAC	3,4-dihydroxyphenylacetic acid

ESI	Electrospray ionization
GABA	γ-aminobutyric acid
GAPDH	Glyceraldehyde 3-phosphate dehydrogenase
Glu	Glutamate
Gln	Glutamine
GPCRs	G-protein coupled receptors
HP	Hippocampus
HPA	Hypothalamic-pituitary-adrenal axis
HPLC	High performance liquid chromatography
HPLC-ECD	High performance liquid chromatography with electrochemical detection
HPLC-UV	High performance liquid chromatography with ultraviolet detection
5-HIAA	5-Hydroxyindoleacetic acid
5-HT	5-Hydroxytryptamine, serotonin
5-HTP	5-Hydroxytryptophan
HVA	Homovanillic acid
IDO	Indoleamine-2, 3-dioxygenase
INF-gamma	Interferon-gamma
IL-1beta	Interleukin-1beta
i.p	Intraperitoneal
IP3	Inositol triphosphate
L-DOPA	L-3,4-dihydroxyphenylalanine
LC	Locus coeruleus
LC-MS	Liquid chromatography–mass spectrometry
M	Multiplet
MAO	Monoamine oxidase
MHPG	3-Methoxy-4-hydroxyphenylglycol
MRI	Magnetic resonance imaging
Myo-inos	Myo-inositol
M/Z ratio	Mass to charge ratio
NA	Noradrenaline

NAA	N- acetyl aspartate
NAAG	N-acetylaspartylglutamate
NAc	Nucleus accumbens
NARIs	Noradrenaline reuptake inhibitors
NET	Noradrenaline transporter
NMDA	N-methyl-D-aspartate
NPC	Niemann-Pick disease type C1
PBS	Phosphate buffered saline
PCA	Principal component analysis
P Chol	Phosphoryl choline
PCR	Polymerase chain reaction
PCx	Parietal cortex
P ethan	Phosphoryl ethanolamine
PFC	Prefrontal cortex
PLS-DA	Partial least squares discriminant analysis
PVN	Paraventricular nucleus
RT-qPCR	Real time quantitative polymerase chain reaction
S	Singlet
SBs	Sphingoid bases
SERT	Serotonin transporter
SIM	Selective ion monitoring
SMPD1	Sphingomyelin phosphodiesterase 1
SNRIs	Serotonin-noradrenaline reuptake inhibitors
SSRIs	Selective serotonin reuptake inhibitors
ST	Striatum
SN	Substantia nigra
t	Triplet
TCA	Tricyclic antidepressant
TH	Tyrosine hydroxylase
TNF-α	Tumour necrosis factor-alpha
TPH	Tryptophan hydroxylase
TSP	3-(trimethylsilyl) propionic-2,2,3,3-d4 acid

VMA	Vanillylmandelic acid
VMAT	Vesicular monoamine transporter
VIP	Variable importance in projection
VTA	Ventral tegmental area
WHO	World Health Organisation
α_1/α_2	Noradrenergic receptors
qu	Quartet

TABLE OF CONTENT

LIST OF FIGURES

LIST OF TABLES

CHAPTER 1

Introduction

1.1. Depression:

Depression is a major psychiatric condition with a prevalence of approximately 4.4% worldwide and is associated with a substantial risk of social dysfunction, psychological disability and suicide (Ambresin et al., 2014; Lan et al., 2009; Organization, 2017; Shneker et al., 2009). It is one of the most common illnesses in the developed countries and according to the world health organisation (WHO), it will constitute the second most important cause of disease induced disability in 2020 (Figure 1.1) (Haenisch and Bönisch, 2011; Moussavi et al., 2007; Murray and Lopez, 1997; Kastrup, 2011). Depression is manifested by a range of emotional symptoms including episodes of consistent low mood, lack of interest in any activity, anhedonia, low self-esteem and loss of cognitive function. In addition, sufferers often develop numerous physical symptoms such as insomnia, restlessness, anorexia and loss of libido (Haase and Brown, 2015). Moreover, the recurrence of symptoms is commonly a feature of major depressive disorder (Jacobs, 2004).

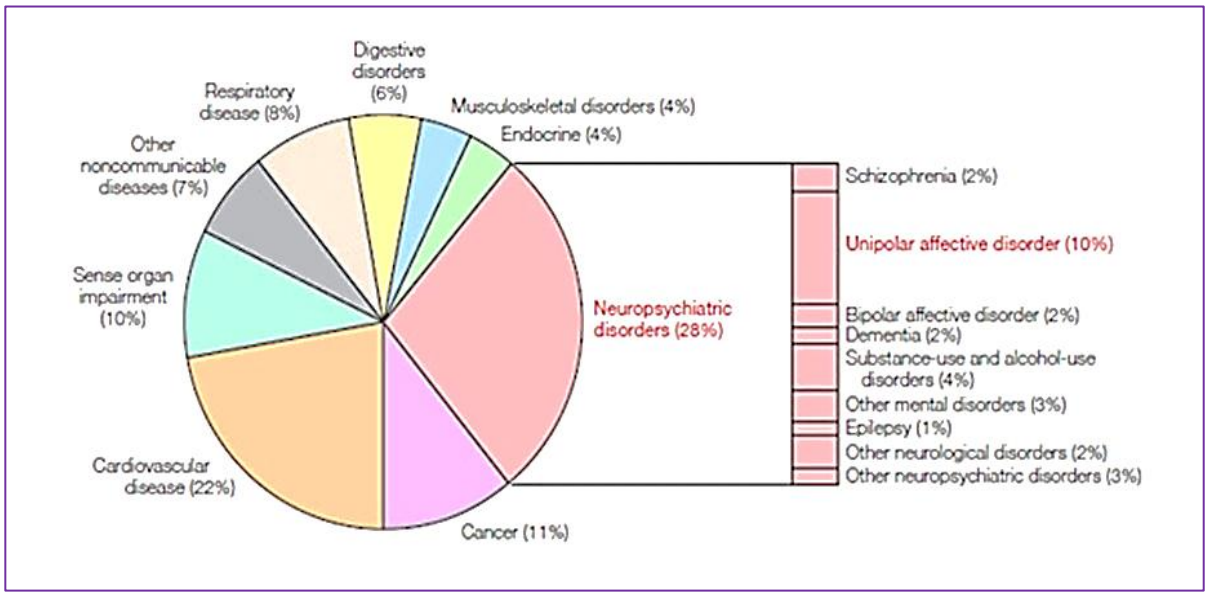

Figure 1.1: Global impact of depression (Prince et al., 2007)**.**

1.2. Historical background:

In Ancient Greece, depression was known as "melancholia" and was described as a distinctive illness with a prolonged feeling of sadness and fear. According to the Greek physician Hippocrates, often referred to as “the father of modern medicine” it was suggested that this mental state was caused by a condition of imbalance in the four essential body fluids or humors with an excessive black bile, and was mentioned as the humoral theory of melancholia in the 4th and 5th centuries BC (Liddell et al., 1996). In the late sixteenth-century the disease was identified as a serious occupancy of the mind with sadness predominantly affecting specific subgroups of the population, including the creative painters and artists (Britton, 2003). During the 17th century it was proposed that melancholia could be cured by performing a “meaningful work”, together with providing a healthy diet, adequate sleep, music as well as discussing the causative problem with a friend (Kent, 2003). Further, in the 18th century the humoral theory of melancholia was challenged by electrical and mechanical explanatory ideas including energy depletion and slowness of circulation (Jackson, 1983). Initially, depression as a term was derived from a Latin word (*deprimere*, meaning “ to press down”) and was primarily used in 1856 by Louis Delasiauve, a French psychiatrist when referring to this psychiatric condition (Berrios, 1988). At the end of the 19th century, the English psychiatrist, Henry Maudsley was the first to use this term in a clinical sense (Lewis, 1934). Eventually, with the beginning of the 20th century and the start of scientific and biomedical discoveries a new concept of depression emerged, and it now began to be considered as a somatic disease along with other organ pathologies such as the heart and kidney (Jacobs, 2004). More recently, in the mid-20th century the monoamine theory of depression evolved. This theory was originally based on a clinical observation that two structurally unrelated medications, namely imipramine (originally used as an antipsychotic drug) and iproniazid (an antituberculosis drug) reduced depressive symptoms (Krishnan and Nestler, 2008). Later, these drugs were found to enhance monoamine neurotransmitter levels particularly noradrenaline (see also section 1.3.1 for further explanation) (Mulinari, 2012).

1.3. Pathogenesis of depression:

1.3.1. The monoamine hypothesis:

The monoamine theory of depression was one of the first theories attempting to elucidate the aetiology of depression. This theory is partly based on the finding from the 1950s that two drugs originally developed for other medical purposes, were found to have antidepressant actions (Schildkraut, 1965). The first one was an anti-tuberculosis drug, iproniazid which was later discovered to increase extracellular monoamine levels by inhibiting the main monoamine degrading enzyme, monoamine oxidase (MAO). The second drug, imipramine was originally developed for the treatment of schizophrenia and subsequently became the archetypal tricyclic antidepressant compound (TCA). This class of drugs raise extracellular monoamine concentrations by blocking the monoamine neuronal transporters including the serotonin transporter (SERT) and the noradrenaline transporter (NET). These observations led to the development of a simplistic hypothesis of depression, the monoamine hypothesis which postulates that depression is associated with the deficiency of monoamine neurotransmitters in the central nervous system (CNS) and subsequently that the increased monoamine neurotransmission induced by antidepressant drugs is responsible for the corresponding alleviation of the depressive symptoms (Schildkraut, 1965). The three centrally acting monoamines implicated in this theory are: noradrenaline (NA), serotonin (also called 5-hydroxytryptamine, 5-HT) and dopamine (DA). However, this theory was conflicted with the fact that the neurochemical effects induced by antidepressant drugs occur much before the onset of their clinical action which is often not seen until approximately 2 weeks of treatment (Mitchell, 2006; Tylee and Walters, 2007), however the full therapeutic action can even be delayed up to 4-6 weeks after starting the treatment (Trivedi et al., 2006). In addition, it was challenged by another contradictory observation that not all depressed patients (i.e. 60-70%) responded to antidepressant drug treatment namely, imipramine (Al-Harbi, 2012; Klerman and Cole, 1965; Rush et al., 2006). Hence, although the monoamine theory gained popularity and support, its validity remains questionable.

1.3.2. The neurotrophic hypothesis:

The concept of neurogenesis, which refers to the ongoing process of generating new neurons from neural progenitor cells in the adult brain, was first established by Altman (1965). In this early study, he demonstrated that neurogenesis occurs continuously in two specific areas of the adult brain: the

subgranular zone of the hippocampal dentate gyrus and the subventricular zone of the lateral ventricles where the newly generated neurons migrate to the olfactory bulb (Altman and Das, 1965; Ming and Song, 2011). Suppression of neurogenesis by stress results in neuronal and glial atrophy specifically in the hippocampus (McEwen et al., 2016). This is proposed to be a critical contributory factor in the aetiology of depression (Krishnan and Nestler, 2008). It has been reported that brain derived neurotrophic factor (BDNF) plays an essential role in regulating the process of neurogenesis. Furthermore, depression may result from a decrease in the expression of BDNF in the limbic areas of the brain, resulting in a reduced neurogenesis in the hippocampus (Lee et al., 2013), which may trigger the detected reduction in the volume of this brain region in depressed patients (Malykhin et al., 2010). These changes can be reversed by the chronic administration of antidepressant drugs (Duman and Li, 2012). In addition, it has been demonstrated that chronic antidepressant drug treatment including noradrenaline-selective reuptake inhibitors (NSRIs) and serotonin-selective reuptake inhibitors (SSRIs) when given for 2-3 weeks increases both BDNF expression and neurogenesis namely in the dentate gyrus of the hippocampus, whereas stress exerts an opposing effect by decreasing hippocampal neurogenesis (Lee et al., 2013; Sahay and Hen, 2007). Additionally, it was reported that the dorsal raphe nucleus of the brain stem (origin of serotonergic neurons) which is implicated in depression (Michelsen et al., 2008) and in mediating the antidepressant drug actions (Rajkumar and Mahesh, 2008) shows a high gene expression level of both BDNF and its receptor, tropomyosin receptor kinase B also known as tyrosine receptor kinase B (TrKB). Thus, it has been suggested that BDNF is not only involved in neurogenesis but might also have a direct neurotrophic action on 5-HT neurons (Madhav et al., 2001).

1.3.3. The lipid hypothesis:

Membrane lipids exert an essential role for neuronal activity of the brain through their function as a physical barrier that separates the intracellular and extracellular compartments. They are also involved in regulating the function and distribution of membrane proteins including neurotransmitter receptors, ion channels, transport proteins (transporters) and membrane enzymes (ceramide activated protein phosphatase) (Alberts et al., 2002), thereby modulating cell signalling and neurotransmission, membrane permeability and cellular growth arrest and apoptosis (Dinoff et al., 2017). Cholesterol, glycerophospholipids and sphingolipids are the major lipid components of the cell membrane in the brain (Fantini and Barrantes, 2009; Jain et al., 2014).

Sphingomyelin is an important membrane sphingolipid which constitutes the main source of ceramide in neuronal cell membranes and undergoes hydrolysis through activation of the enzyme acid sphingomyelinase (ASM) within lysosomes. Interestingly, this process has been shown to be elevated during stress (Kitatani et al., 2008). In this context, a recent animal study demonstrated that chronic stress during a four week period induced a significant up-regulation of ceramide content in the hippocampus and the prefrontal cortex of rats, this with a concomitant decrease of sphingomyelin levels (Oliveira et al., 2016). Furthermore, ceramide levels are also increased through inhibition of the lysosomal acid ceramidase enzyme (AC) which facilitates the conversion of ceramide to sphingosine and free fatty acids in the brain. Importantly, the increased ceramide level has been suggested to be implicated in cell growth arrest and apoptosis (programmed cell death) (Strelow et al., 2000). Further and consistent with a proposed role for ceramide in depression, the lysosomal hydrolysis of sphingomyelin to ceramide through stimulation of ASM, has been reported to be enhanced in patients suffering from major depressive illness (Kornhuber et al., 2008). In addition, a recent study showed that chronic stress to rats (4 weeks of exposure to stressful conditions such as overcrowding, exposure to hot air stream, cold water at 18°C or vibration) induced a behavioural animal pattern associated with depression and this coincided with increased ceramide levels in the hippocampus and prefrontal cortex (Oliveira et al., 2016). Also in support of a role for ceramide in the symptoms of depression are some previous studies demonstrating that antidepressant drugs including the TCA desipramine and the SSRI fluoxetine, inhibit ASM of the mouse hippocampus and consequently modify behaviours associated with antidepressant drug action in mice models (Gulbins et al., 2013; Kölzer et al., 2004). Further, sphingolipids and cholesterol exert an important role for receptor-mediated signaling action as they together form membrane lipid rafts (also referred to as macrodomains or platforms). Such lipid rafts are enriched in various receptors including G-protein coupled receptors (for example the monoamine receptors). Therefore, any change in the composition of these lipid compartments may directly alter the receptors' affinity for ligands as well as their corresponding signaling action (Veiga et al., 2001). Moreover, these macrodomains are important for the activation of the sphingomyelin hydrolysing enzyme, ASM and subsequently could be involved in the generation of ceramide content in the cell membranes in response to stress (Cremesti et al., 2002). Interestingly, a previous study conducted on ASM deficient mice reported a significant reduction of ceramide level in the hippocampus with reduced depressive behaviours (Gulbins et al., 2013). Importantly, the same study also demonstrated another relevant finding that acid ceramidase (AC) deficient mice showed a

significant down-regulation of neurogenesis, neuronal maturation and neuronal survival with an increase of depression-like behaviours (suppressed forced swim test, sucrose preference test and open field test) (Gulbins et al., 2013). Albeit in need of more investigations, these initial and critical observations underpin a newly adopted hypothesis of depression and its treatment which is based on the up-regulation of ceramide level as one of the underlying biological mechanism of depression.

1.3.4. The neuroendocrine hypothesis (The corticosteroid receptor hypothesis):

Dysregulation of the hypothalamic-pituitary-adrenal axis (HPA) (a system composed of the following structures: the paraventricular nucleus of the hypothalamus (PVN), the anterior pituitary lobe and the adrenal gland) is implicated in mediating the stress response and may also represent a contributory factor in the pathogenesis of depression (Duval et al., 2005; Smith and Vale, 2006; Snyder et al., 2011). In response to stress, corticotropin-releasing hormone (CRH, also referred to as corticotropin-releasing factor CRF), is the major regulator of the HPA axis and it is synthesized and released by the hypophysiotropic neurons which are located in the PVN of the hypothalamus (Smith and Vale, 2006). Then, the released CRH binds to the CRH type 1 receptors which are situated on the corticotropic cells in the anterior lobe of the pituitary gland, thus inducing the secretion of adrenocorticotropic hormone (ACTH, also known as corticotropin) into the systemic circulation (Rot et al., 2009; Smith and Vale, 2006; Taylor et al., 2005). Subsequently, the circulating ACTH stimulates the zona fasciculata in the adrenal cortex to release the glucocorticoid hormone (cortisol or corticosterone) through activating the glucocorticoid receptors (Rot et al., 2009). Recent studies suggested that a finding of cortisol hypersecretion was often reflected in depressive patients (Holsboer, 2000; Krishnan and Nestler, 2008). In addition, an enhancement of cortisol secretion has also been detected in rats following exposure to psychological stress (Holsboer, 2000).

1.3.5. The cytokine hypothesis:

It was hypothesized that depression is associated with a concomitantly enhanced production of inflammatory biomarkers namely the pro-inflammatory cytokines (small protein molecules released by specific cells within the immune system to mediate the inflammatory response) including tumour necrosis factor-alpha (TNF-α), interferon-gamma (INF-gamma), interleukin-1beta (IL-1beta) (Maes, 2008; Schiepers et al., 2005). This hypothesis was supported by the observation that chronic autoimmune or inflammatory diseases (e.g. hepatitis C, cancer, rheumatoid arthritis or diabetes mellitus) were often accompanied by depressive symptoms (Schiepers et al., 2005). In this respect,

a preclinical study reported that pro-inflammatory cytokine administration induced depression-like behaviours in rodent models (reduced sexual and exploratory behaviours, loss of appetite, elevated sensitivity of pain as well as social withdrawal) (Schiepers et al., 2005). Additionally, a clinical study indicated that approximately 30% of individuals who received treatment with a synthetic interferon (used for treatment of certain types of leukaemia and skin cancers) developed depression as a common side effect during the course of treatment (Krishnan and Nestler, 2008). Furthermore, the detected increase in cytokine levels may account for the reduced 5-HT levels as well as the increased 5-HT turnover (i.e. increased 5-HIAA/5-HT ratio) which are observed during depression, possibly through activating the tryptophan metabolising enzyme (indoleamine-2, 3-dioxygenase, IDO). Thereby, reducing the tryptophan (the primary amino-acid precursor of 5-HT) and consequently, 5-HT synthesis and levels in the brain (Felger and Lotrich, 2013; Schiepers et al., 2005). In this context, a previous animal study reported that acute treatment with the inflammatory cytokines (e.g. interferon-gamma) or activating the immune response by acute administration of lipopolysaccharide (a cytokine inducer) enhanced the expression of depression-like behaviours in mice (e.g. prolonged immobility in the tail suspension test and forced swim test with a suppressed sexual behaviour) (Lestage et al., 2002; O'Connor et al., 2009). This effect is likely to be mediated by activating the IDO enzyme, therefore increasing tryptophan catabolism and subsequently, reducing 5-HT synthesis (Felger and Lotrich, 2013; O'Connor et al., 2009). Further, the same study showed that administration of 1-methyltryptophan (the IDO antagonist) resulted in attenuation of the depression related behaviours in mice through blockade of IDO activation (O'Connor et al., 2009). In addition, recent studies demonstrated that antidepressant drugs namely the SSRIs including paroxetine, citalopram and sertraline suppress the pro-inflammatory cytokines production, thereby mediating an immunosuppressive effect (Gobin et al., 2014; Shenoy et al., 2013).

1.4. Monoamine neurotransmitters:

1.4.1. Serotonin (5-hydroxytryptamine, 5-HT):

Serotonin (5-HT) is an important neurotransmitter, identified in the late 1940s by Rapport (Rapport et al., 1948) and is known to be responsible for maintaining a broad range of physiological functions including mood, sleep, memory, learning, aggressive behaviour, emotion, appetite, pain, neuroendocrine function and thermoregulation (Murphy and Lesch, 2008).

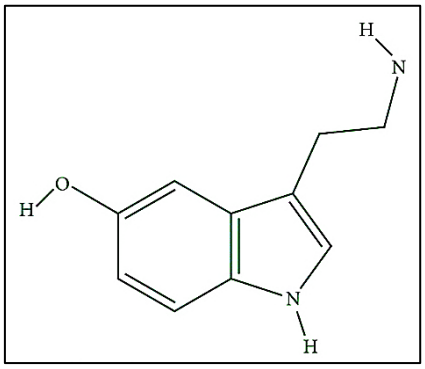

Figure 1.2: Chemical structure of serotonin.

5-HT is an indolamine (Figure 1.2) derived from the dietary amino acid, tryptophan and approximately 90% of the total body 5-HT content is found outside the brain where it is mainly synthetized by the enterochromaffin cells of the GI tract (Berger et al., 2009). In the brain, 5-HT is produced by serotonergic neurons originating in the median and dorsal raphe nuclei of the brain stem, where they send their axonal projections throughout almost the whole brain (Hornung, 2003). Particularly, high levels of 5-HT are detected in brain regions including the prefrontal cortex, nucleus accumbens, hippocampus, striatum and hypothalamus (Zangen et al., 1997). This neurotransmitter is initially biosynthesized from tryptophan in two steps: the first step catalyzes the hydroxylation of the precursor amino acid to form 5-hydroxytryptophan by the action of the rate limiting enzyme tryptophan hydroxylase (TPH) (Welford et al., 2016). TPH is found in two isoforms TPH1 and TPH2, the TPH1 is mainly expressed in the pineal gland and peripheral organs (gut, pancreatic islets of Langerhans, bone, bone marrow, liver and mammary gland) (Amireault et al., 2012), whereas TPH2 is predominantly expressed in the central nervous system (CNS) (Walther and Bader, 2003). Further, the 5-HT synthetic pathway involves decarboxylation of 5-hydroxytryptophan (5-HTP) by the aromatic amino acid decarboxylase enzyme (AADC) to produce 5-hydroxytryptamine (5-HT). Subsequently, the neurotransmitter undergoes further degradation into the final metabolite namely 5-hydroxyindoleacetic acid (5-HIAA) via a combined action of monoamine oxidase (MAO) and aldehyde dehydrogenase enzymes. Finally, 5-HIAA is then excreted in the urine (Figure 1.3) (Berumen et al., 2012; Welford et al., 2016). Following 5-HT biosynthesis, the neurotransmitter is transported to the synaptic vesicles for storage by means of the vesicular monoamine transporter (VMAT). Then, serotonergic transmission is triggered by the release of the stored 5-HT from the presynaptic nerve terminals after the initiation of the action potential and activating the voltage-dependent Ca^{2+} channels (Alekseyenko et al., 2010). Subsequently, Ca^{2+} ions enter into the cell and

bind with the synaptic vesicles membrane, which cause the vesicular compartment to fuse with the cell membrane and release 5-HT into the synaptic cleft by a process of exocytosis (Alekseyenko et al., 2010). Further, the released 5-HT diffuses into the synaptic cleft and binds to the different transmembrane presynaptic and postsynaptic 5-HT receptors. Currently, 7 distinct classes of 5-HT receptors encoded by different genes have been identified including 5-HT1 (5-HT1A, 5-HT1B, 5-HT1D, 5-HT1E and 5-HT1F), 5-HT2 (5-HT2A, 5-HT2B and 5-HT2C), 5-HT3, 5-HT4, 5-HT5 (5-HT5A and 5-HT5B), 5-HT6 and 5-HT7 receptor subtypes (Charnay and Leger, 2010). It was recognized that all the 5-HT receptors are G protein-coupled receptors except the 5-HT3 which form a ligand-gated ion channel (permeable to Na^{+}, K^{+} and Ca^{+2} ions) (Berumen et al., 2012). Additionally, the function of 5-HT in the synapse is terminated via high affinity uptake of 5-HT from the synapse by the serotonin transporter (SERT) which is a target of many effective antidepressant drugs including the SSRIs (see section 1.6.1.1) (Ramamoorthy et al., 2011). The monoamine transporters are protein structures situated on the cell membrane of the monoaminergic presynaptic nerve terminals. Further, they are Na^{+} and Cl^{-} dependent transporters that constitute important members of the SLC6 gene transporter family. Specifically, these protein transporters act to regulate the concentration of the released monoamine neurotransmitters within the synaptic cleft (maintaining a low extracellular level of approximately 5-10 nM for 5-HT) (Calcagno et al., 2009; Crespi et al., 1988). Also, it was reported that 5-HT receptors appeared to have a high affinity state in a nanomolar range (e.g. 5-HT1A receptors in rat cortical tissues showed a high binding affinity of nearly 1 nM for 5-HT) (Daws, 2009; Watson et al., 2000). Thus, SERT modulates signals transmitted by the receptor via regulating the amount of the ligand available to bind to a presynaptic or postsynaptic 5-HT receptor at the specific site of action (Duan and Wang, 2010). In addition, the SERT has a high affinity (approximately 1 nM binding affinity) and selectivity for 5-HT and so strictly regulates the extent and duration of serotonergic neurotransmission (Lundgren et al., 2009; Rudnick, 2006). Therefore, it is considered as a key factor in modulating 5-HT neurotransmission in the CNS. Thus, alteration in SERT function is associated with the treatment of psychological diseases including anxiety and major depressive disorders (Torres et al., 2003).

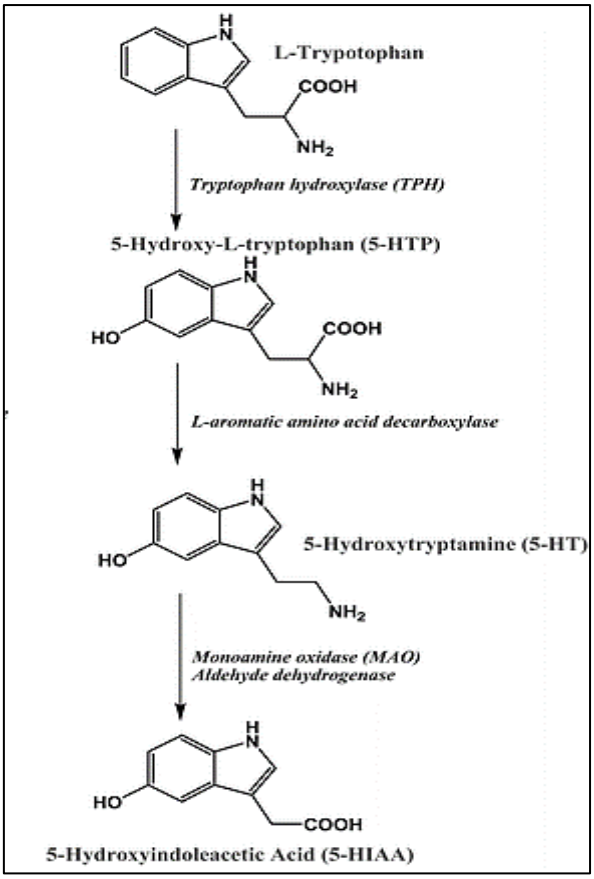

Figure 1.3: 5-HT synthesis and catabolism. Serotonin (5-HT) is synthesized from tryptophan by the rate-limiting enzyme tryptophan hydroxylase (TPH) to form 5-hydroxytryptophan (5-HTP) which in turn decarboxylated by the aromatic amino acid decarboxylase enzyme to produce 5-HT. Then, the neurotransmitter undergoes catabolism into 5-hydroxyindoleacetic acid (5-HIAA) via actions of monoamine oxidase (MAO) and aldehyde dehydrogenase enzymes to be excreted in the urine (Morgan et al., 2012).

1.4.1.1. Serotonin receptors:

Previous pharmacological and biochemical studied indicated that 5-HT receptors (six out of seven groups) are coupled with different types of G proteins, thereby modulating different signaling pathways. Furthermore, 5-HT3 receptors are ligand-gated ion channels (i.e. ionotropic receptors) which mediate a neuronal depolarization through a transient opening of the cations channel with an inward flow of these ions (Frazer and Hensler, 1999). The 5-HT1 and 5-HT5 receptors interact with Gαi/o proteins, thus activating two distinct mechanisms including a decrease in the production of the intracellular cyclic adenylate monophosphate (cAMP, a second messenger) via inhibiting the adenylyl cyclase activity (AC), or mediating a neuronal hyperpolarization which is caused by opening of the K^+ channels and the out flow of K^+ ions to the extracellular space (Frazer and Hensler, 1999). In comparison, 5-HT2 receptors are coupled with Gαq protein activating the phospholipase C,

leading to the production of inositol triphosphate (IP_3) and diacylglycerol (DAG), eventually producing an increase of the intracellular calcium release (McCorvy and Roth, 2015). Additionally, it was observed that, 5-HT4, 5-HT6 and 5-HT7 receptors interact with Gαs proteins activating the AC activity, hence stimulating the production of cAMP and the subsequent activation of other cellular proteins including the protein kinase A enzyme (PKA) (McCorvy and Roth, 2015) and thereby, activating CREB (cAMP response element binding protein) a cellular transcription factor which modifies the level of gene expression) (Berumen et al., 2012). A number of pharmacological and structural studies established that 5-HT receptor subtypes are found to have both a presynaptic localisation (i.e. 5-HT1A, 5-HT1B and 5-HT1D) and a postsynaptic localisation (i.e. 5-HT1A, 5-HT1B, 5-HT1D, 5-HT2A and 5-HT7) (Berumen et al., 2012). In addition, the 5-HT receptor families show a wide neuroanatomical distribution with different expression levels in various brain regions including the cortex, hippocampus, raphe nuclei, substantia nigra, amygdala, hypothalamus, frontal cortex, striatum, nucleus accumbens, olfactory tubercle and thalamus (Charnay and Leger, 2010; Frazer and Hensler, 1999; Taylor et al., 2005). Furthermore, 5-HT1A autoreceptors are abundant somatodendritic presynaptic inhibitory receptors expressed in the raphe nuclei of the mid brain, whereas the 5-HT1A receptors that spread widely in other brain areas mainly in cortico-limbic structures such as the hippocampus are postsynaptic receptors (Celada et al., 2004). Activating these autoreceptors by 5-HT allows opening of the cell membrane potassium channels and pumping the potassium ions out of the cells producing a neuronal hyperpolarization. Therefore, reducing the firing of serotonergic neurons as well as 5-HT biosynthesis and release, hence mediating a negative feedback mechanism that regulates 5-HT release (reducing the terminal release of 5-HT, consequently attenuating excessive increase of extracellular 5-HT level) (Celada et al., 2004; Rajkumar and Mahesh, 2008). It has also been shown that 5-HT1A autoreceptors exert an important role in modulating many behavioural and cognitive functions including learning, sleep, mood, anxiety and depression (Jafurulla et al., 2008). Thus, they represent an important target of various antidepressant drugs such as the SSRIs, TCAs and MAOIs (Celada et al., 2004; Müller et al., 2007). Interestingly, these receptors may interact with membrane lipids (lipid-protein interaction) which may trigger conformational changes that are essential to maintain their structural integrity and function (Singh et al., 2012).

1.4.2. Noradrenaline (NA):

Noradrenaline (NA) is a catecholamine (Figure 1.4) that modulates various behavioural and physiological functions in the brain as well as in the periphery including: heart rate, blood pressure, appetite, mood, sleep, attention, alertness, anxiety and general interest in life (Bönisch and Brüss, 2006).

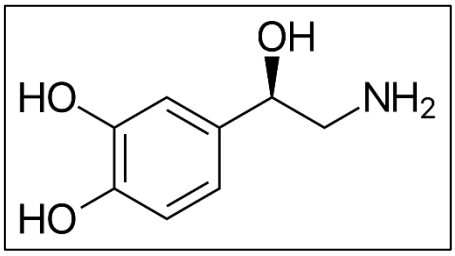

Figure 1.4: Chemical structure of noradrenaline.

Locus coeruleus (LC) of the brain stem is the main site where noradrenergic cell bodies are predominantly located and send their ascending projections to almost the whole of the brain including the prefrontal cortex and the hippocampus (brain regions implicated in the pathology of depressive disorder) (Ramamoorthy et al., 2011). NA is synthesized from its initial precursor, the essential amino acid tyrosine (under tyrosine deficiency, phenylalanine is hydroxylated into tyrosine by phenylalanine hydroxylase enzyme). Then, tyrosine is hydroxylated by the action of the rate limiting cytosolic enzyme tyrosine hydroxylase (TH) to form dihydroxyphenylalanine (DOPA) (Figure 1.5). This reaction is the rate-limiting step in NA biosynthetic pathway and is followed by decarboxylation of DOPA into dopamine via the cytosolic enzyme DOPA decarboxylase (Vieira-Coelho et al., 2009). Then, the neurotransmitter dopamine (DA) is transported via the vesicular monoamine transporter (VMAT) into the synaptic vesicles within the presynaptic nerve terminal. Subsequently, DA is converted by dopamine β-hydroxylase enzyme to NA within the synaptic vesicles to be released following the initiation of an action potential and via a process of exocytosis (Ca^{2+}-dependent exocytosis) into the synaptic cleft. The released NA exerts its action by binding to postsynaptic noradrenergic receptors (also known as adrenoceptors including α_1 α_2 and β_1 β_2 β_3) and the inhibitory presynaptic α_2 autoreceptor (inhibit further NA release) (Gannon et al., 2015; Torres et al., 2003). The α_2 autoreceptor, likewise the serotonin 5-HT1A autoreceptor modulates the chemical signals of the postsynaptic neuron by regulating the amount of neurotransmitter available for the postsynaptic receptors located on it. NA undergoes metabolic degradation via two main enzymes including monoamine oxidase (MAO) and catechol-O-methyl transferase (COMT), giving

rise to its main excretory product 3-methoxy-4-hydroxyphenylglycol (MHPG) which is associated with NA in the brain. MHPG is then further converted to vanillylmandelic acid (VMA) which is the main NA metabolite in the peripheral nervous system. VMA is the biologically inactive end product of NA and is excreted by the kidneys (Figure 1.3) (Fernstrom, 1983). The main termination of the physiological action by NA in the synapse is by reuptake of the monoamine transmitter back into the presynaptic nerve terminals through the action of the plasma membrane noradrenaline transporter (also known as norepinephrine transporter, NET) where NA is either recycled (restored) or undergoes enzymatic degradation by MAO and possibly also COMT into its biologically inactive metabolic products (Eisenhofer et al., 2004; Fernstrom, 1983; Lambert et al., 2001).

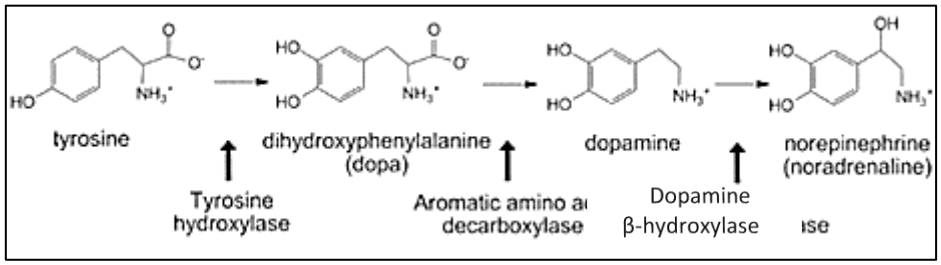

Figure 1.5: Catecholamines biosynthesis. Dopamine (DA) is synthesized from tyrosine that is converted to L-DOPA by tyrosine hydroxylase enzyme (rate-limiting step) and eventually into DA via aromatic amino acid decarboxylase. Then, DA is converted to noradrenaline (NA) via dopamine β-hydroxylase enzyme (Windahl, 2009).

1.4.2.1. Adrenergic receptors:

Detailed studies of the noradrenergic system revealed that effects of NA are mediated via three classes of adrenergic receptors which all belong to the G-protein coupled receptor family including α_1, α_2 and β receptors (Gannon et al., 2015; Sofuoglu and Sewell, 2009). The α_1 subtypes (α_{1A}, α_{1B} and α_{1D}) are excitatory postsynaptic receptors that are coupled to Gq proteins, thus activating the secondary messengers: phospholipase C and phosphoinositol (IP_3) and thereby increasing intracellular calcium levels (Philipp et al., 2002; Sofuoglu and Sewell, 2009). The α_2 adrenergic group includes α_{2A}, α_{2B} and α_{2C} subtypes which are located at both presynaptic and postsynaptic localisations. They are coupled to $Gi_{/o}$ proteins, hence inhibiting the second messenger adenylate cyclase and consequently, reducing the cAMP and calcium levels (Gannon et al., 2015). As already mentioned, the α_2 receptors when located on presynaptic noradrenergic nerve terminals act as inhibitory autoreceptors which modulate NA level through inhibiting further NA release (Gannon et al., 2015). Additionally, the β adrenergic receptors including β1, β2 and β3 subtypes are coupled to

the Gs proteins, activating these receptors result in the increase of adenylate cyclase and cAMP levels (Gannon et al., 2015; Sofuoglu and Sewell, 2009).

1.4.3. Dopamine (DA):

Dopamine is likewise NA, a catecholamine neurotransmitter (Figure 1.6) and plays a critical role in several behavioural and physiological processes including motivation, cognition, attention, reward, learning, memory, sleep, mood and locomotor activity, therefore it is also likely to be involved in the pathophysiology of depressive disorder (Elsworth and Roth, 1997; Hussein, 2016).

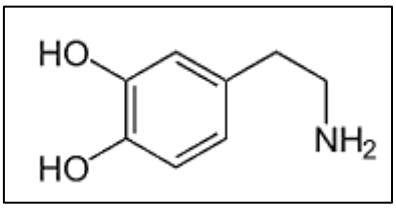

Figure 1.6: Chemical structure of dopamine.

Within the brain, dopaminergic cell bodies are located in two main areas: the substantia nigra of the midbrain (SN) and the ventral tegmental area (VTA) (Brookshire, 2017). The principal dopaminergic pathways implicated in depression are the mesolimbic pathway which originates in the VTA and projects to the nucleus accumbens (also known as ventral striatum) and the mesocortical pathway which also begins in the VTA and innervates the prefrontal cortex (Speed, 2010). After synthesis (Figure 1.5), DA is transported into the synaptic vesicles by the vesicular monoamine transporter (VMAT), and after triggering an action potential the stored DA is released into the synaptic cleft by a process of exocytosis where it interacts with pre and postsynaptic dopamine receptors (D1-D5) (Beaulieu and Gainetdinov, 2011). The dopamine transporter (DAT) located on the cell membrane of presynaptic nerve terminals mediates the termination of dopaminergic neurotransmission by a rapid neuronal reuptake of the released DA back into these presynaptic nerve terminals to be recycled (restored) or to be broken down by enzymatic depredation (MAO-B) (Meiser et al., 2013). Eventually, the released DA is catalysed via the combined action of the two enzymes: MAO and COMT (predominantly a membrane bound form) mainly to dihydroxyphenylacetic acid (DOPAC) and homovanillic acid (HVA) which are excreted in the urine (Elsworth and Roth, 1997; Speed, 2010).

1.4.3.1. Dopamine receptors:

The neurotransmitter dopamine regulates dopaminergic neurotransmission by binding with 5 types of dopamine receptors: D1-D5 which are G protein-coupled receptors (Beaulieu and Gainetdinov, 2011). A number of structural, biochemical and pharmacological studies revealed that dopamine receptors were classified into two main classes: the D1-class which includes the D1 and D5 subfamilies of dopamine receptors and the D2-class including D2, D3 and D4 subtypes of dopamine receptors (Vallone et al., 2000). The D1-class dopamine receptors (D1 and D5) are coupled to $G\alpha s_{/olf}$ type of G proteins, thus stimulating adenylyl cyclase (AC) and subsequently, activating cAMP production. These receptors are predominantly expressed postsynaptically within the striatum, substantia nigra, nucleus accumbens, amygdala, frontal cortex and the olfactory bulb (Beaulieu and Gainetdinov, 2011). In contrast, the D2-class dopamine receptors (D2, D3 and D4) are coupled to $G\alpha i_{/o}$ proteins, hence inhibiting the AC activity and cAMP production. It was established that the D2-class dopamine receptors are expressed significantly at both presynaptic and post synaptic localisations within the striatum, substantia nigra, nucleus accumbens, ventral tegmental area, olfactory tubercle, amygdala and hippocampus (Beaulieu and Gainetdinov, 2011; Vallone et al., 2000). The D2-class dopamine receptors when located presynaptically on DA nerve terminals act as inhibitory autoreceptors. Thus, activation of these receptors provide an important negative feedback mechanism that modulates the firing rate of dopaminergic neurones, DA synthesis and release in response to the increased extracellular DA level (Beaulieu and Gainetdinov, 2011).

1.5. Antidepressant drugs:

The use of the currently prescribed antidepressant medications was originally based (as already mentioned in section 1.3.1) on the early accidental discovery (nearly 70 years ago) of the mood elevating properties of drugs that were initially developed for different medical purposes (Schildkraut, 1965). These drugs were subsequently discovered to enhance the monoamines function in the brain (Hirschfeld, 2000; Mulinari, 2012). Later, they were classified into two main groups of antidepressants including the monoamine oxidase inhibitors (MAOIs) and the tricyclic antidepressant drugs (TCAs). These early observations form the basis of the subsequently postulated proposal of a monoamine hypothesis of depression (Berton and Nestler, 2006; Schildkraut, 1965). In 1987, the first selective serotonin reuptake inhibitor (SSRI) namely zimelidine aimed at a selective enhancement of serotonin neurotransmission in the brain was discovered.

Albeit, it was not used clinically due to its severe side effect, specifically a serious neurological consequence known as Guillain-Barre syndrome (a progressive autoimmune neuropathy which affects the nerve cells, resulting in muscular weakness, pain and paralysis) (Fagius et al., 1985; Ramachandraih et al., 2011). Subsequently, the increased knowledge of drug design and the diverse role of the monoamines in the brain led to the development of many new drugs that represent different antidepressant classes based on their chemical structures and their effects on different monoamine targets.

1.5.1. Classification:

- Monoamine uptake inhibitors:
    1. Selective serotonin reuptake inhibitors (SSRIs)
    2. Noradrenaline reuptake inhibitors (NARIs)
    3. Serotonin-noradrenaline reuptake inhibitors (SNRIs)
    4. Tricyclic antidepressant drugs (TCAs)
- Monoamine oxidase inhibitors (MAOIs)
    1. Reversible monoamine oxidase inhibitors
    2. Irreversible monoamine oxidase inhibitors
- Monoamine receptor antagonists

1.5.1.1. Monoamine uptake inhibitors:

- **Selective serotonin reuptake inhibitors (SSRIs):**

One of the mainstays in the treatment of depression is the use of the SSRIs which represent according to the published data, the most commonly used group of antidepressant drugs. These medications show a high selectivity for serotonin reuptake by blocking the serotonin transporter action (Figure 1.7) and thereby increasing the synaptic as well as the extracellular concentration of 5-HT (Cheung et al., 2006). The following drugs are members of the SSRI group of antidepressant drugs: paroxetine, fluoxetine, sertraline and citalopram (Pies, 2010). Although, they are relatively safe in drug overdose, they are not ideal due to a number of unpleasant side effects including: nausea, sexual dysfunction, gastro-intestinal problems and insomnia. In particular, the use in children has been deemed to be unsuitable, which is due to the increased risk of suicidal attempt

and only fluoxetine is recommended for the treatment of depression in children in the UK (Cheung et al., 2006; Suchard, 2008).

- **Noradrenaline reuptake inhibitors (NARIs):**

Previous preclinical and clinical studies reported that these antidepressant drugs enhance the brain noradrenaline (NA) neurotransmission via their high affinity and selectivity to block the noradrenaline transporter (NET), therefore inhibiting the extracellular reuptake of noradrenaline. Examples of this group of antidepressant drugs include reboxetine and atomoxetine (Hajós et al., 2004).

- **Serotonin-noradrenaline reuptake inhibitors (SNRIs):**

This class of antidepressant drug show likewise the TCAs (albeit chemically different from this group of drugs) a combined action (dual mode of action) to inhibit the reuptake of both 5-HT and NA neurotransmitters by blocking their transporters activity, thus increasing their concentrations in the synaptic cleft (Figure 1.7). It is however, well established that these medications have a variable degree of affinity and selectivity for 5-HT and NA transporters. Venlafaxine for example, shows a higher affinity (30-fold) toward SERT compared to the NET (high potency to inhibit the SERT even at low dose and a lower potency to block NET only at high dose), whereas duloxetine has only 10-fold higher affinity in inhibiting the SERT in comparison with NET (Celikyurt et al., 2012). Unlike the TCAs, SNRIs show a low affinity toward other brain receptors including histamine (H1), cholinergic and α-adrenergic receptors, therefore they lack most of the TCA adverse effects (Celikyurt et al., 2012).

- **Tricyclic antidepressants (TCAs):**

The TCAs represents the first group of antidepressant medications which were "accidently" discovered and then successfully used in a clinical trial for depression in the late 1950s. This drug class is divided into two main groups including tertiary amines (amitriptyline and imipramine) and secondary amines (nortriptyline and desipramine) which result from metabolizing the tertiary amines. The secondary amines have a better tolerability compared to the tertiary amines and hence showing a better compliance due to less incidence of unwanted side effects. It has been suggested that the TCAs exert some of their therapeutic actions by inhibiting the presynaptic reuptake of monoamines, mostly NA and to a lesser extent 5-HT via a competitive blockade of the monoamine transporter binding sites (Figure 1.7) and hence enhancing the transmission of NA and 5-HT (Gillman, 2007). The direct antidepressant effect induced by this mechanism, has however been questioned recently and a number of other hypothesis apart from the monoamine hypothesis

(based on the enhancement of extracellular monoamine levels) have been postulated including the ceramide hypothesis which is in line with the current thesis (see section 1.3.3). Furthermore, it was noted that desipramine shows a higher affinity for NET as compared to SERT, whereas clomipramine has more affinity to bind with SERT comparing with NET (Brunton et al., 2011). Furthermore, these medications may produce a wide range of adverse reactions through their inhibitory effects on other brain receptors such as cholinergic receptors (dry mouth, retention of urine, constipation and blurred vision), α_1 adrenoceptors (postural hypotension), 5-HT receptors and histamine receptors (drowsiness) with a scarce incidence of galactorrhoea, gynaecomastia and cardiac arrhythmias (Gillman, 2007).

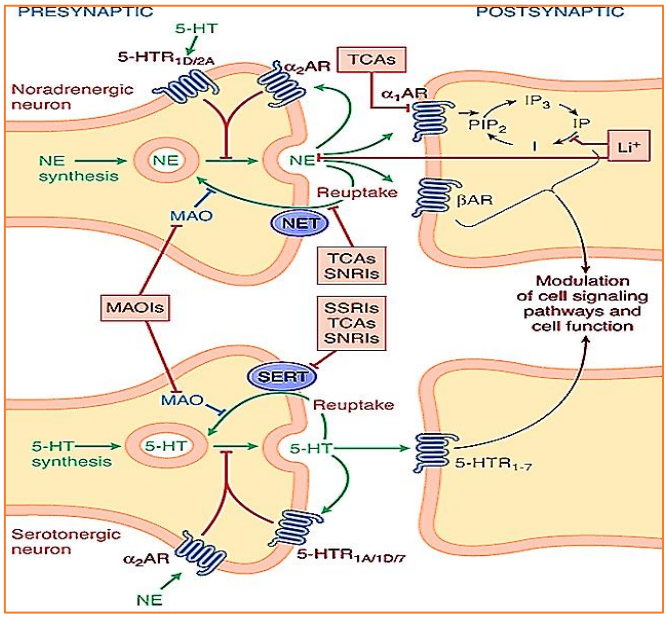

Figure 1.7: Mode of action of antidepressant drugs. Selective serotonin reuptake inhibitors (SSRIs) selectively inhibit the reuptake of serotonin. Serotonin-noradrenaline reuptake inhibitors (SNRIs) block the reuptake of both 5-HT and noradrenaline (NA) by inhibiting their transporters. Tricyclic antidepressant drugs (TCA) inhibit the presynaptic reuptake of NA and 5-HT (Brunton et al., 2011).

1.5.1.2. Monoamine oxidase inhibitors (MAOIs):

Monoamine oxidase (MAO) represents the main enzyme that is responsible for the metabolism and subsequent inactivation of the monoamine neurotransmitters. It is highly expressed within the brain and outside the central nervous system (gastrointestinal tract, liver and platelets) (Fiedorowicz and Swartz, 2004; Finberg and Rabey, 2016). This enzyme exists in two subtypes including MAO-A and MAO-B. The MAO-A isoform specifically metabolizes serotonin and noradrenaline, whereas the MAO-B enzyme catabolizes dopamine, thus inhibition of MAO-A subtype is found to be mainly

correlated with the antidepressant activity of MAOIs (Figure 1.7) (Fiedorowicz and Swartz, 2004). Most first-generation MAOIs act by inducing irreversible inhibition of the monoamine metabolizing enzyme MAO (induce a strong and irreversible linking with MAO, thus irreversibly inhibiting the protein until new enzyme is synthesized to replace it, approximately within two weeks) thereby, preventing monoamine catabolism and hence enhancing their vesicular storage. The commonly prescribed first-generation MAOIs included tranylcypromine, phenelzine and isocarboxazid (Fowler et al., 2009). In addition, moclobemide represents a second-generation reversible MAO-A inhibitor that is currently used in the treatment of depression, while selegeline is a selective MAO-B inhibitor that was approved to be effective in treating parkinsonism (Fiedorowicz and Swartz, 2004; Finberg and Rabey, 2016). Furthermore, the use of first-generation MAOIs was shown to be associated with many undesirable side effects such as insomnia, postural hypotension, weight gain, sexual dysfunction and rarely hypertensive crises and hepatotoxicity (Fiedorowicz and Swartz, 2004).

1.5.1.3. Monoamine receptor antagonists:

- **Mirtazapine:** Mirtazapine enhances NA and 5-HT release by blockade of α_2 adrenoceptors and 5-HT2C receptors.
- **Trazodone:** This antagonist blocks 5-HT2A and 5-HT2C receptors as well as inhibiting 5-HT reuptake.
- **Mianserin:** An α_2 and 5-HT2 receptor antagonist which is due to a considerable bone marrow depressing effect has been ceased from clinical use (Harvey et al., 2008).

1.6. Anatomical and neurophysiological aspects:

Several neuropathological and neuroimaging studies have shown that dysfunction within neural networks in particular within some brain regions are implicated in the pathophysiology of depressive disorder including the prefrontal cortex, hippocampus and the striatum (Figure 1.8) (Drevets et al., 2008; McEwen and Morrison, 2013).

1.6.1. The prefrontal cortex:

The prefrontal cortex (PFC) represents a cortical brain area that lies in the anterior frontal lobe, possessing many subdivisions including orbitofrontal, dorsolateral and ventromedial cortices. Several neuroimaging studies indicated that the PFC receives input from several brain regions such

as widespread areas of the cerebral cortex (occipital, parietal and temporal cortices), also from the limbic system and the brain stem. In addition, it projects to different brain regions including the hypothalamus, brainstem, amygdala and striatum (Siegel and Sapru, 2010). Regarding the monoamine neurotransmitters, the PFC is prominently innervated by serotonergic neurons, also it receives dopaminergic and noradrenergic innervations (Abernathy et al., 2010). It has a high expression level of 5-HT receptors particularly 5-HT1A, 5-HT2A and 5-HT3 receptor subtypes. In addition to the monoamine system, the PFC receives glutamatergic as well as cholinergic inputs from various brain areas (i.e. thalamus, hippocampus and amygdala) (Mattinson et al., 2011; Mesulam et al., 1983; Pirot et al., 1994). Thus, suggesting that this brain region is implicated in the pathogenesis of many psychiatric disorders including depression and schizophrenia possibly through a disruption in serotonergic neurotransmission (Abernathy et al., 2010; Puig and Gulledge, 2011). Functionally, this area is involved in regulating many behavioural and physiological functions through its dense neural network connections including: emotion, memory, learning, attention, decision making and motor response (Euston et al., 2012).

1.6.2. The hippocampus:

The hippocampus is an important region that constitutes one of the brain areas forming the limbic system, it lies under the cerebral cortex within the temporal lobes and adjacent to the amygdala. This limbic structure communicates through dense neural connections with widespread cortical and hypothalamic regions, therefore it is involved in modulating multiple vital functions including memory, learning, motivation, emotional response and cognitive abilities (Amaral and Witter, 1989). Indeed, it was indicated that the hippocampus is highly innervated by serotonergic neurons arising in the raphe nuclei (Moore and Halaris, 1975). Also, it receives a dense noradrenergic innervation from the locus coeruleus, the location of the noradrenergic cell bodies. In total, it has been estimated that the noradrenergic innervation of the hippocampus is approximately twice the noradrenergic connections within the cerebral cortex (Ermine et al., 2016; Oleskevich et al., 1989). The hippocampus is composed of the dentate gyrus (DG) and its principal cell layer consists of granule cells (also known as stratum granulosum). The hippocampus is further subdivided into 5 regions; CA1-CA4 (also referred to as the cornu ammonis) and the subiculum. Additionally, the principal cells within the hippocampal CA layers and the subiculum are all pyramidal cell types (Wible, 2013). Interestingly, many studies in both animals and humans show that hippocampus is

implicated in depression and its treatment (Campbell and MacQueen, 2004; Lee et al., 2013; Sapolsky, 2001). Specifically, a number of imaging studies utilizing magnetic resonance imaging (MRI) and multiple post mortem tissue studies have reported a reduction in hippocampal volume in depressed patients compared to healthy controls, a major finding that may be related to the reduction in neurogenesis (see section 1.3.2) within the hippocampal dentate gyrus, dendritic atrophy and glial cells loss (Campbell and MacQueen, 2004; Sapolsky, 2001; Sheline, 2011).

1.6.3. The striatum:

The striatum is considered to be less involved in the symptoms of depression compared to the prefrontal cortex and the hippocampus (Drevets et al., 2008). This region constitutes one of the four main structures forming the basal ganglia which also contains the substantia nigra, the globus pallidus and the subthalamic nucleus. The striatum is composed of three major nuclei including the caudate nucleus, putamen (both are known as the neostriatum) and the ventral striatum which contains the nucleus accumbens (Andersson et al., 2002). This important subcortical structure participates in motor planning and control as it represents the main input area of the basal ganglia which commonly mediates this action, also it exerts a significant role in reward, motivation, attention, learning, cognitive functions and social behaviours (Lakraj et al., 2014). Moreover, many psychological/neurological conditions including Parkinson's disease, schizophrenia and attention deficit hyperactivity disorder (ADHD) are successfully treated by drugs affecting DA neurotransmission in the striatum. These drugs include psychostimulant drugs such as methylphenidate that block the striatal dopamine transporter (DAT) for ADHD, DA antagonists for schizophrenia and DA enhancing drugs like L-DOPA, MAO and COMT inhibitors for Parkinson's disease (Bortolato et al., 2008; Iversen and Iversen, 2007; Mehler-Wex et al., 2006).

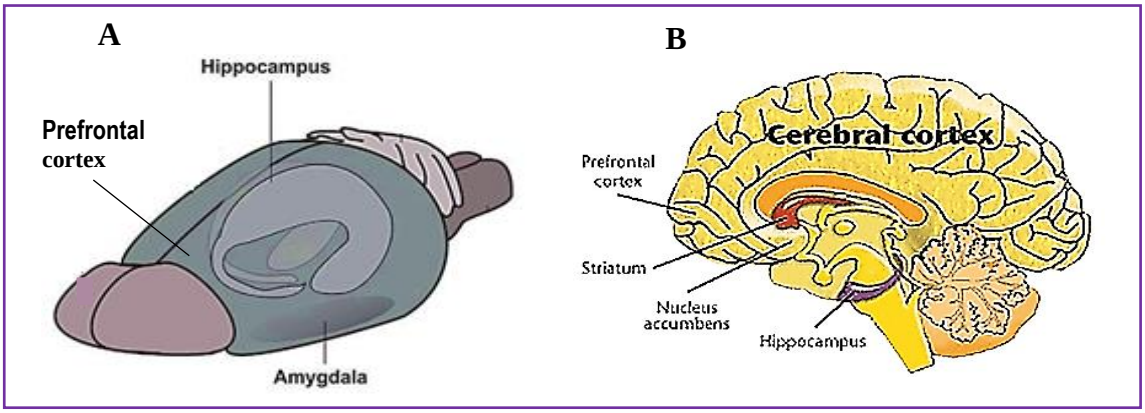

Figure 1.8: Brain regions implicated in depression (A) A representation of rat brain (Dauth et al., 2017). **(B) Human brain** (Clapp et al., 2008)**.**

1.7. Sphingolipids and depression:

Growing evidence from extensive previous preclinical (Dinoff et al., 2017; Gulbins et al., 2013; Müller et al., 2015; Powell et al., 2012; Schneider et al., 2017) and clinical studies (Demirkan et al., 2013; Dinoff et al., 2017; Kornhuber et al., 2005; Rhein et al., 2017) implies that sphingolipids particularly ceramide could have a role in the pathogenesis of depression and other serious psychiatric disorders such as anxiety and schizophrenia (Schneider et al., 2017). One of the reported findings in depression is a reduction in the volume of the hippocampus (hippocampal atrophy) which possibly could be related to a reduced hippocampal neurogenesis (new formation of neurons) in particular in the dentate gyrus of the hippocampus (see section 1.3.2) (Jacobs et al., 2000; Videbech and Ravnkilde, 2004). This process depends entirely on the initial ability of proliferation and differentiation involving both progenitor cells and neuronal stem cells to produce the mature neurons in this particular brain region (Dinoff et al., 2017; Ming and Song, 2011). In this respect, a recent study which utilized a tissue culture of a neuronal pheochromocytoma cell line showed that the application of a specific sphingolipid, namely ceramide resulted in the inhibition of the proliferating activity of these cells (Gulbins et al., 2016). Further, emerging evidence suggests that sphingolipids particularly ceramide is involved in the process of apoptosis of neuronal stem cells in the hippocampus (Dinoff et al., 2017; Wang et al., 2012). Thus, playing an important role in the inhibition of hippocampal neurogenesis which as mentioned already is believed to be implicated in the pathogenesis of depression and possibly the relevant reduction in hippocampal volume (Dinoff et al., 2017; Jacobs et al., 2000; Videbech and Ravnkilde, 2004). Furthermore, another critical neurochemical observation in depression is the reduction in monoaminergic transmission,

particularly 5-HT neurotransmission (Belmaker and Agam, 2008; Hirschfeld, 2000). Indeed, several antidepressant medications exert their therapeutic mode of action by regulating the extracellular levels of monoamines (Hirschfeld, 2000). Sphingolipids, in particular ceramide may promote alteration in cell signaling and monoamine neurotransmission functions via the formation of a ceramide enriched macrodomains that allow clustering of specific proteins including G-protein coupled monoamine receptors (GPCRs) within the cell membrane (see section 1.9.1) (Dinoff et al., 2017; Müller et al., 2015; Schneider et al., 2017). In addition, ceramide has been suggested to contribute in the process of exocytosis and the subsequent neurotransmitter release to the synaptic cleft by aggregating various proteins (i.e. syntaxin 1A and syntaxin 3) that are involved in this process (see section 1.9.1) (Chamberlain et al., 2001; Tsui-Pierchala et al., 2002). Moreover, ceramide may affect serotonin binding to the 5-HT receptors including 5-HT1A receptor subtype, hence modulating serotonergic neurotransmission (Jafurulla et al., 2008). Further, increasing experimental evidence now points to the possible direct involvement of ceramide in depression. This encompass an earlier recorded observation that mice injected with ceramide into the hippocampus showed a marked increase in depression-like behaviours (Gulbins et al., 2013). These depression-related behaviours included: a reduced sucrose consumption in the sucrose preference test, a markedly delayed eating in the novelty suppressed feeding test as well as the apparent neglect of the animal coats in the coat test (Gulbins et al., 2013). Interestingly, another important finding concerning the ceramide role in depression is the fact that many currently used antidepressant drugs inhibit the acid sphingomyelinase enzyme (ASM) when administered chronically (Gulbins et al., 2013). This enzyme catalyzes the degradation of sphingomyelin into ceramide and phosphoryl-choline, a process that is predominantly activated in the membrane lipid rafts (Müller et al., 2015; Reichel et al., 2014; Schneider et al., 2017). Additionally, an important observation is that many SSRIs (paroxetine, fluoxetine and sertraline) and TCAs (e.g. desipramine and nortriptyline) act by inhibiting ASM activity, subsequently reducing brain ceramide level (a possible mechanism of antidepressant action) (see Chapter Five, section 5.1.1.2) (Kornhuber et al., 2008, 2010). This effect is closely associated with the cationic amphiphilic property of these drugs (i.e. the antidepressant drugs such as desipramine and paroxetine) (Funk and Krise, 2012). These small molecules are typically containing both hydrophobic and hydrophilic domains (amphiphilic compounds). Therefore, they have the ability to accumulate inside the acidic lysosomes, thus resulting in a detachment and a subsequent inactivation of the lysosomal enzymes (i.e. ASM). Hence, enhancing high intra-lysosomal accumulation of various lipid species such as sphingomyelin (Kornhuber et al., 2010; Lübke et al.,

2009). Furthermore, a recent study demonstrated that a reduction in hippocampal ceramide level was associated with an inhibition of acid sphingomyelinase activity, concomitantly the mice showed an improvement in their depression-like behaviours following treatment with fluoxetine and amitriptyline in animal models of depression (Gulbins et al., 2013). An important correlation was identified between the reduction in ceramide level which develops after 2-3 weeks of treatment (until the antidepressant drugs accumulate sufficiently within the neuronal lysosomes to inhibit the ASM enzyme) and the period that is consistent with the required time for the onset of the antidepressant action (Kornhuber et al., 2009). Accordingly, the sum of accumulating evidence suggests the concept that sphingolipids, in particular ceramide exerts an important role in the pathogenesis of depression as well as the mechanism of its medical intervention.

1.8. The functional role of sphingolipids in biological membranes:

Lipid bilayers are basic structural components of all the cell membranes which form a critical physical barrier which are mainly composed of four particular phospholipid containing molecules including: sphingomyelin, phosphatidylcholine, phosphatidylserine and phosphatidylethanolamine. Phospholipids are divided into two major classes: glycerophospholipids and sphingophospholipids also termed sphingolipids (Alberts et al., 2002). In an aqueous environment, the lipid bilayers within the cell membrane (3-5 nm in thickness) are spontaneously formed (without energy requirement) with a special organisation of the lipid molecules; the polar hydrophilic heads (readily dissolved in water) facing the exterior aqueous sites while the non-polar hydrophobic tails (water insoluble) are buried in the interior core of the lipid bilayers (Figure 1.9) (Cooper, 2000). Within biological membranes, the packed phospholipids are amphiphilic (also known as amphipathic) molecules that have a polar or hydrophilic head containing a phosphate group and two non-polar or hydrophobic tails which are usually composed of long fatty acid chains that contain a variable number of carbon atoms (14-24) (Alberts et al., 2002). In addition to the other structural constituents of the cell membrane (cholesterol and carbohydrates), the second main component of the cell membrane together with the phospholipids are proteins. These membrane proteins are divided into two main types: transmembrane proteins (also known as integral membrane proteins) and the peripheral membrane proteins (interact indirectly with the transmembrane proteins). The integral proteins are immersed within the lipid bilayers and they are responsible for a variety of specialized functions (Cooper, 2000). Some proteins facilitate membrane permeability and aid the selective transport of

specific particles across the cell membrane such as the ion channels particularly the calcium release-activated channels and the potassium channel Kv 1.3 subtype (Gulbins et al., 1997; Lepple-Wienhues et al., 1999). Others mediate cell signaling actions and subsequent neurotransmission through their functions as neurotransmitter receptors (e.g. G-protein coupled receptors). Additionally, some proteins participate in vital cellular processes serving as enzymes including the intracellular protein phosphatases and protein kinase C enzymes that are for example, involved in stress-induced apoptosis or programmed cell death (Cooper, 2000; Dinoff et al., 2017). The integral membrane proteins are also amphiphilic in nature and will interact strongly through their hydrophobic ends with the lipid bilayers. Not surprisingly, any change in the lipid composition may directly affect properties of the associated proteins, hence their functions will be modulated such as the alteration in receptor affinity, receptor-mediated signaling actions and the selective transporting activity achieved via the membrane ion channels (Alberts et al., 2002; Cooper, 2000).

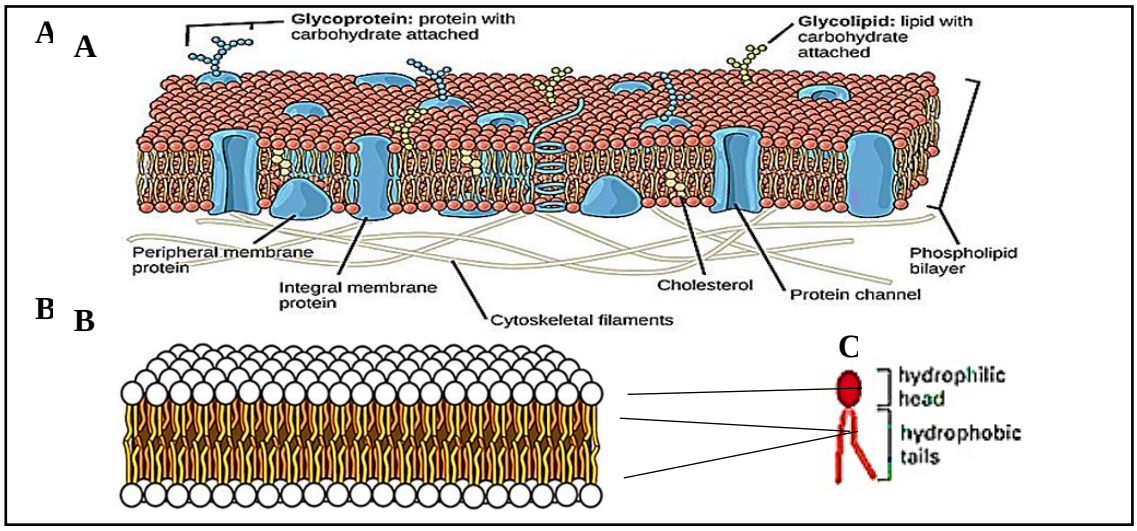

Figure 1.9: Three-dimensional structural models of cell membrane, representing A, B a phospholipid bilayer (Boundless, 2016), and C a phospholipid molecule with a hydrophilic head and two hydrophobic tails (Alberts et al., 2002).

It is well established that sphingolipids are one of the main phospholipid classes within brain membranes and exists in different types including ceramide and sphingosine both of which playing significant roles in modulating neurotransmission and receptor-mediated signal transduction (Dinoff et al., 2017). Within lipid rafts, sphingomyelin (a principal lipid component of the cell membrane) can be catalysed to ceramide and phosphoryl choline by action of the main sphingomyelin catabolizing enzyme, acid sphingomyelinase (ASM) (also known as sphingomyelin phosphodiesterase) which is predominantly activated within these lipid rafts (Kornhuber et al.,

2014; Müller et al., 2015; Reichel et al., 2014; Schneider et al., 2017). Interestingly, the released ceramide molecules have a dramatic ability of spontaneous self-association that result in the formation of small ceramide enriched microdomains (nanoscale) that can further merge producing larger ceramide enriched macrodomains or platforms termed lipid rafts (Figure 1.10) (Dobrowsky, 2000; Hering et al., 2003). These ceramide macrodomains represent tightly packed hydrophobic structures aggregated within the cell membrane that participate in a subsequent re-modelling of the membrane platforms or lipid rafts (Cremesti et al., 2002; Müller et al., 2015; Schneider et al., 2017). Emerging evidence suggests that these lipid rafts (containing the ceramide enriched macrodomains) consequently permit clustering and re-organization of signaling molecules and neurotransmitter receptors including G-protein coupled receptors (GPCRs) (Müller et al., 2015; Schneider et al., 2017). Thus, altering the lipid composition within these membrane macrodomains may directly contribute to a subsequent change in receptor localization and affinity, their signaling action and the synaptic transmission (Fantini and Barrantes, 2009).

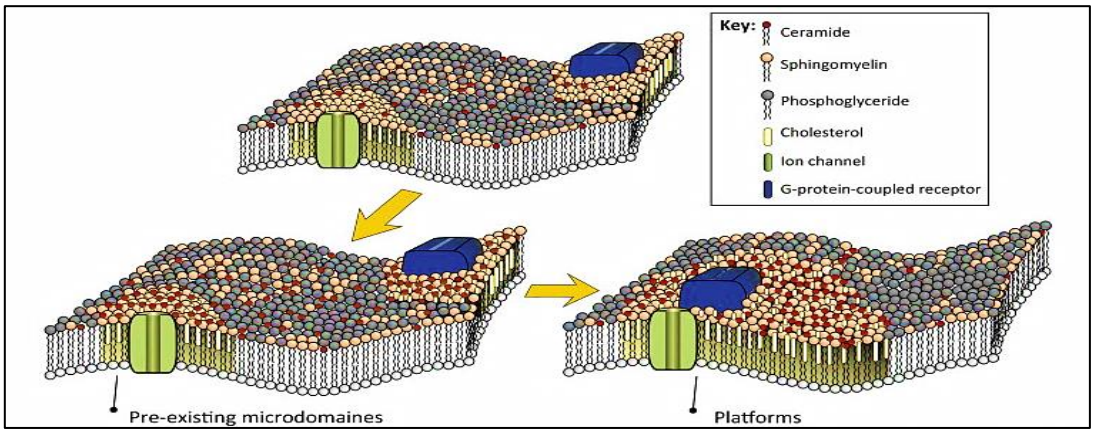

Figure 1.10: The mechanism of ceramide action in biological membranes (Kornhuber et al., 2014).

1.9. The role of lipid raft-sphingolipids in neuronal functions:

1.9.1. Synaptic neurotransmission:

Recent studies indicate that lipid rafts form critical signaling macrodomains within the cell membrane (Dinoff et al., 2017; Müller et al., 2015; Schneider et al., 2017; Tsui-Pierchala et al., 2002). Consequently, these important membrane structures may directly affect cell signaling, synaptic neurotransmission and receptor mediated signal transduction (Fantini and Barrantes, 2009; Hering et al., 2003) (see also section 1.8). Importantly, in addition to clustering of neurotransmitter

receptors resulting in a very high receptor density within the ceramide enriched macrodomains of the cell membranes. These membrane lipid rafts may contribute to synaptic transmission through regulating trafficking and the calcium-dependent fusion of the synaptic vesicles (exocytosis process), and the subsequent neurotransmitter release into the synaptic cleft (Tsui-Pierchala et al., 2002). Recently, it was found that many regulatory biomolecules and proteins implicated in membrane fusion of the synaptic vesicles are densely located within lipid rafts such as syntaxin 1A and syntaxin 3. These presynaptic plasma membrane proteins have been shown to be involved in the process of neuronal exocytosis possibly by forming a stable complex that provides the energy required for the vesicle fusion with the plasma membrane of neuronal cells. Also, they could be implicated in the regulation of calcium influx by binding with both neuronal N- and L-types calcium channels (Kang et al., 2002; Wiser et al., 1996). Accordingly, lipid rafts could promote monoamine neurotransmitter release and consequently, the synaptic neurotransmission function (Chamberlain et al., 2001). It is well established that an important pathophysiological observation in depression is the reduction in serotonergic neurotransmission (Belmaker and Agam, 2008; Hirschfeld, 2000). Further evidence observed that sphingolipids including ceramide may alter monoamine reuptake and signaling, in particular serotonergic transmission either through direct binding to the transporter molecules, hence modulating their transport and functions (i.e. increasing the reuptake of 5-HT) (Gangoiti et al., 2010; Riddle et al., 2003) or by indirect effect via binding and activation of several intracellular proteins and enzymes including phosphatases and kinases (Dinoff et al., 2017; Westwick et al., 1995). In this respect, It was also noted that ceramide may alter serotonin signaling via modulating 5-HT binding to the serotonergic receptors specifically the 5-HT1A subtype (Jafurulla et al., 2008). A previous cell study conducted on a tissue culture of Chinese hamster ovarian cells following sphingomyelinase treatment (using different enzyme concentrations: 25 or 50 IU/L for 90 minutes) reported that sphingolipids, particularly ceramide may affect serotonergic neurotransmission by enhancing the ligand binding activity of 5-HT1A receptors (see section 1.4.1.1). Thus, opens up the possibility that ceramide could modulate brain extracellular 5-HT levels via an inhibition of serotonergic neuronal firing (Jafurulla et al., 2008; Singh et al., 2012). Consequently, growing evidence suggests that a dysregulation in the metabolism of brain membrane sphingolipids particularly ceramide may contribute to alteration in multiple neuronal functions including cell signaling and monoamine neurotransmission. Hence, sphingolipids could be directly implicated in depression and depressive-like behaviours (Gulbins et al., 2013; Kornhuber et al., 2005).

1.9.2. Apoptosis (programmed cell death):

Apoptosis represents a planned process of intrinsic cellular death (Reed, 2000). It is a vital physiological phenomenon possessing a number of morphological and biochemical variations initiated during both early prenatal development and late adult life. However, many histopathological studies indicates that a defect in this regulated intracellular mechanism with a misbalance between cellular death and growth may contribute to the underlying pathogenesis responsible for various CNS disorders such as depression and Parkinson's disease which are expressing apoptotic changes (Eilat et al., 1999; Liu et al., 2017; Wong, 2011), whereas other pathologies may involve a reduced level of apoptosis as in many malignant cancer conditions (Wong, 2011). This critical physiological process is characterized by a series of ordered morphological changes including cellular shrinkage, increased cytoplasmic density, DNA condensation, destruction of the nucleus and finally the formation of apoptotic bodies which undergo phagocytosis by the macrophages (Elmore, 2007; Imajoh et al., 2004). Concomitantly, the main biochemical apoptotic changes include DNA degradation and the activation of particular protease enzymes known as caspases that cleave various cellular proteins to initiate the process of apoptosis (Boatright and Salvesen, 2003; Iglesias-Guimarais et al., 2012; Reed, 2000).

1.9.2.1. Implication of ceramide and sphingosine in apoptosis:

The known membrane sphingolipids, ceramide and sphingosine were recently identified as important mediators of apoptosis (Pettus et al., 2002; Ruvolo, 2003). However, the exact molecular mechanism underlying their contribution to apoptosis is still not fully understood. Recent evidence however, implies that hydrolysis of the sphingolipid molecule, sphingomyelin into the metabolic products: ceramide and sphingosine is increased under stressful conditions (Woodcock, 2006). Consequently, the accumulation of ceramide within the cell membrane results in the formation of lipid rafts containing the ceramide-enriched macrodomains which permit clustering of various proteins, enzymes and receptors (see section 1.8), therefore potentiating the apoptotic mechanisms (Dobrowsky, 2000). In addition, emerging evidence proposes that during programmed cell death ceramide content within the mitochondrial cell membrane is significantly elevated, together with increased permeability of the outer mitochondrial membrane which is due to increased formation of membrane pores, a process triggered by ceramide action. Consequently, these permeable pores may function as ceramide channels that regulate the permeability of the outer mitochondrial

membrane (Siskind, 2005). Thus, allowing the mitochondrial release of pro-apoptotic proteins including procaspases, cytochrome C and other proteins which are important for activating the enzymes (DNase and caspases) that are crucial to initiate the apoptotic mechanism (Siskind, 2005; Woodcock, 2006). Moreover, it has been found that ceramide directly binds to a particular proenzyme known as cathepsin D, hence allowing the release of the active form of the enzyme and subsequently activating a pro-apoptotic protein termed as BID. This protein exerts a critical role in the induction of programmed cell death via promoting the mitochondrial release of cytochrome C into the cytosol (Heinrich et al., 2004; Woodcock, 2006). Interestingly, it has further been reported that ceramide may activate various enzymes involved in apoptosis including protein phosphatases (protein phosphatase 1, PP1 and protein phosphatase 2A, PP2A) and protein kinases (stress-activated protein kinases, SAPKs) (Ruvolo, 2003). In this respect, it was shown that sphingosine may act as a second messenger that mediates programmed cell death by potently inhibiting the protein kinase C enzyme and thereby triggering the apoptotic mechanism (Taha et al., 2006). Sphingosine was also found to promote the activation of BID protein and thereby inducing the mitochondrial release of cytochrome C, hence triggering the mechanism of cellular suicide (Cuvillier et al., 2001; Taha et al., 2006).

1.9.3. Selective transport across the cell membrane:

Recent studies provided evidence that ceramide within membrane lipid rafts may affect selective transport processes and permeability across cell membranes. This is achieved by interacting with certain ion channels that are specifically located in lipid rafts, in particular the potassium channel Kv 1.3 and Kv 2.1 subtypes (Gulbins et al., 1997; Tsui-Pierchala et al., 2002) as well as the presynaptic P/Q-type (Cav 2.1) calcium channels (Lepple-Wienhues et al., 1999; Taverna et al., 2004). Based on these findings, it has been hypothesized that membrane lipid rafts may be required for clustering and localization of these important ion channels, therefore influencing the membrane permeability function (Tsui-Pierchala et al., 2002).

1.10. Aim and objectives of this study:

The overall aim of the present study was to enhance our understanding of the molecular and biochemical actions of two currently prescribed antidepressant drugs namely, paroxetine and desipramine with an emphasis of their effects on the brain sphingolipid pathway. To achieve this

principal aim, the following objectives were pursued by means of a variety of methodologies, using a rat model:

- To assess the regional brain metabolic profile following acute and chronic administration of two different types of antidepressant medications using 1HNMR spectroscopy (Chapter Three).
- To investigate both the drug and region-specific effects of antidepressant treatment on bioactive sphingolipid levels using the methods of: LC-MS and HPLC-UV detection (Chapter Four).
- To investigate the effect of chronic antidepressant drug treatment on the gene expression level of the key enzymes in the brain sphingolipids pathway using RT-qPCR (Chapter Five).
- To examine the effect of the acid ceramidase inhibitor, carmofur on brain level of sphingolipids and monoamines in brain regions implicated in depression by means of LC-MS, HPLC-UV and HPLC-ECD respectively (Chapter Six).

CHAPTER 2

Materials and methods

2.1. Animals and drug treatment:

2.1.1. Habitation and environmental conditions:

Adult male Sprague-Dawley rats weighing (290-300 g) were used for the acute (single injections) experimental part of the current project (Table 2.1). For the chronic experiments, (daily injections for 15 days at 10 am) the body weights ranged from 180-200 g at the start of the treatment (Table 2.2). All rats were purchased from (Charles River, UK) and were housed four or six animals per cage under automatically controlled environmental temperature (20-22°C), lighting condition (light 07:00-19:00) and humidity (45-50%). All the animals had free access to food and drinking water and were maintained in this environment with regular handling for one week before the start of the experiment. All procedures involving animals described in this study were carried out in strict accordance with UK Home Office regulations and Animals Scientific Procedures Act (1986) under requisite project and personal licence authority and were approved by DMU Ethical Review Committee. In total, 126 male Sprague-Dawley rats were used to perform the experimental work of the present study, 60 rats were used for the acute administration groups, whereas the remaining 66 animals were used for chronic treatment, which included both control and drug treated groups.

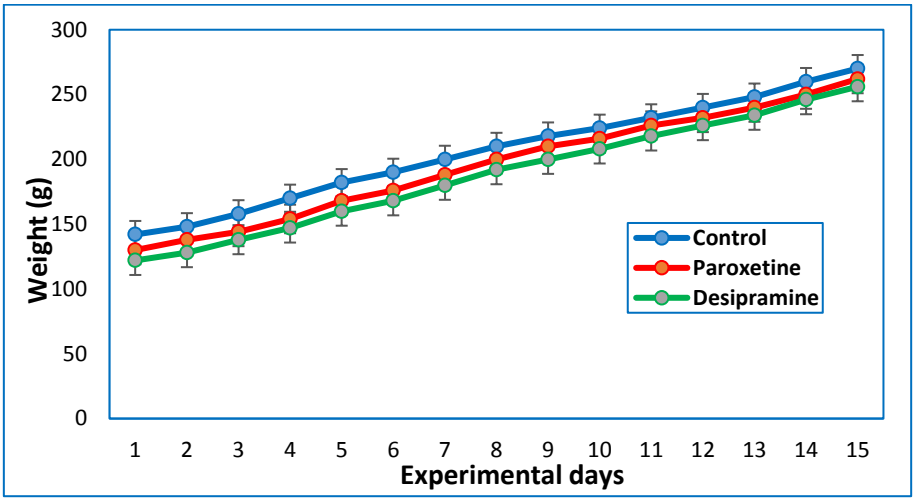

Figure 2.1: A growth diagram showing the increase in body weight in grams of the total chronically treated animals in this project including both control and drug-treated rats across the experimental days (1-15 days). A total of 66 rats were used for the chronic treatments, which included both control (saline-treated) and drug-treated (paroxetine and desipramine) groups. Generally, at the end of the treatment period, body weights of control animals (average body weight = 270 g, n = 30) were slightly higher compared to the drug-treated rats (average body weight for paroxetine = 262 g and for desipramine = 256 g, for both groups n = 18), however, the difference was not statistically significant (one-way ANOVA p value = 0.510).

2.1.2. Drug treatment:

Animals were randomly separated into two groups (control and drug treated) and each group depending on the experimental protocol and the analytical/molecular technique used comprised of either six or twelve animals. Chronically treated animals were weighed every day, the body weights were recorded, and the injection volume adjusted accordingly. The body weights of the rats injected chronically with antidepressant drugs were not statistically different from their corresponding controls during the period of injections (Figure 2.1). Rats in control groups received either a single intraperitoneal (i.p) injection of saline (0.9% of sodium chloride, 1 ml/kg) (acute group) or were injected once daily with saline at 10 am for 15 days (chronic group). The corresponding drug treatment groups received injections of either: paroxetine (5 mg/kg, i.p), a selective serotonin reuptake inhibitor (SSRI) or desipramine (10 mg/kg, i.p), a tricyclic antidepressant (TCA). Immediately prior to injections, both paroxetine and desipramine were dissolved (solutions made up daily) in saline at 5 mg/ml and 10 mg/ml respectively. In man, plasma concentration of desipramine associated with clinical efficacy is usually between 50-300 ng/ml (Gillman, 2007), whereas the reported therapeutic plasma level for paroxetine is 30-120 ng/ml (Hiemke et al., 2011). In the present study, chosen doses of the utilised antidepressant drugs were selected, in accordance with previously published data (Detke et al., 1997; Hajós-Korcsok et al., 2000; Mathes and Spector, 2011) where detectable biochemical and behavioural changes were indicated following similar drug regimes in animal models of depression. Furthermore, a preclinical study conducted in rats reported that paroxetine administration in a dose of 5 mg/kg, i.p (identical to the dose used in this study) resulted in plasma concentration of 55-100 ng/ml which is well within the range of the therapeutic plasma concentration of 30-120 ng/ml measured in patients treated with paroxetine (Benmansour et al., 1999). Additionally, desipramine administration in a dose of 15 mg/kg/day i.p (the present study used 10 mg/kg, i.p) was found to attain a plasma level at a range of 265-430 ng/ml following 7-10 days of treatment in rats (Benmansour et al., 1999; Kaye et al., 1989). Thus, based on previous studies, the doses of paroxetine and desipramine used in the present study, are likely to reach plasma concentrations similar to levels associated with therapeutic response in humans (Benmansour et al., 1999; Brimberg et al., 2007; Gundersen et al., 2013; Kozisek et al., 2007; Mathes and Spector, 2011). At the end of the designated period rats were sacrificed according to Schedule one procedure (Home Office, Animal act, 1986), trunk blood was collected, and the brain was removed. For biochemical analysis of brain tissue and in some cases plasma (see Chapters Three,

Four and Six) rats were killed one hour after the last injection. For the gene expression study (Chapter Five) animals were sacrificed at 24 hour after the final injection, based on previous gene expression studies (Andriamampandry et al., 2002; Lee et al., 2010; Nakatani et al., 2004; Yamada et al., 2003). Generally, on the day of the experiment, the overall body weights for the treated animals were not statistically different compared to the corresponding controls after acute treatment (p value = 0.277) (Table 2.1 and Figure 2.2) and this was also the case following chronic administration (p value = 0.370) (Student's t-test) (Tables 2.2 and Figure 2.2).

Table 2.1: The mean +/- SEM for body weights and corresponding brain sections weight in grams following acute administration for the control and treatment groups (n = 6 or 12 per group). Abbreviations: PFC, prefrontal cortex; HP, hippocampus and ST, striatum.

Acute administration	Body weight (g)	PFC (g)	HP (g)	ST (g)
Control	304 ± 4	0.180 ± 0.009	0.222 ± 0.012	0.397 ± 0.026
Treatment	297 ± 4	0.188 ± 0.009	0.228 ± 0.012	0.384 ± 0.027

Table 2.2: The mean +/- SEM for body weights and corresponding brain sections weight in grams following chronic administration for the control and treatment groups (n = 6 or 12 per group).

Chronic administration	Body weight (g)	PFC (g)	HP (g)	ST (g)
Control	270 ± 7	0.193 ± 0.011	0.218 ± 0.006	0.411 ± 0.026
Treatment	262 ± 6	0.206 ± 0.012	0.211 ± 0.008	0.430 ± 0.027

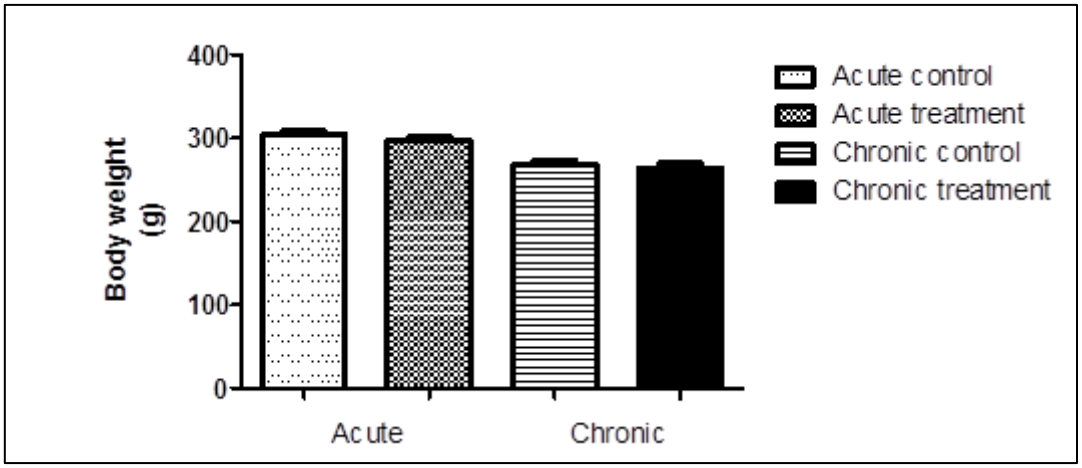

Figure 2.2: Animals body weight in grams for the whole control and treatment groups across the experiments. Data presented as mean ± SEM ($p > 0.05$) (Student's t-test).

2.1.3. Brain tissues dissection:

On the day of the experiment, the animals were weighed, treated and killed according to a precise timetable, making sure that all animals were terminated at one hour after the injection or in the case of the gene expression study (Chapter Five) at 24 hours. The whole brain was then removed, and brain regions were dissected out rapidly on ice into three targeted brain regions (Figure 2.3). The dissection was performed in correspondence with the Rat Brain Atlas (Paxinos and Watson, 2006). The brain was cut into four separate planes (see Figure 2.3), firstly the olfactory bulb was removed and then the prefrontal cortex was cut out with a scalpel. The striatal region was obtained by cutting a section posteriorly at the hypothalamus (Quansah, 2017), eventually, the hippocampus was acquired via sectioning anterior to the brain stem structures and both halves of the hippocampus were carefully released from the adherent cortical tissues. The brain samples were then snap frozen in isopentane on dry ice, weighed and stored at - 80°C until subsequent preparation for biochemical analysis.

A

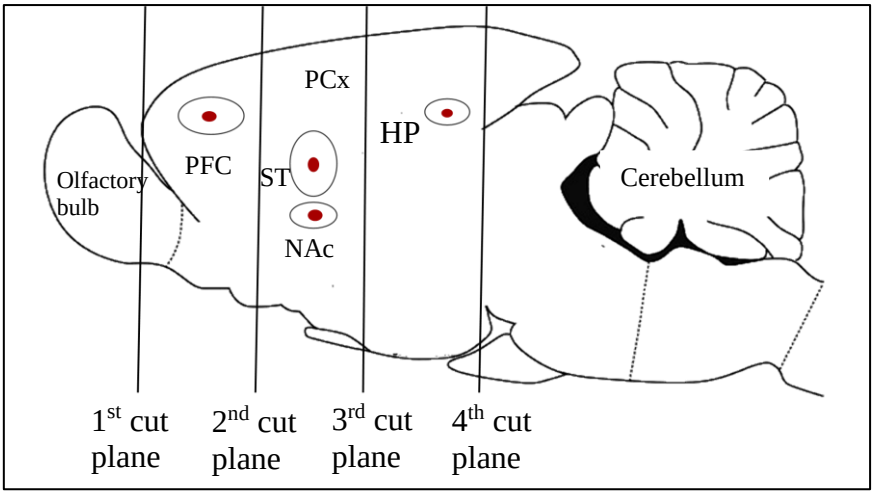

B

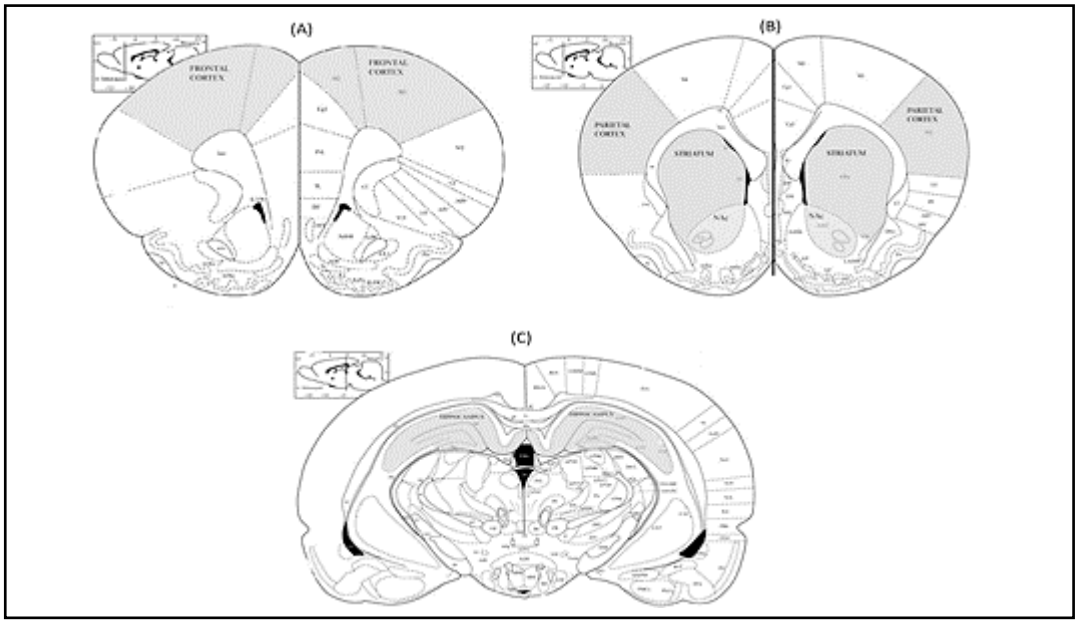

Figure 2.3: (A) The dissection planes. (B) A representation of the three examined regions in the rat brain. (A) Prefrontal cortex; (B) striatum and (C) hippocampus, based on Paxinos and Watson rat brain atlas (Paxinos and Watson, 2006). Abbreviations: PFC, Prefrontal cortex; PCx, parietal cortex; ST, striatum; NAc, nucleus accumbens; HP, hippocampus.

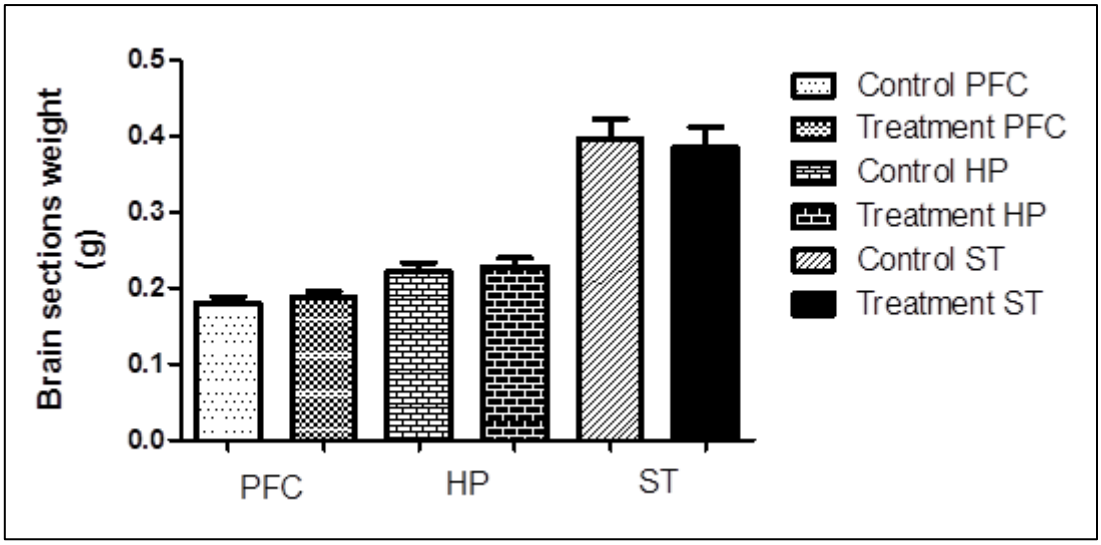

Figure 2.4: Brain sections weight in grams following acute administration for the control and treatment groups in all the achieved experiments. Data presented as mean ± SEM ($p > 0.05$) (Student's t-test). Abbreviations: PFC, the prefrontal cortex; HP, the hippocampus; ST, striatum.

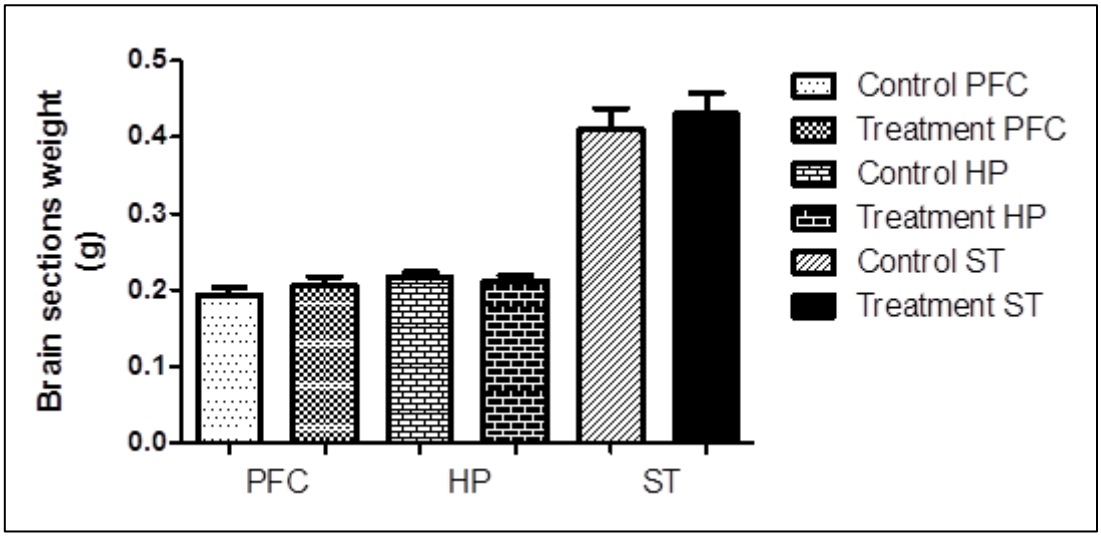

Figure 2.5: Brain sections weight in grams following chronic administration for all the control and treatment groups in all the accomplished experiments. Data presented as mean ± SEM ($p > 0.05$) (Student's t-test).

In addition, the overall brain sections weight within both control or treatment groups and following either acute or chronic administration were not statistically different ($p > 0.05$) (Student's t-test) which reflects the consistency in performing the brain dissection (Tables 2.1, 2.2, Figures 2.4 and 2.5).

2.1.4. Drugs and chemicals:

The drugs and chemicals used in the whole experimental work of the present study with their suppliers are summarized in the list below:

- Acetonitrile was of LC-MS grade (Fisher Scientific, UK).
- Carmofur was a gift from LKT Laboratories (Germany).
- Ceramide and sphingosine standards were of LC-MS grade (Sigma-Aldrich, UK).
- Chloroform was of LC-MS grade (Rathburn Chemicals Ltd, UK).
- Desipramine hydrochloride was purchased from Sigma-Aldrich, USA.
- Deuterium oxide (99.8%; Acros Organics) and deuterium oxide containing 3-(trimethylsilyl) propionic – 2, 2, 3, 3 – d4 acid (TSP) sodium salt (Acros Organics BVBA).
- DNA ladder (Bioline, UK), 2% agarose was obtained from (ThermoFisher Scientific, UK).
- Ethanol was of LC-MS grade (Fisher Scientific, UK).
- iScript cDNA Synthesis Kit was purchased from Bio-rad, UK.
- Methanol was of HPLC (Stratlab, UK) and LC-MS grades (Rathburn Chemicals Ltd, UK).
- Monoamine neurotransmitters and their metabolite standards were obtained from Sigma-Aldrich, UK.
- My Taq red master mix (Bioline, UK).
- Paroxetine hydrochloride hemihydrate was a gift from Glaxo Smith Kline (i.e. GSK).
- Perchloric acid (Rathburn Chemicals Ltd, UK).
- RNeasy Mini Kit was purchased from Qiagen, UK.
- SensiFAST SYBR HI-ROX was obtained from Bioline, UK.
- Turbo DNAse-AM free kit (Ambion Inc, USA) and 96-well reaction plates were supplied by Thermo Fisher Scientific, UK.
- Water of HPLC grade and (LC-MS Chromasolv) from Strat Lab, UK and Sigma-Aldrich, UK.

2.1.5. Data presentation and statistical analysis:

The effect of acute and chronic antidepressant drugs as well as after acute carmofur administration were statistically analysed using Prism 5.0 Software (Graph Pad Prism). Statistical analysis of the recorded two datasets (saline versus drug-treated) groups were performed by Student´s t-test (see Chapter Six and Chapter Four section 4.3.2). On the other hand, multiple datasets were tested using either two-way analysis of variance (two-way ANOVA with Bonferroni post-hoc test) (see Chapter four section 4.3.1 and Chapter Six) or one-way analysis of variance (one-way ANOVA with Bonferroni t-test) (see Chapter Five) for multiple comparison. All data were presented either as means or fraction of controls ± standard errors of the mean (SEM) for each group. Statistically significant difference was considered at a level of $p < 0.05$. For analysis of NMR data see section 2.2.6.

2.2. Proton nuclear magnetic resonance spectroscopy (^{1}H NMR spectroscopy):

^{1}H NMR spectroscopy is a powerful analytical technique that has been widely employed in number of applications including: chemical, clinical, biomedical and biological research, pharmaceutical production as well as in the food, medicine and chemical industry (Günther, 2013; Powers, 2009). This spectroscopic tool (Figure 2.6) has been extensively used to investigate the structural configuration and physical properties of certain molecules within a tissue sample. In addition, it allows the determination of metabolic changes and also the identification of a wide range of metabolites in biological fluids in response to external conditions such as diet or various drug applications (Cloarec et al., 2005).

2.2.1. Basic principles of NMR spectroscopy:

The atomic nuclei are electrically charged units (carry a positive charge) and usually they possess a specific intrinsic property of spinning randomly around their axis in different directions (termed as nuclear spin, I). The tendency of a nucleus to spin (I) is totally dependent upon its internal structure, i.e. the number of protons and neutrons contained within the nucleus, if the total number is even, then the nucleus has no spin (zero spin) such as ^{16}O or ^{12}C, whereas other atoms are composed of odd number of protons and neutrons (odd mass number), hence they have a non-zero spin or (I) = ½ or one of its multiples (3/2 or 5/2,…) and these elements include for example, hydrogen 1 (^{1}H),

^{19}F and ^{13}C which are all particularly useful for the analysis by NMR spectroscopy. In particular, the proton or ^{1}H is the most commonly used element in NMR studies with a high magnetic activity (García-Álvarez et al., 2016; Günther, 2013). Furthermore, irradiating the sample with a pulse of radiofrequency waves promotes transition of the hydrogen nuclei within the analysed sample from a lower energy level to a higher energy level which is accompanied by the subsequent absorption of energy (known as excitation of the nuclei). Then, the excited nuclei may flip back to the initial lower energy state (termed as relaxation) and hence, emitting the absorbed energy as resonant signals that can be detected by the receiver of the utilized instrument, thus generating the NMR spectrum across the sample (García-Álvarez et al., 2016; Wong, 2014)

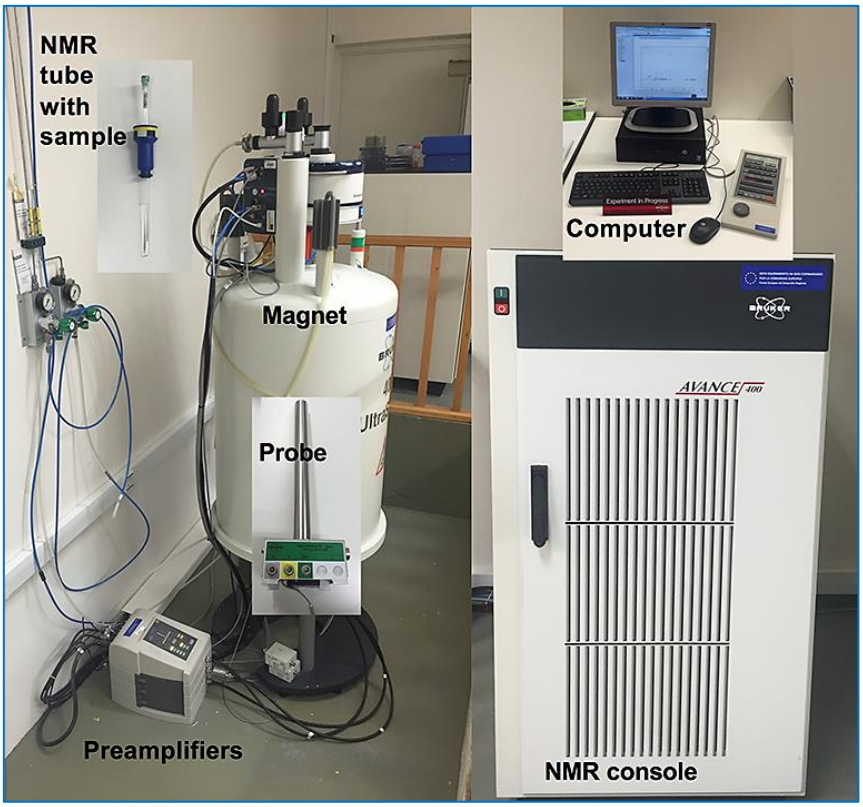

Figure 2.6: NMR spectrometer components (García-Álvarez et al., 2016)**.**

2.2.2. Chemical shift:

Throughout the NMR spectra, a series of resonant signals spread over a horizontal axis from zero parts per million (ppm) unit to ten ppm scale range (Figure 2.7). Additionally, within each analysed sample a reference compound (trimethylsilylpropanoic acid, TSP) is used as a standard that gives a resonant signal (a reference signal) at the zero point of the chemical shift (Günther, 2013). Importantly, preparing a sample for the NMR analysis necessitates the use of specific solvents that do not contain ^{1}H hydrogen atoms such as deuterium oxide (D_2O) to avoid introducing an interfering signal within the spectrum.

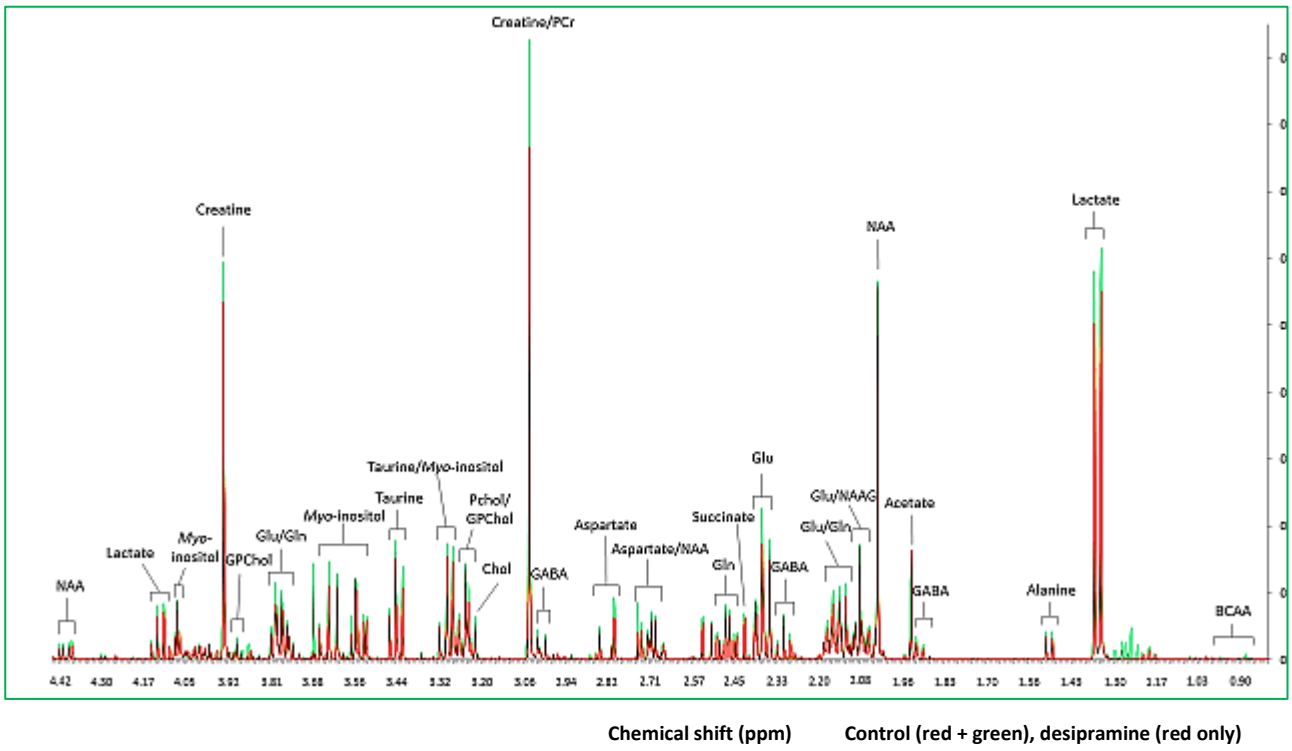

Figure 2.7: ^{1}H NMR spectra of hippocampal extracts obtained from control (red + green) and treated rats (red only) showing different metabolites identified following acute desipramine treatment. Abbreviations: Glu, glutamate; NAAG, N-acetylaspartylglutamate; Gln, glutamine; NAA, N-acetyl aspartate; Chol, choline; Pho ethanol, phosphoryl ethanolamine; Pho creatine, phosphocreatine; P cho, phosphoryl choline; ATP, adenosine triphosphate; Tau, taurine; Aspart, aspartate; Myo-inos, myo-inositol; BCAA, branched chain amino acid.

2.2.3. Sample preparation for NMR spectroscopic analysis:

2.2.3.1. Preparation of brain samples:

The preparation of brain samples for NMR spectroscopic analysis was based on previously published protocols (Adinehzadeh et al., 1999; Lan et al., 2009; Shi et al., 2007). The frozen brain samples were thawed and homogenized in 1.5 ml cold acetonitrile and water (1:1 volume ratio) of HPLC-grade from Fisher Scientific, UK using the Polytron PT3000 at 2600 rpm for 15 seconds. The homogenates were then centrifuged in 2ml plastic centrifuge tubes at 1000 g for 5 minutes at 4^{o}C (Sorvall Legend Micro 17R, Thermo Scientific, UK). This was followed by separation and evaporation of the supernatant to dryness under vacuum for two hours. The sediments of the brain homogenates were then preserved and stored at - 80^{o}C for further lipophilic extraction and analysis (see Chapter Four and Chapter Two, section 2.3). The dried supernatant residue was reconstituted with 550 µl of D_2O containing 0.9 mM trimethylsilylpropanoic acid (TSP) (Sigma Aldrich, UK) and 50 µl of 1M phosphate buffer (138 g NaH_2PO_4-H_2O in 1 litre dH_2O) at pH 7.0 and vortex- mixed for 10 seconds. The samples were then centrifuged at 1000 g for 10 minutes at 4^{o}C. Finally, the supernatants were placed into the NMR tubes (5 mm in diameter) (Norell, UK) for subsequent NMR analysis.

2.2.3.2. Preparation of plasma samples:

The preparation of plasma samples for NMR spectroscopic analysis was based on previously published protocols (Deprez et al., 2002; Shi et al., 2007; Zira et al., 2013). Blood samples collected in heparin tubes (BD, USA) were centrifuged for 10 minutes at 1300 g for complete separation of the plasma from the whole blood. Then 500 µl of separated serum was removed and transferred to the centrifuge tubes with the addition of 55 µl of D_2O (Fisher Scientific, UK). The samples were centrifuged again at 1000 g for 10 minutes at 4°C. Lastly, the supernatants were transferred to 5.0 mm NMR tubes (Norell, UK) for analysis.

2.2.4. NMR spectroscopy and experimental conditions:

^{1}H NMR analysis was conducted with a Bruker Avance AM-400 spectrometer operating at a frequency of 399.94 MHz and a probe temperature of 298 K (25°C). Scanning of the analysed samples was performed with the application of 128 scans, a relaxation delay of 3 seconds and a spectra width of 4800 Hz.

2.2.5. Data collection and pre-processing:

NMR spectra of all groups were interpreted and processed manually via ACD/NMR Processor Academic Edition (Ontario, Canada) software prior to statistical analysis using Metabo Analyst 3.0 software (Xia et al., 2015; Xia and Wishart, 2002, 2016). In addition, all areas including noise peaks, also the spectral regions representing the water signal at 4.60-5.10 ppm of the chemical shift were deleted from all the spectra before eventually starting data analysis.

2.2.6. Statistical analysis of NMR data:

Using the Metabo Analyst software (Xia et al., 2015), the normalised integral data were investigated by means of both Univariate and Multivariate analytical methods, and on the bases of the literature values (Gao et al., 2013; Govindaraju et al., 2000; Liu et al., 2014). Multivariate statistical analysis was performed by both Principal Component Analysis (PCA) and the Partial Least Squares Discriminant Analysis (PLS-DA) to maximize the experimental groups' separation and samples clustering and to identify those metabolites significantly affected by drug treatment using the variable importance in projection (VIP) scores. Univariate statistical analysis was carried out using the Student´s t-test to identify the significant changes of these metabolites within each explored brain region (see Chapter Three). Statistically significant changes were defined as those demonstrating a probability $p < 0.05$. Moreover, fold changes were calculated to assess the results and to determine the direction of metabolite changes in treatment groups in comparison with the relevant control groups.

2.2.6.1. Multivariate analysis methods:

Principal Component Analysis (PCA) is a statistical method used to provide a viewed summary of the clustering pattern for the analysed samples, hence allowing the detection of any abnormal point that represents an outlier value to be excluded from the overall study. Further analysis was conducted by means of Partial Least Squares Discriminant Analysis (PLS-DA) which enables data discrimination and metabolic identification via performing the two-dimensional (2D) (Figure 2.8) and the three-dimensional (3D) scores plot (Figure 2.9. A), thus demonstrating the visualized graphical output for experimental groups separation. Identification of the underlying metabolites responsible for this separation pattern was implemented using the variable importance in projection (VIP) scores (investigating the first 25 selected spectral bins for the included metabolites accountable for groups separation (Figure 2.9, B) (Xia et al., 2015).

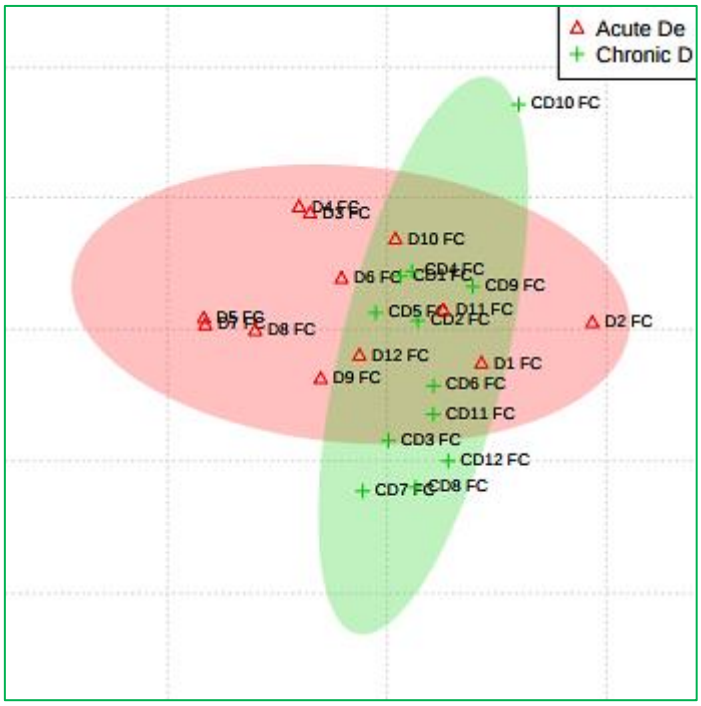

Figure 2.8: PLS-DA 2D Scores Plot of control and treatment groups.

A

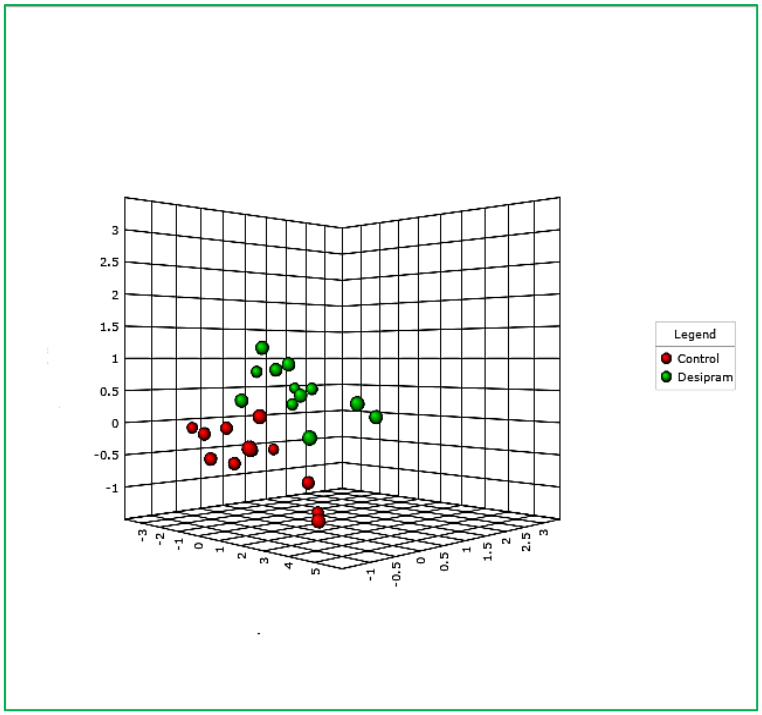

B

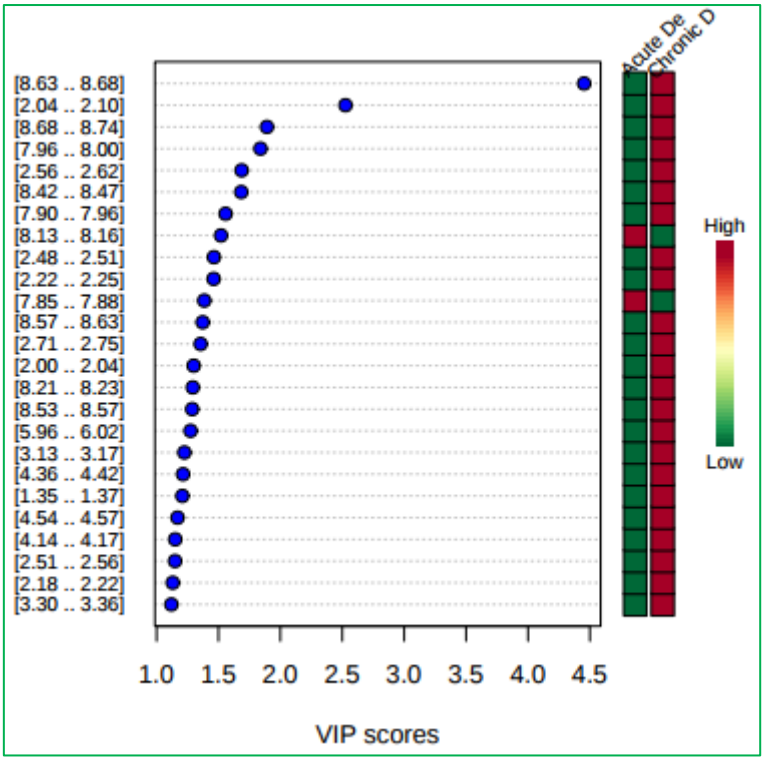

Figure 2.9: PLS-DA (A) 3D Scores Plot of control and treatment groups. (B) Variables of importance in projection (VIP) scores. The coloured boxes on the right indicate the relative concentration of the metabolites identified within the selected spectral bins on the left in each group under study.

2.3. Liquid chromatography–mass spectrometry (LC-MS):

Liquid chromatography–mass spectrometry (LC-MS or HPLC-MS) (Figure 2.10) is a micro analytical tool that combines the separation capability of HPLC with the effective mass analysing specificity of mass spectrometry. It provides a sensitive and highly selective technique that is extensively utilized in a broad range of clinical, biological and chemical applications, allowing the simultaneous detection and quantification of various metabolites and biomolecules ranging from large organic compounds such as proteins and peptides to small pharmaceutical molecules (Kang, 2012; Pitt, 2009). Additionally, LC-MS can successfully identify the structure and accurate molecular weight of the analyte in a sensitive, affordable and less time consuming approach compared to other analytical methods including HPLC-EC (Pitt, 2009).

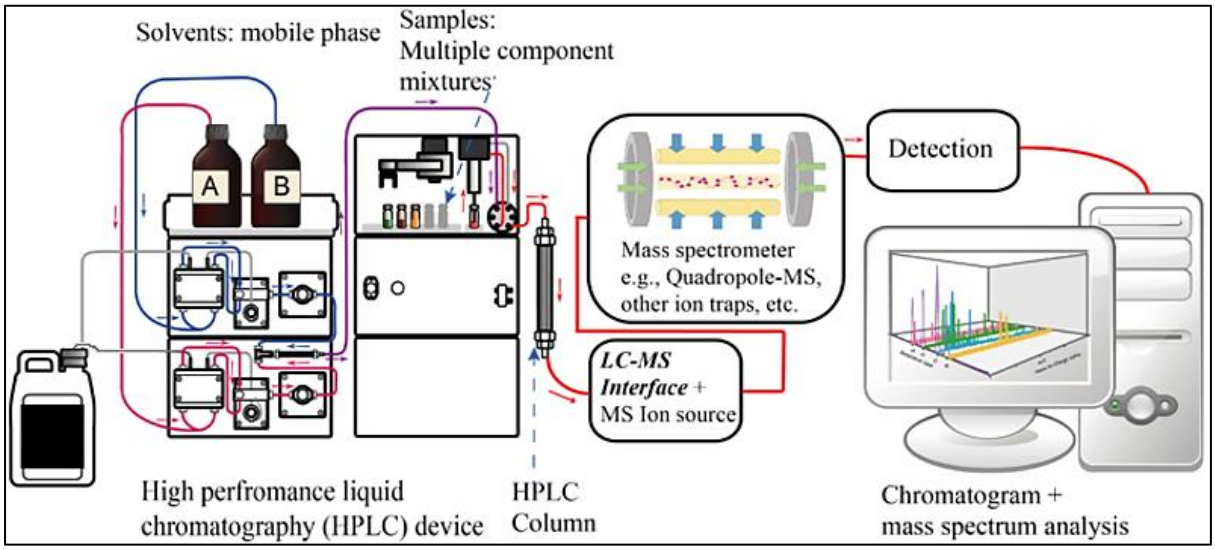

Figure 2.10: A schematic diagram of the basic components of the LC-MS (YassineMrabet, 2017)**.**

2.3.1. Basic principles of LC-MS:

Typically, the LC-MS system offers a coupling of two components, a high resolution HPLC separation and a sensitive mass spectrometric detection system, hence determining the structure of the analyte in a biological sample. The liquid chromatographic extraction was achieved using a reversed phase column for molecular separation (polar mobile phase with non-polar stationary phase). Furthermore, the separation capability of the desired molecule

is mainly dependent upon its affinity to interact with the stationary phase, thus the analyte that expresses a higher lipophilic affinity requires a longer time to be eluted, whereas a molecule with a lower tendency to interact with the stationary phase shows a shorter eluting time (Kang, 2012; Parasuraman et al., 2014). When the separated neutral compound within the current HPLC mobile phase reaches the mass spectrometry detector (Figure 2.10), it undergoes heating and subsequent vaporization. This is followed by ionization via electrospray ionization technique (ESI) which leads to the formation of positively charged particles or ions in a gaseous phase (molecular or protonated ions, M^+). Subsequently, the molecular ions are guided and accelerated through the mass analyzer that represents the heart of the MS-system, promoting the separation and deflection of the ions path by the surrounding electromagnetic field according to their mass to charge (m/z) ratios (light ions show a high deflection capability, whereas heavy ions display a lower bending property (Parasuraman et al., 2014). Then, the emerging ions from the mass analyzer are directed toward the detector, generating an electrical signal which in turn is converted into a digital response that can detected and stored by the computer, thus measuring the relative abundance of the target ion species (counting the number of ions of a particular m/z value) (Kang, 2012).

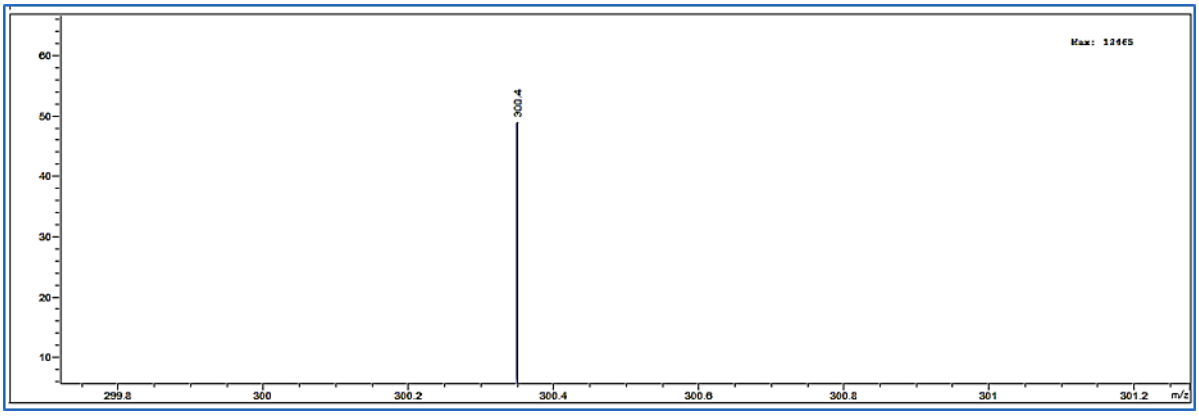

Figure 2.11: LC-MS spectrum showing sphingosine signal in the scan mode (m/z = 300.4) in a rat hippocampal sample

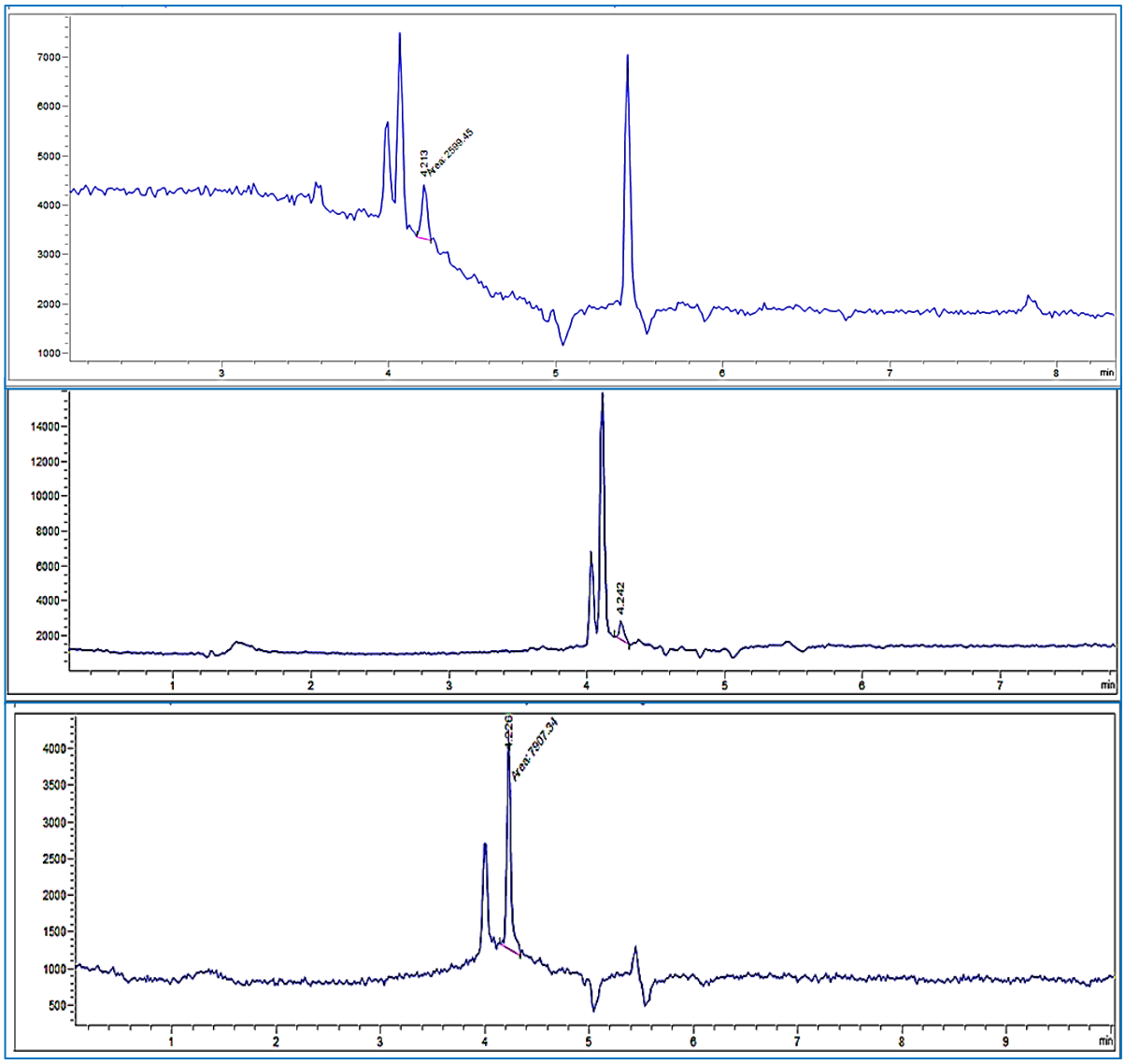

Figure 2.12: LC-MS chromatogram of frontal cortical samples obtained from upper: control and middle: treated rats showing sphingosine peaks at a retention time of 4.213 and 4.242 minutes respectively. Lower: sphingosine standard peak at a concentration of 10 mg/L and a retention time of 4.226 minute.

2.3.2. Sample preparation and lipid extraction:

The achieved drug treatment method was already described in section 2.1.2. The lipid extraction procedure used in the present study was based on the published methods (Bligh and Dyer, 1959; Merrill et al., 2005; Sullards et al., 2011). After completing the aqueous extraction for the initial metabolic study using the NMR technique, the frozen tissue pellets were placed in Pyrex 13 x 100 mm borosilicate tubes with Teflon-lined caps. Borosilicate tubes were used to minimize the lipid loss, because lipids may stick to some types of glass.

The brain samples were then homogenized at 1:3 wet weight per volume in cold phosphate buffered saline (PBS). For the blood samples 100 µl from each blood sample was used for the lipid extraction procedure. Specific volumes (as described below) of chloroform/methanol mixture (1:2 v/v) then chloroform and water were added to the tissue homogenates or the blood samples according to the relative ratios: 1 volume of the sample; 3.75 volume of 1:2 $CHCl_3$:MeOH; 1.25 volume $CHCl_3$; 1.25 volume of dH_2O in a total volume of 7.25 volumes (Bligh and Dyer, 1959). The samples were sonicated for 30 seconds and incubated overnight in sealed Pyrex tubes at 48 °C in a water bath. After cooling the samples, 150 µl of 1 MKOH in methanol (5.6 g of KOH in 100 ml of MeOH) were added. Samples were then sonicated for 30 seconds and incubated for 2 hours at 37°C (Sullards et al., 2011). The tubes were cooled to room temperature and pH adjusted to 7 by the addition of 6 µl of glacial acetic acid followed by the addition of 1.25 volume each of chloroform and water and vortexing, then centrifugation to separate the samples into upper and lower phases. Then, the lower layer was carefully removed with Pasteur pipette leaving behind the protein in the interphase. Re-extraction of the upper layer was achieved by adding 1.25 volume of chloroform followed by vortexing, centrifugation and collection of the lower layer which was then pooled with the first lower phase and evaporated to dryness under a stream of nitrogen (without overheating). Subsequently, the dried organic phase residues were reconstituted in 300 µl of the mobile phase, sonicated for 15 seconds and centrifuged for 10 minutes. Finally, 50 µl of the clear supernatants were transferred into glass inserts placed inside 2 ml glass vials for LC-MS analysis.

2.3.3. LC-MS protocol:

Chromatographic separation of sphingosine, a ceramide metabolite was successfully separated from the other lipid species using either: a) Thermo Scientific BDS HYPERSIL C18 Reversed Phase column (4.6 x 150 mm, 5 µm) or b) ACE UltraCore 5 Super C18 Reversed Phase column (4.6 x 150 mm, 5 µm). The mobile phase(s) A and B used for both columns contained: A) 60% methanol, water, acetic acid (58/41/0.1, v/v/v) and ammonium formate at 5 mM and B) 40% methanol, acetic acid (99/0.1, v/v) and ammonium formate at 5 mM, flow rate was set at 1 ml/min. Using an on-line LC-MS detector, the mobile phase was flowing through the column by the use of an Agilent 1260 Infinity LC-system (Agilent Technologies) and the

optimal MS conditions were the following: nitrogen gas temperature was set at 350°C; the drying gas flow was 11 L/min; the fragmentor voltage was 100 V; with a nebulizer pressure of 53 psig and the gain was 1 A. Electrospray ionization (ESI) was achieved in the positive mode and selective ion monitoring (SIM) mode was set to a fragment ion of m/z 300.4 at a retention time of approximately 5.39 – 5.40 minutes in the samples investigated which was confirmed by the m/z value and the retention time of sphingosine standards (Figures 2.11 and 2.12). Because of the setup of the available LC-MS system, there was a subsequent failure of detecting a molecule with a mass exceeding 500 on the SIM mode (i.e. the C18 ceramide, m/z = 566.7), hence the required ceramide analysis was unachievable. Thus, a separate HPLC-UV system was set up for the analysis of ceramide (see section 2.4). In order to normalise the samples, the Bradford assay was carried out to determine the total protein concentration of individual samples (section 2.3.5).

2.3.4. Calibrations for quantitative analysis of sphingosine:

Standard curves were generated with each analysed group of samples to quantify sphingosine concentration in our samples. Sphingosine standard was dissolved in methanol to produce a stock solution at 200 mg/L and stored at - 80˚C. Immediately before the analysis of individual sample sets, 50 mg/L working stock and subsequent fresh serial dilutions were made up in methanol to provide concentrations ranging from 0.2 – 15 mg/L. Validation of the method was examined by observing the linearity of the standard curves. Further, the standard curves and their linear coefficient of variation (R^2) values for the different brain tissue and plasma groups are outlined below (Tables 2.3, 2.4 and Figures 2.13, 2.14).

Table 2.3: Linear coefficient of variation (R^2) of the analytical method for sphingosine standard curve measurement from brain samples in all treatment groups.

	Group	R^2
1	Acute paroxetine	0.995
2	Acute desipramine	0.9989
3	Chronic paroxetine	0.9951
4	Chronic desipramine	0.9941

Table 2.4: Linear coefficient of variation (R^2) of the analytical method for sphingosine standard curve measurement from plasma samples in all treatment groups.

	Group	R^2
1	Acute paroxetine	0.9956
2	Acute desipramine	0.9956
3	Chronic paroxetine	0.9986
4	Chronic desipramine	0.9956

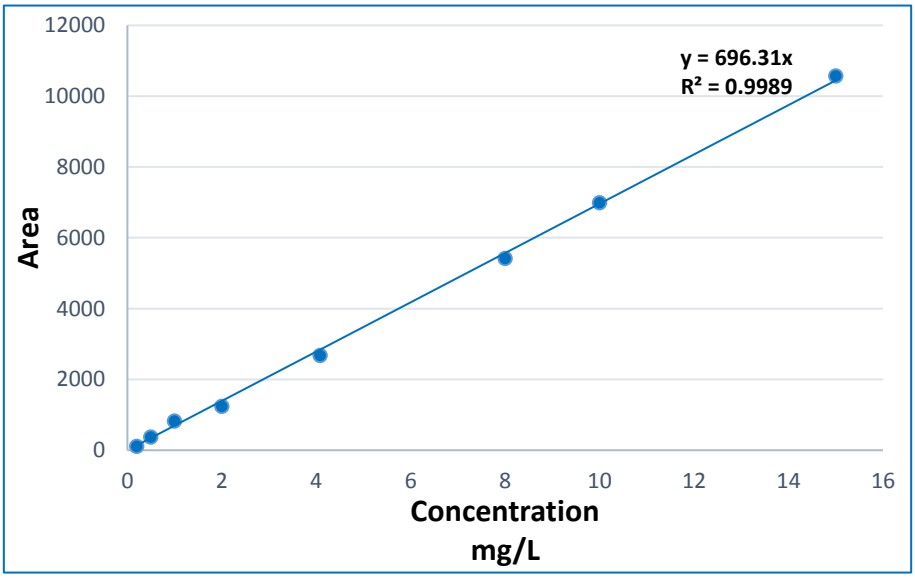

Figure 2.13: A standard (calibration) curve used for sphingosine concentration measurement in rat brain samples.

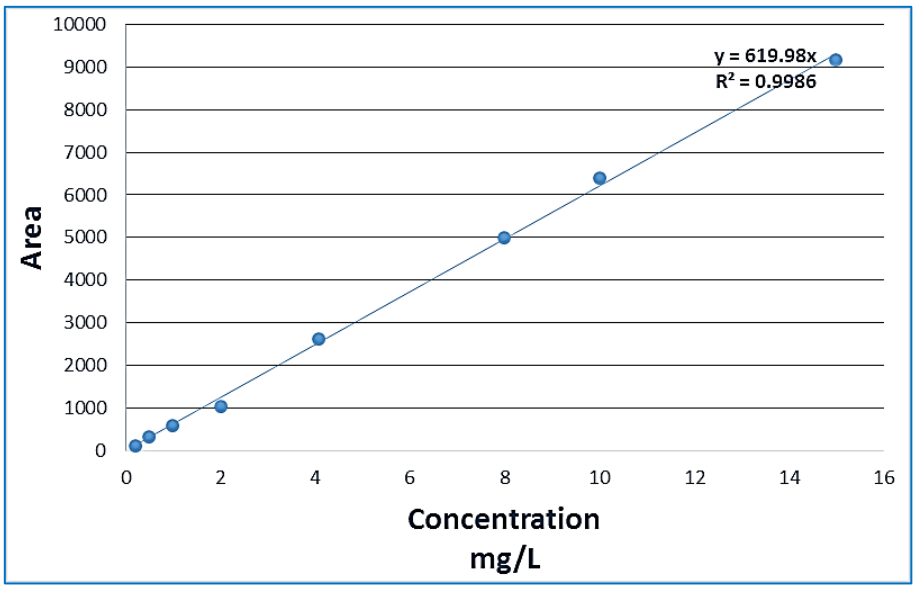

Figure 2.14: A standard (calibration) curve used for sphingosine concentration measurement in rat plasma samples.

2.3.5. Determination of total protein concentration in tissue samples:

Total protein concentration of tissue samples was determined using the Bradford assay. A dilution of 1 mg/ml of bovine serum albumin (BSA) in distilled H_2O (dH_2O) was prepared in order to generate a standard protein curve by preparing duplicates of serial concentrations from the initial BSA stock of 1 mg/ml at intervals of 0.1 mg/ml (Stoscheck, 1990). Tissue homogenates were prepared in dilutions of 1 to 8 (diluting 5 µl of the tissue homogenates in 40 µl of dH_2O) and were loaded in a 96-well plate (polystyrene multi-well plate, Fisher Scientific, UK). Finally, 200 µl of the Bradford reagent (Sigma Aldrich, UK) was added to the wells during gentle mixing. Samples were then incubated for 30 minutes at 37°C (Stoscheck, 1990) allowing them to cool and finally placing the plate in a micro plate reader (Bio Tek, USA) which was set at a wave length of 595 nm to measure the total protein concentration (mg/ml) in the analysed samples.

2.4. High-performance liquid chromatography with ultraviolet detection (HPLC-UV):

High-performance liquid chromatography with UV detection (HPLC-UV) offers a reliable and a sensitive analytical technique that can be applied for the detection and quantification of UV absorbing organic compounds in biological samples. This method was used in the present study (see Chapter Four) for the detection of ceramide in rat brain samples from animals treated with antidepressant drugs or saline. Basically, following a derivatization reaction, brain samples were analysed for the content of ceramide using a reversed phase HPLC system with a UV detector set at a wave length of 230 nm (Figure2.15) (Cremesti and Fischl, 2000; Iwamori et al., 1979; Tepper and Blitterswijk, 2000).

2.4.1. Basic principles of HPLC-UV:

Samples (30 µl) to be analysed were manually injected by a Hamilton glass syringe into a Rheodyne injector equipped with a 50 µl injection loop, then transported within the continuously running stream of the polar mobile phase through the HPLC column (non-polar stationary phase) under high pressure to separate the analytes of the brain samples. This set up allowed the non-polar molecules within the injected sample to move slowly through the

packed column, whereas the polar compounds travel rapidly through the column resulting in a chromatographic separation of the analytes within the investigated samples (Bird, 1989). Subsequently, as the sample exits the column and reaches the UV-detector, a beam of ultraviolet light is directed across a flow cell toward a sensor that measures the absorbance of UV-light passing through the sample within the flow cell at a specific wave length (Figure 2.15), resulting in the amplification of the produced electrical signal that is recorded by the computer, thus generating a series of peaks in the recorded UV-spectrum (Bird, 1989). For details of the HPLC-UV system used in this study see section 2.4.3.

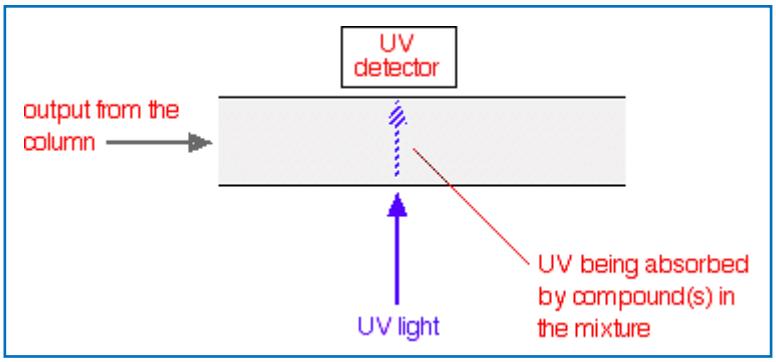

Figure 2.15: Detection principals of HPLC-UV (Esmaeilzadeh et al., 2016)**.**

Since the ceramide molecule lacks a chemical group that absorbs light (i.e. a chromophore such as the benzoyl group) identification of the ceramide by the HPLC with UV-detection was not initially possible. To overcome this problem a derivatization method was developed which was based on a benzoylation reaction, using benzoyl chloride to form the ceramide benzoate, a compound that can be readily detected by UV absorption at a wave length of 230 nm via the HPLC-UV system (Figure 2.16) (Cremesti and Fischl, 2000; Iwamori et al., 1979; Tepper and Blitterswijk, 2000).

2.4.2. Sample preparation and benzoylation of ceramide:

Lipid extraction was conducted via the previously mentioned procedure (see Chapter Two, section 2.3.2) based on the published methods by (Bligh and Dyer, 1959; Sullards et al., 2011). The totally extracted lipids were then benzoylated using 50 µl of benzoyl chloride and 500 µl of pyridine (1:9, v/v) at 70°C for 3 hours. The benzoylation reaction was then stopped by the addition of 500 µl of water and 30 minutes incubation at room temperature. The pyridine content was then evaporated, and the dried lipid residue reconstituted with 1.5 ml of 5%

sodium bicarbonate. After vortexing the samples and centrifugation for 5 minutes at 1000 rpm, which allowed the partitioning of the extract into two distinct layers with the upper layer containing the ceramide content. The ceramide content was then extracted twice with 2 ml of hexane and the clear upper layers were collected and pooled in clean Pyrex 13 x 100 mm borosilicate tubes with Teflon-lined caps. Then, the hexane was washed with 500 µl of 5% sodium bicarbonate and thoroughly dried under a stream of nitrogen. Finally, the benzoylated ceramide was reconstituted with 200 µl of acetonitrile and 35 µl aliquots were injected into the HPLC-UV system for analysis.

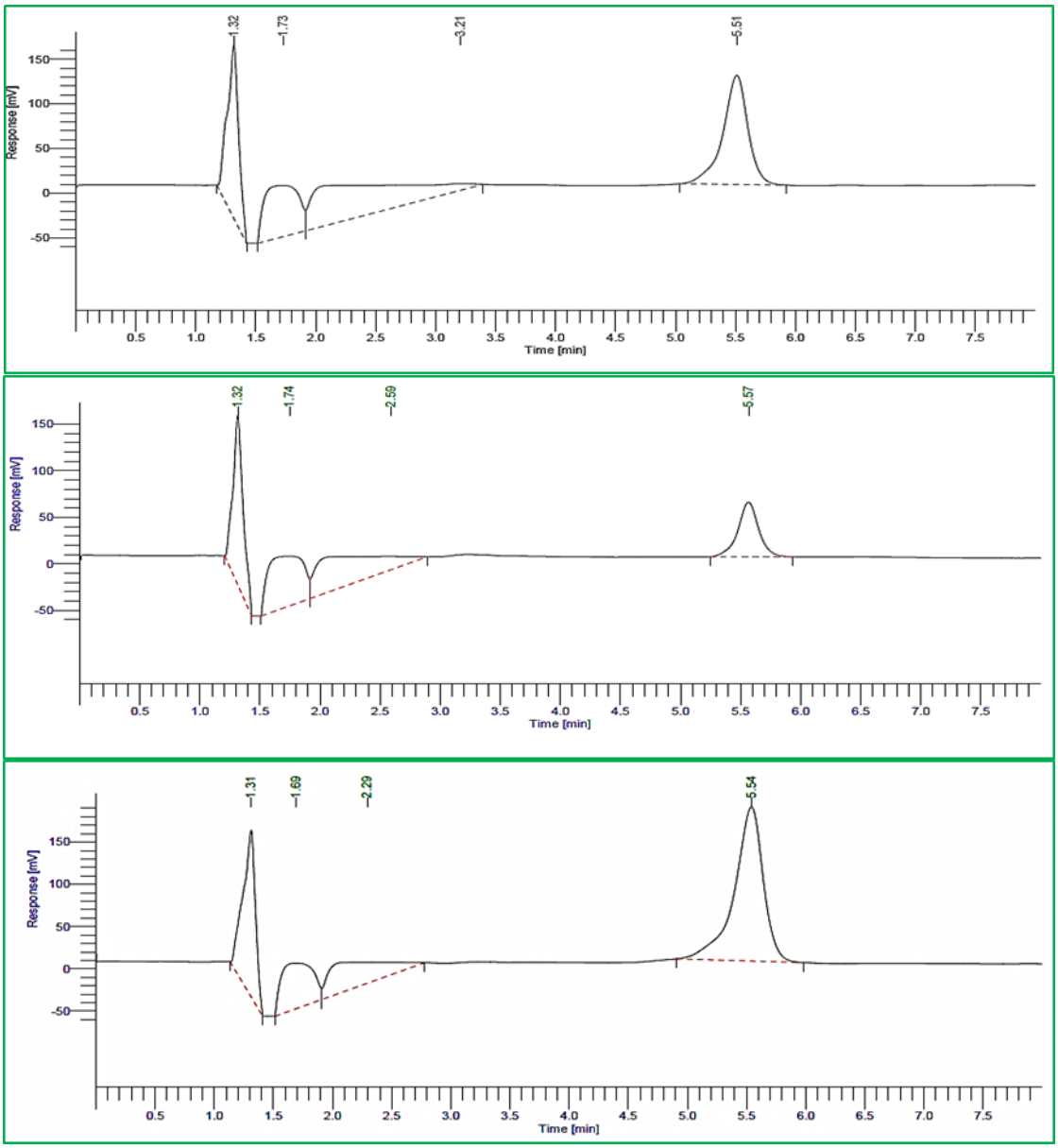

Figure 2.16: UV-HPLC chromatogram of hippocampal samples obtained from upper: control and middle: treated animals following chronic paroxetine administration showing ceramide peaks at a retention time of 5.51 and 5.57 minutes respectively. Lower: ceramide standard peak at a concentration of 40 mg/L and a retention time of 5.54 minutes.

2.4.3. HPLC-UV protocol:

The identification and analysis were performed using a Perkin Elmer Series 200 HPLC system. The benzoylated ceramide was separated on an ACE UltraCore 5 Super C18 Reversed Phase column (4.6 x 150 mm, 5 µm) using 40% methanol and acetic acid (99/1, v/v) as a mobile phase A and 60% water with formic acid (99.9/0.1, v/v) as a mobile phase B at a flow rate of 1 ml/min and an operating pressure of 1500-2000 psig (pounds per square inch, gage). Both mobile phase mixtures were degassed before use by sonication. The benzoylated ceramide content was detected using an UV absorbance detector set at 230 nm. In order to adequately analyse ceramide concentration in individual brain samples, standard curves were generated before the analysis of each experimental group. For this purpose, powdered ceramide was dissolved in methanol to produce a stock solution at a concentration of 1000 mg/L which was stored at - 80˚C. For the generation of standard curves, a 50 mg/L working stock and subsequent fresh serial dilutions were made in methanol to obtain concentrations ranging from 0.5 – 40 mg/L. Validation of the method was assessed by the level of linearity of the standard curves (Figure 2.17). The complete running time for the samples was set at 8 minutes and the ceramide peaks were eluted at a retention time of 5.1 - 5.7 minutes.

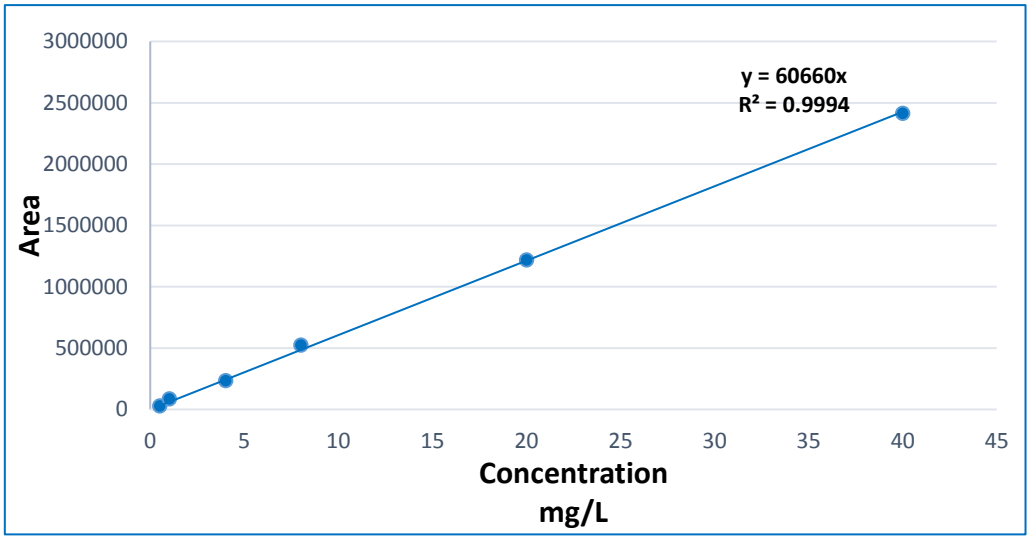

Figure 2.17: A typical standard curve for ceramide measurement.

2.5. High-performance liquid chromatography with electrochemical detection (HPLC-ECD):

HPLC with electrochemical detection (HPLC-ECD) is a sensitive and rapid analytical tool for the simultaneous measurements of monoamine neurotransmitters including catechol and indole amines and their corresponding acidic metabolites in brain tissue samples. It has been used successfully for the measurement of a variety of compounds that display electrochemical responses including oxidation or reduction reactions. The method is further well established for the measurements of electroactive neurotransmitters and drugs in biological samples including: cultured cells, brain tissues, plasma, cerebrospinal fluid and dialysates from brain microdialysis sampling (Yang and Beal, 2011).

2.5.1. Basic principles of HPLC-ECD:

After manual injection of the sample, it will be carried by the polar mobile phase through the HPLC column (Waters Spherisorb reversed phase C18 column, 4.6 x 100 mm and particle size of 3 µm), which is packed with non-polar particles forming a non-polar stationary phase. Basically, the polar molecules within the introduced sample pass rapidly through the column (low attraction) whereas the non-polar compounds cross slowly (high attraction). Subsequently, the sample containing an electrochemically active substance exits the column and it enters the detector and passes through the electrochemical flow cell where a reaction (oxidation or reduction) takes place at the surface of the working electrode when an electrode potential is applied (+ 0.70 V in this study) (Yang and Beal, 2011). Additionally, the electrochemical cell has two other electrodes; the auxillary or the counter electrode (during oxidation, at the surface of the working electrode electrons are produced and subsequently moving towards the auxillary electrode which then helps to transmit an electrical current). The third electrode of the ECD set up encompasses the reference electrode which stabilises the applied potential (i.e. + 0.70 V) (Figure 2.18). Then, the resultant electrical signal from the analyte is recorded by the computer as a corresponding peak, hence generating an ECD chromatogram for the target neurochemicals in the analysed sample (Figure 2.19) (Yang and Beal, 2011).

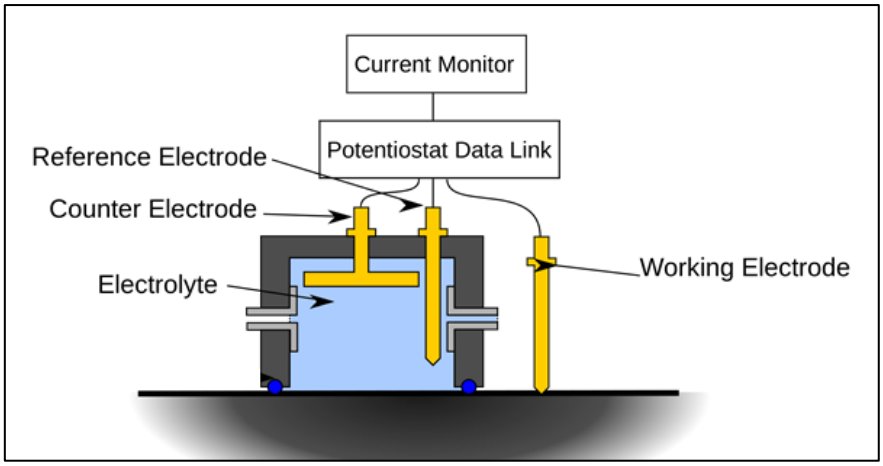

Figure 2.18: A schematic diagram of a flow cell within an HPLC-ECD system (Mason, 2015).

The electrochemical reactions for monoamines are summarized below:

1. 5-HT: In an acidic solution, the electrochemical oxidation of 5-HT results in the formation of 5,7-dihydroxytryptamine (5,7-DHT), then further oxidation occurs leading to another intermediate namely 4,5,7-trihydroxytryptamine and ultimately, the final oxidation product is 5-hydroxytryptamine-4,7-dione (Wrona et al., 1986).
2. Dopamine: Increasing the cell potential results in oxidation of dopamine into dopamine-o-quinone which will be reduced back to dopamine when the potential is decreased (Ss et al., 2015).
3. Noradrenaline: Oxidation of the neurotransmitter noradrenaline results in the production of its ortho-quinone form (noradrenaline-o-quinone) which can be reduced back to NA following a reduction of the applied potential (Fox and Wightman, 2017).

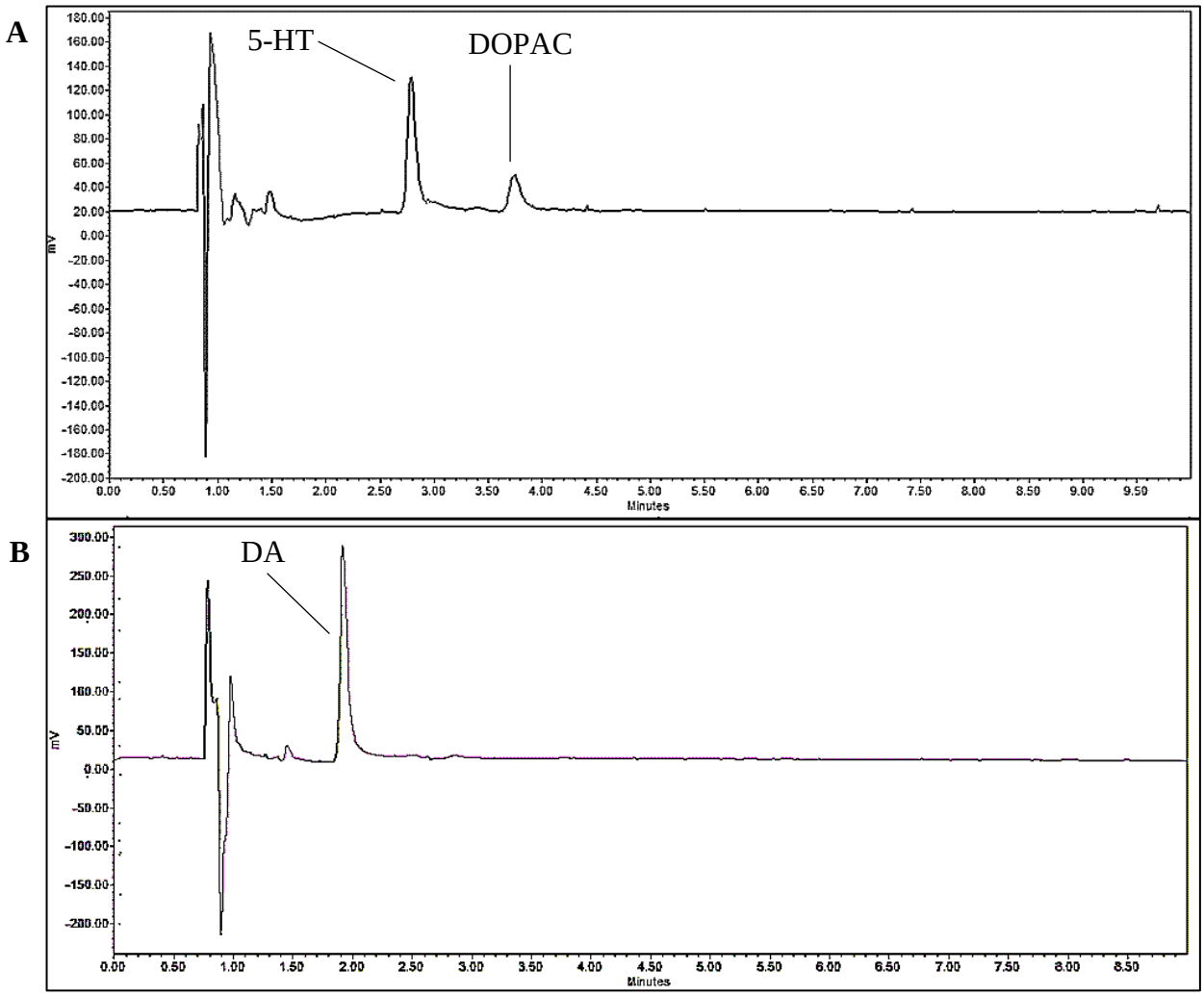

Figure 2.19: (A) HPLC-ECD chromatogram showing 5-HT and 3, 4-dihydroxyphenylacetic acid (DOPAC) standard peaks at a concentration of 20 ng/ml and a retention time of 2.78 and 3.50 minutes respectively. (B) HPLC-ECD chromatogram showing dopamine (DA) standard peak at a concentration of 50 ng/ml and a retention time of 1.912 minute.

2.5.2. Carmofur treatment:

A detailed description of carmofur administration is fully described in Chapter Six, section 6.2.1.1, whereas the brain dissection and sample collection are described in detail in Chapter Two, sections 2.1.2 and 2.1.3.

2.5.3. Sample preparation:

Total tissue extraction method was based on the previously described procedure by (Colado et al., 1997; Yang and Beal, 2011; Zhou et al., 2009). Removal of proteins (e.g. removal of enzymes which breaks down the monoamines) from the frozen brain samples was obtained

by homogenization in cold 0.2 M perchloric acid (PCA, 1:3 weight per volume). The Eppendorf tubes were then capped and vortexed immediately after adding the PCA to prevent gelling of the proteins in the samples. This was followed by the disruption of the brain tissue using the Polytron PT3000 for 20 seconds at 1000 rpm. Subsequently, the samples were centrifuged for 5 minutes at 10 000 g, 4°C and the clear supernatants were transferred into clean centrifuge tubes. Finally, the collected supernatants were utilized for the measurement of 5-HT, DA, NA, 5-HIAA and DOPAC levels using the highly sensitive HPLC-ECD system, whereas the sediments of the tissue homogenate were preserved at - 80°C for further lipophilic extraction and ceramide analysis by the UV-HPLC technique.

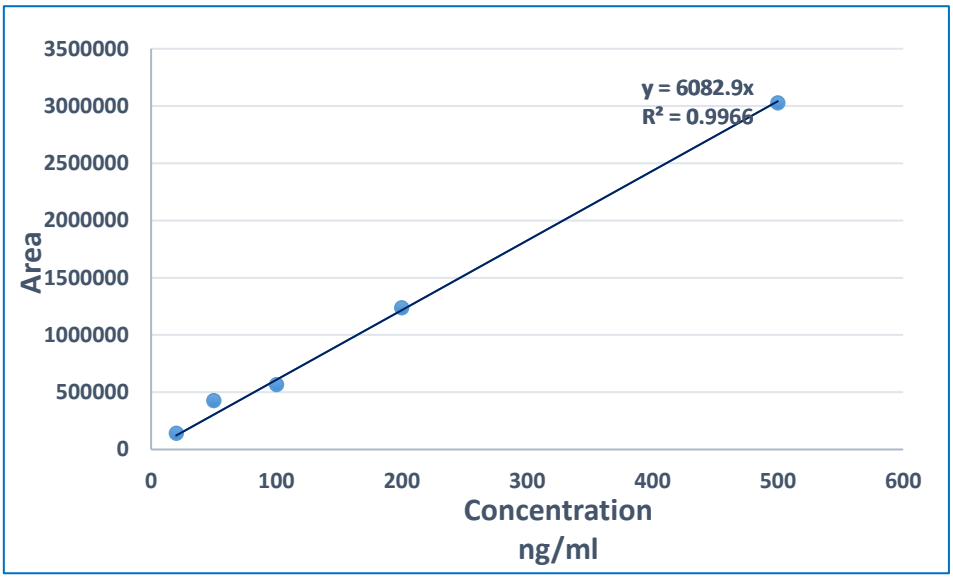

Figure 2.20: A typical standard curve used for 5-HT measurement in brain samples.

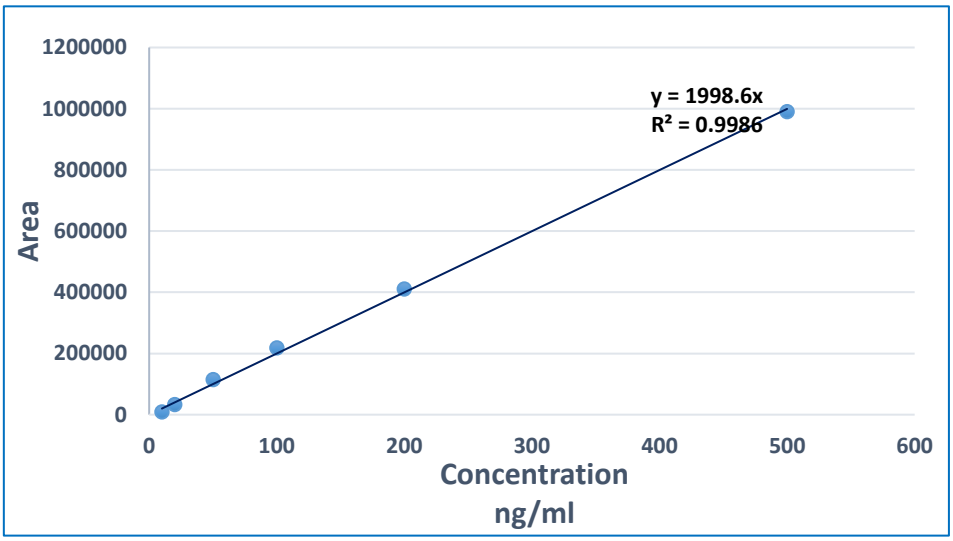

Figure 2.21: A typical standard curve for DOPAC measurement in brain samples.

A

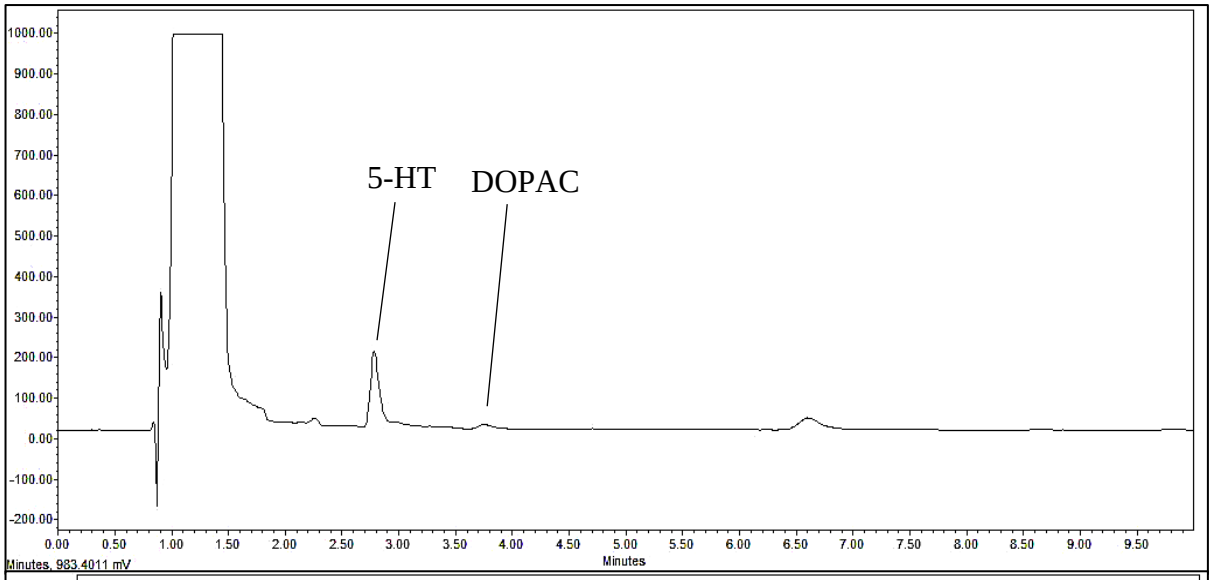

B

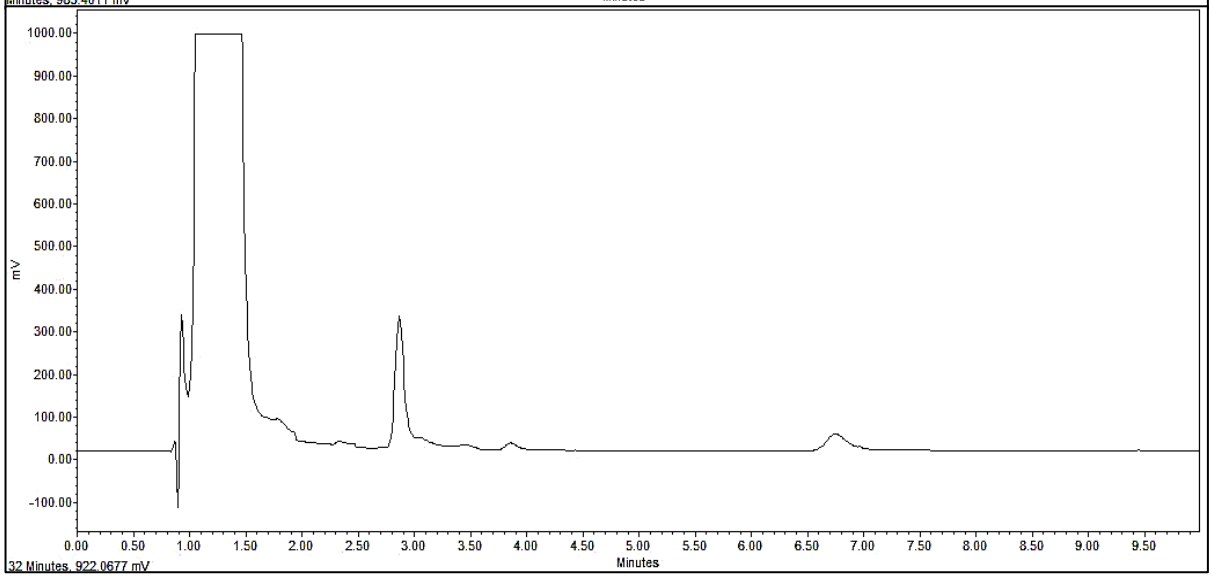

Figure 2.22: HPLC-ECD chromatogram of frontal cortical samples obtained (A) from a control animal and (B) from a carmofur treated animal showing 5-HT peak at a retention time of 2.77 and 2.82 minutes and DOPAC peak at a retention time of 3.50 and 3.61 minutes respectively.

2.5.4. HPLC-ECD protocol:

2.5.4.1. Mobile phase:

The monoamine neurotransmitters and their metabolites were separated using the following mobile phase (Hajós-Korcsok et al., 2000; Pei et al., 1995; Zetterström et al., 1988):

5-HT mobile phase:

- 600 ml of 1M NaH_2PO_4. $2H_2O$ (adjust pH at 3.0 by phosphoric acid)
- 14.9 ml of 10% EDTA
- 4550 ml H2O
- 0.022 g sodium octanyl sulphonate
- 590 ml of methanol
- pH = 3.8 (adjust using sodium hydroxide)

Dopamine mobile phase:

- 600 ml of 1M NaH_2PO_4. $2H_2O$ (adjust pH at 3.0 by phosphoric acid)
- 14.9 ml of 10% EDTA
- 3400 ml H_2O
- 0.322 g sodium octanyl sulphonate
- 710 ml of methanol
- pH = 3.8 (adjust using sodium hydroxide)

Noradrenaline mobile phase:

- 500 ml of 1M NaH_2PO_4. $2H_2O$ (adjust pH at 3.0 by phosphoric acid)
- 14.9 ml of 10% EDTA
- 3900 ml H_2O
- 2.16 g sodium octanyl sulphonate
- 600 ml of methanol
- pH = 4.6 (adjust using sodium hydroxide)

All of the above described mobile phases were degassed for 30 minutes and filtered through Whatman filter discs (Whatman, UK) prior to their usage on the HPLC-ECD system.

2.5.4.2. Sample analysis using HPLC-ECD:

Following the manual injection of 50 µl aliquots into a Rheodyne injector (model 7725i) fitted with a 50 µl loop, monoamines and their metabolites were separated on a C18 Spherisorb column (4.6 x 100 mm and particle size of 3 µm; Waters Ltd, UK) which was connected to a pre-column equipped with a filter of pore size 0.5 µm (Waters, Ltd, UK). Flow rate was set at 1.2 ml/min with a Waters 1515 Isocratic HPLC pump. Content of the samples were finally analysed using the on-line Waters 2465 Electrochemical Detector (Waters Ltd, UK) equipped with the ECD flow cell (Waters model 282065). The optimal operating parameters were the following: the operating pressure, 2000 psig; column temperature, 30°C; injection volume, 50 µl and the applied detection potential was set at + 0.70 V. Preparation of fresh serial dilutions of the individual monoamine and metabolite standards were done daily in 0.2 M PCA to obtain concentrations ranging from 10-500 ng/ml and were then loaded on the system to identify the representative peaks, their retention times and the area under each peak following a pronounced chromatographic separation. Then, a standard calibration curve was plotted with each investigated group to calculate the concentration of the corresponding neurotransmitters and their metabolites in each analysed brain sample (Figures 2.20 and 2.21). Validation of the method was assessed by observing the linearity of the standard curves. The complete assay was achieved within 10 minutes and 5-HT, DA, NA, 5-HIAA and DOPAC peaks were approximately eluted at the following retention times: 2.7, 1.9, 5.2, 4.7 and 3.5 minutes respectively using Breeze 2 software (Waters Ltd, UK) (Figure 2.22).

2.6. Real-time quantitative polymerase chain reaction assay (RT-qPCR):

Quantitative polymerase chain reaction (qPCR) is a valuable, highly sensitive and widely used molecular technique that facilitates studying and quantification of the gene expression level of specific genes through the generation of millions or billions of copies of a selected DNA sequence in a broad range of biological samples. It has become an essential tool that is used in various applications and research fields including pathology, biology, forensic sciences, pharmacology and cancer studies. This method allows a selective amplification (production of multiple copies or amplicons) of a particular DNA fragment which is complementary to the sequence of interest (Giri, 2015; Pestana et al., 2009).

2.6.1. Basic principles of RT-qPCR:

2.6.1.1. Main components of PCR reaction:

- The DNA template: a double stranded DNA (complementary DNA, cDNA) that is extracted from the sample.
- The primers: short segments or pieces of single stranded DNA (20-30 base pairs in length) that are identical to certain parts of the target DNA sequence. The primers serve as a starting point for adding nucleotides that are required for constructing the new DNA strand.
- Deoxynucleotides: DNA bases which are the substrates of the DNA including four bases: adenine (A), thymine (T), cytosine (C) and guanine (G) (Giri, 2015; Pestana et al., 2009).
- DNA polymerase: a thermally stable enzyme that does not denature under high temperature (98°) and it exerts an essential role in adding the deoxynucleotide bases to the initial DNA template, thereby synthesizing a new DNA strand that is complementary to the DNA template strand (Giri, 2015).
- Potassium or magnesium Buffers: These are required for providing the optimal reaction conditions (Staněk, 2013).

2.6.1.2. Main steps of PCR:

- **Denaturation (step one):**

The reaction mixture containing the DNA template is heated to a high temperature approximately 94°C for 20-30 seconds which facilitates breaking the weak hydrogen bonds that hold the double DNA strands together. Thus, splitting (denaturing) the double strands completely into two single stranded DNA (Giri, 2015; Pestana et al., 2009).

- **Annealing (step two):**

Lowering the temperature of the PCR reaction to a particular temperature (a primer-specific temperature) usually between 50-60°C for 20-40 seconds and therefore, enabling the primers to be bound (annealed) to a specific site (the complementary sequence) on the single DNA template strand (Staněk, 2013).

- **Extension or elongation (step three):**

Finally, raising the reaction temperature to 72-80°C for 2 minutes (usually 72°C) which is the optimal temperature that permits the DNA polymerase enzyme to start adding the deoxynucleotides to the attached primer at a rate of 1000 base pairs per minute. Thereby, extending the primer using the target DNA sequence, thus constructing a new complementary copy of a double stranded DNA molecule containing one old strand attached to another new one (Giri, 2015). Within one PCR cycle, a single molecule of double stranded DNA template will be amplified into two double stranded DNA pieces (two copies) which undergo further amplification in the following cycles (Giri, 2015). Eventually, with using the PCR analysis enough copies of the gene of interest are obtained after repeating the PCR steps for 30-40 cycles (usually 35 cycles).

2.6.1.3. Real time quantitative PCR assay (RT-qPCR) (melting curve analysis):

Quantification of the target gene is accomplished by real time quantitative PCR assay (RT-qPCR) via melting curve assessment (measuring the fluorescence intensity against the temperature changes). In the qPCR, a fluorescent double stranded DNA binding dye is used to bind to a double stranded DNA molecule, therefore generating a single fluorescent peak by increasing the temperature (Figure 2.23. A). Using the programmed thermal cycler to run the qPCR after completing the amplification cycles, the temperature sets above the primer specific temperature (approximately 65°C). As the dye is incorporated with the double stranded DNA, the level of the measured fluorescence is significantly increased producing a fluorescent signal. Subsequently, the temperature is raised and the double DNA strands are separated or denatured forming two single stranded DNA, the dye becomes dissociated resulting in a decrease in the detected fluorescence (Figure2.23) (Pryor and Wittwer, 2006).

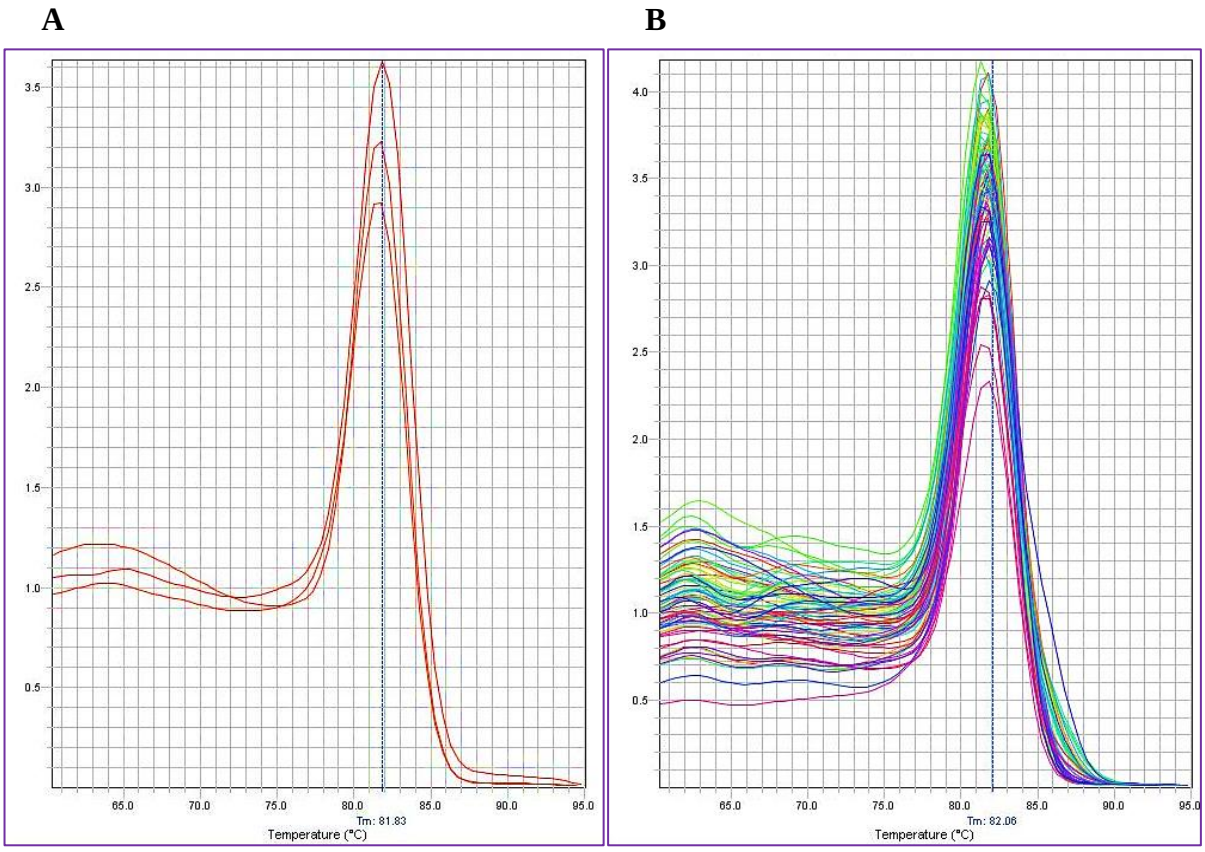

Figure 2.23: (A) Fluorescent signals of a triplicate. (B) Melting curve from qPCR of the ASAH1 gene. The figure shows the relation between the level of the detected fluorescence and the temperature, displaying a single amplicon peak, thus verifying one PCR product.

2.6.2. Drug treatment:

Details of the antidepressant drug treatment, brain regions dissection and samples collection were fully described in Chapter Five, section 5.2.1 as well as in Chapter Two, sections 2.1.2. and 2.1.3.

2.6.3. Total RNA extraction:

Total RNA was extracted from all collected brain samples using RNeasy Mini Kit following the previously published method by Logmann (Logmann et al., 1987). Samples were treated with 10 µl of β-mercaptoethanol and 1 ml of Buffer RLT (lysis buffer). Twenty milligrams of each frozen sample were separated and homogenized in 350 µl of lysis buffer followed by careful removal of the supernatant. Then, 350 µl of 70% ethanol was added to the lysate and mixed by pipetting without centrifugation. The whole sample (700 µl) was transferred into an RNeasy Mini Spin column placed in a 2 ml collection tube and centrifuged for 1 minute at 10

000 g. After changing the collection tube, 700 µl of Buffer RW1 (washing buffer) was added to the sample in a spin column and centrifuged for 1 minute at 10 000 g and the flow through was then discarded. This was followed by the addition of 500 µl of buffer RPE (washing buffer) to the sample, centrifuged for 1 minute at 10 000 g and the flow through was discarded. Then, 500 µl of the same buffer solution were added followed by centrifugation for 2 minutes at 10 000 g. The collection tubes were changed, and further centrifugation was carried out for 1 minute at 10 000 g to dry the membrane. Under strict sterilization, new collection tubes were placed under the RNeasy spin columns and 30 µl of RNase-free water were added directly to the spin columns containing the RNA samples and centrifuged for 2 minutes at 10 000 g. Repeated centrifugation for another 2 minutes was performed to obtain approximately 30 µg of highly refined RNA samples which were transferred into new tubes and stored in - 80°C for subsequent analysis.

2.6.4. Turbo DNA digestion:

DNA digestion in all the samples was performed following the manufacturer´s instructions to eliminate any DNA contamination by DNAse treatment using the Turbo DNAse-AM free kit. All RNA samples were treated with 3 µl of Turbo DNAse buffer and 1 µl of Turbo DNAse. Then, samples were incubated for 30 minutes at 37°C on a hot block and 3 µl of DNAse inactivation reagent was added to each sample followed by incubation at room temperature for 5 minutes with intermittent mixing. Samples were centrifuged for 1.5 minutes at 10 000 g and the supernatants were transferred into new tubes. Finally, RNA concentration in all the samples was evaluated and recorded using a Nanodrop spectrophotometer (Thermo Scientific Nanodrop Lite spectrophotometer, UK).

2.6.5. Complementary DNA (cDNA) synthesis:

The cDNA was synthesized in all samples using an iScript cDNA Synthesis Kit (Bio-rad, UK) according to the manufacturer's guidelines. In brief, 1 µg of clean, total RNA was used as a template to generate the cDNA in a 20 µl reaction mixture in each sample (4 µl of 5x iScript Reaction Mix, 1 µl of iScript Reverse Transcriptase, 15 µl of RNA and Nuclease-free water) and all the preparations were done on ice. Then, samples were incubated in a programmable thermal cycler (PTC-200 Peltier Thermal Cycler) and the conditions for thermocycling

reactions were priming for 5 minutes at 25°C, reverse transcription for 20 minutes at 46°C and reverse transcription inactivation for 1 minute at 95°C. Finally, the prepared cDNA samples were maintained in - 20°C for subsequent PCR amplification.

2.6.6. PCR Amplification and gel electrophoresis:

In order to assess the integrity of the RNA samples (absence of DNA contamination), the purity of the synthesized cDNA samples as well as testing the utilised primers condition, PCR amplification was subsequently performed using primer pairs supplied by IDT (Integrated DNA Technologies, Belgium). The genes of interest which were investigated in this study included the ASAH1 gene (encodes acid ceramidase enzyme), the SMPD1 gene (encodes acid sphingomyelinase enzyme) and two reference genes namely: beta-actin (β-actin) and glyceraldehyde 3-phosphate dehydrogenase (GAPDH) both of which were selected based on previously published studies (Bonefeld et al., 2008; Swijsen et al., 2012). The selected primers were designed via Primer3Plus (http://primer3plus.com/cgi-bin/dev/primer3plus.cgi) using the following reaction conditions: annealing temperature of 57-63°C with an optimal temperature of 60°C, guanine-cytosine content (GC content) of 20-80 % (an ideal GC content of 50 %), a primer size of 18-27 base pairs (bp) with an optimal primer length of 20 bp and a maximal product size of 200 bp. The amplicon secondary structures were evaluated using the Mfold Web Server (http://unafold.rna.albany.edu/?q=mfold) without any interfering secondary structures at both binding sites of each primer. The primer sequences for the selected amplicons and their optimized parameters are shown in Table 2.5.

Table 2.5: The utilized primers sequence and the relevant optimized conditions for each.

	Primer name	Primer sequence (5'--->3')	Product size (bp)	Annealing temperature (°C)	GC content
1	ASAH1	F: ACCGTGGACAGAAGATTGCA	151	55	50
		R: AGTTCTCAACACAGGTGCCT			50
2	SMPD1	F: CTCTGGAAACCCTGGCTTGAT	162	59	52.4
		R: TGCTGGGTCTGTCTTGTTCAG			52.4
3	GAPDH	F: TCACCACCATGGAGAAGGC	168	53	45
		R: GCTAAGCAGTTGGTGGTGCA			55
4	β-actin	F: TGTCACCAACTGGGACGATA	165	55	50
		R: GGGGTGTTGAAGGTCTCAAA			50

A reaction mixture (My Taq Red Master Mix) (Bioline, UK) contained 5 µl of My Taq Red Mix reagent, 0.2 µl of the forward primer, 0.2 µl of the reverse primer, 1 µl of each cDNA (or 1 µl of RNA or 1 µl of nuclease free water) and 4.1 µl of RNase-free water was made up to a total volume of 10.5 µl. The reaction mixtures were subjected to thermocycling conditions for 35 cycles which included an initial denaturation at a temperature of 95°C for 15 seconds, followed by annealing for 15 seconds at the primer specific temperature (see Table 2.5) and a final extension (elongation) for 10 seconds at 72°C. The PCR amplifications were performed using Lab tech. com Thermal Cycler (G-Storm). Consequently, 5 µl of the PCR products (the analysed samples, RNA, the negative control or the blank and the DNA ladder) were loaded and separated on a 2 % agarose gel after running the set for 30 minutes at 90 V (Figure 2.24) and then were visualised using a Gel Doc EZ Imager (Bio-Rad, UK).

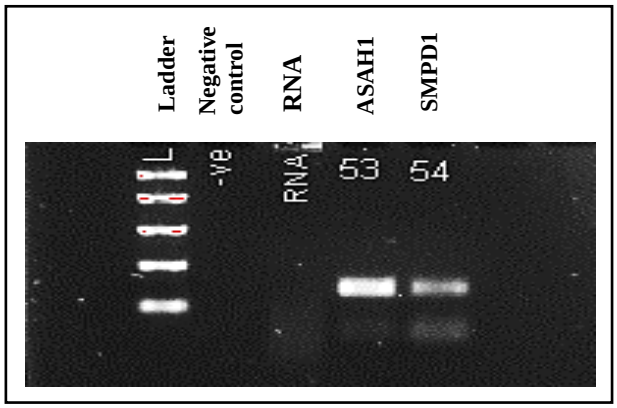

Figure 2.24: PCR products visualisation by agarose gel electrophoresis. The first lane represents the ladder or the standard marker, then the PCR products of the negative control and the RNA (no visible bands) followed by the cDNA of the target genes: ASAH1 and SMPD1 genes.

2.6.7. Real-time quantitative PCR (RT-qPCR):

The real-time qPCR analysis was performed using the Real-time PCR Machine (Applied Bio System, UK) using Step One Plus Real-Time PCR system. Each reaction mixture contained 5 µl of SensiFAST reagent (SensiFAST SYBR HI-ROX), 0.2 µl of the forward primer, 0.2 µl of the reverse primer, 0.5 µl of the cDNA of each sample and 4.1 µl of RNase-free water to a total volume of 10 µl and triplicates were used for each sample. Real-time PCR amplification conditions were the following: Holding stage (95°C for 2 minutes), cycling stage (40 cycles at 95°C for 10 seconds and 30 seconds at each primer specific temperature) and melt curve stage (95°C for 15 seconds, 60°C for 1 minute and 95°C for 15 seconds). Analysis of the generated melting curve was accomplished following the amplification of each primer and standard curves were plotted using 10-fold serial dilutions of the PCR products of the utilized primer pairs (Figure 2.25). Levels of the gene expression in all regional brain samples were evaluated relative to the reference genes: GAPDH and β-actin (normalizing factors). In addition, quantification of the target genes was performed by the qBASE+ relative quantification software (Qbase, UK) via $2^{-\Delta\Delta CT}$ for data processing and by using the Ct values generated from each RT-qPCR experiment, then results were entered into Graph Pad Prism and one-way ANOVA with Bonferroni t-test for groups comparison.

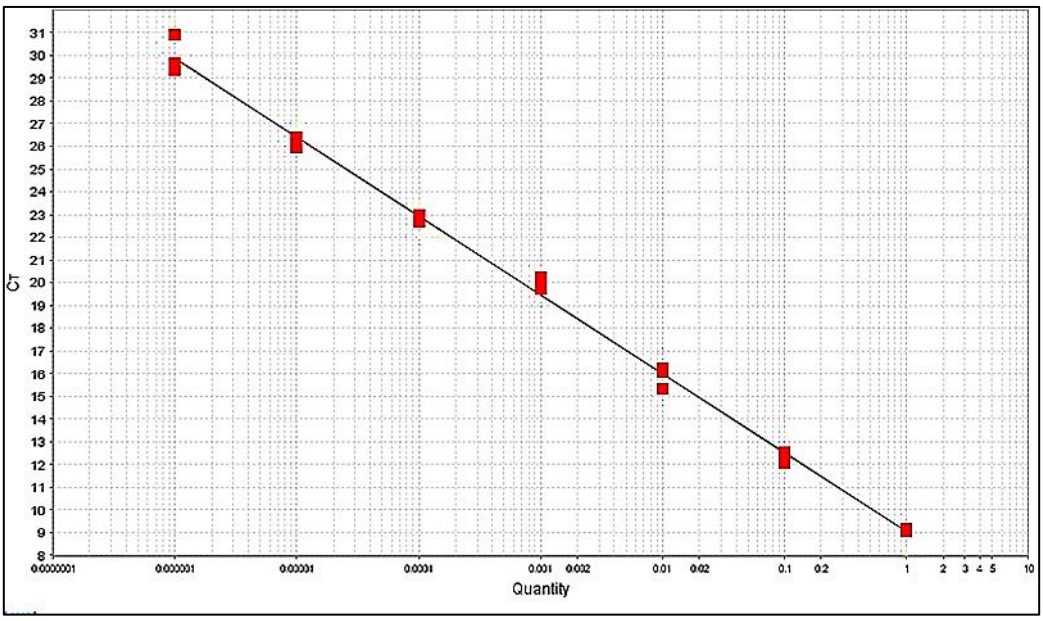

Figure 2.25: A standard curve for the β-actin gene. The CT-value represents the number of cycles required for the generated fluorescent signal to cross the background fluorescence.

CHAPTER 3

Analysis of rat brain metabolic profile following acute and chronic antidepressant drugs by ^{1}H NMR

3.1. Introduction:

Depression is a common and serious psychiatric condition that requires an effective medical treatment. Despite the extensive research efforts into the mechanism of action by antidepressant drugs, which indeed have resulted in some progress (Bai et al., 2015; Leonard, 2000; Taylor et al., 2005), to the best of our knowledge the molecular mechanism underlying the drugs therapeutic actions still remain to be fully understood. Recently, NMR-based metabonomic studies as well as structural imaging studies utilizing MRI technique (Brigitta, 2002; Lan et al., 2009; Strakowski et al., 2005; Tsang et al., 2005) have been applied to investigate brain metabolic alterations following drug treatment of depression. However, further biochemical information related to the efficacy of antidepressant drugs is still essential to elucidate the drug-induced metabolic consequences of both short and long-term administration of the current antidepressant medications. ^{1}H NMR spectroscopy has been increasingly utilized to explore such metabolic profiling in tissues as well as biological fluids which allows a higher sensitivity and a greater accuracy of biochemical detection and quantification compared to the magnetic resonance spectroscopy technique (MRS) (Tsang et al., 2005). Additionally, the NMR methodology has been widely used in many studies to investigate the biochemical changes of psychiatric diseases and their drug treatments particularly bipolar disorders (Lan et al., 2009) and schizophrenia (Holmes et al., 2006). In this respect, further brain research performed on schizophrenic patients compared to controls utilizing the non-invasive MRS technique identified metabolic reduction in the level of N-acetyl aspartate (NAA, a biomarker of neuronal integrity) (Ohrmann et al., 2007) and elevated lactate level (Halim et al., 2008). Furthermore, another biochemical study conducted on depressed patients in comparison with normal controls utilizing the proton MRS approach identified changes in various metabolites including glutamate, glutamine and γ-amino butyric acid (GABA) within specific brain regions: the prefrontal cortex, amygdala and hippocampus (Yüksel and Öngür, 2010). In addition, a metabolic screening analysis using NMR spectroscopy was conducted on postmortem brain samples from patients diagnosed with bipolar disorder identified numerous biomolecules within the prefrontal cortex that might be related to the pathogenesis of the disease including metabolites and amino acids such as glutamate, GABA and myo-inositol as well as creatine (Lan et al., 2009; Smith et al., 2014; Strakowski et al.,

2005). To date, however, these studies have not revealed any consistent pattern of brain metabolic changes related to depressive illness or antidepressant drug administration.

3.1.1. Aim:

In this study, ^{1}HNMR spectroscopy was employed to investigate the postulated differential effects of both acute and chronic administration of two antidepressant drugs (paroxetine and desipramine) in rats on aqueous metabolite levels in plasma and brain regions implicated in the pathogenesis of depression including the prefrontal cortex, hippocampus and the striatum. In particular, the study examined drug and region-specific alterations in a wide range of brain metabolites. Moreover, the study specifically aimed to evaluate the possibility of differential changes following acute and chronic treatment which may give further insight into the therapeutic mode of action of the currently available antidepressant agents.

3.2. Material and methods:

3.2.1. Drug administration and brain dissection:

A full description of animal housing conditions, drug treatments, brain dissection and sample collection is described in Chapter Two, section 2.1. To examine the effects of acute drug administration, 48 male Sprague-Dawley rats were separated into two sets and each set into two groups comprising 12 animals per group and were housed in groups of 4 animals per cage. Within the first set, the first group (control) received a single i.p. injection of saline (1 ml/kg) and the second group (paroxetine) received a single i.p. injection of paroxetine (5 mg/kg). The second set of experiments also consisted of a drug group (n = 12) and a saline group. The drug group received desipramine (10 mg/kg, i.p). All rats were sacrificed one hour after injection via schedule one procedure (Home Office, Animal act, 1986) and blood samples were collected immediately after lesion of the jugular vein. The whole brain was dissected out rapidly on ice into three specific brain regions in correspondence with the Rat Brain Atlas (Paxinos and Watson, 2006): the prefrontal cortex, hippocampus and striatal region. The brain samples were rapidly frozen using isopentane on dry ice, weighed and stored at - 80°C until subsequent preparation for NMR analysis

To examine the effects of chronic drug administration, forty-eight male Sprague-Dawley rats were divided into control and drug treated groups (12 rats per group). The first group (control group) received a single i.p. injection of saline (1 ml/kg/day) for 15 days. The desipramine group received a single i.p. injection of desipramine (10 mg/kg/day) for 15 days. The paroxetine group received a single i.p injection of paroxetine (5 mg/kg/day) for the same period. Then, at the end of the treatment, rats were sacrificed one hour after the last injection. Brains were dissected out, weighed and plasma samples were collected. All samples were stored at - 80°C until needed for ^{1}HNMR analysis.

3.2.2. NMR spectroscopy and sample preparation:

A detailed description of ^{1}H NMR analysis and procedures for sample preparation was shown in Chapter Two, sections 2.1 and 2.2 respectively.

3.3. Data collection and statistical analysis:

NMR spectra of all groups were processed using Metabo Analsyt 3.0 software (Xia et al., 2015). Multivariate statistical analysis was performed by partial least squares discriminant analysis (PLS-DA) to maximize the experimental groups' separation (determining whether the control and treatment groups are clearly different). In addition, it allows the identification of the variables that contribute to this actual groups separation (specifying the metabolites or biomarkers significantly affected by drug treatment) using the variable importance in projection (VIP) scores. Univariate statistical analysis was carried out using the Student t- test to identify significant changes of these metabolites within each brain region. Statistically significant changes were defined as those demonstrating a probability $p < 0.05$. In addition, fold changes were calculated to assess the results and to determine the direction of metabolite changes in treatment groups in comparison with the relevant control groups.

3.4. Results:

3.4.1. ^{1}H NMR spectra of rat brain extract:

The ^{1}H NMR spectra acquired from analysing the aqueous brain extracts of drug and saline treated rats within a spectral region of 0.8-4.5 ppm displayed resonances of a large number of metabolites within the investigated brain regions, as shown in Figures 3.1 and 3.2.

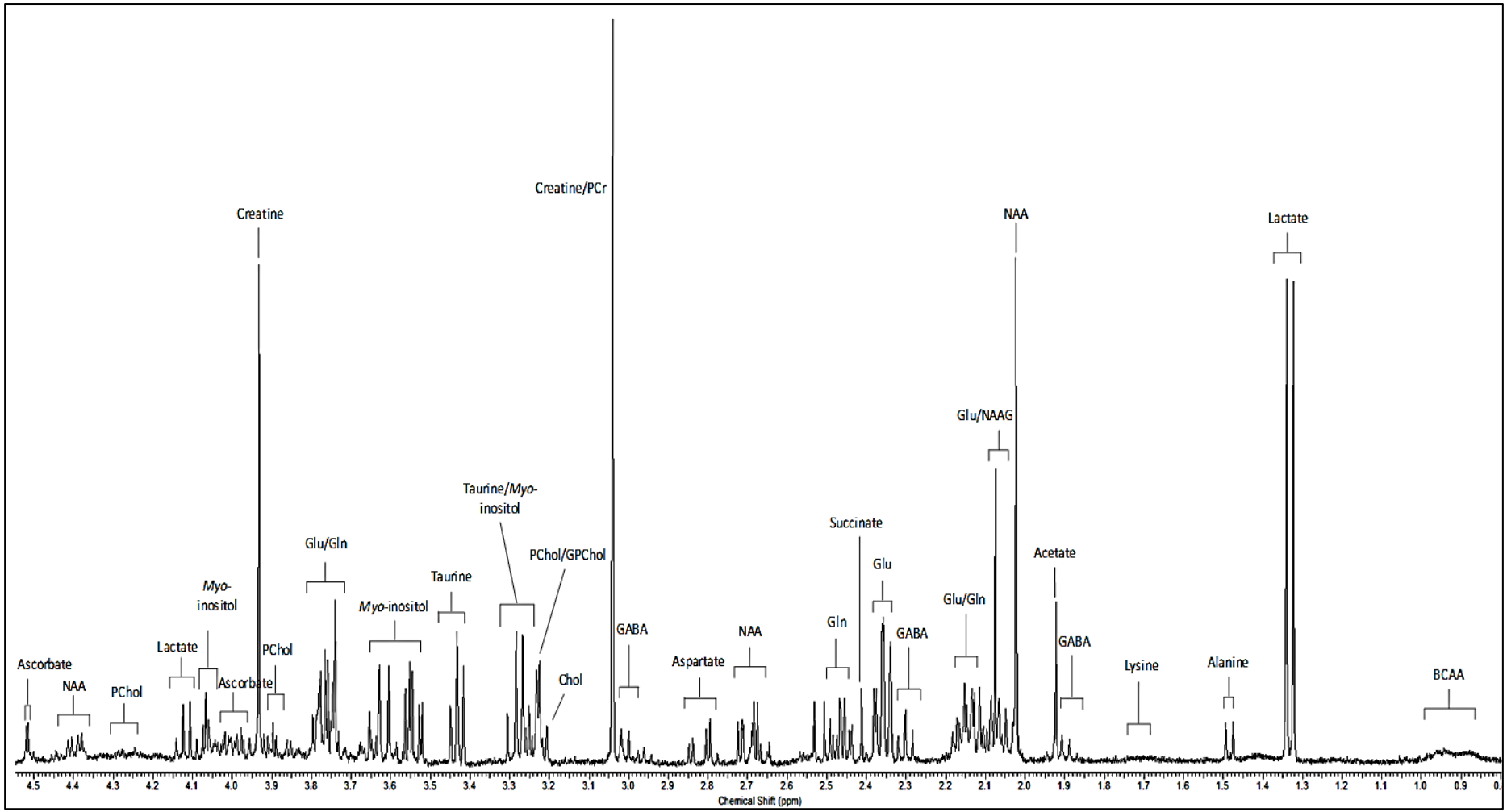

Figure 3.1: ^{1}H NMR spectra of a frontal cortical extract obtained from control rat showing different metabolites. Abbreviations: Glu, glutamate; NAAG, N-acetylaspartylglutamate; Gln, glutamine; NAA, N-acetyl aspartate; Chol, choline; GABA, Gamma amino butyric acid; PCholi, Phpshporyl choline; GPChol, Glycerolphosphyl choline; BCAA, branched chain amino acids.

A

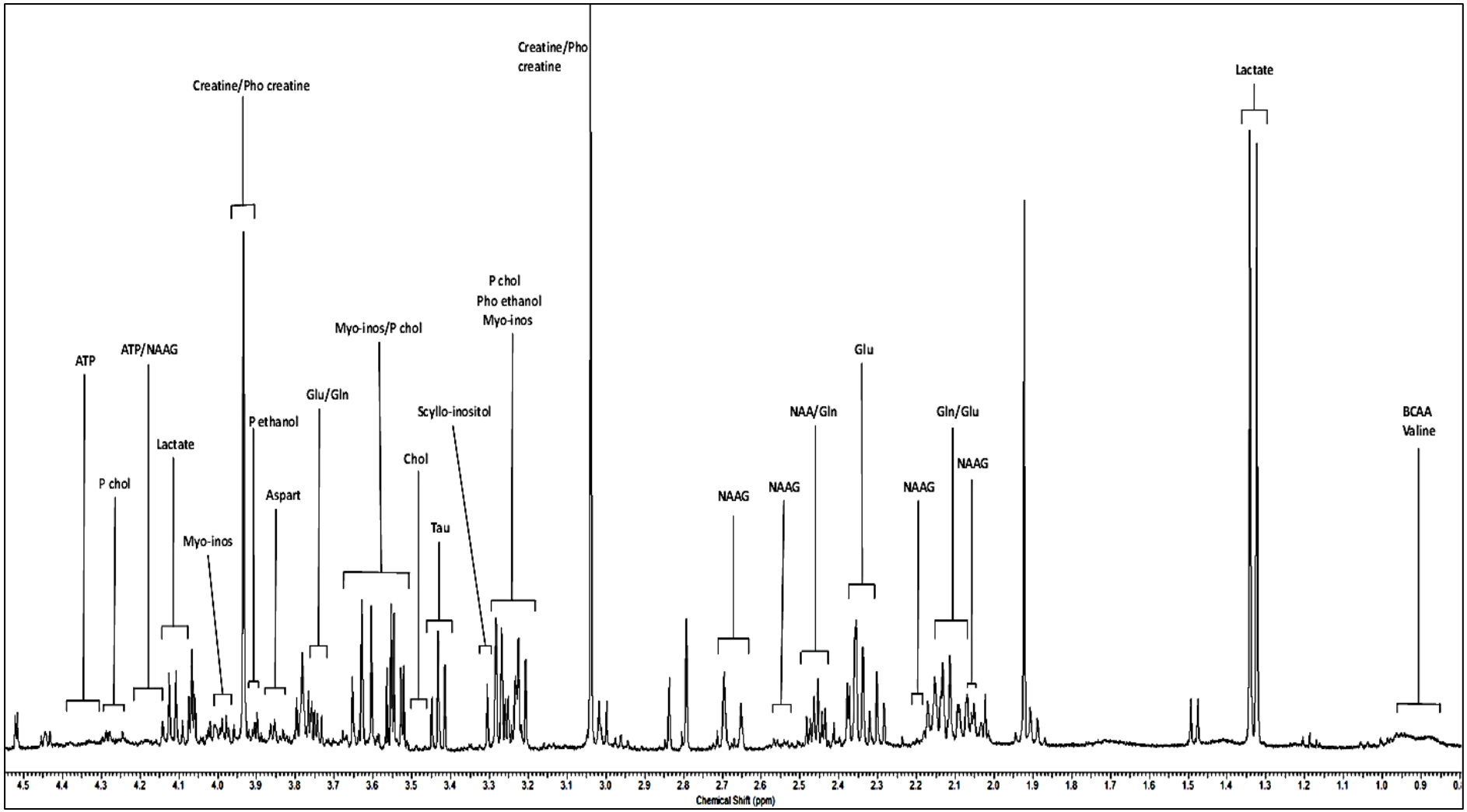
Creatine/Pho creatine
Creatine/Pho creatine
Lactate
P chol
Pho ethanol
Myo-inos
Myo-inos/P chol
ATP
ATP/NAAG
Glu/Gln
Glu
P ethanol
Scyllo-inositol
NAA/Gln
Gln/Glu
BCAA
Valine
Lactate
P chol
Chol
NAAG
NAAG
NAAG
NAAG
Aspart
Tau
Myo-inos
4.5 4.4 4.3 4.2 4.1 4.0 3.9 3.8 3.7 3.6 3.5 3.4 3.3 3.2 3.1 3.0 2.9 2.8 2.7 2.6 2.5 2.4 2.3 2.2 2.1 2.0 1.9 1.8 1.7 1.6 1.5 1.4 1.3 1.2 1.1 1.0 0.9
Chemical Shift (ppm)

B

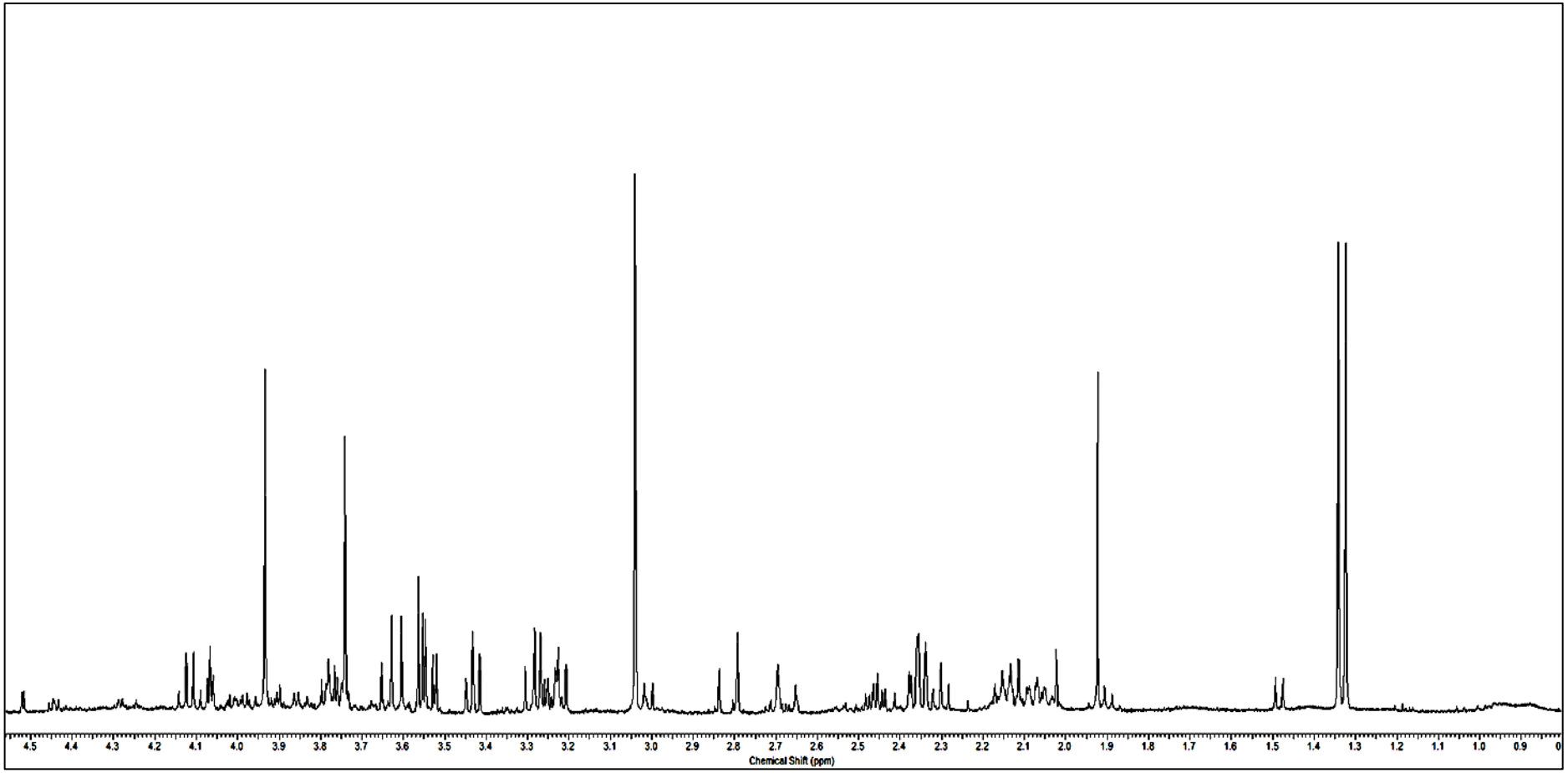

Figure 3.2: ^{1}H NMR spectra of hippocampal tissue extracts obtained from control (A) and treated rats (B) showing different metabolites significantly changed identified within the hippocampus following acute desipramine treatment. Abbreviations: Glu, glutamate; NAAG, N-acetylaspartylglutamate; Gln, glutamine; NAA, N-acetyl aspartate; Chol, choline; Pho ethanol, phosphoryl ethanolamine; Pho creatine, phosphocreatine; P cho, phosphoryl choline; ATP, adenosine triphosphate; Tau, taurine; Aspart, aspartate; Myo-inos, myo-inositol; BCAA, branched chain amino acid.

3.4.2. Acute paroxetine and desipramine treatment:

3.4.2.1. Metabolic changes in the prefrontal cortex following acute drug administration:

Acute treatment with paroxetine significantly decreased a number of metabolites within the prefrontal cortex (Table 3.1 and Figure 3.1). The PLS-DA scores plot in Figures 3.3 and 3.4 shows the separation between the treatment and control groups. In contrast, data analysis following acute desipramine treatment exhibited no significant differences in any metabolite within the prefrontal cortex (data not shown).

Table 3.1: Metabolites significantly changed identified within the prefrontal cortex following acute paroxetine treatment (Student t-test). Abbreviations: d, doublet; t, triplet and m, multiplet.

	Metabolites	Chemical shift (ppm)	Multiplicity	P-value	Fold changes
1	Valine	0.83 - 1.00	d	0.019	-1.39
2	Leucine	0.97 - 1.01	t	0.021	-1.45
3	ATP	4.15 - 4.23	m	0.043	-1.30
4	Glutamate	2.33 - 2.39	m	0.043	-1.26
5	D-Glucose (β)	4.51 - 4.53	d	0.057	-1.36

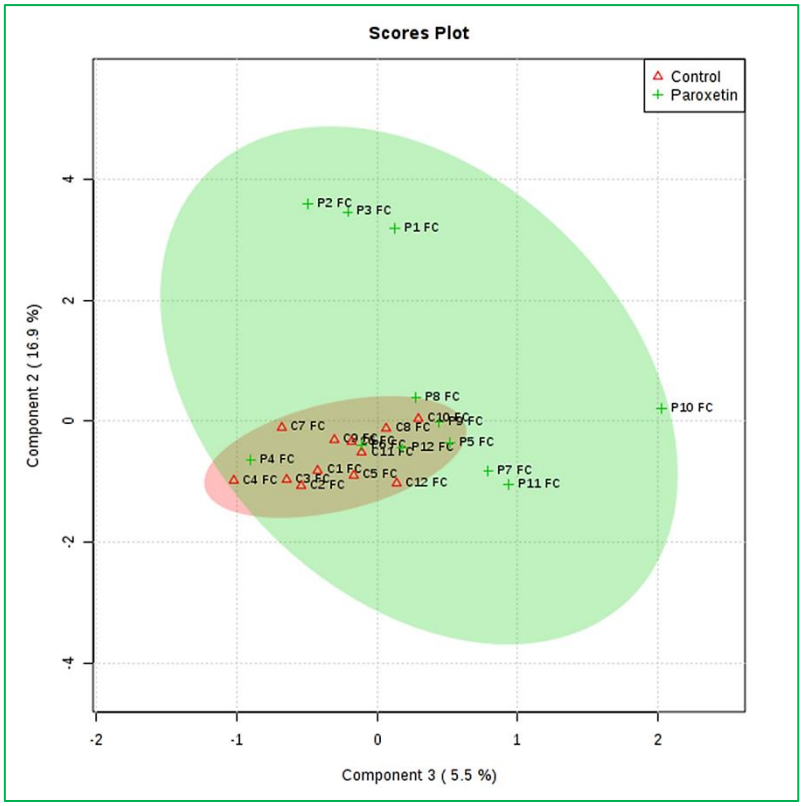

Figure 3.3: PLS-DA 2D Scores Plot of control and acute paroxetine treatment groups in the prefrontal cortex.

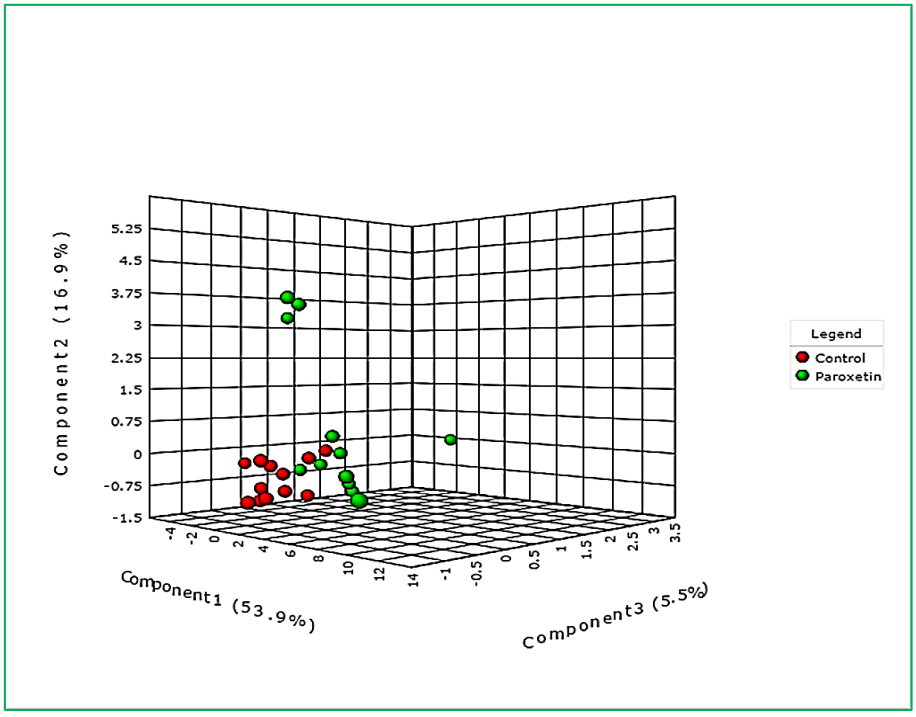

Figure 3.4: PLS-DA 3D Scores Plot of control and acute paroxetine treatment groups in the prefrontal cortex.

3.4.2.2. Metabolic changes in the hippocampus following acute drug administration:

Both acute paroxetine and desipramine administration induced a significant reduction in the level of several metabolites identified within the hippocampus. However, acute desipramine treatment was associated with a higher number of significantly changed metabolites compared with the acute paroxetine treatment group (see Figure 3.2).

A. Acute paroxetine treatment:

Identification of the significant metabolic changes within the hippocampus after acute paroxetine treatment showed significantly decreased levels of 4 metabolites (Table 3.2 and Figure 3.2). The PLS-DA scores plot in Figures 3.5 and 3.6 shows the separation between the treatment and control groups.

Table 3.2: Metabolites significantly changed identified within the hippocampal tissue following acute paroxetine treatment (Student t-test). Abbreviations: d, doublet; t, triplet and dd, doublet of doublet.

	Metabolites	Chemical shift (ppm)	Multiplicity	P-value	Fold changes
1	Serine	3.84 - 3.87	dd	0.027	-1.18
2	D-Glucose(α)	3.81 - 3.84	dd	0.042	-1.18
3	Valine	3.58 - 3.59	d	0.044	-1.19
4	Myo-inositol	3.60 - 3.66	t	0.044	-1.19
		3.51 - 3.56	dd	0.054	-1.17

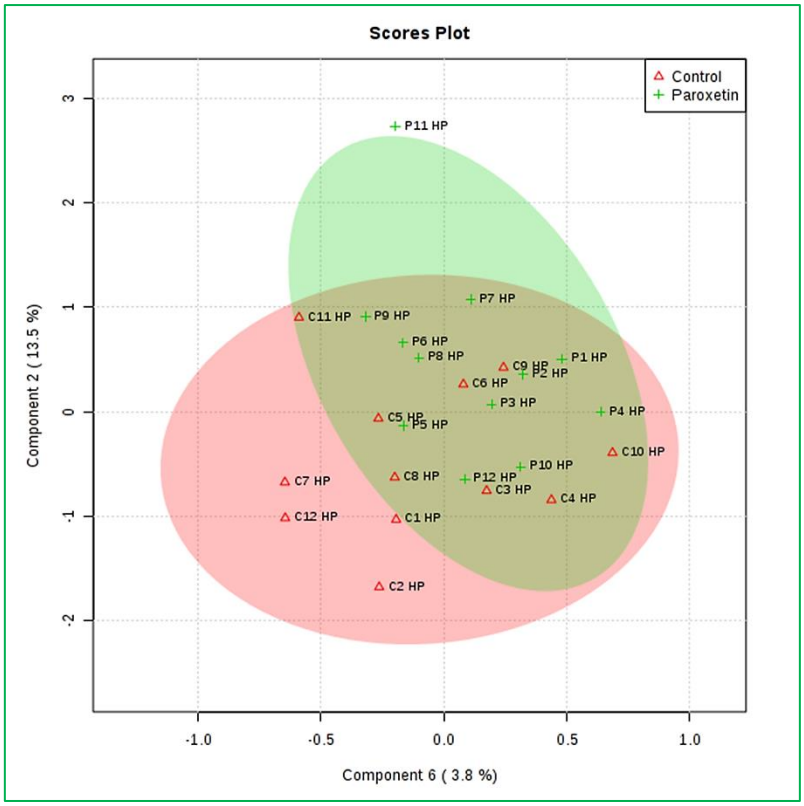

Figure 3.5: PLS-DA 2D Scores Plot of control and acute paroxetine treatment groups in the hippocampus.

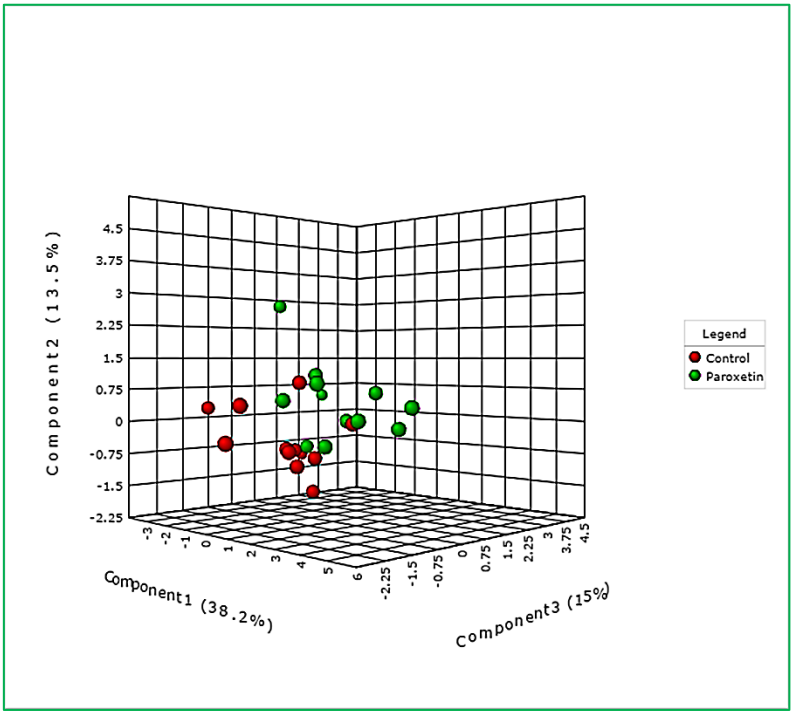

Figure 3.6: PLS-DA 3D Scores Plot of control and acute paroxetine treatment groups in the hippocampus.

B. Acute desipramine treatment:

Acute desipramine administration induced a significant decrease in 9 metabolites within hippocampal tissue extract as displayed in Figures 3.2, 3.9 and Table 3.3. The PLS-DA method showed a clear separation between the drug treatment group and control groups following acute desipramine treatment as demonstrated in Figures 3.7 and 3.8.

Table 3.3: Metabolites significantly changed within the hippocampal tissue following acute desipramine treatment (Student t-test). Abbreviations: d, doublet; t, triplet; dd, doublet of doublet; m, multiplet; qu, quartet and s, singlet.

	Metabolites	Chemical Shift (ppm)	Multiplicity	P-value	Fold changes
1	N-Acetylaspartylglutamate	2.52 - 2.57	dd	0.002	-1.33
		2.18 - 2.23	m	0.005	-1.33
		2.68 - 2.73	dd	0.009	-1.31
2	Glutamine	2.43 - 2.47	m	0.004	-1.33
		2.11 - 2.18	m	0.024	-1.27
3	N-Acetyl aspartate	2.47 - 2.51	dd	0.004	-1.33
4	Lactate	1.31 - 1.35	d	0.012	-1.36
		4.08 - 4.15	qu	0.012	-1.35
5	Myo-inositol	3.60 - 3.66	t	0.014	-1.30
		3.51 - 3.56	dd	0.015	-1.30
		3.26 - 3.29	t	0.050	-1.28
6	Scyllo-inositol	3.30 - 3.31	s	0.015	-1.36
7	Glutamate	3.73 - 3.77	dd	0.022	-1.26
		2.33 - 2.38	m	0.041	-1.28
8	Phosphoryl ethanolamine	3.22 - 3.26	m	0.031	-1.29
9	Choline	3.46 - 3.51	m	0.044	-1.92
10	Creatine / Phosphocreatine	3.03 - 3.05	s	0.054	-1.26
		3.92 - 3.94	s	0.055	-1.25

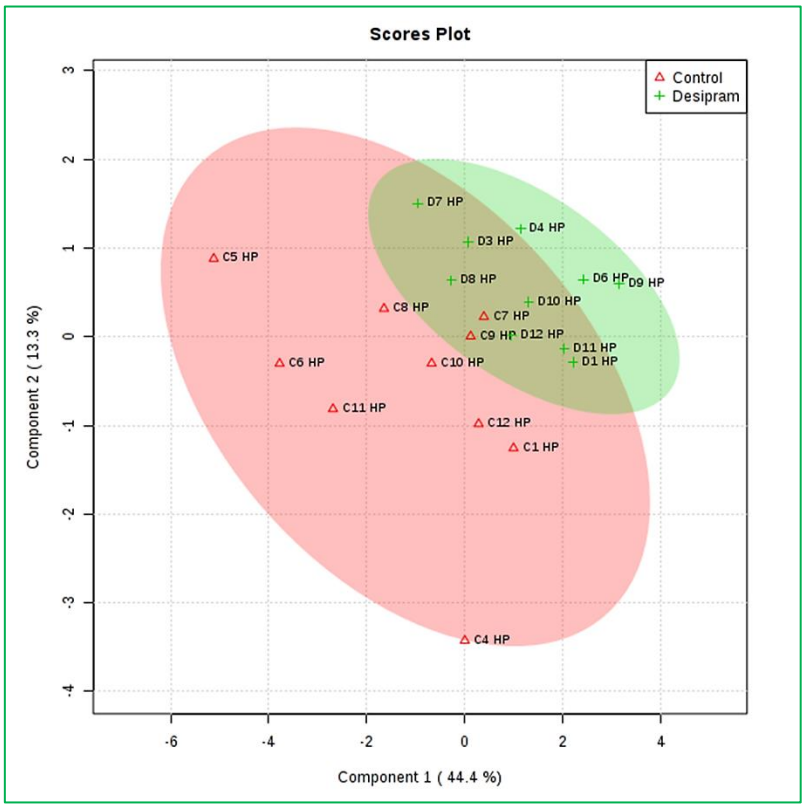

Figure 3.7: PLS-DA 2D Scores Plot of control and acute desipramine treatment groups in the hippocampus.

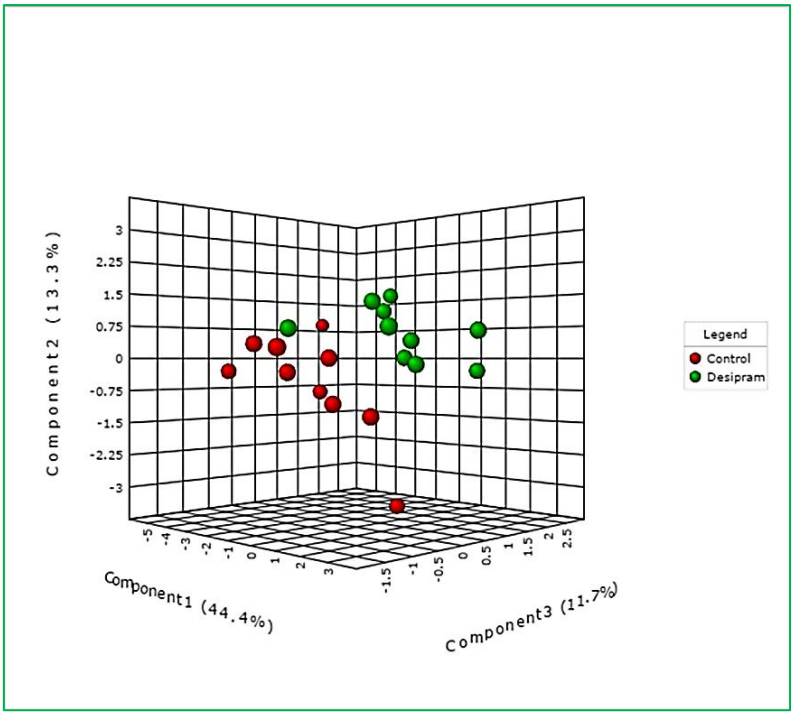

Figure 3.8: PLS-DA 3D Scores Plot of control and acute desipramine treatment groups in the hippocampus.

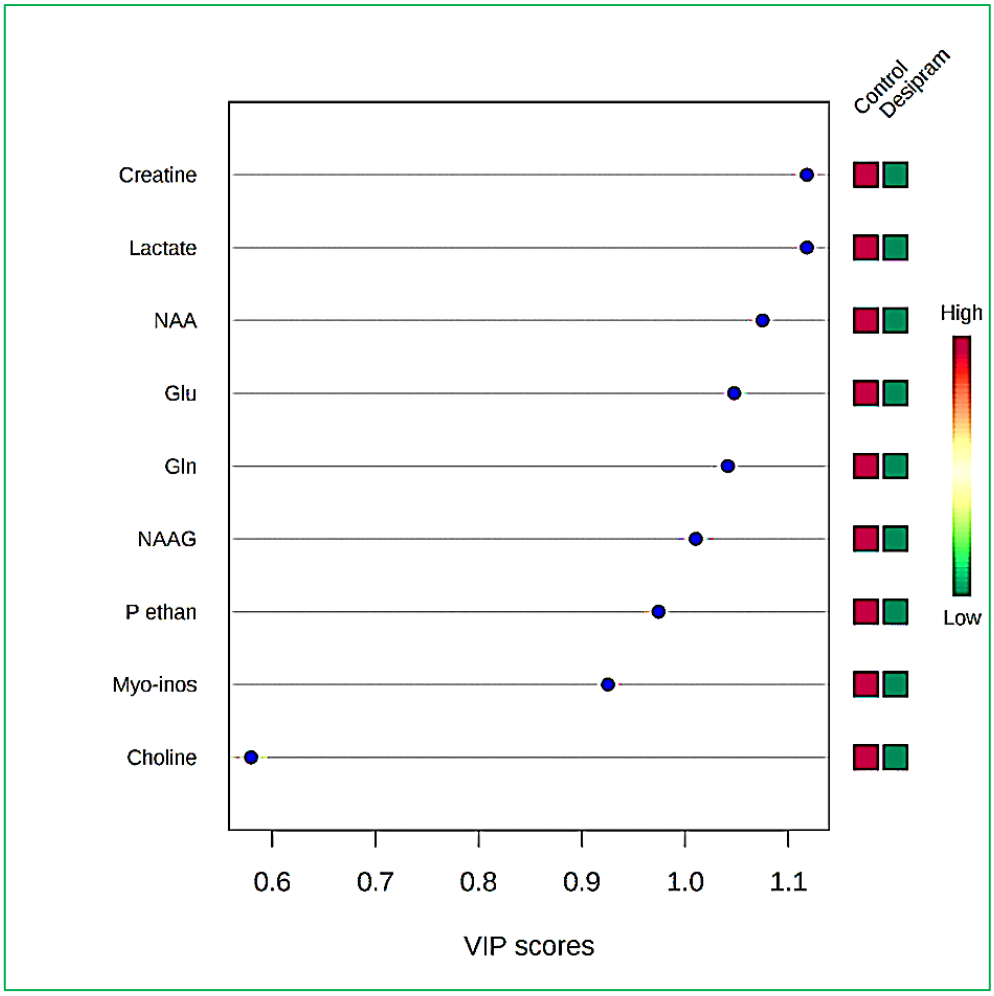

Figure 3.9: Variables of importance in projection (VIP) scores for the significantly changed metabolites in the PLS-DA of control and acute desipramine treatment groups in the hippocampus. The panel to the right indicates the direction of metabolite changes in both groups. Abbreviations: NAA, N-acetyl aspartate; Glu, glutamate; Gln, glutamine; NAAG, N-acetylaspartylglutamate; P ethan, phosphoryl ethanolamine; myo-inos, myo-inositol.

3.4.2.3. Metabolic changes in the striatal region following acute drug administration:

Analysis of data obtained from the rat striatal region showed different effects following acute paroxetine and desipramine treatment. Thus, acute paroxetine administration did not result in any significant changes in this particular brain region whereas, acute desipramine treatment revealed the highest number of significant metabolic changes in this region. Interestingly, these changes were overall opposite compared to those seen in the prefrontal cortex and the hippocampus, thus in the striatum desipramine generally caused an up-regulation of a range of metabolites as compared to its effect in the two other brain regions

examined, where the drug in contrast reduced the levels of a number of metabolites (Figures 3.1, 3.12 and Table 3.4). The PLS-DA scores plot in Figures 3.10 and 3.11 shows the separation between the treatment and control groups.

Table 3.4: Metabolites significantly changed identified within the striatal tissue following acute desipramine treatment (Student t-test). Abbreviations: d, doublet; t, triplet; dd, doublet of doublet; m, multiplet and s, singlet.

	Metabolites	Chemical shift (ppm)	Multiplicity	P-value	Fold changes
1	N-Acetylaspartylglutamate	4.17 - 4.21	dd	0.008	+1.40
		2. 07 - 2.08	s	0.016	+1.29
2	ATP	4.15 - 4.23	m	0.008	+1.40
		4.30 - 4.37	m	0.014	+1.38
		4.37 - 4.42	m	0.016	+1.30
3	Phosphoryl choline	4.27 - 4.30	m	0.012	+1.38
		3.21 - 3.22	s	0.016	+1.34
		3.66 - 3.70	m	0.020	+1.28
4	Taurine	3.41 - 3.45	t	0.016	+1.30
		3.24 - 3.26	t	0.016	+1.34
5	Phosphoryl ethanolamine	3.97 - 4.05	m	0.016	+1.30
		3.22 - 3.24	m	0.016	+1.34
6	Glutamate	2.04 - 2.10	m	0.016	+1.29
		2.33 - 2.38	m	0.030	+1.24
		3.74 - 3.77	dd	0.056	+1.24
7	Valine	0.84 - 1.00	d	0.031	+1.32
		3.58 - 3.59	d	0.025	+1.27
8	Glutamine	2.48 - 2.47	m	0.019	+1.27
		2.11 - 2.18	m	0.022	+1.26
		3.77 - 3.79	t	0.056	+1.24
9	Aspartate	3.88 - 3.92	dd	0.020	+1.26
10	Creatine	3.92 - 3.94	s	0.020	+1.26
	Phosphocreatine	3.03 - 3 .05	s	0.020	+1.26
11	Myo-inositol	3.60 - 3.66	t	0.020	+1.28
		4.05 - 4.08	t	0.021	+1.28
		3.26 - 3.29	t	0.023	+1.27
		3.51 - 3.56	dd	0.029	+1.26
12	Scyllo-inositol	3.30 - 3.31	s	0.035	+1.29

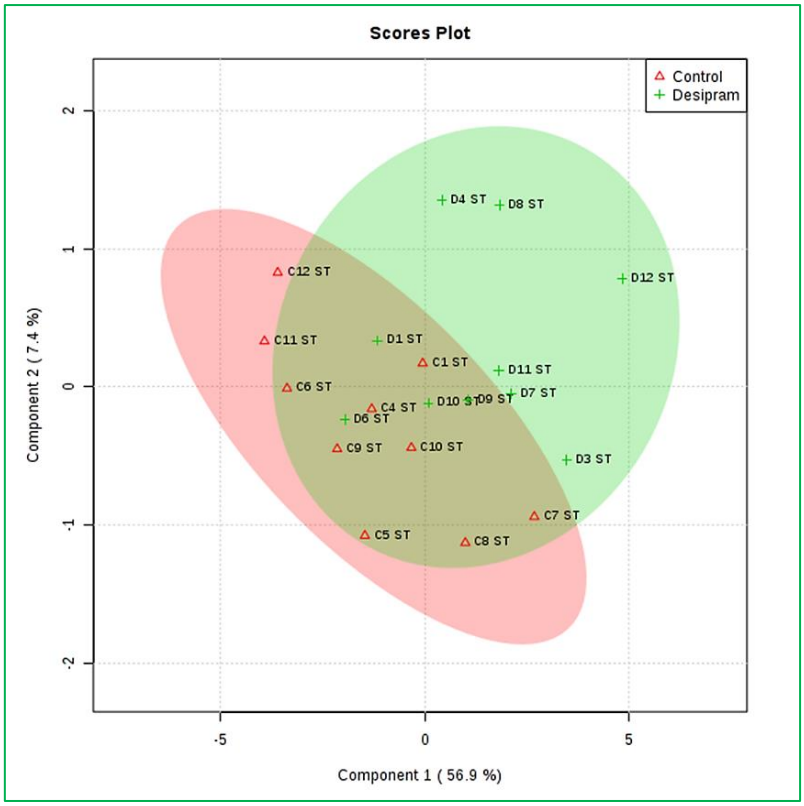

Figure 3.10: PLS-DA 2D Scores Plot of control and acute desipramine treatment groups in the striatal region.

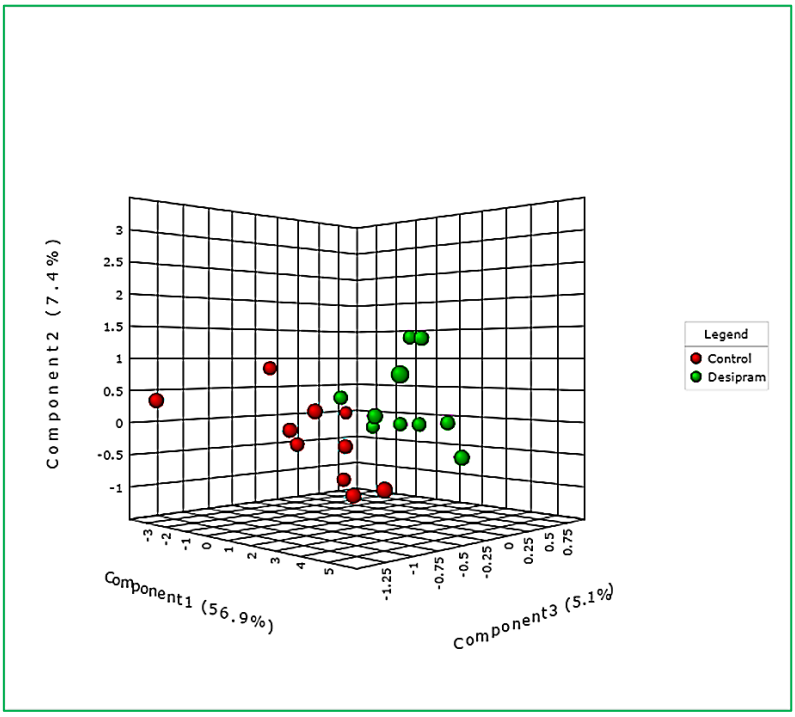

Figure 3.11: PLS-DA 3D Scores Plot of control and acute desipramine treatment groups in the striatal region.

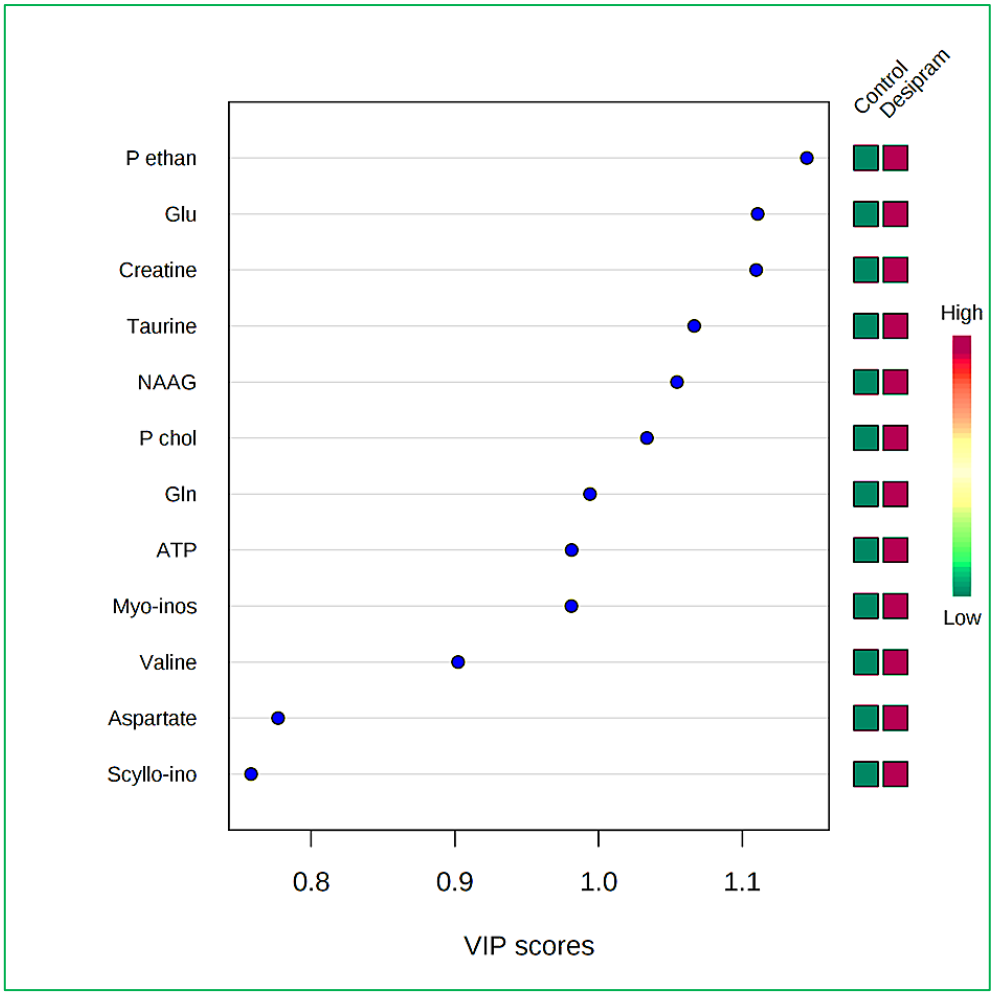

Figure 3.12: Variables of importance in projection (VIP) scores for the significantly changed metabolites in the PLS-DA of control and acute desipramine treatment groups in the striatal region. The panel to the right indicates the direction of metabolite changes in both groups. Abbreviations: P ethan, phosphoryl ethanolamine; Glu, glutamate; NAAG, N-acetyl aspartylglutamate; P chol, phosphoryl choline; Gln, glutamine; ATP; adenosine triphosphate; myo-inos, myo-inositol; scyllo-ino, scyllo-inositol.

3.4.2.4. Metabolic changes in the plasma following acute drug administration:

The plasma samples of the two acute treatment groups varied in number for technical reasons (i.e. difficulties with blood sampling). The acute paroxetine group contained 12 plasma samples; 6 controls and 6 treatment samples whereas acute desipramine treatment group included 24 samples; 12 controls and 12 treatment samples. Spectral analysis of the plasma samples obtained from the acute desipramine group did not show any significant variation between the control and the treatment animals (data not shown), whereas the acute paroxetine group showed a significant decrease of some metabolites as indicated in Table

3.5. The PLS-DA scores plot in Figure 3.13 and Figure 3.14 displays the separation between the paroxetine treatment and control groups.

Table 3.5: Metabolites significantly changed identified within the plasma following acute paroxetine treatment (Student t-test). Abbreviations: d, doublet; and s, singlet.

	Metabolites	Chemical Shift (ppm)	Multiplicity	P-value	Fold changes
1	Serine	4.23 - 4.40	d	0.016	-1.63
2	α-Hydroxyisovalerate	4.17 - 4.24	d	0.024	-1.45
3	Succinate	2.64 - 2.66	s	0.031	-1.56
4	Creatine	3.08 - 3.09	s	0.043	-1.85

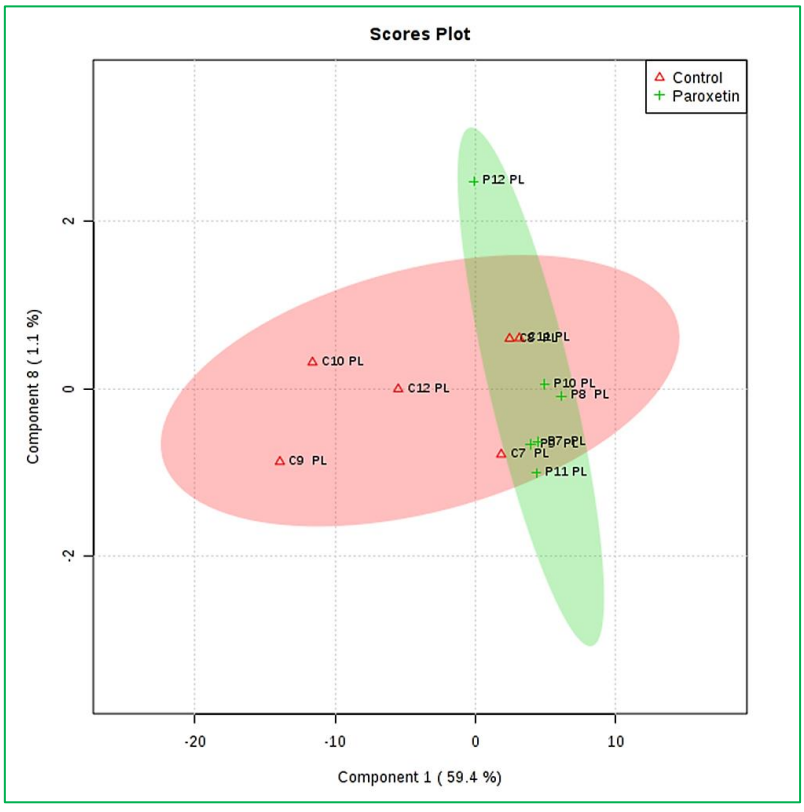

Figure 3.13: PLS-DA 2D Scores Plot of control and acute paroxetine treatment groups in the plasma.

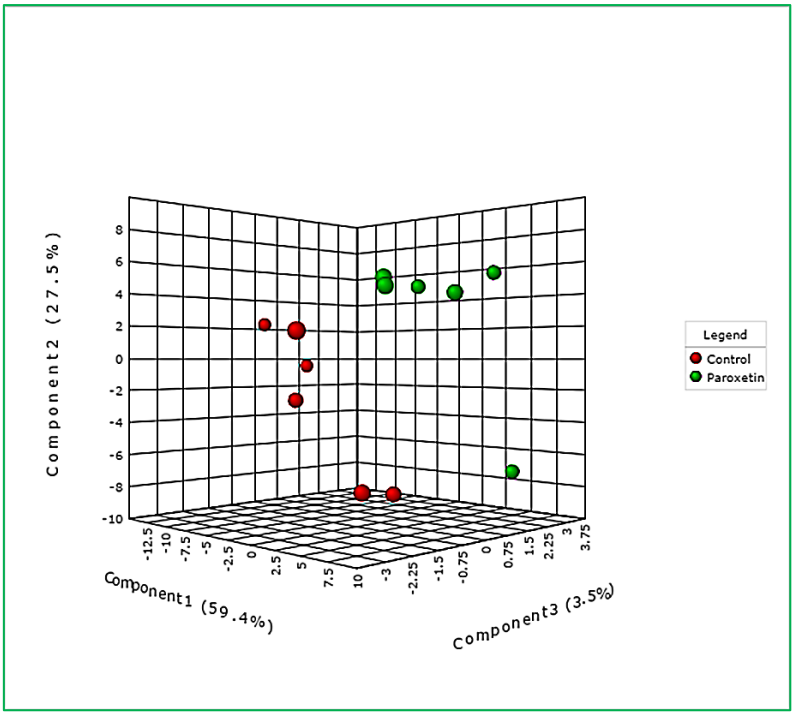

Figure 3.14: PLS-DA 3D Scores Plot of control and acute paroxetine treatment groups in the plasma.

3.4.3. Chronic paroxetine and desipramine treatment:

3.4.3.1. Metabolic changes following chronic paroxetine administration:

A. Metabolic changes in brain regions:

Analysis of chronic paroxetine data revealed a significant reduction in the level of succinate (Student t-test, p = 0.04) with a trend to decrease in myo-inositol level within the hippocampus (p values for the myo-inositol peaks = 0.067, 0.073, 0.096 respectively) (Table 3.6) without any significant alteration in any metabolite within the prefrontal cortex and the striatal regions.

Table 3.6: Metabolites significantly and non-significantly changed identified within the hippocampal tissue following chronic paroxetine treatment (Student t-test). Abbreviations: t, triplet; dd, doublet of doublet; and s, singlet.

	Metabolites	Chemical shift (ppm)	Multiplicity	P-value	Fold changes
1	Myo-inositol	3.51 - 3.56	dd	0.067	-1.58
		3.60 - 3.66	t	0.073	-1.58
		4.05 - 4.08	t	0.096	-1.56
2	Succinate	2.40 - 2.42	s	0.040	-1.85

B. Metabolic changes in the plasma:

Spectral analysis of the plasma samples obtained from the chronic paroxetine group did not show any significant variation between the control and the treatment animals (data not shown).

3.4.3.2. Metabolic changes following chronic desipramine administration:

A. Metabolic changes in brain regions:

Comprehensive analysis of chronic desipramine data displayed no statistically significant changes in any metabolite between control and desipramine treatment rats within any of the three brain regions (data not outlined).

B. Metabolic changes in the plasma:

Spectral analysis of the plasma samples obtained from the chronic desipramine group showed a significant increase in the level of creatinine only (Student t-test p value = 0.030) with a trend to an increase in serine level (p value = 0.077). The PLS-DA scores plot in Figure 3.15 and Figure 3.16 shows the separation between the drug treatment and control groups.

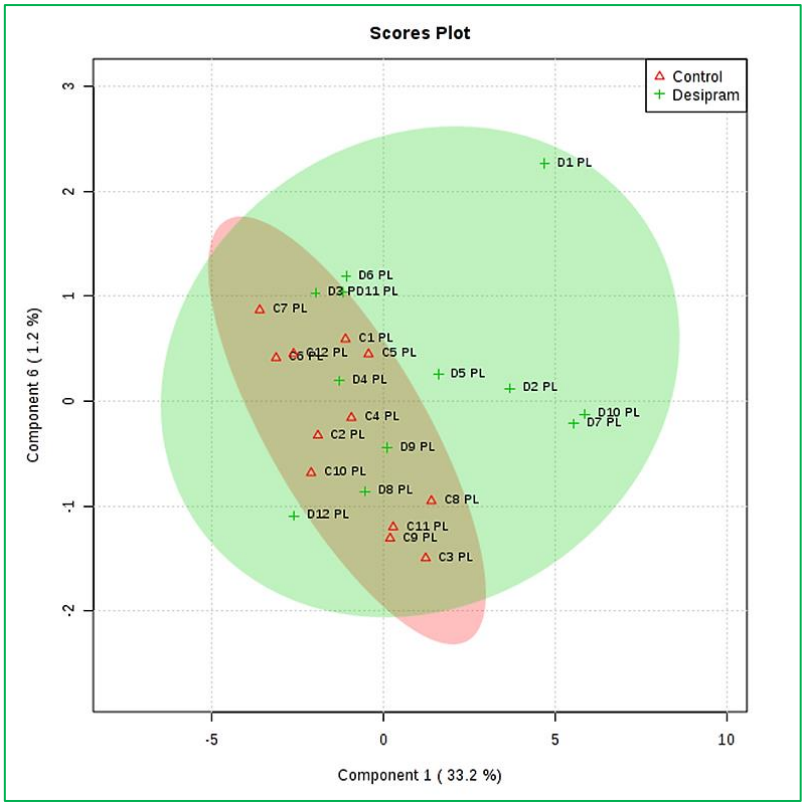

Figure 3.15: PLS-DA 2D Scores Plot of control and chronic desipramine treatment groups in the plasma.

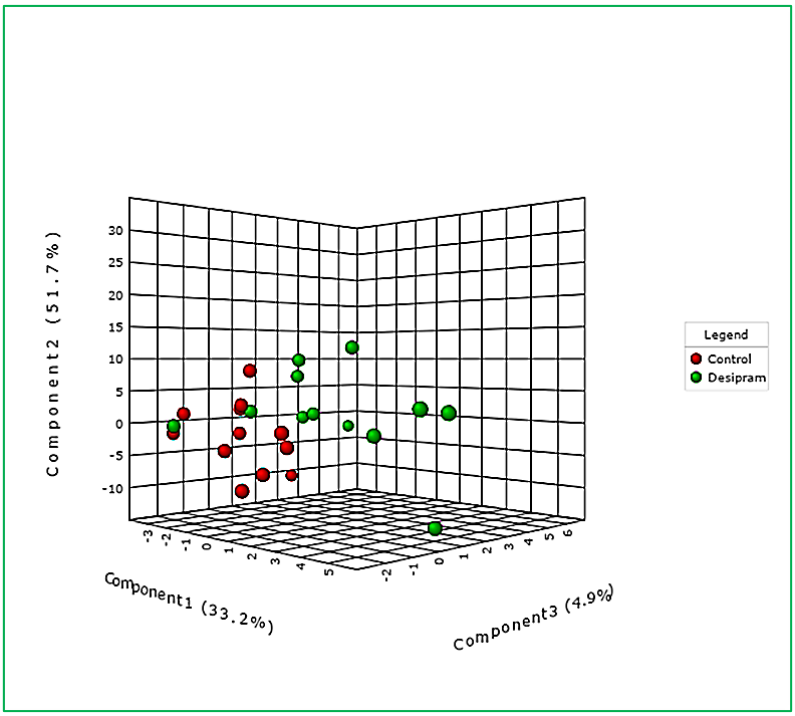

Figure 3.16: PLS-DA 3D Scores Plot of control and chronic desipramine treatment groups in the plasma.

3.5. Discussion:

Along with the theories attempting to elucidate the pathogenesis of depression and its available therapy, the neurochemical alterations of various important brain biomolecules that may be associated with depression and the relevant treatment remain to be determined. Recent studies have investigated the metabolic effects of antidepressant drug treatment using different technologies. Thus, a previous clinical imaging study using MRI (magnetic resonance imaging) scans revealed a decreased metabolic activity within the dorsolateral prefrontal cortex, as well as an increased metabolic activity within the ventrolateral prefrontal cortex, the orbitofrontal cortex and the inferior orbital gyrus in depressed subjects. These changes were normalized following successful paroxetine treatment (Brody et al., 1999). In line with this study, a magnetic resonance spectroscopy (MRS) study in depressed patients implied that there were regional abnormalities of several brain metabolites some of which were also changed by antidepressant drugs in the current study including: choline, glutamate, glutamine and NAA levels in the brain of the affected subjects (Yildiz-Yesiloglu and Ankerst, 2006). In this regard, a recent post mortem study using NMR spectroscopy identified a number of metabolic alterations involving glutamate, GABA, myo-inositol and creatine that may be associated with psychological disorders (Lan et al., 2009).

In order to better understand the mechanism of action by antidepressant drugs, the present study investigated the metabolic effects of two different antidepressant drugs in three separate brain regions (the prefrontal cortex, hippocampus and the striatum) implicated in the mechanism of action by antidepressant drugs. This was done following either acute (single injection) or chronic (once daily for 15 days) treatment regimes. Metabolic changes were also recorded in the corresponding plasma samples. For this purpose, we used ^{1}H NMR spectroscopy to investigate for the first time the effect of antidepressant drugs on brain metabolites in rat brain regions thought to be associated with depression. Two antidepressant drugs from different classes were utilized in the study: paroxetine and desipramine. Paroxetine is an SSRI that blocks extracellular 5-HT uptake by inhibiting its neuronal transporter (SERT). The other drug, desipramine is a TCA which inhibits the neuronal noradrenaline transporter (NET) and to a much lesser extent also SERT. By preventing the uptake of these monoamines, these drugs cause an increase in the concentration of 5-HT and

NA within the synaptic cleft. An effect likely to contribute to the drugs well known antidepressant action (David et al., 2003; Hyman and Nestler, 1996).

The present study found that acute administration of paroxetine and desipramine induced significant metabolic changes, which frequently depended on duration of treatment and were often both brain region and drug specific. These differential results probably reflect the fact that desipramine and paroxetine primarily block different types of transporters, NET and SERT and therefore preferentially increase extracellular levels of NA and 5-HT respectively, thereby stimulating receptors with differential distribution and actions in the different brain regions investigated. In contrast following chronic administration, very few metabolic effects were detected.

The brief function of the main metabolites identified as being significantly modified by the antidepressant drugs of brain regions and in plasma samples are summarized below in section 3.7.1 (see Figures 3.1 and 3.2).

3.5.1. List of antidepressant-induced changes of metabolites identified in ^{1}H NMR spectra:

- Adenosine triphosphate (ATP): ATP is the principle source of energy production (Erecińska and Silver, 1989).
- Aspartate: This amino acid acts as an excitatory amino acid neurotransmitter in the brain and also enhances the immune response by facilitating immunoglobulin and antibody production (Klunk et al., 1996).
- Choline: Choline is an essential substrate of phospholipids and is involved in the synthesis of the neurotransmitter acetylcholine (Pouwels and Frahm, 1998).
- Creatine and phosphocreatine: These compounds participate in cerebral energy production. They are required for the synthesis and metabolism of ATP in the brain (Crespo et al., 2008; Smith et al., 2014).
- D-Glucose: Glucose is the main source of energy (Gruetter et al., 1996).
- Glutamate: Glutamate is the main excitatory neurotransmitter in the brain and the major source of GABA (Van Zijl and Barker, 1997).

- Glutamine: Glutamine is a precursor to glutamate and hence also a source for the inhibitory amino acid GABA (Pouwels and Frahm, 1998).
- Lactate: Lactate is an important substrate in cerebral energy metabolism. It is produced by the anaerobic breakdown of glucose (Fillenz, 2005; Van Zijl and Barker, 1997).
- Leucine: Leucine is a branched amino acid which plays an important role in insulin release (Garlick, 2005).
- Myo-inositol: Myo-inositol is an essential osmolyte which can be used as an indicator of intracellular osmolarity (Brand et al., 1993; Tsang et al., 2006).
- N-acetyl aspartate (NAA): NAA is the source of NAAG and exhibits the same function of NAAG in transferring the metabolic water to the extracellular space to maintain the neuronal integrity that is necessary for the neuronal activity (Baslow, 2003).
- N-acetylaspartylglutamate (NAAG): NAAG is synthesized from N-acetyl aspartate (NAA) and glutamate in neurons. This substance participates in the maintenance of normal neuronal osmolarity by releasing the free metabolic water to the extracellular compartment opposite the concentration gradient of water and thereby, maintaining a normal neuronal structure (Baslow and Guilfoyle, 2006). It achieves an important role in the excitatory neurotransmission to astrocytes. Therefore, liberates a considerable amount of energy needed for the neuronal neurotransmission and it is also a precursor of glutamate (Pouwels and Frahm, 1997).
- Phosphoryl ethanolamine: This compound originates from the alcohol part of the phosphoglyceride ethanolamine (Govindaraju et al., 2000).
- Scyllo-inositol: A form of inositol which is found in a lower concentration compared to that of myo-inositol in a ratio of 12:1 (Michaelis et al., 1993).
- Serine: Serine is an important amino acid required for several vital functions including a precursor for myelin sheath, maintenance of normal glucose level, normal muscle growth and NMDA receptor neurotransmission (Panatier et al., 2006).
- Succinate: This metabolite exerts an essential role in generating ATP in the mitochondria (Mills and O'Neill, 2014).
- Taurine: This amino acid functions as an inhibitory neurotransmitter in the CNS and a cell membrane stabilizer by increasing the level of the brain threshold in epilepsy.

Taurine is also involved in regulation of cellular osmolarity (Hardy and Norwood, 1998).

- Valine : Valine is a branched chain amino acids essential for protein synthesis and energy production (Siegel et al., 1989).

3.5.2. Metabolic alteration in the prefrontal cortex following acute antidepressant drug administration:

Compared to the corresponding saline treated control group, acute paroxetine treatment resulted in a significant reduction in 4 metabolites: valine, leucine, ATP, and glutamate. In contrast, the acute desipramine treatment group did not exhibit any significant metabolic difference within this particular brain region. ATP is the main source of energy within the cells and glutamate apart from acting as the main excitatory amino neurotransmitter and the metabolic precursor of GABA in the brain, also plays an indirect role in the process of glycolysis in the brain (Schousboe et al., 2007). This observation suggests that acute paroxetine medication but not desipramine targets amino acid metabolism and the cerebral pathway of glucose metabolism. Further, reduced level of valine and ATP indicates that paroxetine acutely may decrease energy production within the prefrontal cortex. Moreover, previous clinical studies reported a pronounced hypoglycaemia with an enhanced insulin release following both acute and chronic paroxetine treatment in both diabetic patients as well as normoglycemic control subjects (Derijks et al., 2008; Han et al., 2016). In this regard, a recent experimental study revealed a similar finding which indicated that acute paroxetine administration at a dose of 5 mg/kg resulted in hypoglycaemia with an increased insulin release in mice (Kadioglu et al., 2011). Thus, the drug-induced hypoglycaemia following acute paroxetine treatment is possibly reflecting the initial metabolic alteration, in particular the recorded reduced leucine level in the prefrontal cortex.

3.5.3. Metabolic alteration in the hippocampus following acute antidepressant drug administration:

The hippocampal data analysis after acute paroxetine treatment showed a statistically significant reduction in 4 metabolites as compared to the controls, including: serine, D-glucose, valine and myo-inositol. Acute desipramine induced significant down-regulation

within the hippocampus of NAAG, glutamine, NAA, lactate, myo-inositol, scyllo-inositol, glutamate, phosphoryl ethanolamine and choline. Taken together, this suggests that the hippocampus is affected by the two drugs in a similar way to the effect detected in the prefrontal cortex following acute paroxetine treatment.

3.5.4. Metabolic alteration in the striatal region following acute antidepressant drug administration:

Analysing the striatal data after acute treatment with the two antidepressant drugs displayed a strikingly drug dependent metabolic effect within this brain region. Thus, while acute paroxetine treatment did not reveal any significant effects within the striatal brain region. On the contrary, acute desipramine administration exhibited the highest number of significant metabolite changes within this brain region. Interestingly, the desipramine induced effects of brain metabolites in the striatum were in contrast, to those seen in the other two brain regions (i.e. decreases) increased in the striatum. An important finding that was consistent with a previous ^{1}H NMR study following chronic methylphenidate treatment in rats (Quansah, 2017). Detected increases were indeed recorded for up to twelve different functionally important brain metabolites and included: NAAG, ATP, phosphoryl choline, taurine, phosphoryl ethanolamine, glutamate, aspartate, creatine and phosphocreatine, myo-inositol and scyllo-inositol.

3.5.5. Metabolic alteration in the plasma following acute antidepressant drug administration:

Spectral analysis of plasma samples obtained from the acute desipramine group did not reveal any significant variation compared to the control group, whereas, analysing the data of the acute paroxetine group showed a significant reduction of serine, α-hydroxyisovalerate, succinate and creatine.

3.5.6. Metabolic changes specific for acute desipramine administration:

3.5.6.1. N-acetyl aspartate (NAA) and N-acetylaspartylglutamate (NAAG):

NAAG and NAA are important amino acids present in high concentration in the brain. Both exert an essential role in maintaining normal neuronal structure, activity, plasticity and energy production (Baslow and Guilfoyle, 2006). Acute desipramine treatment resulted in a significant reduction of both NAAG and NAA in the hippocampus and in contrast, a significant increase in aspartate, a precursor of NAA and NAAG levels in the rat striatal brain region. These observed changes suggest that acute desipramine may exert an initial region-specific effect on neuronal viability and energy production. Interestingly, a recent MRS study on bipolar patients found that these patients showed a regional abnormality of NAA brain levels (Yildiz-Yesiloglu and Ankerst, 2006). Further, a previous metabolomic study utilized gas chromatography-mass spectrometry showed a down-regulation of NAA and glutamate in the hippocampus of stressed mice following sub-chronic treatment with imipramine and fluoxetine for 14 days (Zhao et al., 2015). In addition, a previous MRS study reported that depressed patients who received chronic lithium treatment had increased NAA brain levels compared to control subjects (Moore et al., 2000). In comparison, another study showed no significant changes in NAA level following chronic lithium treatment, similarly a previous rat brain study also failed to show effects on NAA levels following chronic lithium administration (Brambilla et al., 2004; Lan et al., 2009; O'Donnell et al., 2003).

3.5.6.2. Glutamate and glutamine:

Acute desipramine treatment also significantly decreased levels of the main excitatory amino acid glutamate and its precursor glutamine in the hippocampus. In contrast, in the striatal region their levels were increased while in the prefrontal cortex no significant changes were recorded. Glutamine is stored in the glial cells and taken up by neurons where it is converted to glutamate. The rate of this glutamate-glutamine cycle between cell types in the brain is indicative of glutamatergic neurotransmission (Van Zijl and Barker, 1997). Thus, the observed change in glutamate and glutamine levels may indicate that acute desipramine produces a change in brain glutamatergic activity and that this effect varies in different parts of the brain (decreases in the hippocampus while increases in the striatum). In this respect a number of functional magnetic resonance imaging studies showed alterations in neural activity in

depressed patients, although the reported results were inconsistent (Chang et al., 2004; Strakowski et al., 2005; Yüksel and Öngür, 2010).

3.5.6.3. Myo-inositol, scyllo-inositol and taurine:

Acute desipramine treatment resulted in a significant reduction of both myo-inositol and scyllo-inositol levels in the hippocampus and in contrast a significant increase in their levels were detected in the striatal region. Myo-inositol is an important intracellular osmolyte in the CNS that contributes to maintaining an osmotic balance in the cell by regulating its transport across the plasma membrane (Haris et al., 2011). Furthermore, myo-inositol constitutes an important precursor of the cell membrane inositol containing phospholipids and myelin sheath and also a key marker for glial integrity as it is present in a higher concentration in glia cells compared to neurons (Brand et al., 1993; Chiappelli et al., 2015; Tsang et al., 2006). This essential metabolite is synthesized via the enzymatic action of inositol monophosphatase enzyme which is inhibited by lithium, a mood stabilising drug used in bipolar disorder treatment (Ohnishi et al., 2014; Rango et al., 2008). Moreover, previous brain imaging studies of patients with depressive disorder reported a reduction in myo-inositol level in comparison with healthy controls (Chiappelli et al., 2015; Rango et al., 2008). In addition, taurine, an amino acid which is also involved in the intracellular osmo-regulatory function (Brand et al., 1993; Fisher et al., 2002; Hardy and Norwood, 1998) was similarly to myo-inositol increased in the striatal region by acute desipramine treatment. The observed findings therefore suggest that acute desipramine administration initially alters tissue osmo-regulation and hence may acutely modulate glial cell volume and structure. Possible related to the finding of the present study includes a previous study demonstrating changes in myo-inositol levels in the frontal cortex of depressed patients compared to normal controls, and that such effect was partly reversed by chronic lithium treatment (O'Donnell et al., 2003). Also a significant reduction of myo-inositol level was reported in the striatum and hippocampus of the rat following lithium treatment (Lan et al., 2009).

3.5.6.4. Phosphoryl ethanolamine, choline and phosphoryl choline:

All three of these metabolites are known to be important for the synthesis of membrane phospholipids. Interestingly, alterations in membrane lipid metabolism has been reported in

the brain of patients suffering from bipolar disorder (Frey et al., 2007). In this study, the observed significant changes (Tables 3.3 and 3.4) of these metabolite levels suggest that desipramine may transiently exert a region-specific regulatory role on neuronal membrane phospholipids.

3.5.6.5. Energy metabolism:

Many studies indicate that brain energy metabolism is altered in depressive disorder (Pieczenik and Neustadt, 2007; Stork and Renshaw, 2005). In the current study, several metabolites involved in cerebral energy metabolic pathways were found to be significantly altered following acute desipramine treatment including: lactate, ATP, creatine and phosphocreatine. The observed findings therefore, suggest that acute but not chronic desipramine treatment may target pathways related to cerebral energy production.

3.5.7. Metabolic changes specific to acute paroxetine administration:

Acute paroxetine treatment significantly reduced valine and glucose levels in the hippocampus. In comparison, within the prefrontal cortex there was only a trend by paroxetine to decrease glucose level. However, in the hippocampus, paroxetine significantly reduced ATP, glutamate and valine levels. These metabolites are all known to play roles in various pathways related to energy metabolism and indeed recent studies showed that glutamatergic neurotransmission is of particular importance in this respect (Schousboe et al., 2007; Stork and Renshaw, 2005). Importantly, the glutamate-glutamine cycle is an energy demanding process, hence it is closely linked to cerebral glucose oxidation and energy production (Schousboe et al., 2007). In this context, abnormalities of energy metabolic pathways have recently been identified in depressed patients (Pieczenik and Neustadt, 2007; Stork and Renshaw, 2005). Additionally, in line with our results, a previous *in vivo* study conducted on rat revealed that acute citalopram administration induced a significant reduction of glutamate in the prefrontal cortex following a single intraperitoneal injection at a dose of 20 mg/kg, hence acute SSRI treatment may affect glutamatergic neurotransmission and the excitatory system in the brain (Gołembiowska and Dziubina, 2000).

Myo-inositol:

Acute paroxetine treatment resulted in significant decrease of myo-inositol and serine levels in the rat hippocampus but not in the prefrontal cortex or the striatum which may initially represent a region-specific alteration in tissue osmo-regulatory function within the brain.

3.5.8. Metabolic changes in the brain regions and plasma following chronic administration of paroxetine:

In the present study, while acute paroxetine treatment significantly decreased the level of a number of metabolites in the prefrontal cortex and hippocampus, chronic paroxetine administration clearly revealed fewer metabolic changes in one brain region (see Table 3.6). Thus, in the hippocampus only a significant reduction of succinate was recorded and a trend to decrease myo-inositol level compared to the controls. Further, chronic paroxetine treatment failed to alter metabolite levels in the prefrontal cortex and the striatum as well as in plasma samples which may suggest the occurrence of neuroadaptive changes to the acute metabolic responses seen after short-term paroxetine treatment. Succinate exerts a crucial role in the generation of adenosine triphosphate (ATP) which represents the main source of energy in the mitochondria (Mills and O'Neill, 2014). Together with the finding of the present study that acute paroxetine changes levels of some metabolites including valine, glucose and ATP which likewise succinate are related to energy metabolism, it is likely that metabolic pathways involved in the generation of energy are targeted by paroxetine. Further, it is possible that this drug effect is related to its therapeutic action. In support of this, a recent animal study demonstrated that chronic paroxetine treatment normalizes the increase of hippocampal energy metabolism in a stress model of depression in rats (Khedr et al., 2015). Additionally, chronic paroxetine administration resulted in a non-significant hippocampal reduction in myo-inositol level which is an important marker for glial integrity (Tsang et al., 2006). This effect may reflect the possible role of paroxetine in modulating the tissue osmo-regulatory function as well as glial cells structure.

3.5.9. Metabolic changes in the brain regions and plasma following chronic administration of desipramine:

Chronic desipramine treatment, in contrast to its acute administration which revealed a number of changes of water soluble brain metabolite levels (see Tables 3.3 and 3.4), failed to show any significant differences between chronically treated rats and their corresponding controls within the explored brain regions. In addition, spectral analysis of the plasma samples obtained from the chronic desipramine group showed a significant increase in the level of creatinine only.

Our results with the TCA desipramine and the SSRI paroxetine are in contrast to a previous study, investigating the metabolic profile following chronic administration of a different TCA namely imipramine and the SSRI fluoxetine. Similar to this study, Zhao et al, treated rats for two weeks although in contrast to the present study they reported significant down regulation of: leucine, valine, glutamic acid, aspartic acid, glycine, NAA, and lysine within the hippocampus by both drugs while fluoxetine also significantly reduced myo-inositol levels (Zhao et al., 2015). The discrepancy between our study and the study by Zhao et al, might be explained by the fact that we used normal rats while their study was conducted on ''stressed'' rats which in itself could have caused neuroadaptive changes resulting in a modified response to chronic antidepressant drug administration (Herman, 2013). In addition, a recent brain imaging study utilizing the MRI technique indicated a widespread activation throughout specific brain regions including the cerebral cortex and the hippocampus after acute citalopram administration in rats. However, localization of the reported changes was observed following chronic treatment which may suggest the development of neuroadaptive responses (Sekar et al., 2011). In this respect, a recent experimental study conducted on the frontal cortex of freely moving mice utilising the *in vivo* microdialysis technique revealed that a single antidepressant drug administration (paroxetine, citalopram or venlafaxine at three different doses: 1, 4 and 8 mg/kg, i.p) induced a pronounced increase in the extracellular levels of 5-HT and NA in the cortical dialysates. An effect that would be expected to occur by the blockade of 5-HT and NA transporters (David et al., 2003).

While acute antidepressant drug administrations caused widespread changes of several brain metabolites in the present study, the lack of response by chronic treatment could possibly reflect the onset of a neuroadaptive effect by the drug following chronic administration. In parallel with this observation, a previous animal study recorded that chronic desipramine treatment has been indicated to promote adaptive changes in specific brain regions, especially in the hippocampus of rats (Sacchetti et al., 2001). Such adaptive response in the noradrenergic neurons, have been shown to encompass down-regulation of the presynaptic inhibitory α_2 autoreceptors and the postsynaptic β-adrenergic receptors following chronic administration of antidepressant drugs including the TCAs (Hyman and Nestler, 1996; Sacchetti et al., 2001; Schultz et al., 1981; Sulser et al., 1978; Taylor et al., 2005). Thus, initially, acute antidepressant treatment (TCA) increases the synaptic levels of noradrenaline by blocking its transporter function which will cause hyper-stimulation of presynaptic α_2 autoreceptors as well as postsynaptic β-adrenergic receptors. Subsequently, this response will result in phosphorylation of the stimulated receptors through activation of specific synaptic enzymes, namely the G protein-coupled receptor kinases leading to desensitization of these receptors (Lefkowitz, 1993). In addition, acute SSRI administration increases the synaptic level of 5-HT via blocking the serotonin transporter, which in turn activates the presynaptic inhibitory receptors (i.e. the somatodendritic 5-HT1A autoreceptors) resulting in a decreased serotonergic neurotransmission at the level of the raphe nuclei, the origin of the 5-HT neurons. Accordingly, these 5-HT1A autoreceptors also become desensitised and hence contributing to the subsequently elevated 5-HT level. This enhancement of 5-HT neurotransmission is attributed to the completely recovered firing activity of the serotonergic neurons as a consequence of long-term drug exposure (2-3 weeks of treatment) (Blier and de Montigny, 1994; Mnie-Filali et al., 2013; Sekar et al., 2011).

3.6. Conclusion:

The current study was aimed at the detection of drug-induced alterations of water soluble metabolites using ^{1}H NMR following the administration of two antidepressant drugs by either acute or chronic treatment. The findings of the study show that both acute paroxetine and desipramine treatment influence the brain levels of a number of metabolites involved in important mechanisms of the brain including: energy consumption, neurotransmission and neuronal integrity. The study investigated the effect of two antidepressant drugs in three separate brain regions relevant to depression and its treatment namely: prefrontal cortex, hippocampus and the striatum. Overall, the recorded changes of metabolite levels following an acute injection varied, depending on both brain regions and drug type. However, these observed drug-associated metabolic responses were not maintained after chronic treatment which may suggest the occurrence of neuroadaptive changes following repeated drug administrations. Further studies are needed to better understand if these acute effects of paroxetine and desipramine on functionally important brain metabolites are part of a chain of events resulting in the therapeutic effect or even the undesirable adverse effects seen after chronic treatment in patients.

CHAPTER 4

LC-MS and HPLC-UV analysis of sphingosine and ceramide content in rat brain following acute and chronic antidepressant drug treatment

4.1. Introduction:

The main structural components of all biological membranes are proteins, lipids and small amounts of carbohydrates. In mammalian cells, the plasma membrane lipids are predominantly composed of phospholipids and cholesterol (Fahy et al., 2005). Phospholipids are divided into two major families: glycerophospholipids with the glycerol backbone and sphingophospholipids which contain the sphingoid base backbone. Sphingophospholipids (or sphingolipids) are bioactive compounds that contain sphingoid bases (SBs) which are di- or trihydroxy long chain alkanes of 14 to 22 carbon atoms linked to longer chain fatty acids (Figure 4.1) (Gault et al., 2010). Sphingoid bases encompass 60 different species where sphingosine, phytosphingosine or sphinganine are the main distinctive SBs. The wide array of sphingolipids results from the possible variation in the sphingoid base type, position and number of the double bonds, hydroxyl groups and the length of the fatty acid chains (Gault et al., 2010; Kolter and Sandhoff, 1999). Ceramide belongs to a class of hydrophobic sphingolipid molecules that represent a central core in sphingolipid biosynthetic pathways as well as an important precursor of other simple sphingolipid species including sphingosine and sphingosine-1-phosphate (Gault et al., 2010). A growing body of evidence indicates an important role of these highly bioactive molecules in a wide range of vital cellular functions including cell signaling and synaptic neurotransmission (see Chapter One, section 1.10.1) (Dinoff et al., 2017; Gracia-Garcia et al., 2011; Müller et al., 2015; Schneider et al., 2017). Additionally, ceramide may contribute to functions related to membrane permeability by interacting with specific ion channels (see Chapter One, section 1.10.3) (Gulbins et al., 1997; Lepple-Wienhues et al., 1999; Tsui-Pierchala et al., 2002). In addition, it has been shown that ceramide could be involved in the regulation of growth arrest (Dinoff et al., 2017) as well as apoptosis or programmed cell death that occurs specifically in the mitochondria (see Chapter One, section 1.10.2) (Pettus et al., 2002; Ruvolo, 2003).

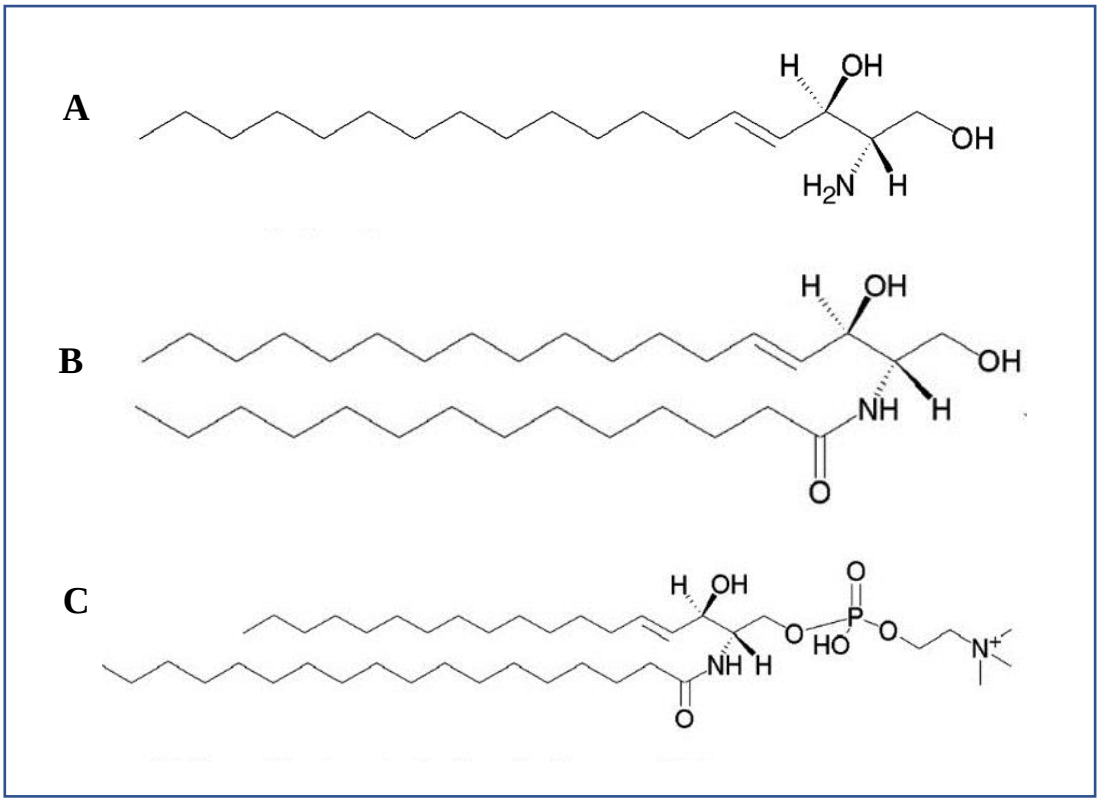

Figure 4.1: Chemical structure of sphingolipids. (A) Sphingosine. (B) Ceramide (N-acylsphingosine). (C) Sphingomyelin (ceramide phosphocholine) (Fahy et al., 2005).

4.1.1. Sphingolipid biosynthesis:

Ceramide or N-acyl sphingosine is the essential building block of the sphingolipids and can be generated through three main pathways (Gault et al., 2010) as illustrated in Figure 4.2 and outlined below:

4.1.1.1. Lysosomal sphingomyelin hydrolysis:

Sphingomyelin constitutes a major and complex sphingolipid component of the cellular plasma membrane in the brain. The degradation of sphingomyelin (utilised as a substrate) into ceramide and phosphorylcholine particularly within the membrane lipid rafts is catalysed via the activity of the acid sphingomyelinase enzyme (also known as sphingomyelin phosphodiesterase which is encoded by the SMPD1 gene), a process that is enhanced in response to stress (i.e. food deprivation for 24 hour) (Grassmé et al., 2015; Gulbins et al., 2015; Kornhuber et al., 2014). Interestingly, it was found that this pathway represents the most common way of ceramide production (Dinoff et al., 2017; Goñi and Alonso, 2002).

4.1.1.2. The *de novo* pathway:

The *de novo* biosynthesis of ceramide is initiated by the condensation of the amino acid serine and the fatty acid palmitate to form 3-ketodiydrosphingosine (3-ketosphinganine) through the action of the rate-limiting enzyme serine palmitoyltransferase in the cytoplasm of the endoplasmic reticulum (the main site for lipid biosynthesis) (Hanada, 2003). Subsequently, 3-ketosphinganine is reduced to sphinganine (diydrosphingosine) via the enzyme 3-ketosphinganine reductase (3-ketodihydrosphingosine reductase). Then, sphinganine is acylated by the enzyme dihyro ceramide synthase to produce dihydroceramide (Pewzner-Jung et al., 2006). Eventually, the last reaction in ceramide production is catalysed by the action of the enzyme dihydroceramide desaturase to generate ceramide (Rother et al., 1992). Subsequently, a cytoplasmic transfer protein namely the ceramide transporter (CERT) mediates the transport of ceramide from the endoplasmic reticulum to the Golgi apparatus where ceramide undergoes further conversion to liberate other complex sphingolipids such as sphingomyelin (Hanada, 2006).

4.1.1.3. The salvage pathway:

This pathway includes the lysosomal hydrolysis of complex sphingolipids such as: glucosylceramide (formed by adding a glucose molecule to ceramide) and sphingomyelin which results eventually in the production of sphingosine (the major product of ceramide catabolism) (Gault et al., 2010; Tafesse et al., 2006). The sphingosine released from the lysosome is then reused through recycling or re-acylation to serve as a substrate for further regeneration of ceramide in the endoplasmic reticulum via the action of the ceramide synthase enzyme (Kitatani et al., 2008; Tettamanti, 2004).

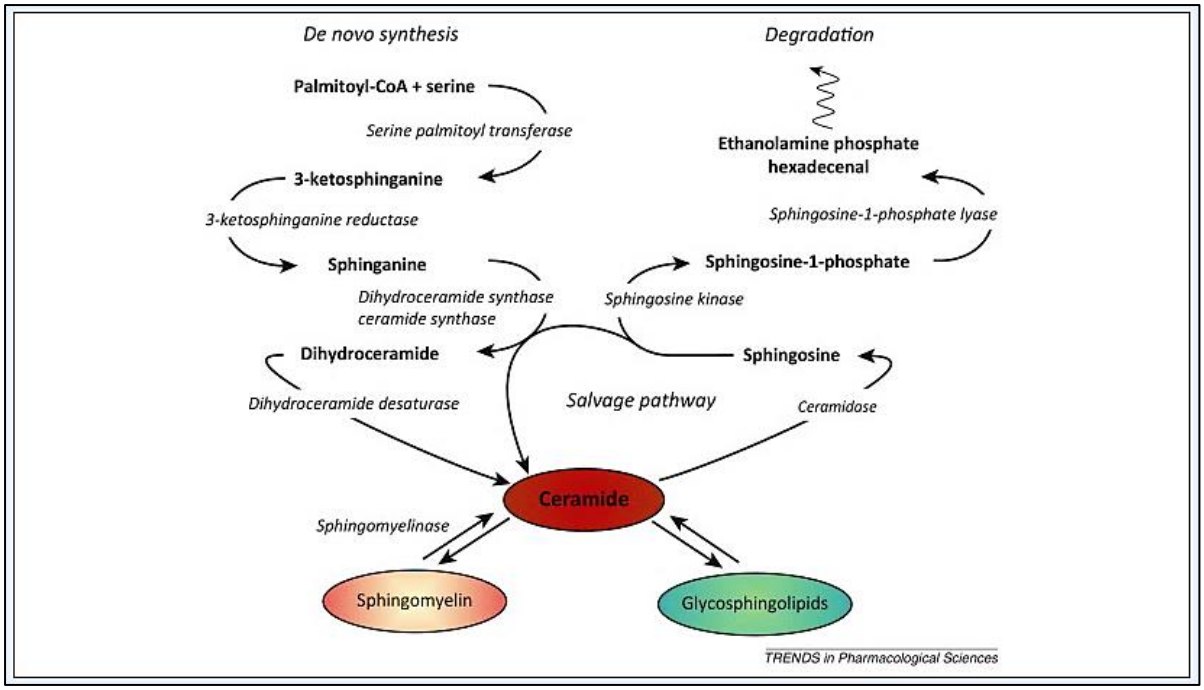

Figure 4.2: The biosynthetic pathways of sphingolipids (Kornhuber et al., 2014).

4.1.2. Biological functions of sphingosine:

Sphingosine (the main metabolite of ceramide) is a simple sphingolipid molecule produced within the plasma membrane, lysosomes, endoplasmic reticulum and the Golgi complex by degradation of ceramide through the action of the enzyme acid ceramidase (Gault et al., 2010; Sun et al., 2008). Sphingosine has been reported to be implicated in the process of apoptosis (see Chapter One, section 1.10.2.1) (Cuvillier, 2003; Suzuki et al., 2004) as well as in the pathogenesis of a neurodegenerative disease termed Niemann-Pick disease type C1 (NPC1) (te Vruchte et al., 2004). This disease is an inherited lysosomal storage disease characterized by accumulation of various lipids such as sphingosine, sphingomyelin and cholesterol with a concomitant reduction in the calcium concentration within the lysosomes compared to normal cells (Höglinger et al., 2015; Lloyd-Evans et al., 2008; te Vruchte et al., 2004). A recent study conducted on both human and mouse cultured fibroblast cells with sphingosine incubation observed that an acute increase of sphingosine levels was immediately followed by an enhanced release of lysosomal calcium compared to cells not incubated with sphingosine (Höglinger et al., 2015). This intracellular response was found to trigger autophagy (a controlled destruction of proteins and other cellular components) (Höglinger et al., 2015).

Furthermore, the increased calcium level was shown to promote a translocation of the transcription factor EB (TFEB) to the cellular nucleus and consequently activating genes that are involved in the process of autophagy (Höglinger et al., 2015; Medina et al., 2015). Additionally, it was reported that two proteins located on the surface of the lysosomes, two-pore channel 1 and 2 (TPC1) and (TPC2), were activated by the action of the sphingosine. Subsequently, they may act as channels to allow the release of calcium ions from the lysosome, thus mediating a reduced lysosomal calcium concentration following a significantly increased sphingosine level within these organelles which is a known feature in Niemann-Pick disease type C1 patients (Höglinger et al., 2015; Lloyd-Evans et al., 2008).

In the current study, initially it was planned to employ liquid chromatography coupled with mass spectrometry (LC-MS) approach to explore the effect of acute and chronic antidepressant drug treatment on ceramide content in lipid samples extracted from rat brain. However, the limitations of the operating LC-MS system available failed to detect molecules with a mass exceeding 500. Since ceramide has a molecular weight of 567, it was not possible to use this technique for the direct quantification of ceramide content. Instead, sphingosine which represents the major metabolic product of ceramide as well as its precursor in the salvage pathway of ceramide synthesis (see Figure 4.2) was measured using the LC-MS technique. Sphingosine has a molecular mass of 300 and hence could be directly quantified using the equipment available within the School of Pharmacy. Subsequently, measurements of ceramide content in hippocampal brain samples following antidepressant drug treatment was successfully undertaken via the development of an already published method (Couch et al., 1997; Iwamori et al., 1979). Thus, ceramide analysis was achieved by means of chemical derivatisation of the extracted ceramide followed by high-performance liquid chromatography with ultraviolet detection technique (HPLC-UV). Additional studies were undertaken to confirm the proposed correlation between these two measured sphingolipid molecules.

4.1.3. Ceramide, biological functions and depression:

Recently, the major lipid components of the cell membrane: sphingolipids, particularly ceramide species have been focussed on for their implication in depression (see Chapter One, section 1.8) (Dinoff et al., 2017; Gulbins et al., 2013, 2015). In the cell membranes, these bioactive hydrophobic molecules aggregate in organized membrane compartments termed lipid rafts which may consequently, merge to form larger ceramide-rich platforms. These membrane platforms permit re-organisation and clustering of numerous proteins and signaling molecules including receptors (i.e. G-protein coupled receptors, GPCRs) and thereby, altering neuronal firing and signal transduction (see Chapter One, section 1.9) (Dinoff et al., 2017; Gulbins et al., 2013, 2015; Schneider et al., 2017). In this respect, these ceramide-rich platforms play important role in various biological functions such as cell signaling and monoamine neurotransmission, also affecting membrane permeability by regulating ion channels, in particular the calcium channels as well as the potassium channels (i.e. Kv 1.3) (see Chapter One, section 1.10) (Dinoff et al., 2017; Müller et al., 2015; Schneider et al., 2017; Tsui-Pierchala et al., 2002). In addition, ceramide exerts an essential role in vital cellular mechanisms such as growth arrest and apoptosis (see Chapter One, section 1.10.3) (Pettus et al., 2002; Ruvolo, 2003). Furthermore, recent studies indicate that lipid rafts are the main site for the activation of the enzyme acid sphingomyelinase (ASM) which in turn results in the enhancement of ceramide generation and the subsequent formation of the membrane ceramide-rich platforms (Gulbins et al., 2015; Schneider et al., 2017). Growing evidence suggests that many antidepressant drugs induce inhibition of ASM by promoting a proteolytic degradation of this enzyme (Dinoff et al., 2017; Gulbins et al., 2013, 2015). Consistent with these emerging findings, a previous animal study reported that administration of the antidepressant drugs: amitriptyline and fluoxetine at therapeutic plasma concentrations inhibited the activity of the enzyme ASM resulting in reduced ceramide concentrations in the hippocampus. This was coincided with a reduction of depression-like behaviours in a mouse model of depression (Gulbins et al., 2013). Overall, more studies are required to fully understand the role of ceramide in depression and its therapeutic intervention.

4.1.4. Aim:

With the recent findings in hindsight that sphingolipids could be implicated in depression and its treatment, the present study was aimed at investigating the effect of acute and chronic antidepressant drug treatment on brain levels of two of the bioactive lipid molecules in the sphingolipid pathway namely: ceramide and its major metabolite sphingosine in the rat. The experiments were designed to test the hypothesis that chronic antidepressant drug treatment lowers the brain level of the sphingolipid molecules, specifically ceramide and sphingosine. In order to assess this, the below experiments were performed:

- By using the LC-MS technique, levels of sphingosine were determined in regional brain extracts and plasma samples from groups of rats treated with acute or chronic antidepressant drugs namely, the SSRI paroxetine or the TCA desipramine.
- The effects of antidepressant drug treatment on sphingosine level in cultured mouse macrophages cells was investigated via the LC-MS.
- An HPLC-UV method was developed for the measurements of ceramide in hippocampal brain extracts from rats treated chronically with the SSRI paroxetine.

4.2. Materials and method:

4.2.1. Sphingosine analysis by liquid chromatography coupled with mass spectrometry (LC-MS):

4.2.1.1. Sphingosine analysis in cultured mouse macrophages:

The preparation of the cultured cells for the sphingosine analysis using the LC-MS technique was based on previously published protocols (Couch et al., 1997; Elojeimy et al., 2006; Shaner et al., 2009). Mouse macrophages cell line (RAW 264.7), a common type of the monocyte-derived cell line was used in this limited preliminary study to test the effect of two antidepressant drugs (desipramine and paroxetine) treatment at a concentration of 10 µM on sphingosine content after 30 minutes or 60 minutes incubation periods and prior to a detailed animal study. The cells were cultured (at 5 x 10^5 cells/ml) and were grown in RPMI culture medium (Fisher Scientific, UK), which was supplemented with 200 µg/ml streptomycin and 200 units/ml penicillin. The frozen cells were collected from the liquid nitrogen, then the stored vial was thawed in a warm water bath. In a sterilized cell culture hood, the cell

suspension was transferred from the vial for incubation in a humidified incubator under controlled conditions: 95% relative humidity, 5% CO_2 and a temperature of 37˚C. Subsequently, the cultured cells were split and regularly examined under the microscope every day for any sign of contamination. The investigated antidepressant drugs: desipramine and paroxetine were added to the cultured cells at a concentration of 10 µM (Elojeimy et al., 2006) and were incubated for 30 minutes or 60 minutes under the same conditions. Following the specified incubation periods, the cells were washed several times with an ice-cold phosphate buffered saline (PBS) and centrifuged at 500 g for 5 minutes at room temperature. The supernatants were then removed, and the residues were stored at - 80˚C for a subsequent lipid extraction and LC-MS analysis. The frozen cell pellets were thawed and re-suspended in 500 µl of cold PBS, then lipids were extracted using the described method in Chapter Two, section 2.3.2.

4.2.1.2. Sample preparation and lipid extraction:

Full details of animal housing conditions, drug administration, brain dissection and samples collection are described in Chapter Two, section 2.1, whereas the sample preparation and the subsequent lipid extraction procedure is described in detail in Chapter Two, section 2.3.2. For both acute and chronic treatment studies, male Sprague-Dawley rats (266-301 g body weight) were separated into four groups, each comprising 12 animals. Rats were housed four animals per cage. Two antidepressant drugs were utilized in this study: paroxetine, a selective serotonin reuptake inhibitor (SSRI) was administered at 5 mg/kg intraperitoneally (i.p). The other drug: desipramine, a tricyclic antidepressant (TCA) was administered at 10 mg/kg i.p. The control animals received i.p saline 0.9 % (1ml/kg). In the acute study, treatment was administered once only, and the rats were sacrificed 1 hour later. In the chronic study, treatment was repeated once daily at 10 a.m. for 15 consecutive days and the rats were sacrificed 1 hour after the final injection. Consequently, blood samples were collected immediately after lesion of the jugular vein and the whole brain was dissected out rapidly on ice into three specific brain regions: prefrontal cortex, hippocampus and the striatal region. The brain samples were rapidly frozen using isopentane cooled with dry ice, weighed and then stored with the blood samples at - 80°C for subsequent lipid analysis. Lipid extraction

was based on a previously published method (Bligh and Dyer, 1959; Merrill et al., 2005; Sullards et al., 2011) and was fully described in Chapter Two, section 2.3.2.

4.2.1.3. LC-MS protocol:

The liquid chromatographic separation conditions, the optimal MS conditions, type of columns and the mobile phases used in the performed LC-MS analysis are described in detail in Chapter Two, section 2.3.3. Because of the restriction of the operating LC-MS, it was impossible to detect and analyse C18 ceramide (molecular mass = 566.7 g/mol) on the selective ion monitoring mode (SIM) with the available equipment. However, LC-MS analysis of the main ceramide metabolite, sphingosine (m/z 300.4) was achievable. Thus, detection and quantification of sphingosine content was carried out in the extracted lipid samples which was confirmed by the m/z value (mass-to-charge ratio) and the retention time of sphingosine standards (Figure 4.3). The Bradford assay was used to determine the total protein concentration in each sample and subsequently, was used as a normalizing parameter to quantify the sphingosine concentration in the investigated samples (see Chapter Two, section 2.3.5).

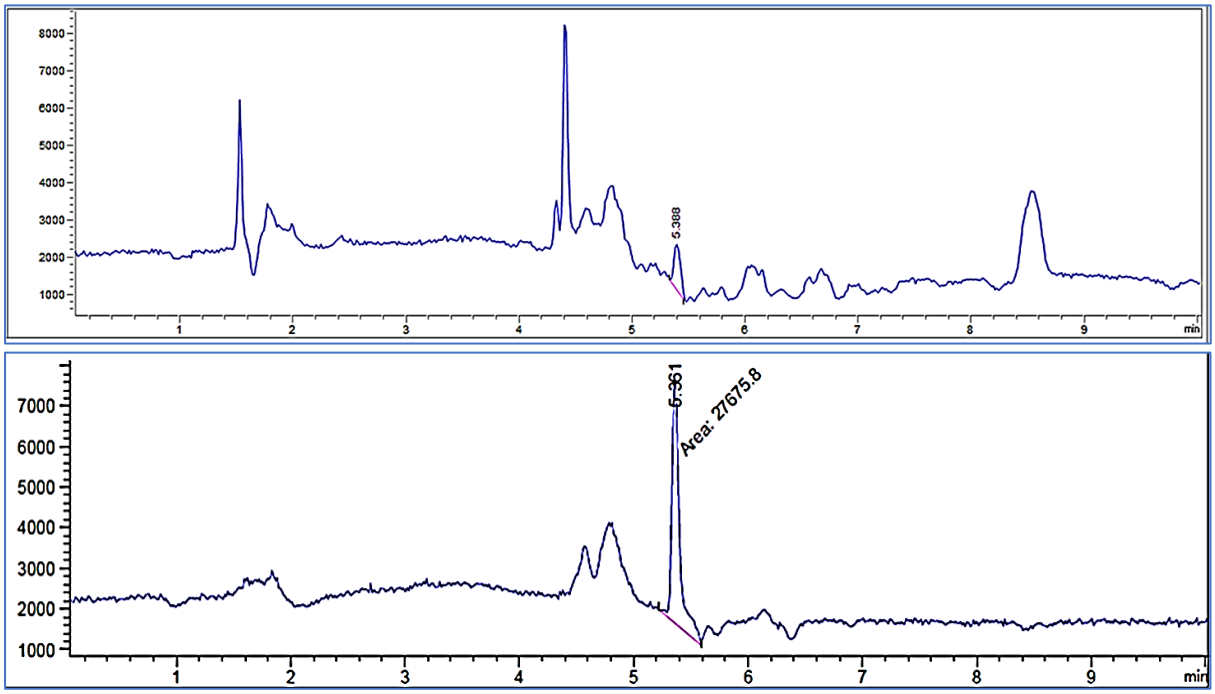

Figure 4.3: Lower: Sphingosine standard peak at a concentration of 40 mg / L and a retention time of 5.361 minute. Upper: LC-MS chromatogram of hippocampal tissue obtained from a rat following chronic desipramine treatment; showing sphingosine peak at a retention time of 5.388 minute.

4.2.1.4. Data presentation and statistical analysis:

Datasets generated from the LC-MS study of the sphingosine were analysed statistically either by two-way analysis of variance (two-way ANOVA with Bonferroni post-hoc test) or via one-way analysis of variance (one-way ANOVA followed by Bonferroni post-hoc test) for multiple comparison. On the other hand, statistical analysis of the HPLC-UV ceramide data was established by means of the Student's t-test, data obtained from both sphingosine and ceramide study were tested using Prism 5.0 Software (Graph Pad Prism Software, version 5). Values were presented as means ± standard errors of the mean (SEM) for each group and they were expressed as mg sphingosine or ceramide/mg protein in all the analysed samples (using the area under the peak for each integrated signal). Statistically significant difference was considered at a level of $p < 0.05$.

4.2.1.5. Calibrations for quantitative analysis of sphingosine:

Determination of sphingosine concentration after generating a standard curve was performed with each analysed group of samples, together with the used standards, chemicals and solvents in the sphingosine assay are fully described in Chapter Two, section 2.3.5 and section 2.3.6.

4.2.2. Ceramide analysis by high-performance liquid chromatography with ultraviolet detection (HPLC-UV):

Direct quantitation of ceramide via high-performance liquid chromatography with ultraviolet detection method (HPLC-UV) was not feasible due to the lack of a UV-absorbing chemical group at a specific wave length region within the ceramide molecule. Therefore, a benzoylation reaction was performed to allow a quantitative analysis of the resultant ceramide benzoates at 230 nm using the HPLC-UV technique (Figure 4.4). This method was successful albeit time consuming and required the use of carcinogenic chemicals such as pyridine and benzoyl chloride and, hence experiments had to be performed in a fume cupboard (Cremesti and Fischl, 2000).

4.2.2.1. Sample preparation and benzoylation of ceramide:

The procedure for ceramide quantification following a benzoylation reaction using HPLC-UV used in this study relied on a number of previously published method (Couch et al., 1997; Iwamori et al., 1979; Ogawa et al., 2010; Tepper and Blitterswijk, 2000). For a full description of the performed method involving preparation of samples, the ceramide benzoylation steps, HPLC protocol, the generated standard curves and the utilized reagents and chemicals see Chapter Two, section 2.4.2, section 2.4.3 and section 2.4.4 respectively.

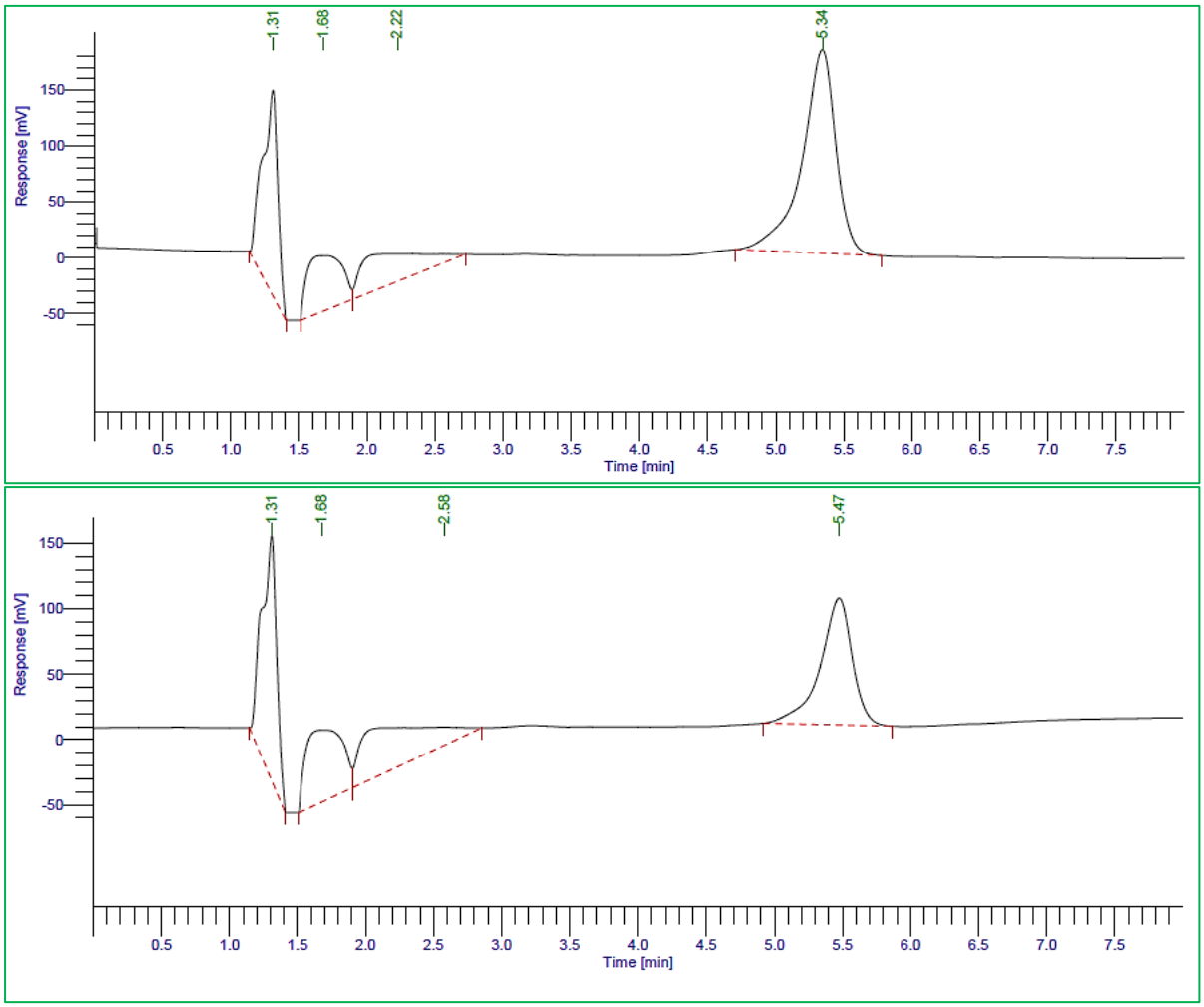

Figure 4.4: Lower: UV-HPLC chromatogram of a hippocampal sample obtained from a control animal showing the ceramide peak at a retention time of 5.47. Upper: ceramide standard peak at a concentration of 40 mg/L and a retention time of 5.34 minute.

4.3. Results:

4.3.1. LC-MS analysis of sphingosine in rat brain and plasma following acute and chronic antidepressant drug administration:

4.3.1.1. Regional differences in the basal sphingosine level among the control groups in rat brain:

Prior to the evaluation of the sphingosine level in rat brain and plasma samples following short and long-term antidepressant drug treatment, a reliable assessment of the basal sphingosine level was performed among all the acute as well as the related chronic control groups by means of the LC-MS technique. Statistical analysis using one-way analysis of variance (one-way ANOVA) with Bonferroni t-test for multiple comparison showed that the expression of this sphingolipid molecule follows a region-specific manner. The present study found that there was a clear distinction in the basal level of sphingosine in the brain regions examined (PFC, HP and ST). Accordingly, acute control data analysis indicated that there was a significantly lower basal sphingosine content in the striatum compared to its recorded level in the other two brain regions (the PFC and HP) ($p = 0.001$, $F(2,68) = 7.243$) (Figure 4.5).

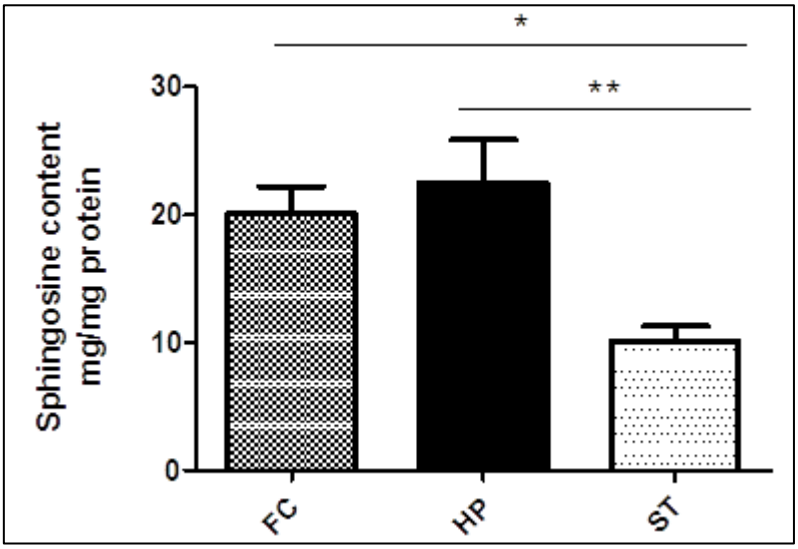

Figure 4.5: Basal sphingosine content (mg/mg protein) in the three investigated brain regions in the acute control groups. All values represent mean ± SEM (n = 24). Abbreviations: PFC, prefrontal cortex; HP, hippocampus and ST, striatum. * $P < 0.05$ and ** $p < 0.01$ (one-way ANOVA with Bonferroni t-test).

Also, a similar expression level was observed by analysing the chronic control groups (p = 0008, F (2,67) = 7.890) (Figure 4.6).

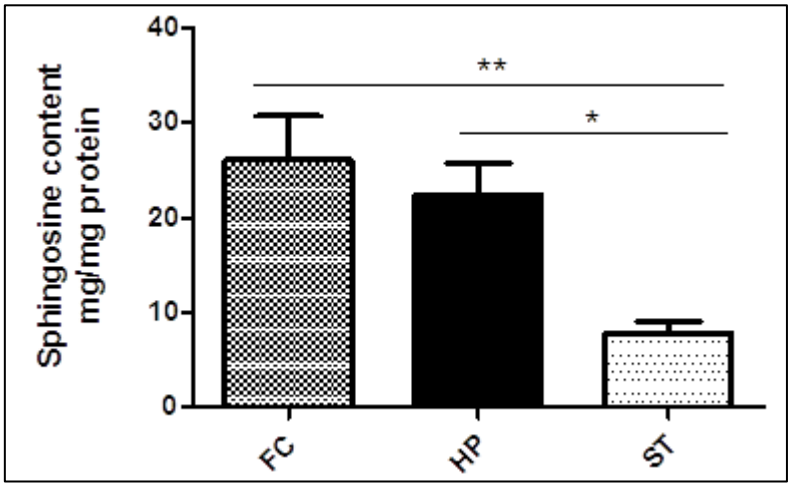

Figure 4.6: Basal sphingosine content (mg/mg protein) in the three investigated brain regions in the chronic control groups. All values represent mean ± SEM (n = 24). Abbreviations: PFC, prefrontal cortex; HP, hippocampus and ST, striatum. * P < 0.05 and ** p < 0.01 (one-way ANOVA with Bonferroni t-test).

Additionally, to exclude the possible stressful effect of the repeated animals handling as well as their daily injections on the analysed sphingosine level, a subsequent comparison of the acute saline-treated rats with the corresponding chronic control animals was established using two-way ANOVA followed by Bonferroni t-test. Consequently, no significant alteration in basal sphingosine level was detected between the overall acute and the relevant chronic saline-injected controls (p = 0.70) (Figure 4.7).

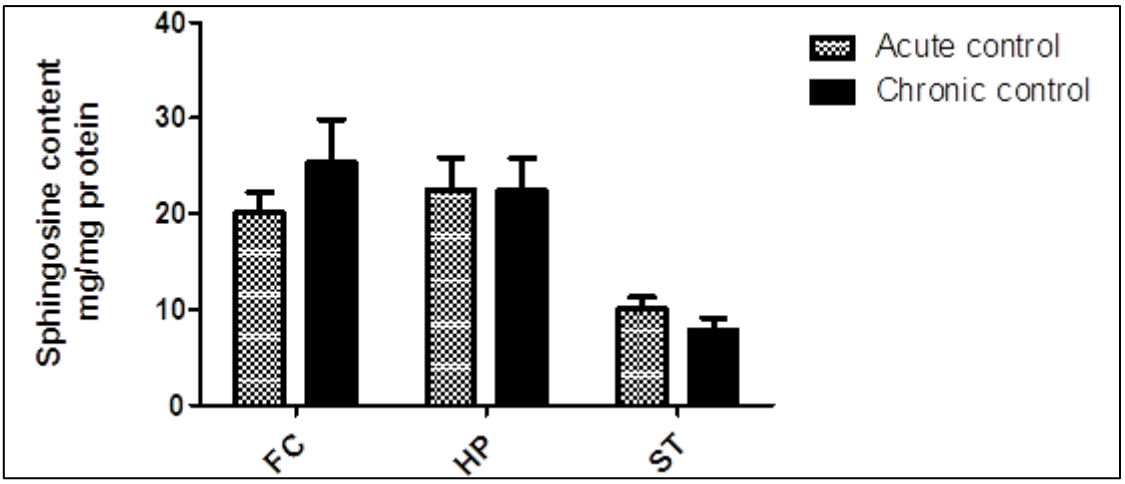

Figure 4.7: A comparison of the basal sphingosine content (mg/mg protein) in the three investigated brain regions following both acute and chronic saline administration. All values represent mean ± SEM (n = 24). Abbreviations: PFC, prefrontal cortex; HP, hippocampus and ST, striatum.

4.3.1.2. Effect of acute and chronic paroxetine treatment on sphingosine level in rat brain:

In the present study, for the two antidepressant drugs tested, two-way analysis of variance (two-way ANOVA) was performed for each analysed treatment group to test for the effects of treatment (paroxetine or desipramine versus saline) and brain region (the prefrontal cortex, hippocampus and striatal regions). Two-way ANOVA indicated a clearly significant effect of brain region on sphingosine level following acute paroxetine treatment ($p < 0.0001$, $F(2,64) = 12.78$) without a statistically significant interaction effect between the two assessed variables (i.e. no brain region versus treatment interaction). The highly significant effect of brain region detected is possibly related to the observation that the striatum had a significantly lower sphingosine level compared to the other two brain regions including the prefrontal cortex and hippocampus and this was seen following acute administration of paroxetine as well as desipramine in both acute treatment groups (see Chapter Four, section 4.3.1.1). Subsequently, the Bonferroni post hoc analysis did not show any statistically significant changes in the level of sphingosine within any of the three investigated brain regions after acute treatment with paroxetine (Figure 4.8 and Table 4.1) compared to the saline treated controls.

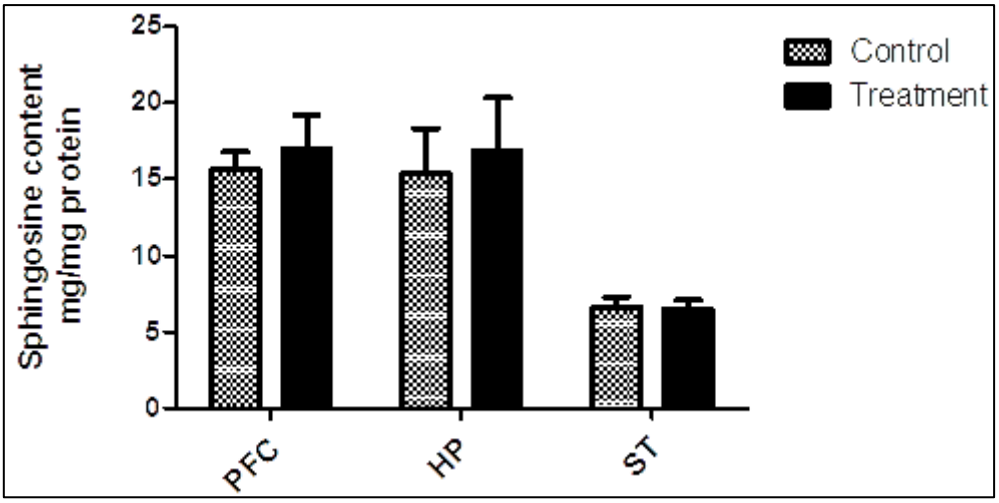

Figure 4.8: Sphingosine content (mg/mg protein) in brain of rats following acute paroxetine treatment. All values represent mean ± SEM (n = 12). Abbreviations: PFC, prefrontal cortex; HP, hippocampus and ST, striatum.

Similar to the effect observed with the acute paroxetine administration data, two-way ANOVA following chronic treatment of this SSRI revealed a clearly significant effect of brain region

($p < 0.0001$, $F(2,65) = 18.42$) (Figure 4.9). In contrast to acute treatment of paroxetine, post-hoc analysis using the Bonferroni t-test indicated a significant paroxetine induced decrease in sphingosine content in both the prefrontal cortex ($p < 0.001$) (Figures 4.9, 4.12 and 4.13) and hippocampus ($p < 0.001$) (Figures 4.9 and 4.14). This was however, not seen in the striatum, where chronic paroxetine treatment failed to significantly reduce sphingosine levels compared to the corresponding control group (Figure 4.9).

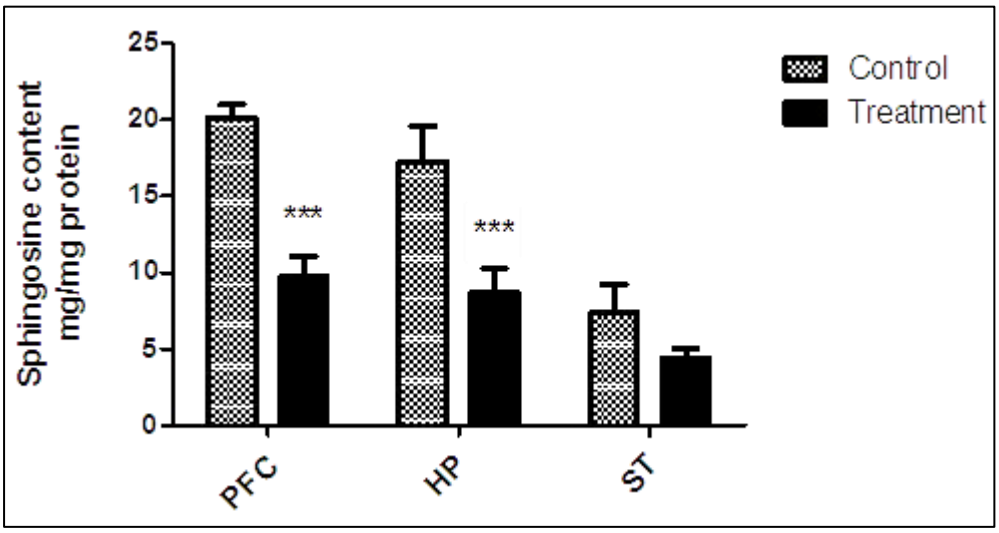

Figure 4.9: Sphingosine content (mg/mg protein) in brain of rats following chronic paroxetine treatment. All values represent mean ± SEM (n = 12). Abbreviations: PFC, prefrontal cortex; HP, hippocampus and ST, striatum. *** $P < 0.001$ for both the PFC and HP but not significant for the striatum (two-way ANOVA with Bonferroni t-test).

To compare the effects of acute and chronic paroxetine administration, two-way ANOVA was undertaken within each brain region. In prefrontal cortex there was a highly significant interaction between treatment and duration ($p < 0.001$, $F(1,42) = 10.94$) and the Bonferroni t-test indicated a significant reduction in sphingosine level after chronic but not acute treatment (Figure 4.10 and Table 4.1).

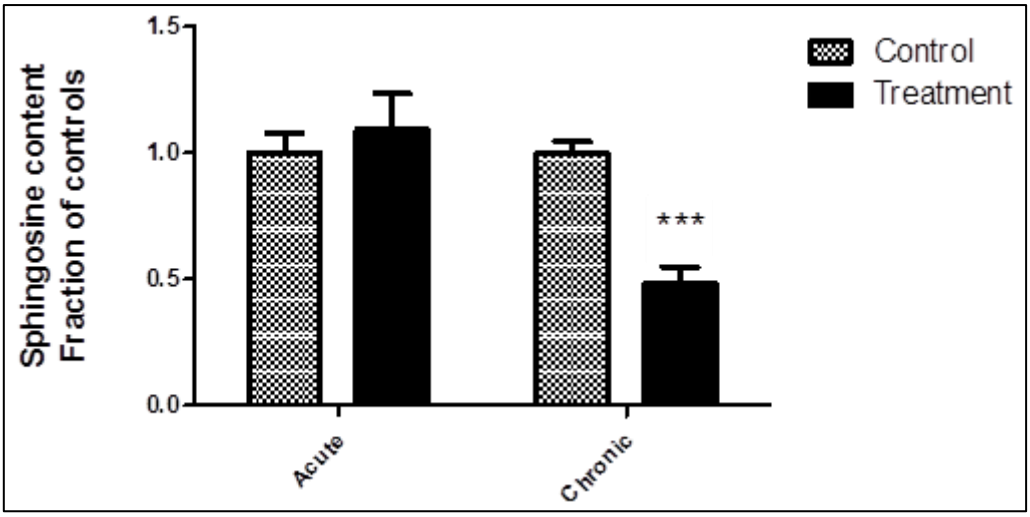

Figure 4.10: Sphingosine content (mg/mg protein) in the prefrontal cortex following acute and chronic paroxetine treatment. All values represent fraction of controls ± SEM (n = 12). Abbreviations: PFC, prefrontal cortex; HP, hippocampus and ST, striatum. *** P < 0.001 for the chronic paroxetine group (two-way ANOVA with Bonferroni t-test).

In the hippocampus, the interaction effect between treatment and duration did not quite reach statistical significance (p = 0.086, F (1,44) = 3.095) and although, qualitatively similar changes were seen as in PFC, these were not statistically significant according to the Bonferroni test (Figure 4.11 and Table 4.1).

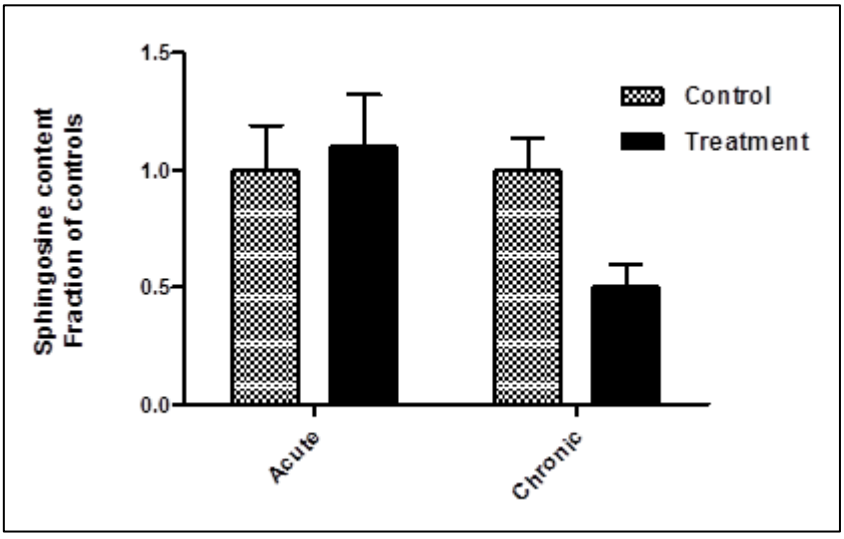

Figure 4.11: Sphingosine content (mg/mg protein) in the hippocampus following acute and chronic paroxetine treatment. All values represent fraction of controls ± SEM (n = 12). Abbreviations: PFC, prefrontal cortex; HP, hippocampus and ST, striatum.

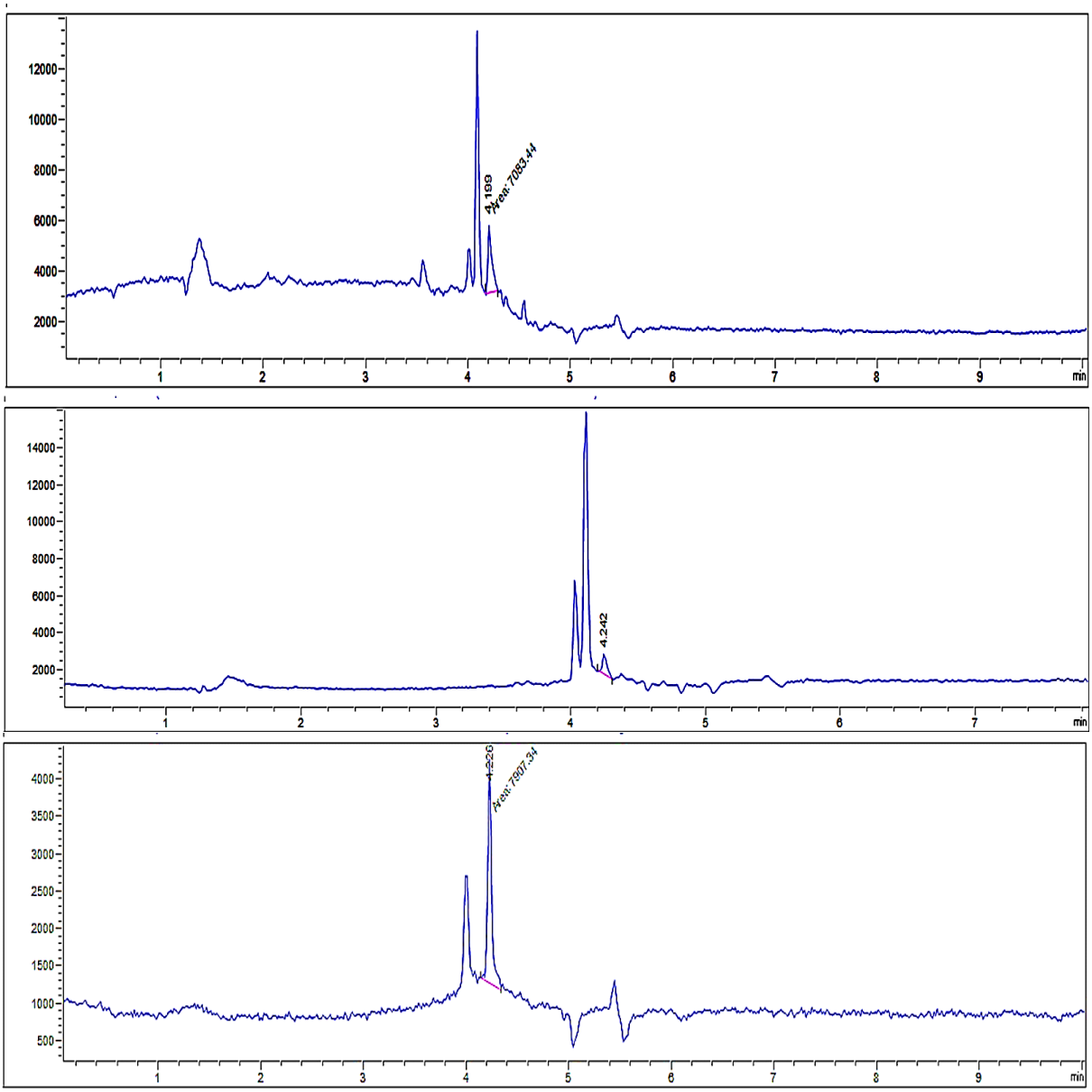

Figure 4.12: LC-MS chromatogram of frontal cortical samples obtained from upper: control and middle: treated rat following chronic paroxetine administration showing sphingosine peak at a retention time of 4.199 and 4.242 minute respectively. Lower: LC-MS chromatogram showing sphingosine standard peak at a concentration of 10 mg/L and a retention time of 4.226 minute.

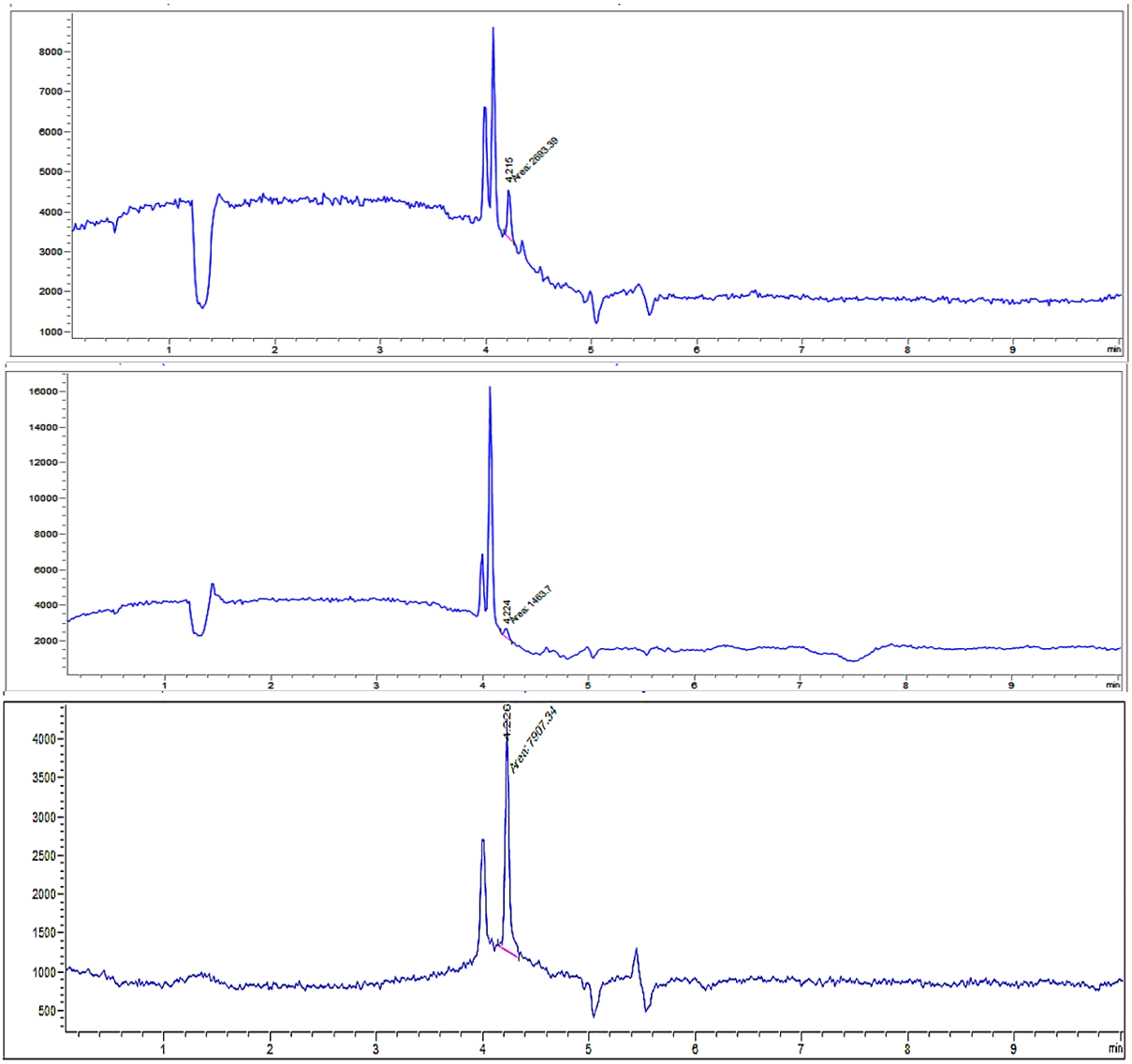

Figure 4.13: LC-MS chromatogram of frontal cortical samples obtained from upper: control and middle: treated rat following chronic paroxetine administration showing sphingosine peak at a retention time of 4.216 and 4.224 minute respectively. Lower: LC-MS chromatogram showing sphingosine standard peak at a concentration of 10 mg/L and a retention time of 4.226 minute.

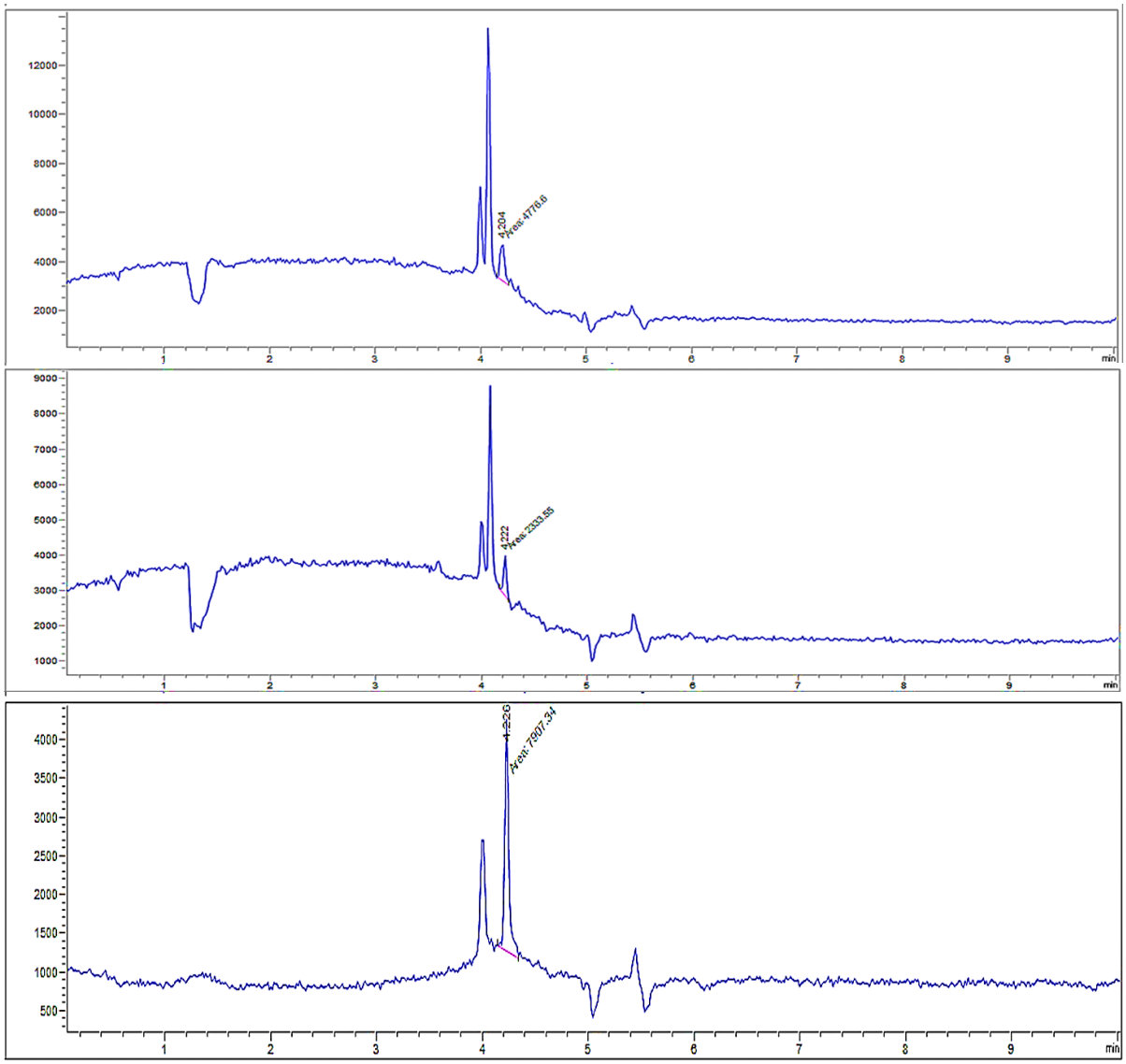

Figure 4.14: LC-MS chromatogram of hippocampal samples obtained from upper: control and middle: treated rat following chronic paroxetine administration showing sphingosine peak at a retention time of 4.204 and 4.222 minute respectively. Lower: LC-MS chromatogram showing sphingosine standard peak at a concentration of 10 mg/L and a retention time of 4.226 minute.

4.3.1.3. Effect of acute and chronic desipramine treatment on sphingosine level in rat brain:

Acute desipramine administration revealed a clearly significant effect of brain region ($p = 0.001$, $F(2,62) = 7.718$), whereas no significant effect of treatment or interaction effect (brain region x treatment) was observed. A subsequent Bonferroni post hoc analysis did not show any statistical significance in the sphingosine level in any of the three brain regions explored of the drug treated rats compared to their saline treated controls (Figure 4.15 and Table 4.2).

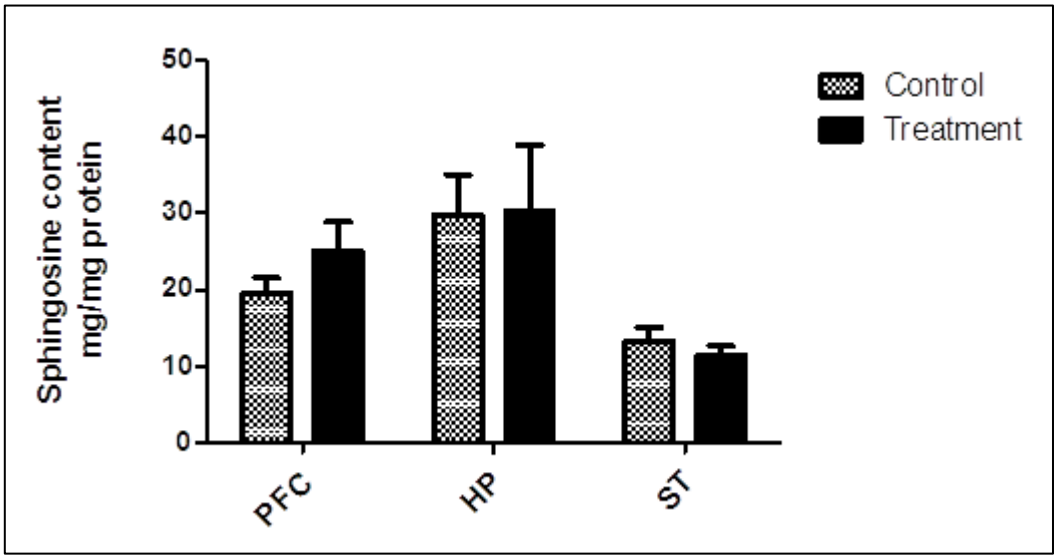

Figure 4.15: **Sphingosine content (mg/mg protein) in brain of rats following acute desipramine treatment.** All values represent mean ± SEM (n = 12). Abbreviations: PFC, prefrontal cortex; HP, hippocampus and ST, striatum.

Two-way ANOVA following chronic desipramine administration indicated a significant effect of brain region ($p < 0.05$, $F(2,62) = 4.445$) (Figure 4.11) but post-hoc analysis did not indicate significant changes in any of the three brain regions. However, there was a non-significant trend to a reduction of sphingosine level in the PFC and HP (Figure 4.16).

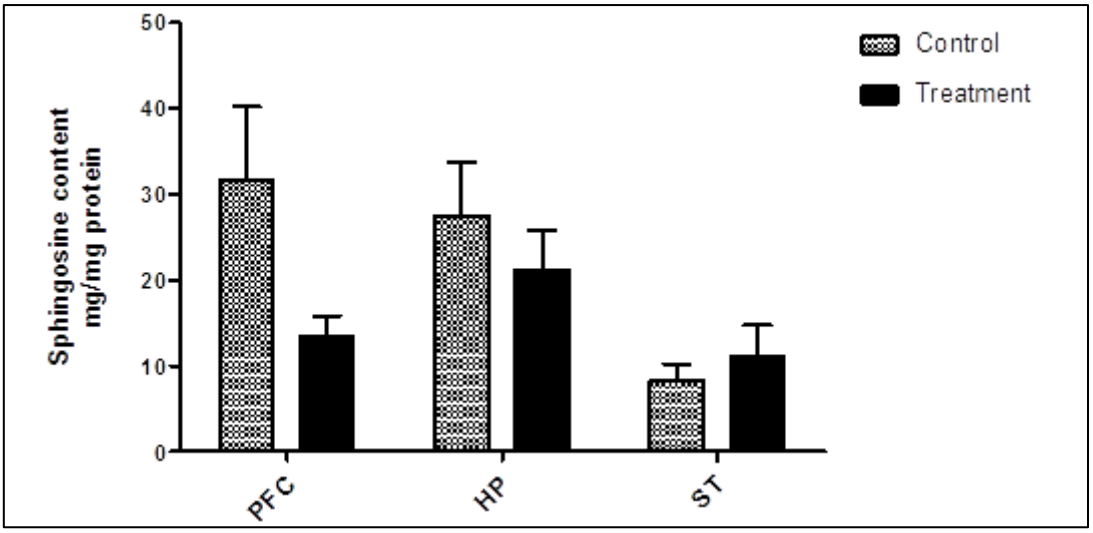

Figure 4.16: Sphingosine content (mg/mg protein) in brain of rats following chronic desipramine treatment. All values represent mean ± SEM (n = 12). Abbreviations: PFC, prefrontal cortex; HP, hippocampus and ST, striatum.

Consistent with the reported finding after chronic paroxetine administration, treatment with desipramine in prefrontal cortex indicated a significant interaction between treatment and duration ($p < 0.05$, $F(1,40) = 4.798$) and Bonferroni post hoc analysis revealed that chronic but not acute desipramine treatment significantly decreased sphingosine content (Figure 4.17 and Table 4.2). Within both the hippocampus and striatal region, no significant changes were recorded following either acute or chronic desipramine compared with the relevant controls (Figure 4.16 and Table 4.2).

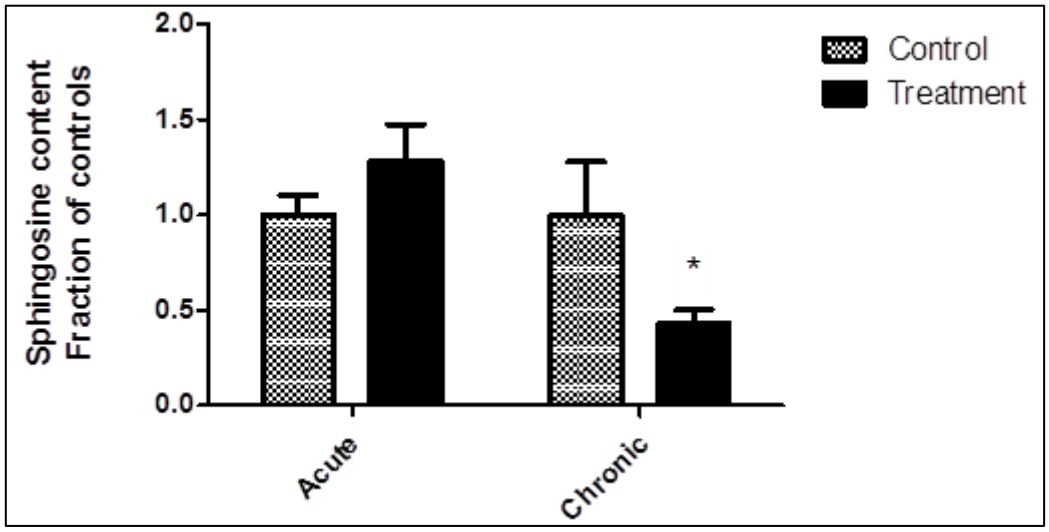

Figure 4.17: Sphingosine content (mg/mg protein) in the prefrontal cortex following acute and chronic desipramine treatment. All values represent fraction of controls ± SEM (n = 12). Abbreviations: PFC, prefrontal cortex; HP, hippocampus and ST, striatum. * $P < 0.05$ for the chronic desipramine group (two-way ANOVA with Bonferroni t-test).

4.3.1.4. Effect of acute and chronic antidepressant drug treatment on plasma level of sphingosine:

Analysis of the generated plasma data is detailed below: the two-way ANOVA indicates no significant interaction effect comparing acute versus chronic desipramine treatment in plasma. However, the subsequent Bonferroni t-test showed a significant difference ($p < 0.05$) between control and treatment groups following acute desipramine treatment but not after chronic administration (Figure 4.18). In contrast, similar qualitative changes were seen in the plasma following paroxetine treatment, although the two-way ANOVA revealed no significant interaction effect comparing acute versus chronic paroxetine treatment. The post hoc analysis displayed a trend toward a reduced sphingosine level in plasma after acute paroxetine administration without any detected significant difference following its chronic treatment (Figure 4.19).

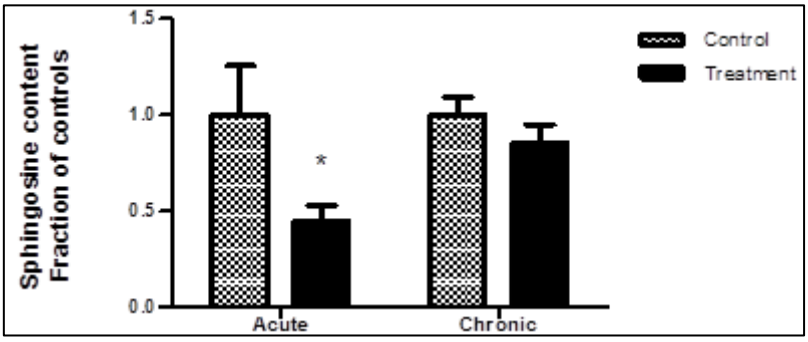

Figure 4.18: Sphingosine content (mg/mg protein) in plasma of rats following acute and chronic desipramine treatment. All values represent fraction of controls ± SEM (acute desipramine n = 8) (chronic desipramine n = 12). * $P < 0.05$ for the acute desipramine group (two-way ANOVA with Bonferroni t-test).

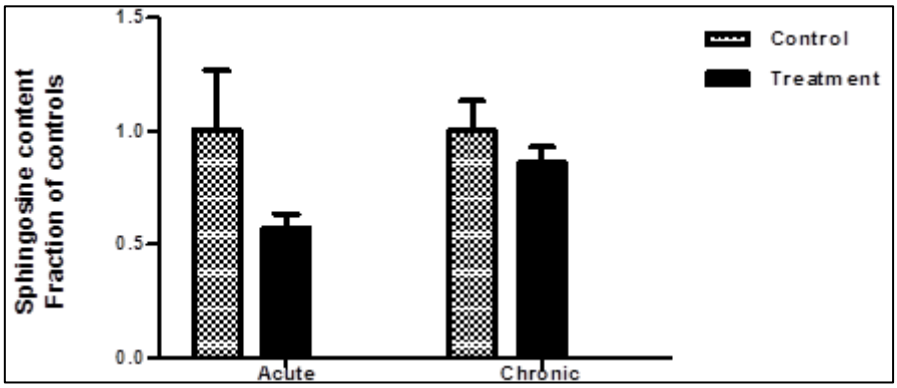

Figure 4.19: Sphingosine content (mg/mg protein) in plasma of rats following acute and chronic paroxetine treatment. All values represent fraction of controls ± SEM (acute paroxetine n = 6) (chronic paroxetine n = 12).

Table 4.1: Summary of effects of acute and chronic paroxetine (5 mg/kg) on sphingosine in rat brain and plasma.

	PFC (mg/mg protein)	HP (mg/mg protein)	ST (mg/mg protein)	Plasma (mg/mg protein)
Acute				
Control	15.59 ± 1.218	15.38 ± 2.934	6.604 ± 0.681	1.849 ± 0.496
Paroxetine	17.03 ± 2.211	16.89 ± 3.440	6.515 ± 0.574	1.056 ± 0.119
Chronic				
Control	20.15 ± 0.857	17.25 ± 2.378	7.351 ± 1.872	2.055 ± 0.274
Paroxetine	9.721 ± 1.327 ***	8.708 ± 1.563 ***	4.389 ± 0.661	1.765 ± 0.145

Values indicate sphingosine content (mg sphingosine/mg protein) as mean ± SEM (n=12).

*** P < 0.001 (two-way ANOVA with Bonferroni t-test). Abbreviations: PFC, prefrontal cortex; HP, hippocampus and ST, striatum.

Table 4.2: Effects of acute and chronic desipramine (10 mg/kg) on sphingosine in rat brain and plasma.

	PFC (mg/mg protein)	HP (mg/mg protein)	ST (mg/mg protein)	Plasma (mg/mg protein)
Acute				
Control	19.53 ± 2.023	29.68 ± 5.395	13.29 ± 1.672	2.036 ± 0.517
Desipramine	25.04 ± 3.787	30.31 ± 8.527	11.44 ± 1.228	0.914 ± 0.160 *
Chronic				
Control	31.50 ± 8.759	27.49 ± 6.225	8.242 ± 1.955	1.858 ± 0.167
Desipramine	13.45 ± 2.397	21.18 ± 4.605	11.14 ± 3.607	1.590 ± 0.173

Values indicate sphingosine content (mg sphingosine/mg protein) as mean ± SEM (n=12).

* P < 0.05 (two-way ANOVA with Bonferroni t-test). Abbreviations: PFC, prefrontal cortex; HP, hippocampus and ST, striatum.

4.3.1.5. Effect of antidepressant drug treatment on sphingosine level in cultured mouse macrophages:

This initial study was established to examine whether the utilized antidepressant drugs induce an alteration of the main ceramide metabolite: sphingosine content in whole cell lysates from cultured mouse macrophages (RAW 264.7 cells) using LC-MS. Our data showed that treatment of the cultured cells with desipramine or paroxetine at a concentration of 10 µM for different incubation periods (either 30 minutes or 60 minutes) did not induce any detectable alteration of the sphingosine content compared to the corresponding control cells following the same treatment (Figure 4.20). Protein measurement of the cell homogenate aliquots was undertaken for normalization and determination of the sphingosine concentration in the analysed cell samples was achieved after generating a standard curve.

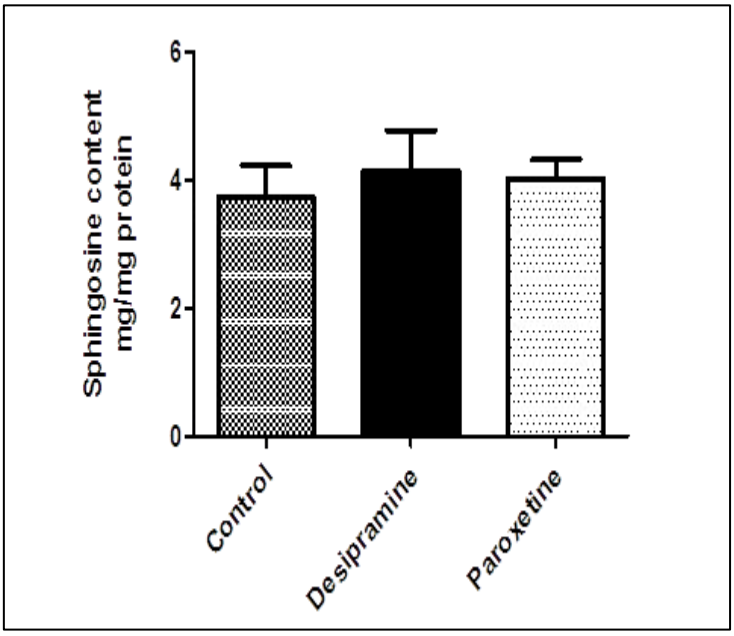

Figure 4.20: Effect of desipramine and paroxetine treatment (10 µM) in RAW 264.7 cells on sphingosine content (mg/mg protein) after one-hour incubation. All values represent mean ± SEM (n = 4).

4.3.2. Analysis of ceramide in rat brain following chronic paroxetine administration by the HPLC-UV:

As indicated previously, a reliable detection and quantification of the ceramide content in the extracted lipid content from brain extracts following chronic antidepressant drug treatment was possible via a developed method, using high-performance liquid chromatography with ultraviolet detection technique (HPLC-UV). This analysis was undertaken using the same samples from the hippocampus of rats chronically treated with saline or paroxetine which had previously been assayed for sphingosine content. In order to evaluate if changes of the ceramide metabolite (sphingosine) reflected changes of its precursor (ceramide), we measured ceramide levels from the hippocampus after chronic paroxetine using this method. Student's t-test was performed to determine statistical differences between the analysed group means representing both the treatment group and the corresponding saline treated animals. Consistent with the reported sphingosine data in the hippocampus following chronic paroxetine administration (Figures 4.9 and 4.23), this treatment protocol also resulted in a highly significant reduction of ceramide levels in this brain region compared to the saline injected controls ($p < 0.0001$) (Figures 4.21, 4.22 and Table 4.3).

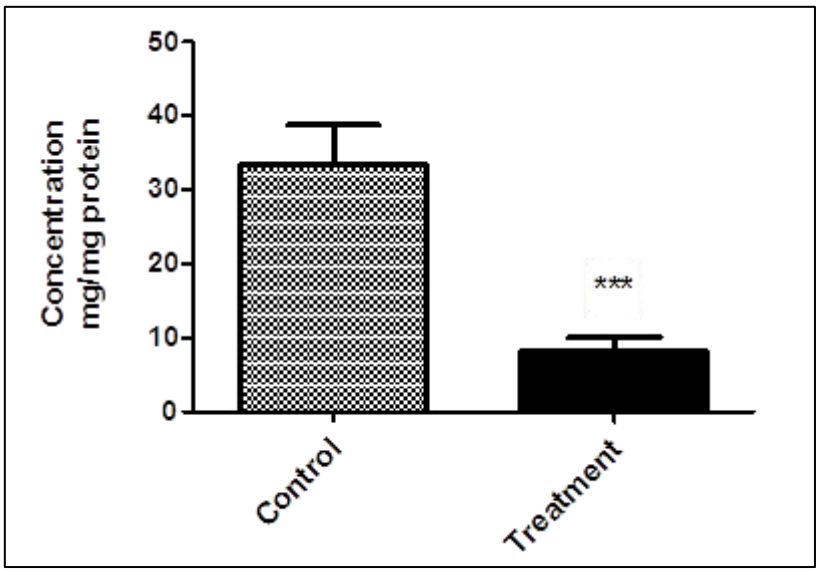

Figure 4.21: Ceramide content (mg/mg protein) in the rat hippocampus following chronic paroxetine treatment. All values represent mean ± SEM (n = 12); *** $p < 0.001$ (Student's t-test).

Table 4.3: Effect of chronic paroxetine treatment (5 mg/kg/day) for 15 days on ceramide content (mg/mg protein) in rat hippocampus. All values represent mean ± SEM (n = 12); *** p < 0.001 (Student's t-test).

	Ceramide content (mg/mg protein)
Control	33.45 ± 4.360
Chronic paroxetine	8.25 ± 1.534

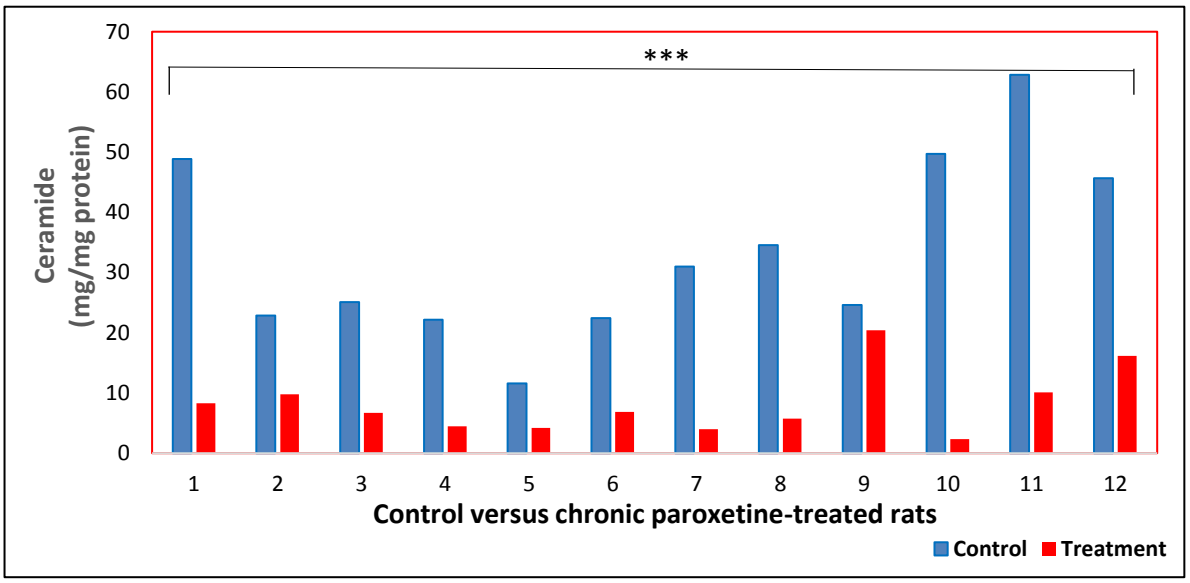

Figure 4.22: Ceramide content (mg/mg protein) in the rat hippocampus comparing control versus chronic paroxetine-treated animals (n = 12); *** p < 0.001 (Student's t-test).

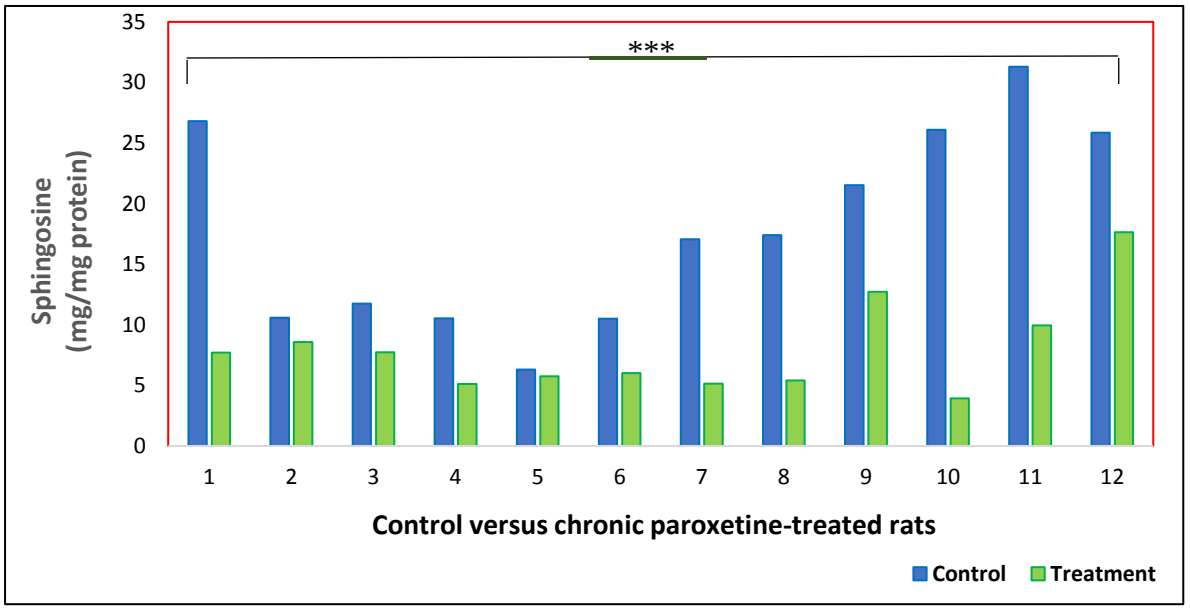

Figure 4.23: Sphingosine content (mg/mg protein) in the rat hippocampus comparing control versus chronic paroxetine-treated animals (n = 12); *** p < 0.001 (two-way ANOVA with Bonferroni t-test).

In order to investigate the association between the ceramide content and its major metabolite, sphingosine data from the same hippocampal brain samples were analysed by linear regression analysis. Such analysis indicated that there was a highly significant correlation between ceramide and sphingosine in both control groups ($p < 0.0001$, $F(1,10) = 522.4$, $R^2 = 0.981$) (Figure 4.24) and treatment groups ($p < 0.0001$, $F(1,10) = 275$, $R^2 = 0.965$) (Figure 4.25) in the hippocampus of saline as well as paroxetine-treated rats (Figure 4.26).

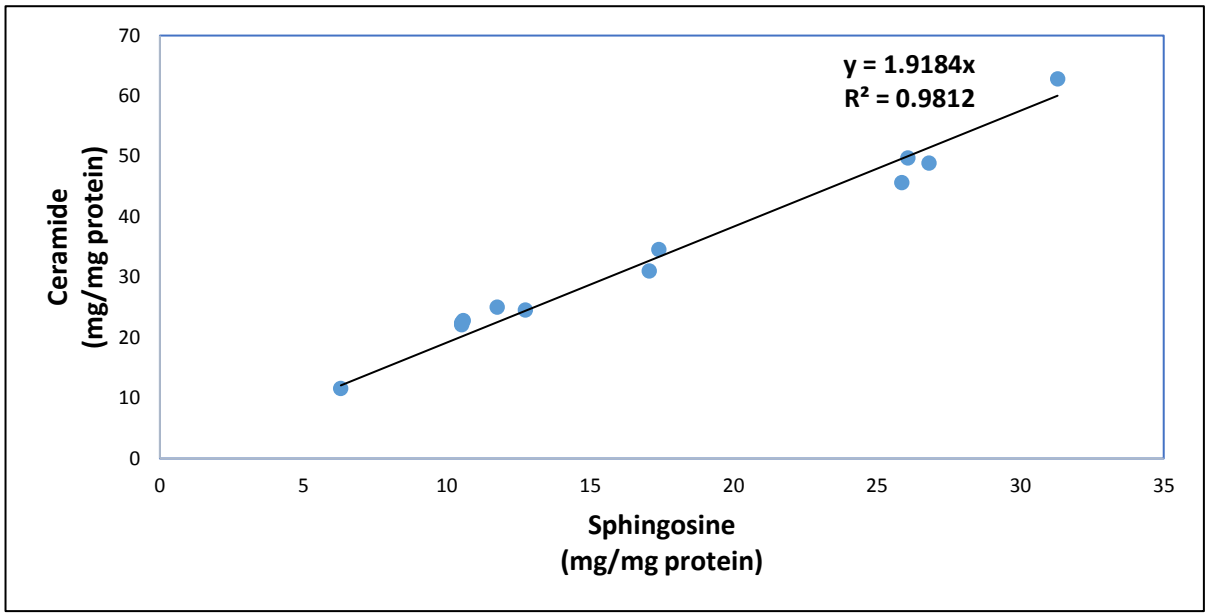

Figure 4.24: Linear regression analysis of ceramide (mg/mg protein) and sphingosine content (mg/mg protein) in the rat hippocampus of the control groups following chronic saline treatment. All values represent mean (n = 12).

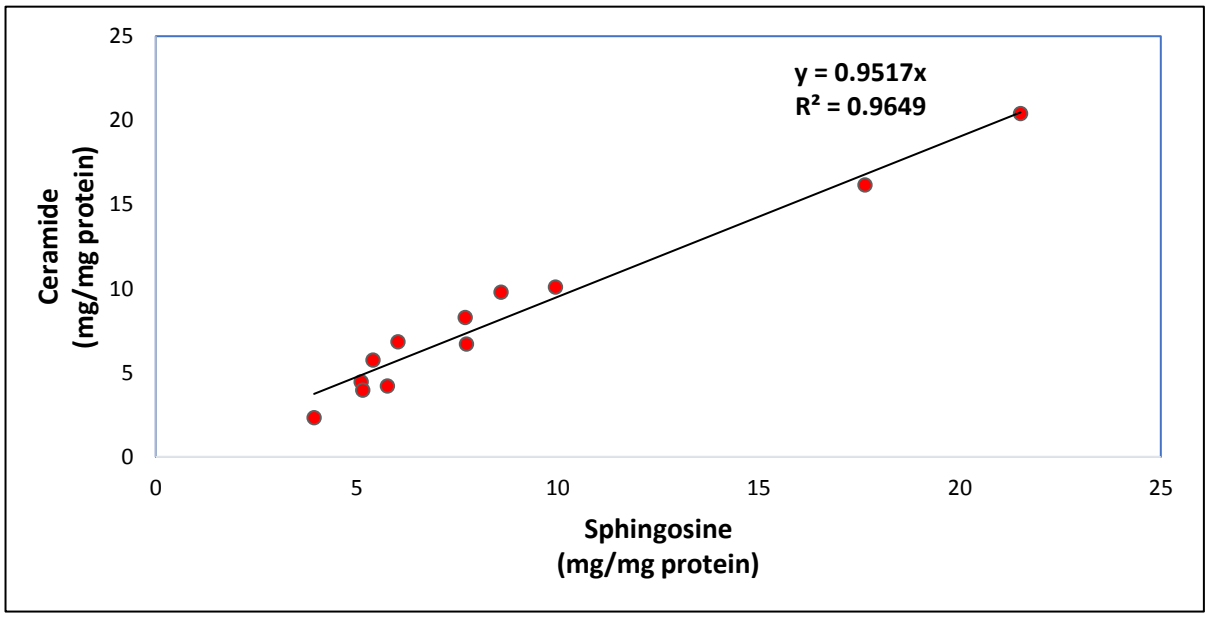

Figure 4.25: Linear regression analysis of ceramide (mg/mg protein) and sphingosine content (mg/mg protein) in the rat hippocampus of the treatment groups following chronic paroxetine administration. All values represent mean (n = 12).

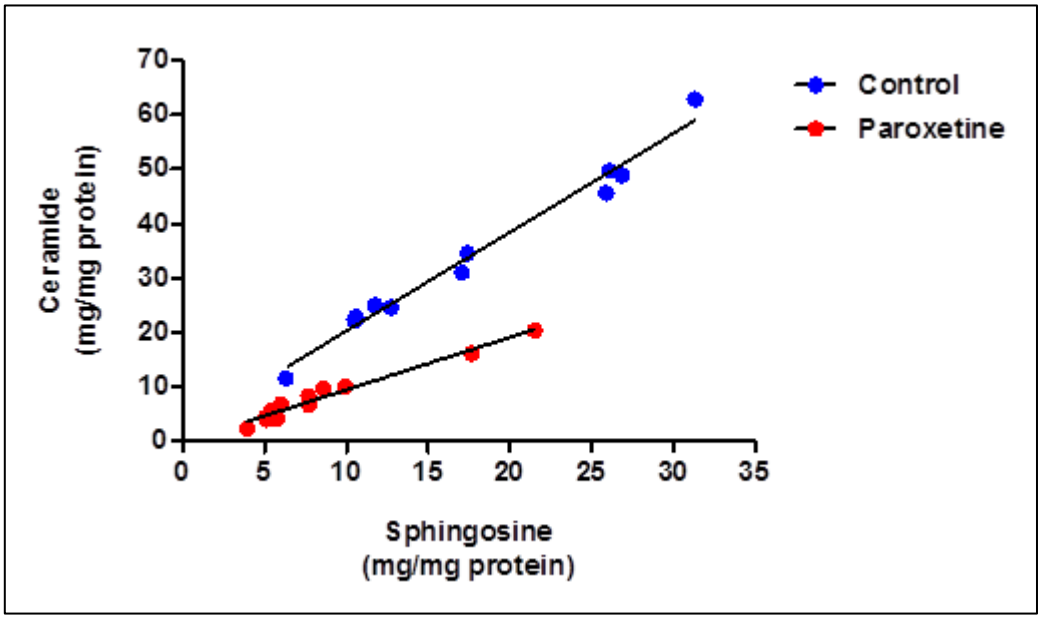

Figure 4.26: Linear regression analysis of ceramide (mg/mg protein) and sphingosine content (mg/mg protein) in the rat hippocampus of both control and treatment groups following chronic paroxetine administration. All values represent mean (n = 24).

Furthermore, the overall regression analysis of hippocampal ceramide and sphingosine data revealed that there was a statistically significant relationship between the two molecules of interest ($p < 0.0001$, $F(1,22) = 155.1$, $R^2 = 0.876$) in paroxetine treated samples and their corresponding controls (Figure 4.27).

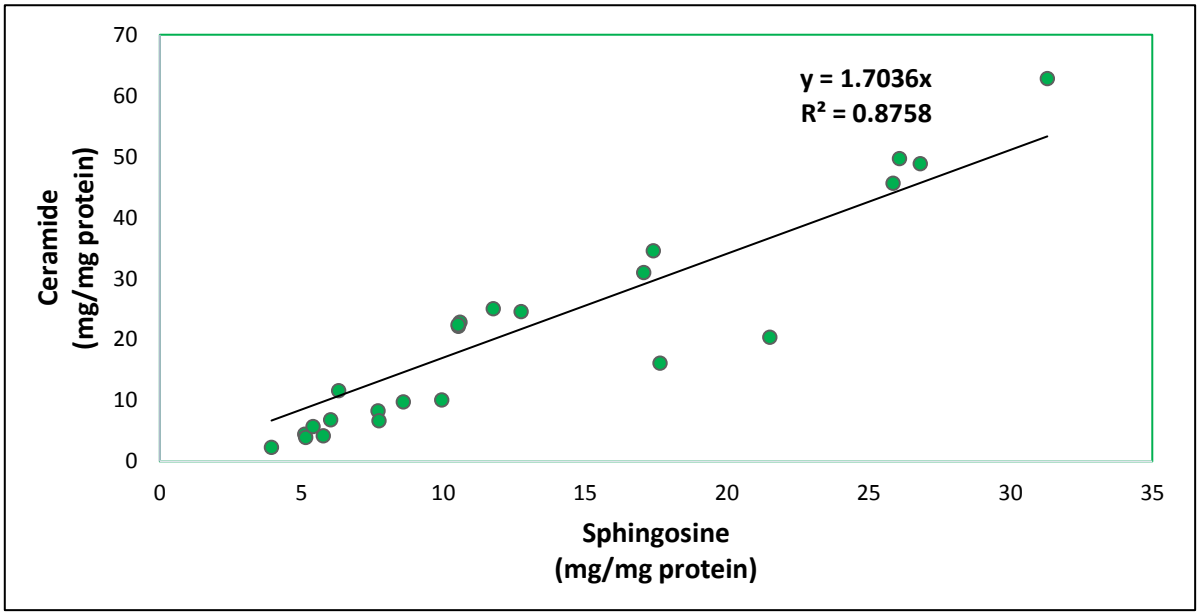

Figure 4.27: Linear regression analysis of ceramide (mg/mg protein) and sphingosine content (mg/mg protein) in the rat hippocampus of all control and treatment data following chronic paroxetine administration. All values represent mean (n = 24).

Taken together, these experiments show that sphingosine is generally a good index of its parent sphingolipid ceramide.

4.4. Discussion:

4.4.1. Principal findings:

Recent studies have indicated a role of sphingolipids in depression. Therefore, the current study was conducted to investigate the effect of acute and chronic treatment of two antidepressant drugs: the SSRI paroxetine and the TCA desipramine on brain sphingolipid levels in treated rats and their corresponding saline injected controls. For this purpose, levels of sphingosine and its precursor, ceramide were measured in brain regions implicated in depression. These two sphingolipid molecules were reliably measured in brain structures that have been reported to be involved in the symptoms of depression: the prefrontal cortex, hippocampus and striatum (Holmes, 2008; Sheline, 2011) using LC-MS and HPLC-UV techniques for the measurements of sphingosine and ceramide respectively. The results revealed that chronic antidepressant drug administration induced a pronounced reduction of sphingosine content in two of the brain regions investigated (a region-specific effect) namely, the prefrontal cortex and hippocampus (a similar trend for a reduced sphingosine level in the hippocampus after chronic desipramine administration was also detected) (see Figures 4.9 and 4.16). Thus, the observed changes in sphingosine content were stronger in the prefrontal cortex, whereas the striatum failed to display any significant changes. Interestingly, the marked decrease in sphingosine level was recorded only following chronic and not after the acute treatment.

In contrast, acute treatment with desipramine and paroxetine exhibited no statistically significant changes in the level of sphingosine in any of the three brain regions examined (see Figures 4.8 and 4.15). On the other hand, the obtained plasma data showed a significant reduction after acute desipramine and a trend to a reduced sphingosine level after acute paroxetine treatment. In contrast both drugs failed to significantly alter plasma levels after chronic administration of both drugs (see Figures 4.18 and 4.19). Additionally, an initial cell study conducted on mouse macrophages cells indicates that there was no significant

alteration in the sphingosine content in cultured cells following treatment with antidepressant drugs compared to the corresponding control cells. Consistent with the sphingosine data, using the HPLC-UV, the hippocampal ceramide level indicated a significant reduction in the treated animals compared to their corresponding saline injected controls (Figure 4.20) with a significant correlation between hippocampal ceramide and sphingosine levels following chronic paroxetine treatment (see Figures 4.24, 4.25, 4.26 and 4.27 respectively).

4.4.2. Chronic antidepressant induced alteration of sphingolipids:

In the present study, mass spectrometry as well as HPLC-UV data showed that chronic antidepressant drug treatment resulted in a significant reduction of sphingosine levels in the hippocampus and the prefrontal cortex but not in the striatum. In addition, there was a concomitantly pronounced decrease in hippocampal ceramide content in paroxetine-treated rats compared to their corresponding saline-injected controls. The study also clearly demonstrated that in the hippocampal samples, levels of sphingosine were significantly correlated with its parent lipid ceramide in both control and treated animals. Therefore, sphingosine levels appear to be a reliable index of ceramide in rat brain extracts. Interestingly, the observed findings from our study were consistent with a previous study reporting a similar reduction of hippocampal ceramide level following long-term antidepressant drug therapy (Gulbins et al., 2013). Several preclinical studies indicate that chronic stress to rodents, results in enhanced depression-related behaviours when using animal models of depression (Bai et al., 2017; Gulbins et al., 2013, 2015; Kornhuber et al., 2014; Schneider et al., 2017). In this respect, a recent animal study revealed that exposure to chronic unpredicted stress for four weeks via applying a randomized daily exposure for one hour to one of the following stressful conditions: vibration, overcrowding, exposing the animal to a cold water at 18°C or a hot air stream resulted in increased ceramide level in the prefrontal cortex and hippocampus. Likewise, indicating an increased synthesis of ceramide, a decrease in the content of the precursor to ceramide namely sphingomyelin was recorded in these brain regions of the same chronically stressed rats compared to their relevant controls (Oliveira et al., 2016). This previously reported effect could be explained by an activation of the ASM enzyme which converts sphingomyelin to ceramide. In addition, other

pathways of ceramide synthesis such as the *de novo* and the salvage pathways (see pages 3 and 4 in the introduction) could also contribute to these chronic stress induced enhancements of ceramide (Gault et al., 2010; Oliveira et al., 2016). In accordance with a recent study (Gulbins et al., 2013), the present findings from our lipid measurements suggest that the detected sphingolipids alteration following chronic antidepressant drug treatment in the prefrontal cortex and hippocampus may be related to a dysregulation of the main sphingolipid metabolizing enzymes, in particular acid sphingomyelinase (ASM) in both brain regions (for detailed information see the relevant Chapter Five). Furthermore, a number of animal and human studies indicated that these particular brain regions which are implicated in the pathogenesis of depression may undergo a structural as well as functional impairment following exposure to chronic stress (reduction in cortical and hippocampal volume, altered transmission, impaired synaptic plasticity of the hippocampus) (Bai et al., 2017; Oliveira et al., 2016; Sousa and Almeida, 2012). Indeed, these brain regions are reported to have neurophysiological abnormalities in depressed patients as indicated by previous post-mortem and neuroimaging studies (Drevets, 2000; Lee et al., 2009). As being the focus of many recent studies and in support of our data, it was mentioned that the stress induced increase of ceramide level can be reversed or normalized by the potential use of antidepressant drugs such as fluoxetine, paroxetine, desipramine and maprotiline (Dinoff et al., 2017; Gulbins et al., 2013, 2015, Kornhuber et al., 2008, 2011, 2014). Consistent with our findings, a previous animal study demonstrated that chronic administration of fluoxetine and amitriptyline at similar doses to those which achieve therapeutic plasma concentrations in depressed patients resulted in a reduced activity of acid sphingomyelinase and decreased ceramide concentration in the hippocampus of “depressed” mice (Gulbins et al., 2013). Further, this coincided with an increase of neuronal maturation and proliferation (i.e. neurogenesis) compared to the corresponding controls. In addition, a reduction of depression-like behaviours was noted (reduced sucrose preference and neglect of the animal coats) (Gulbins et al., 2013). Taken together, these studies indicate a relationship between antidepressant induced reduction of ceramide and a reduction in signs of depression in animals. In this regard, the same study also revealed that non-stressed mice over-expressing acid sphingomyelinase or had a deficiency of the acid ceramidase enzyme or where injected with C16 ceramide into the hippocampus showed a decrease in neurogenesis which coincided with increased depressive-like behaviours. Moreover, all of these reported findings could then be

normalized by antidepressant drug treatment (Gulbins et al., 2013). Hence, the recorded findings in the current study are in line with previously reported work on ceramide and its implication in depression as well as its pharmacological treatment. Overall, the present study is unique, since it performed regional measurements of sphingosine following both acute and chronic administration of paroxetine and desipramine. In this respect, the current study also detected marked regional differences in the effect of both drugs. Thus, effects were generally more pronounced in brain regions strongly associated with symptoms and treatment of depression i.e. the prefrontal cortex and the hippocampus compared to the striatum (Drevets et al., 2008; Lee et al., 2013; McEwen and Morrison, 2013). In summary, the generated data from the present study appear to support and extend the knowledge of the recently emerged lipid hypothesis of depression and its drug treatment (see Chapter One, section 1.3.3).

4.5. Conclusion:

The current study showed that chronic antidepressant drug treatment induced a clear reduction of sphingosine level in the prefrontal cortex and hippocampus of the rat. In this respect, chronic administration of the SSRI paroxetine appeared to be more effective compared to chronic treatment of the TCA desipramine. In contrast, no significant changes were recorded in the level of sphingosine within any of the three-investigated brain regions following acute treatment. Strikingly, chronic paroxetine administration also induced a highly significant reduction of ceramide level in the hippocampus of paroxetine treated rats compared to the corresponding saline injected controls. Furthermore, regression analysis of hippocampal ceramide and sphingosine data revealed that there was a statistically significant correlation between the two sphingolipid molecules after chronic paroxetine or saline treatment. Therefore, indicating that brain sphingosine levels serve as reliable index of its precursor sphingolipid ceramide. In this regard, here the reported reduction of sphingolipids following chronic antidepressant drug treatment could be due to a dysregulation of the main sphingolipid-metabolizing enzymes particularly acid sphingomyelinase. Thus, in Chapter Five, we have extended this study by looking into the possibility that this enzyme and/or acid ceramidase are indeed implicated in the effects seen in the current chapter. This was achieved by measuring mRNA levels for these two enzymes by using the RT-PCR technique. Importantly, and in line with the established delay in onset of antidepressant action by these

drugs, our results show that long-term treatment with antidepressant drugs may be required to induce reductions of the brain ceramide content as well as its main metabolite sphingosine and thereby, may achieve their therapeutic effectiveness.

CHAPTER 5

Effects of antidepressant drug treatment on gene expression for two key enzymes of the rat brain sphingolipid pathway using real-time quantitative polymerase chain reaction (RT-qPCR)

5.1. Introduction:

Ceramide is an important biomolecule of the sphingolipid family and has a central role for the normal function of biological cell membranes. Also, it is a main sphingolipid precursor which undergoes synthesis and metabolism to generate other simple (e.g. sphingosine) or complex sphingolipids (e.g. sphingomyelin) through actions of the key metabolizing enzymes: acid sphingomyelinase (ASM) and acid ceramidase (AC) respectively (see Figure 5.2) (Dinoff et al., 2017; Gangoiti et al., 2010). Recently, it has been suggested that membrane sphingolipids possibly via changes in the expression of ASM and AC play a role in the pathogenesis of depression and the therapeutic effect of antidepressant drugs (Canals et al., 2011; Müller et al., 2015; Osherovich, 2013). Ceramide is involved in cell growth arrest and apoptosis (Hannun and Obeid, 2008). In comparison, the ceramide metabolite sphingosine (which is formed by the enzyme AC) when phosphorylated into sphingosine-1-phosphate mediates cellular growth and proliferation (Futerman and Hannun, 2004). The balance between these different sphingolipids which often regulate opposing biological functions is critical in maintaining a proper dynamic, regarding the balance between cellular growth and death and thereby, determining cellular fate (Cuvillier et al., 2001; Spiegel, 1999). In addition, it has been reported that activation of the enzyme ASM with the resultant accumulation of ceramide has been linked to several brain disorders including Alzheimer's disease and major depressive disorder (He et al., 2010; Kornhuber et al., 2005, 2011). In this context, a previous clinical study conducted on depressed patients recorded an increase of ASM activity during episodes of depressive symptoms compared to corresponding healthy controls (Kornhuber et al., 2005). Moreover, a number of recent studies identified several antidepressant drugs as functional inhibitors of ASM activity such as the TCA drugs: desipramine, imipramine, amitriptyline and nortriptyline; the tetracyclic antidepressant drug maprotiline (Canals et al., 2011; Kornhuber et al., 2010) as well as the SSRIs: fluoxetine, paroxetine and sertraline (Kornhuber et al., 2008, 2011). Further and in line with these previously reported findings, another study indicated that administration of the antidepressant drugs, fluoxetine and amitriptyline at doses similar to those which achieve therapeutic plasma concentrations in patients with depression resulted in a decline in hippocampal ceramide concentration. An effect which coincided with a reduction of ASM activity and a prevention of depression-like behaviours in a mouse model of depression (Gulbins et al., 2013, 2015). Further, some

previous genetic and pharmacological studies showed that genetic deficiency of AC or over expression of ASM enzymes in mice induced depression-related behavioural effects such as a pronounced reduction in sucrose preference, a notable delay in the novelty-suppressed feeding test, a delayed forced swim test and a marked neglect of the animal coats. Interestingly these enhanced effects in models of depression coincided with increased levels of hippocampal ceramide compared to the corresponding controls. Further, and in support of a role for ceramide in depressive behaviours, ceramide levels were normalized following chronic antidepressant drug treatment (Gulbins et al., 2013, 2015).

5.1.1. The main sphingolipid metabolizing enzymes:

Ceramide undergoes generation or degradation via action of the enzymes outlined below and as illustrated in Figure 5.2:

5.1.1.1. Acid sphingomyelinase (ASM):

Sphingomyelin phosphodiesterase 1 (SMPD1) is the gene that encodes the acid sphingomyelinase (ASM) glycoprotein, a water-soluble lysosomal hydrolase that is active in its membrane-bound form to catalyse the hydrolysis of sphingomyelin into ceramide and phosphorylcholine at an acidic pH (the optimum pH for the peak enzyme activity is 5.0) (Figure 5.2) (Canals et al., 2011; Linke et al., 2001). The enzyme ASM is present in different cellular locations: lysosomes, mitochondria and on the outer surface of the plasma membrane as well as the extracellular space (Grassme et al., 2001; Gulbins et al., 2015).

5.1.1.2. Functional inhibition of acid sphingomyelinase (ASM):

By using both *in vivo* as well as in cell culture models, a class of drugs have recently been identified which all share an important property regarding the function of ASM. This diverse group includes many drugs i.e. various antidepressant drugs (e.g. paroxetine, fluoxetine, desipramine and amitriptyline), amlodipine (a calcium-channel blocker), clomiphene (an ovulatory stimulant), promethazine (a phenothiazine with antipsychotic and antihistamine actions), mebeverine (an anticholinergic), loperamide (an anti-diarrhoeal) and promazine (an antipsychotic) (Kornhuber et al., 2008, 2010, 2011). These compounds are often described as cationic amphiphilic drugs as they contain both a hydrophilic domain with an ionisable amine

group and a hydrophobic (a lipophilic) domain (Funk and Krise, 2012; Kornhuber et al., 2010). Also, most of these small molecules are weak bases with a molecular weight lower than 500 and are likely to cross the blood-brain barrier (BBB) (Kornhuber et al., 2010, 2011). Thus, they have the ability to accumulate inside the acidic lysosomal apparatus of the neurons and therefore, they can potentially induce an indirect or a functional inhibition of the enzyme ASM without directly inhibiting the activity of the enzyme (Kornhuber et al., 2009, 2010, 2011). Hence, this group of drugs are referred to as "functional inhibitors of ASM" (Figure 5.1). As a consequence of this action, it could be speculated that this type of drugs (e.g. paroxetine and desipramine) dependent on the validity of the "ceramide hypothesis of depression" could contribute to their usefulness in the treatment of this condition (Kornhuber et al., 2010, 2011). Inside the acidic lysosomal compartment a pH of 4.8 is maintained by an energy dependent proton pump and the inner surface of the lysosomal membrane is shown to be negatively charged, whereas the enzyme (i.e. ASM) carries a positive charge (Kölzer et al., 2004; Kornhuber et al., 2009, 2014). Therefore, ASM is electrostatically attached to the inner phase of the lysosomal membrane, thereby it will be protected from its inactivation by the low pH in the acidic lysosomal lumen as well as from proteolytic degradation via the lysosomal proteases (Bohley and Seglen, 1992; Kölzer et al., 2004; Kornhuber et al., 2010, 2011). Potential functional inhibitors of ASM such as the two amphiphilic antidepressant drugs paroxetine and desipramine used in the present study have been shown to pass through the lysosomal membrane in their neutral or uncharged forms by a process of passive diffusion (Kornhuber et al., 2009, 2014). Thus, due to the amphiphilic nature of the drug (i.e. the TCA desipramine) inside the lysosome, desipramine becomes positively charged and hence, loses its ability to pass through the lysosomal membrane, which is mainly permeable to uncharged molecules (Kornhuber et al., 2010). Subsequently, the intra-lysosomal concentration of the drug becomes high (intra-lysosomal accumulation of the positively charged or protonated drug form) and thereby, resulting in a displacement of the positively charged ASM from its binding place within the inner lysosomal membrane(Beckmann et al., 2014; Kornhuber et al., 2010, 2014). The resultant detachment of the ASM enzyme from the intra-lysosomal membrane promotes its subsequent inactivation by the low pH and/or by a proteolytic breakdown. This process is outlined in Figure 5.1 and could be achieved by one of the two antidepressant drugs investigated in the present study as an example of a functional inhibitor of ASM namely, the TCA desipramine (Beckmann et al., 2014; Kornhuber et al., 2010, 2014).

Possibly of clinical relevance, it has also been reported that a functional inhibition of ASM by fluoxetine and amitriptyline was seen at a plasma concentration within the therapeutic range for the clinical treatment of depression (Gulbins et al., 2013; Kornhuber et al., 2014).

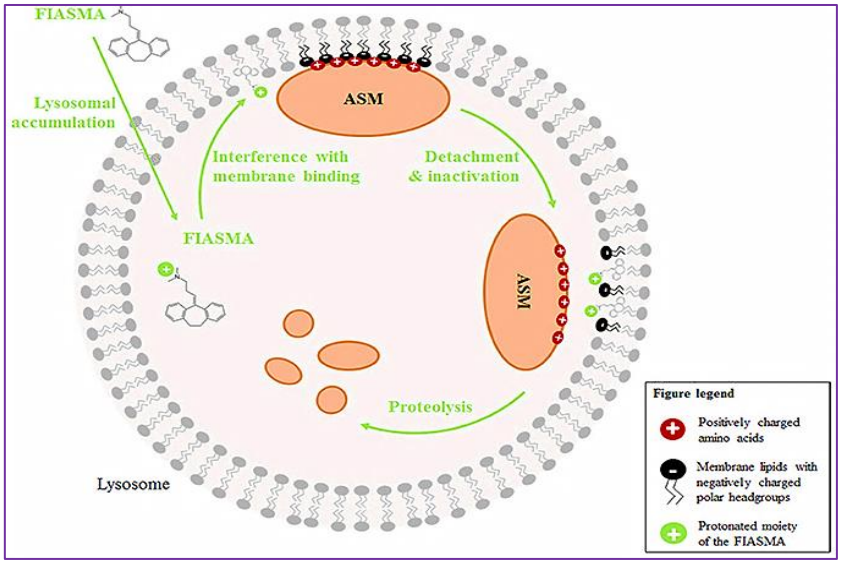

Figure 5.1: Mechanism of action of the functional inhibitors of ASM (Beckmann et al., 2014). The amphiphilic tricyclic compound (i.e. desipramine) accumulates in its charged form inside the acidic lysosomes, thus displacing ASM from the inner lysosomal membrane leading to inactivation or proteolysis of the enzyme in the acidic lysosomal lumen. This mechanism is known as functional inhibition of ASM.

5.1.1.3. Acid ceramidase (AC):

The N-acylsphingosine amidohydrolase 1 (ASAH1) gene encodes the acid ceramidase (AC) enzyme, a lysosomal protein that hydrolyzes ceramide into sphingosine and free fatty acid at an optimum pH of 4.5 (Figure 5.2) (Canals et al., 2011; Kornhuber et al., 2010). It was reported that AC activity has shown to be stimulated by various cellular stressors such as exposure to UV radiation or chemotherapy (Canals et al., 2011; Linke et al., 2001). In support of the effect of antidepressant drugs on the AC enzyme, a previous study demonstrated that the TCA desipramine induced a down-regulation of the AC activity in cultured cancer cell lines, an effect that is accompanied by its inhibitory effect on the enzyme acid sphingomyelinase (dual effect of desipramine on both ASM and AC) (Elojeimy et al., 2006). In this context, recent studies recorded that activity of the enzyme AC appears to be lower compared to the ASM activity as determined in postmortem brain tissues from patients with Alzheimer's disease and normal controls (He et al., 2010; Kornhuber et al., 2010). Furthermore, previous studies have demonstrated that genetic deficiency of the AC enzyme is implicated in Farber disease

(inherited deficiency of AC, resulting in lysosomal accumulation of ceramide in the brain and several other body organs including: kidney, lungs, around the joints and in the subcutaneous tissues) (Canals et al., 2011; Ehlert et al., 2007; Koch et al., 1996). On the other hand, it has been shown that up-regulation of the AC enzyme is associated with tumour progression and enhanced resistance of tumour cells to anticancer treatment including both radiotherapy and chemotherapeutic treatments (Saied and Arenz, 2014).

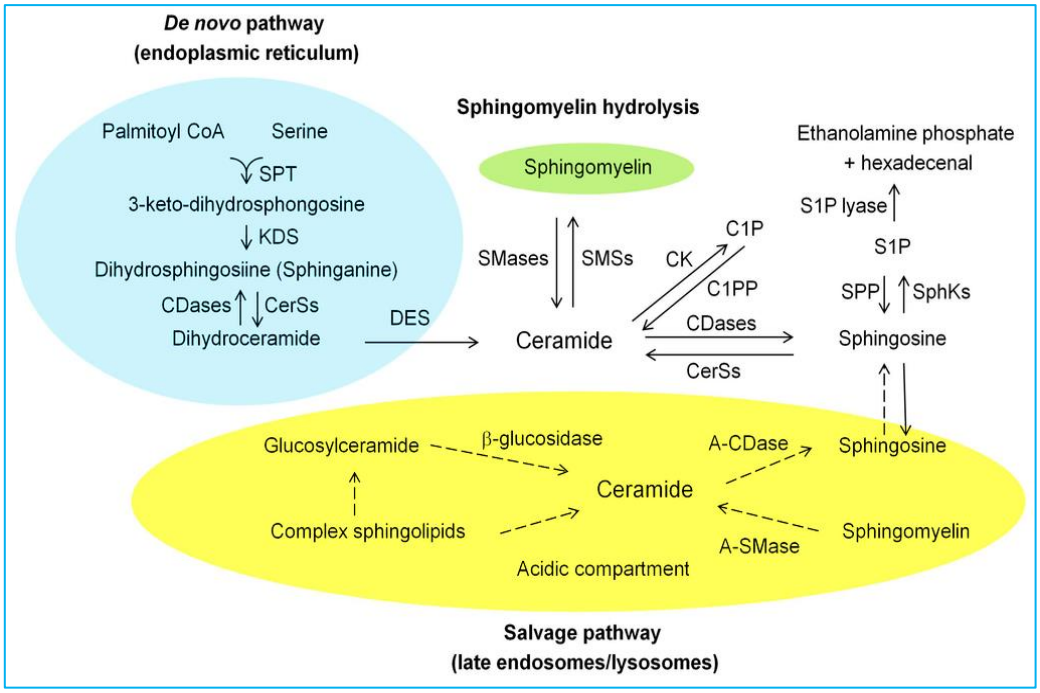

Figure 5.2: Metabolic pathways of sphingolipids including the main metabolizing enzymes. A-SMase, acid sphingomyelinase; A-CDase, acid ceramidase; CerSs, ceramide synthases; C1P, ceramide-1-phosphate; CK, ceramide kinase; C1PP, ceramide-1-phosphate phosphatase; KDS, 3-keto-dihydrosphingosine reductase; DES, dihydroceramide desaturase; SMSs, sphingomyelin synthases; SphKs, sphingosine kinases; SPP, sphingosine-1-phosphate phosphatase; S1P, sphingosine-1-phosphate; SPT, serine palmitoyl transferase (Ueda, 2015).

5.1.2. Aim:

In chapter Four, this project showed that two different types of antidepressant drugs namely, the SSRI paroxetine and the TCA desipramine significantly reduced levels of ceramide and its main metabolite sphingosine in rat brain regions following chronic but not acute administration. To better understand the mechanism of action behind this effect, the current study was designed to investigate the effect of these two antidepressant drugs on gene expression levels of the main sphingolipid-regulating enzymes (ASM and AC). In particular,

the experiments of the current chapter aimed to test the hypothesis that chronic antidepressant drug treatment reduces the gene expression level for SMPD1 and ASAH1 the genes encoding, the ASM and AC enzyme proteins respectively. This study was established in the same brain regions explored in Chapter Four (the prefrontal cortex, hippocampus and striatum). Specifically, the present study examined the following:

- By using the real-time quantitative polymerase chain reaction technique (RT-qPCR), the expression levels of the SMPD1 and ASAH1 genes were recorded in brain samples from rats chronically treated (once daily injections for 15 days) with antidepressant drugs (desipramine or paroxetine) or the corresponding vehicle controls.
- To investigate the occurrence of any brain region-specific effect by chronic antidepressant drug treatments on the gene expression of SMPD1 and ASAH1.

5.2. Materials and method:

5.2.1. Drug treatment:

Full details of the antidepressant drug treatment were previously described in Chapter Two, section 2.6.4. Briefly, to investigate the effect of chronic antidepressant drug administration on the gene expression level for the key sphingolipid-metabolizing enzymes (ASM and AC), 18 male Sprague-Dawley rats (body weights ranging from 122-142 g at the start of the experiment) were separated into three groups (6 animals/group/cage). All rats were weighed throughout the injection period and the first group (control group) received a single saline injection 0.9% (1 ml/kg/day, i.p), the second group (paroxetine group) received a single paroxetine injection (5 mg/kg/day, i.p), whereas the third group (desipramine group) received a single desipramine injection (10 mg/kg/day, i.p). All animals were injected once daily at 10 am for 15 days. Based on previously published studies investigating biochemical/molecular long-term effects of antidepressant drugs, rats were sacrificed 24 hour after the final injection (Andriamampandry et al., 2002; Bock et al., 2013; Gąska et al., 2012; Lee et al., 2010; Nakatani et al., 2004; Yamada et al., 2003). Then, the whole brain was removed and brain regions including the prefrontal cortex (PFC), hippocampus (HP) and the striatum (ST) were rapidly dissected out on ice as before. The regional brain samples were then quickly snap-frozen in isopentane on dry ice, brain samples were then weighed and stored at - 80°C until subsequent PCR analysis.

5.2.2. Measurement of the mRNA of genes encoding the sphingolipid-regulating enzymes, ASM and AC after chronic antidepressant drug treatment:

In this chapter, the real-time quantitative polymerase chain reaction (RT-qPCR) assay was employed to quantify changes in mRNA levels of SMPD1 and ASHA1, genes encoding the ASM and AC enzymes respectively (see Chapter Two, Figure 2.24). This was performed in regional brain samples from rats treated chronically with either paroxetine, desipramine or the corresponding vehicle (saline) once daily for 15 days. The primers used were designed and selected as previously described (Chapter Two, section 2.6.8) and the procedures of RNA extraction, DNA digestion, complementary DNA (cDNA) synthesis and the RT-qPCR process have been described in detail in Chapter Two, sections 2.6.5-2.6.9 respectively.

5.2.3. Data presentation and statistical analysis:

The SMPD1 and ASAH1 mRNA levels were measured following chronic antidepressant drug treatment (paroxetine and desipramine) in the three examined brain regions (PFC, HP and ST). The recorded values indicate the normalised expression levels of the mRNA of the two analysed genes of interest: SMPD1 and ASAH1 and were expressed as fraction of controls ± standard errors of the mean (SEM) for all regional brain samples (treated and controls). Additionally, the generated data were evaluated and normalised relative to two reference genes: beta-actin (β-actin) and glyceraldehyde 3-phosphate dehydrogenase (GAPDH) which were selected based on published studies investigating effects in rodent brain tissue (Bonefeld et al., 2008; Swijsen et al., 2012). Statistical analysis was performed by one-way analysis of variance (one-way ANOVA followed by Bonferroni t-test) using Prism 5.0 Software (Graph Pad Software) and statistically significant difference was set at a level of $p < 0.05$.

5.3. Results:

5.3.1. Effect of chronic antidepressant drug administration on the mRNA levels for the reference gene (β-actin):

The reference genes utilized in this study were selected and adopted on the bases of previously published studies (Bonefeld et al., 2008; Swijsen et al., 2012), taking into account their expression stability following exposure to the experimental treatment and under the

assay conditions. From these previous studies two different reference genes (housekeeping genes) were chosen and tested for normalisation of the generated data namely, β-actin (ACTB) and glyceraldehyde 3-phosphate dehydrogenase (GAPDH) (Figures 5.3 and 5.4). Based on these initial experiments, the β-actin gene (ACTB) showed the most stable expression and therefore, used for the further normalisation of our data.

Figure 5.3: Visualisation of the β-actin PCR products by 2% agarose gel electrophoresis. The first lane represents a ladder (a standard marker), then a negative control which is followed by the PCR products of the housekeeping gene (β-actin).

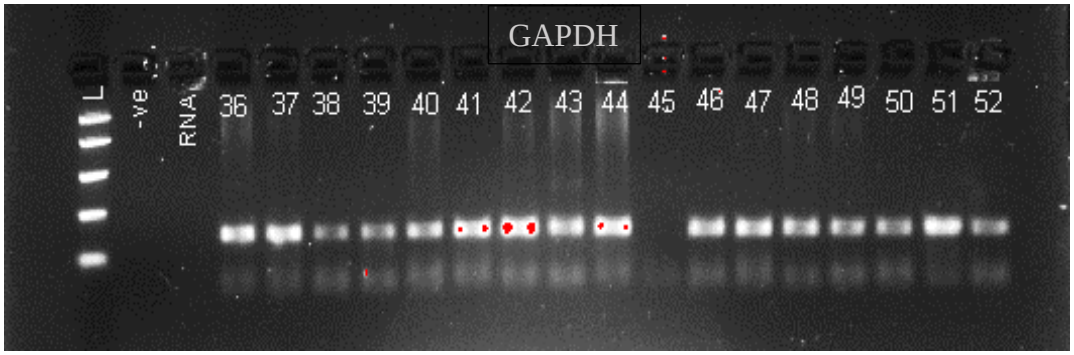

Figure 5.4: Visualisation of the GAPDH PCR products by 2% agarose gel electrophoresis. The first lane represents a ladder (a standard marker), then a negative control and the RNA product of this gene (no visible band) followed by the PCR products of the housekeeping gene (GAPDH).

Statistical analysis using one-way analysis of variance (one-way ANOVA) revealed no significant alteration in the average expression level of β-actin in the three investigated brain regions following either chronic paroxetine or desipramine treatment in comparison with the relevant saline-injected controls. Thus, indicating a stable expression level of the reference gene (β-actin) used in the present experimental model ($p > 0.05$) (Figures 5.5, 5.6 and 5.7).

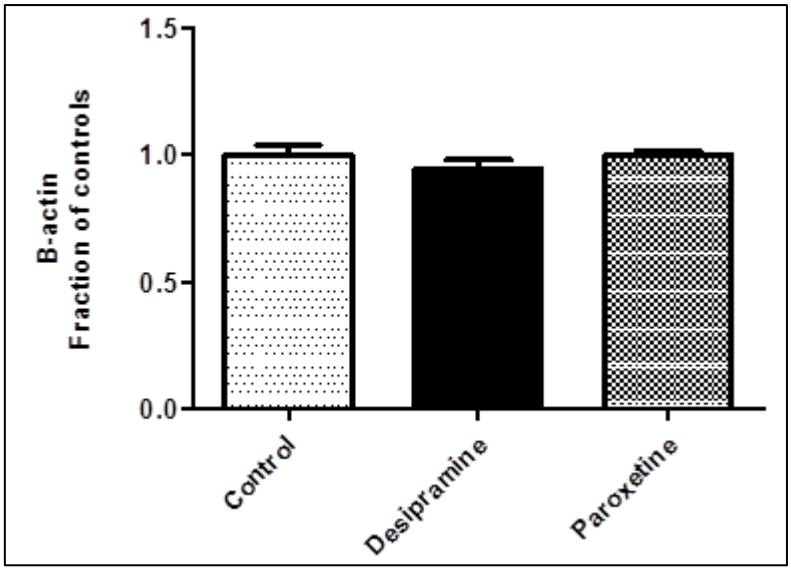

Figure 5.5: A comparison of the average expression levels of β-actin (ACTB) in the prefrontal cortex following both chronic saline (control) and drug treatment (desipramine and paroxetine). All values represent fraction of controls ± SEM (n = 6).

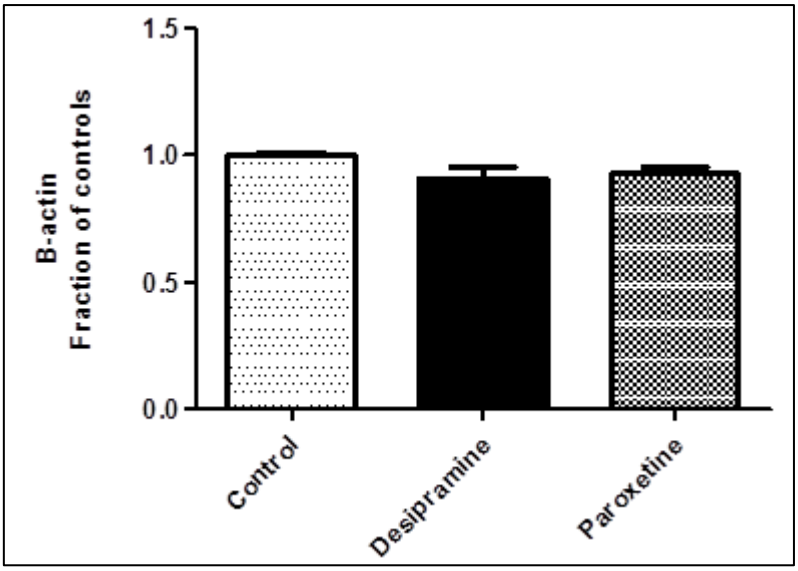

Figure 5.6: A comparison of the average expression levels of β-actin (ACTB) in the hippocampus following both chronic saline (control) and drug treatment (desipramine and paroxetine). All values represent fraction of controls ± SEM (n = 6).

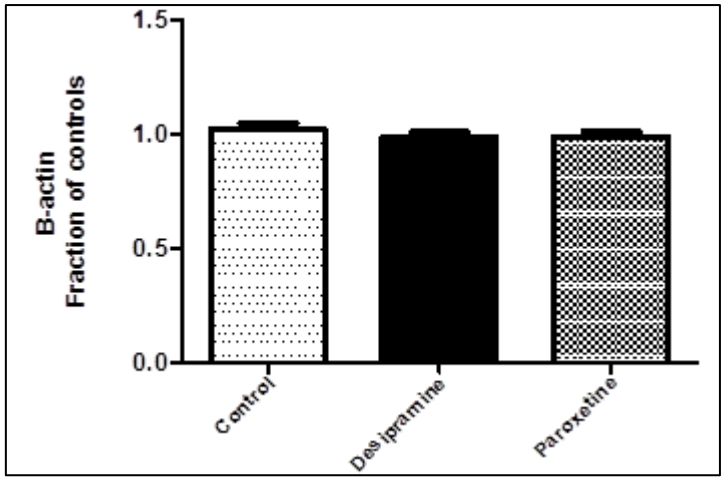

Figure 5.7: A comparison of the average expression levels of β-actin (ACTB) in the striatum following both chronic saline (control) and drug treatment (desipramine and paroxetine). All values represent fraction of controls ± SEM (n = 6).

5.3.2. Effect of chronic antidepressant drug administration on SMPD1 mRNA levels:

5.3.2.1. Effect of chronic paroxetine treatment on SMPD1 mRNA levels:

The expression of the SMPD1 gene which encodes the ASM enzyme was measured following long-term paroxetine treatment (once daily for 15 days) in rat brain regions (prefrontal cortex, hippocampus and striatum) using RT-qPCR method. The Bonferroni t-test indicated a significant reduction of SMPD1 mRNA levels in the hippocampus of the chronic paroxetine-treated rats compared to their corresponding saline-injected controls ($p = 0.015$, $F(2,17) = 5.610$) (Figure 5.8 and Table 5.1).

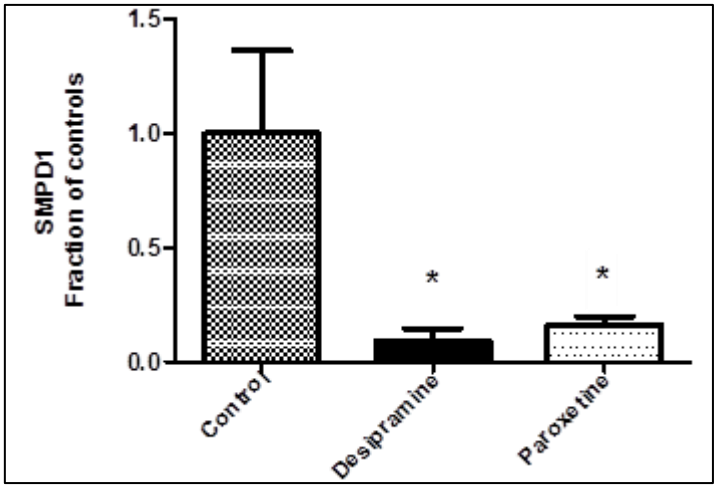

Figure 5.8: Normalised expression level of the SMPD1 gene in the hippocampus following chronic desipramine and paroxetine treatment (β-actin normalisation). All values represent fraction of controls ± SEM (n = 6). * $P < 0.05$ (one-way ANOVA with Bonferroni t-test).

In the prefrontal cortex, similar qualitative changes were observed following chronic paroxetine treatment, however and according to the Bonferroni t-test, this reduction failed to reach significance (p = 0.116) (Figure 6.9 and Table 6.1). In the striatum, paroxetine also had a tendency to decrease levels of the SMPD1 gene, however likewise in the prefrontal cortex, this effect remained non-significant here too (p = 0.322) (Figure 5.10 and Table 5.1).

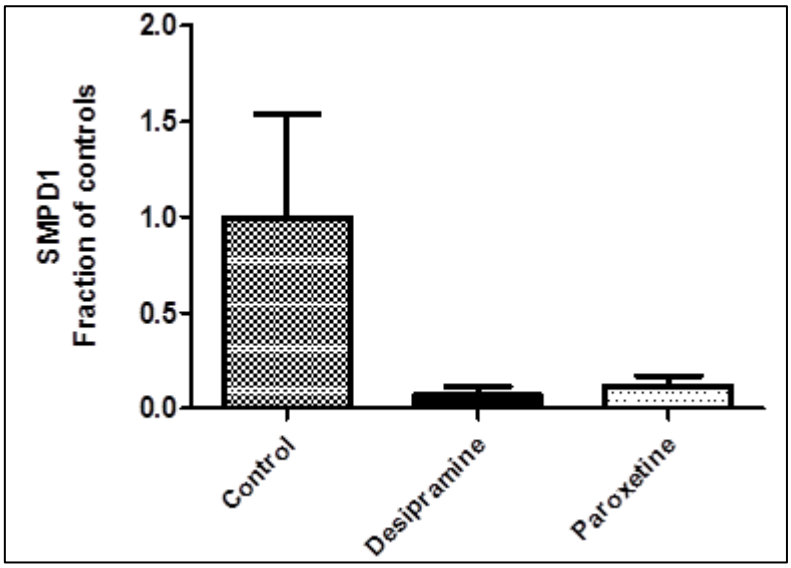

Figure 5.9: Normalised expression level of the SMPD1 gene in the prefrontal cortex following chronic desipramine and paroxetine treatment (β-actin normalisation). All values represent fraction of controls ± SEM (n = 6).

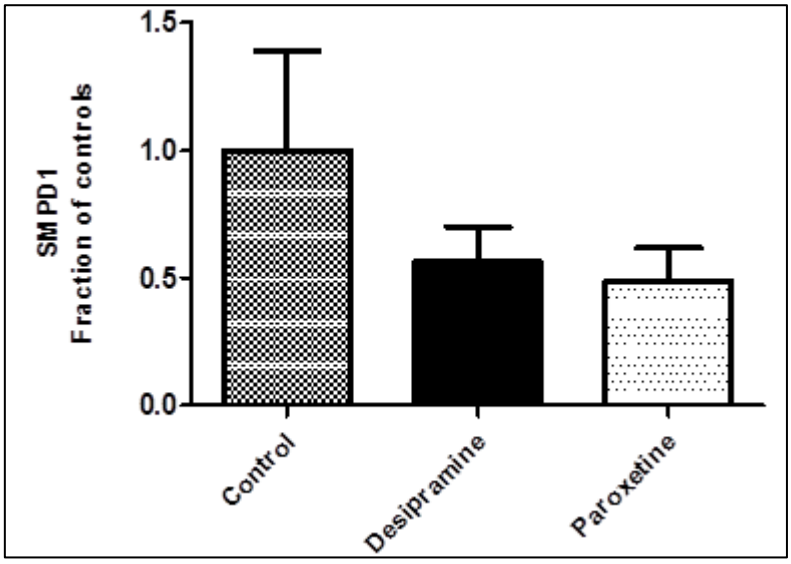

Figure 5.10: Normalised expression level of the SMPD1 gene in the striatum following chronic desipramine and paroxetine treatment (β-actin normalisation). All values represent fraction of controls ± SEM (n = 6).

5.3.2.2. Effect of chronic desipramine treatment on the SMPD1 mRNA level:

Consistent with the recorded findings after chronic paroxetine administration, in the hippocampus, treatment with desipramine similarly showed a significant reduction of SMPD1 mRNA levels in the drug-treated samples compared to the relevant controls as revealed by the Bonferroni t-test ($p < 0.05$, $F(2,17) = 5.610$) (Figure 5.8 and Table 5.1). Also, in the prefrontal cortex, there was a non-significant trend towards a reduced expression level of the SMPD1 gene (Figure 5.9 and Table 5.1). Further likewise with paroxetine in the striatum desipramine failed to significantly reduce expression levels of SMPD1 (Figure 5.10 and Table 5.1).

5.3.3. Effect of antidepressant drug administration on the ASAH1 mRNA level:

5.3.3.1. Effect of chronic paroxetine treatment on the ASAH1 mRNA level:

Measurement of the expression level of the ASAH1 gene which encodes the acid ceramidase (AC) enzyme was successfully established after chronic paroxetine treatment (once daily injections for 15 days) in the three investigated rat brain regions by means of the RT-qPCR technique. With regards to the SSRI paroxetine, it was found that in two of the three analysed brain regions, namely the prefrontal cortex and hippocampus, chronic paroxetine treatment induced a non-significant trend to reduce ASAH1 mRNA levels (Figures 5.12, 5.11 and Table 5.1). However, in the striatum, samples from paroxetine treated rats had very similar levels of ASAH1 mRNA as compared to their corresponding control samples (Figure 5.13 and Table 5.1).

5.3.3.2. Effect of chronic desipramine treatment on ASAH1 mRNA levels:

In comparison, to the effect by the SSRI paroxetine which failed to significantly alter ASAH1 mRNA levels, chronic administration of the TCA desipramine (once daily for 15 days) significantly reduced the expression of the ASAH gene in the hippocampus. Thus, the Bonferroni t-test revealed a significantly reduced ASAH1 mRNA level in comparison with the related controls ($p = 0.043$, $F(2,15) = 4.031$) (Figure 5.11 and Table 5.1).

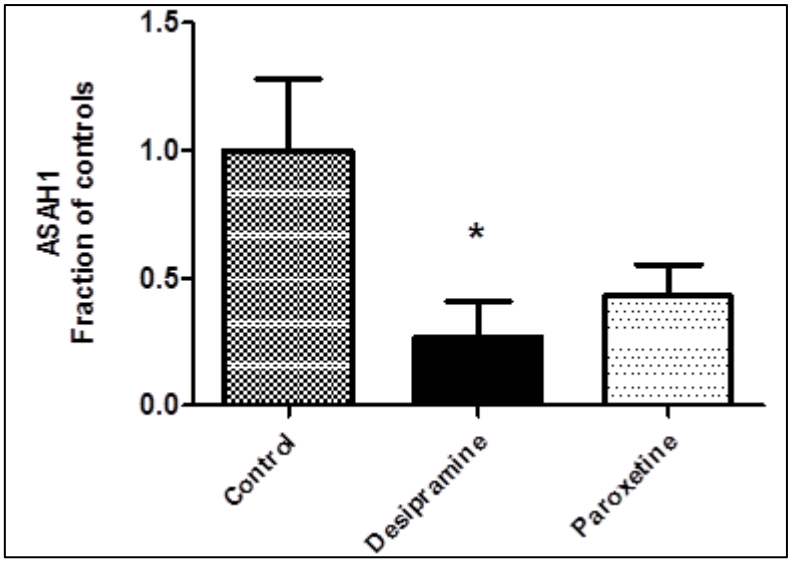

Figure 5.11: Normalised expression level of the ASAH1 gene in the hippocampus following chronic desipramine and paroxetine treatment (β-actin normalisation). All values represent fraction of controls ± SEM (n = 6). * P < 0.05 (one-way ANOVA with Bonferroni t-test).

In addition, similar qualitative changes were observed in the prefrontal cortex, although they were not statistically significant (p = 0.126) (Figure 5.12 and Table 5.1). Likewise, to paroxetine in the striatum, samples from desipramine treated rats had marginally similar levels to samples collected from the corresponding saline injected control group (Figure 5.13 and Table 5.1).

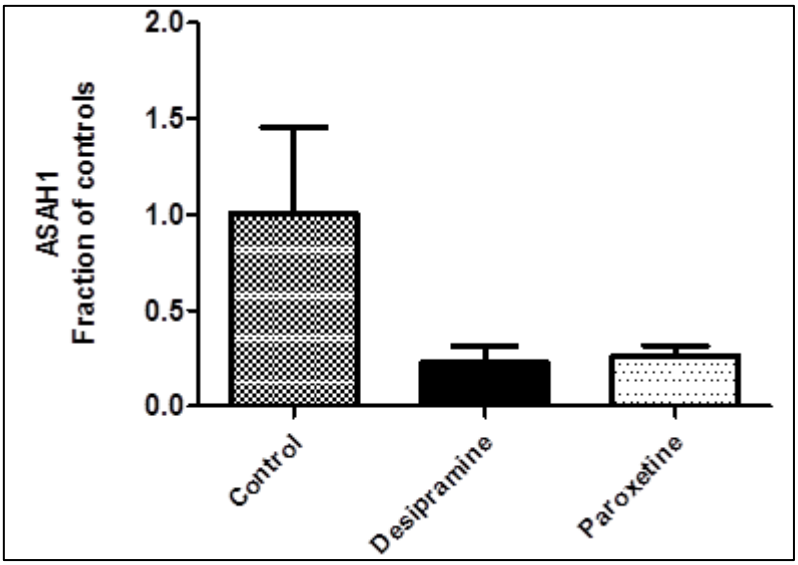

Figure 5.12: Normalised expression level of the ASAH1 gene in the prefrontal cortex following chronic desipramine and paroxetine treatment (β-actin normalisation). All values represent fraction of controls ± SEM (n = 6).

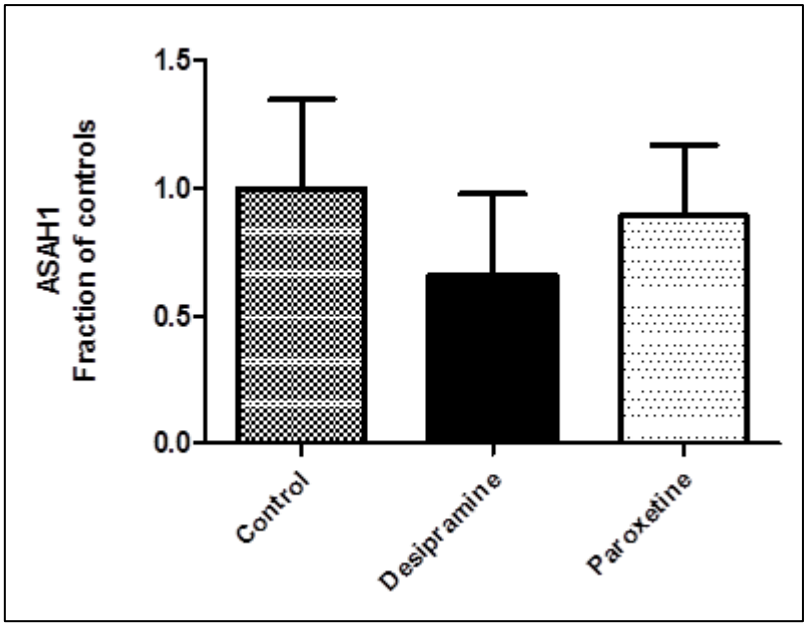

Figure 5.13: Normalised expression level of the ASAH1 gene in the striatum following chronic desipramine and paroxetine treatment (β-actin normalisation). All values represent fraction of controls ± SEM (n = 6).

Table 5.1: Normalised expression level of the target genes in rat brain following chronic desipramine and paroxetine treatment (β-actin normalisation) using real-time qPCR technique. Abbreviations: PFC, prefrontal cortex; HP, hippocampus and ST, striatum.

Gene symbol		PFC Normalised gene Expression level	HP Normalised gene Expression level	ST Normalised gene Expression level
ASAH1	Control	2.005 ± 0.910	4.572 ± 1.279	1.403 ± 0.486
	Desipramine	0.459 ± 0.168	1.226 ± 0.638 *	0.920 ± 0.454
	Paroxetine	0.520 ± 0.113	1.959 ± 0.504	1.525 ± 0.288
SMPD1	Control	7.012 ± 3.774	6.388 ± 2.326	1.060 ± 0.414
	Desipramine	0.488 ± 0.310	0.578 ± 0.353 *	0.597 ± 0.148
	Paroxetine	0.843 ± 0.372	1.025 ± 0.239 *	0.515 ± 0.139

Values indicate the normalised expression level of the target genes: ASAH1 and SMPD1 as mean ± SEM (n = 6). * $P < 0.05$ (one-way ANOVA with Bonferroni t-test).

5.4. Discussion:

5.4.1. Principal findings:

Clinical and pharmacological research have shown that high expression levels of AC in different cancer cells (i.e. melanoma, head and neck cancers, prostate and colon cancers) render these tumour cells to be more resistant to the pharmacological induction of apoptosis compared to normal cells (Pizzirani et al., 2013; Zeidan et al., 2008). This is likely to be associated with the enhanced tumour resistance to radiotherapy or chemotherapy, thus resulting in an increased risk of cancer relapse and progression (Pizzirani et al., 2013; Saied and Arenz, 2014). Indeed, small-molecules were recently identified as chemosensitizing compounds (i.e. carmofur) which promote death of cancer cells via AC inhibition (Canals et al., 2011; Pizzirani et al., 2013). Additionally, extensive work in another field of research has focussed on the regulation of ceramide synthesis and metabolism by the lipid-metabolizing enzymes acid sphingomyelinase (encoded by the SMPD1 gene) and acid ceramidase (encoded by the ASAH1 gene) respectively (Canals et al., 2011; Gulbins et al., 2013, 2015; Kornhuber et al., 2011). However, growing body of evidence also suggests that these two enzymes have potential roles in depression and its therapeutic interventions (Dinoff et al., 2017; Gulbins et al., 2013; Kornhuber et al., 2008, 2009; Jernigan et al., 2015). In Chapter Four, it was shown that two different antidepressant drugs: paroxetine and desipramine decreased levels of sphingolipids in brain areas related to the symptoms of depression. In this chapter, we therefore, sought to find a possible link between this action and two of the key target sphingolipid-processing enzymes. For this purpose, we used the polymerase chain reaction technique for the detection and quantification of the two target genes, SMPD1 and ASAH1. These two genes encode the ceramide synthesising enzyme acid sphingomyelinase and the ceramide metabolising enzyme acid ceramidase (breaks down ceramide to sphingosine) respectively. Using this technique, we reliably measured mRNA levels for SMPD1 and ASAH1 in rat brain regions (PFC, HP and ST) after chronic paroxetine and desipramine administration once daily for 15 days as well as from the corresponding controls receiving saline injection for the same period of time. To the best of our knowledge, this is the first study which examines these two genes or the corresponding proteins (i.e. AC or ASM) in regional brain samples from rats following antidepressant drug treatment. Interestingly expression levels for both SMPD1 and ASAH1 were quite similar in the hippocampus and prefrontal cortex but substantially

lower in the striatum (Table 5.1). In support of a lower activity of these genes in the striatum, this brain region also showed the lowest sphingosine levels (Chapter Four, Tables 4.1 and 4.2). Importantly, results from this chapter revealed that chronic paroxetine as well as desipramine treatment induced a significant reduction of SMPD1 mRNA levels in the hippocampus of the drug-treated rats compared to their corresponding saline-injected controls (Figure 5.8). Similarly, administration of both drugs resulted in a reduction of SMPD1 mRNA levels in the prefrontal cortex, this reduction however, in contrast to what was seen in the hippocampus, turned out to be a non-significant (Figure 5.9). In the striatum, both drugs failed to significantly alter the expression of the SMPD1 gene and generally the percentage reduction was smaller in this part of the brain (Figure 5.10). In addition, statistical analysis showed a significantly reduced expression level of the ASAH1 gene in the hippocampus after long-term desipramine administration (Figure 5.11), whereas a non-significant trend toward a reduced expression level of this target gene was observed following paroxetine treatment in the same specified brain region. Also, a similar trend was recorded in the ASAH1 mRNA level in the prefrontal cortex (Figure 5.12) without any detectable alteration in the expression level of this gene in the striatum after chronic treatment with both antidepressant drugs (Figure 5.13).

5.4.2. Effect of antidepressant drug administration on the expression of the SMPD1 gene:

In the present study, the generated data showed that chronic administration of paroxetine and desipramine resulted in a significant reduction of the SMPD1 mRNA levels, in the hippocampus and a similar non-significant trend was also recorded in the prefrontal cortex, but not in the striatum of the drug-treated animals in comparison with the relevant controls. In correspondence with these findings, our previously stated results in Chapter Four indicating that a similar antidepressant induced reduction of the targeted sphingolipids (sphingosine and ceramide) was observed only following chronic and not acute treatment (see Figures 4.9, 4.16 and 4.21 respectively). In connection with the possible role of ceramide in depression and its treatment, recent studies have explored the consequences of enhanced ceramide synthesis. This was established using a genetically modified mice strain that over expresses the ceramide synthesising enzyme ASM, which should theoretically lead to higher levels of ceramide compared to normal mice. More specifically, it was indeed reported that these

genetically modified mice with increased ASM activity showed higher hippocampal ceramide levels compared to normal mice. Moreover, such elevated ceramide levels coincided with enhanced depression-like behaviours in these mice compared to genetically non-modified mice. These animal models of depression included: suppression of feeding and sucrose preference as well as various behavioural tests such as the forced swim test and the coat test (Gulbins et al., 2013). In support of the role of elevated ceramide levels in depression; the depression like behaviours in the mice with elevated expression of the gene (i.e. the SMPD1 gene) encoding the ASM enzyme were significantly attenuated following administration of the SSRI fluoxetine or the TCA amitriptyline when administered in the drinking water at a concentration of 80 mg/L and 180 mg/L respectively. Drinking water containing the antidepressant drugs were made up fresh every 48 hours and treatment continued for 35 days (Gulbins et al., 2013). In this context, previous studies have reported that many antidepressant drugs act as functional inhibitors of acid sphingomyelinase activity as they all share a property of inhibiting this enzyme (see section 5.1.1.2) including various SSRIs (i.e. paroxetine) and all of the TCAs (i.e. desipramine) (Dinoff et al., 2017; Kornhuber et al., 2008, 2010, 2014). Thus, it was indicated that inside the acidic lysosomal compartment of the neurone, a slow intra-lysosomal accumulation of the antidepressant drug is developed. Accordingly, the charged or the protonated form of the compound become accumulated and trapped inside the lysosome via a continuous proton pump across the lysosomal membrane, this process is known as acid trapping or lysosomotropism (Kornhuber et al., 2009, 2011, 2014), see also Figure 5.1. Consequently, this increased drug concentration inside the lysosome induces a detachment and subsequent inactivation of ASM activity in the acidic lysosomal lumen (Kornhuber et al., 2009, 2014). Interestingly, it was found that this functional inhibition of ASM action develops slowly and takes 2-3 weeks to occur until the antidepressant drug accumulates in adequate amount in the brain tissues particularly inside the neuronal lysosomes (Dinoff et al., 2017; Kornhuber et al., 2009). Hence, the time required for the ASM inhibition is consistent with the time needed for the onset of the therapeutic action of the antidepressant drugs (Kornhuber et al., 1995, 2009, 2014), thus suggesting further evidence for the implication of ceramide in depression and the mechanism of antidepressant drug action.

5.4.3. Effect of antidepressant drug administration on the expression of the ASAH1 gene:

The present experimental dataset demonstrated that chronic desipramine administration induced a significant reduction of the ASAH1 gene which encodes the acid ceramidase enzyme specifically in the hippocampus. On the other hand, long-term paroxetine treatment showed only a non-significant trend towards a reduced expression level of the target gene in the same brain region of the drug-treated rats compared to their corresponding controls. Of specific interest, a previous cell culture study which used Chinese hamster ovary cells found that both ASM and AC enzymes are under a parallel regulation and a detected over-expression of the AC was also associated with an enhanced ASM level. Hence, suggesting that the expression level of these two enzymes are correlated. Although, the specific activity and abundance inside the lysosomes of the ASM and AC enzymes are still unknown, the specific activity of the ASM in the total human brain tissue was shown to be higher compared to that of AC (100-fold more) (He et al., 1999, 2003; Kornhuber et al., 2010). Accordingly, recent post mortem human studies on brain tissues of patients with Alzheimer's disease showed an increased expression of both ASM and AC enzymes. Also, there was a concomitant elevation of both ceramide and its metabolite sphingosine, while levels of the ceramide precursor sphingomyelin were found to be reduced in these patient brain samples compared to the normal controls (He et al., 2010). However, it was suggested that the TCA desipramine induces a non-selective functional or indirect inhibition of both lysosomal ASM as well as AC enzymes to the same extent (dual effect) (Arenz, 2010; Elojeimy et al., 2006; Kornhuber et al., 2010). In contrast, the SSRIs (e.g. paroxetine and fluoxetine) were shown to preferentially inhibit ASM activity over AC (Kornhuber et al., 2010). The results of the present study are in line with this finding, thus desipramine significantly inhibited hippocampal gene expression for both enzymes while paroxetine only showed significant reductions for the gene encoding ASM but not for the one encoding AC (Table 5.1). Furthermore, it was reported that the desipramine-induced inhibition of the AC enzyme was mediated by cathepsins B and L degradation (lysosomal proteases that are implicated in the intra-lysosomal proteolysis) (Elojeimy et al., 2006; Saied and Arenz, 2014). To the best of our knowledge, the current study is the first to investigate the effect of antidepressant drugs on the expression levels of SMPD1 and ASAH1 genes that encode two important lipid-processing enzymes namely, ASM

and AC respectively in brain regions implicated in depression. However, further research should be undertaken to improve our understanding of the mechanism underlies this action.

5.5. Conclusion:

The present study revealed that chronic antidepressant drug administration resulted in a significant reduction of the SMPD1 mRNA level in the hippocampus of the drug-treated rats compared to the corresponding saline-injected controls. Similarly, administration of both paroxetine and desipramine induced a non-significant trend to a reduction of the SMPD1 mRNA level in the prefrontal cortex but not in the striatum. Additionally, our data showed a significantly reduced expression level of the ASAH1 gene specifically in the hippocampus after chronic desipramine administration, whereas a non-significant trend toward a reduced expression level of this gene was observed following paroxetine treatment in the same brain region. Also, a similar trend was recorded in the ASAH1 mRNA level in the prefrontal cortex without any detected alteration in the striatum after chronic treatment with both antidepressant drugs. In this experimental set, the recorded reduction in the expression level of the target genes particularly in the rat hippocampus could be related to a functional or indirect inhibition of the corresponding lysosomal protein. However, and with respect to the ASAH1 gene, there was a more pronounced effect following chronic desipramine administration (a drug-specific effect) indicating a similar and a non-selective inhibition of both enzymes in the hippocampus after desipramine treatment. In summary, our findings show that long-term antidepressant drug treatment in the rat may induce a notable down-regulation of two hippocampal genes encoding two key enzymes of the brain sphingolipid pathways. Future studies should further proceed on investigating the functional inhibitors of ASM, aiming to diagnose a new antidepressant drug with a high efficacy and a faster action.

CHAPTER 6

Measurement of monoamine and metabolite levels in rat brain regions following acute carmofur treatment using high performance liquid chromatography with electrochemical detection (HPLC-ECD)

6.1. Introduction:

According to the monoamine hypothesis of depression, a reduction of the monoamine neurotransmitters including noradrenaline (NA), 5-HT and dopamine (DA) underlies the symptoms of depression (Schildkraut, 1965). Subsequently, extensive clinical and biochemical research regarding the cause of depression have focussed on central monoaminergic transmission. This particularly emphasising the brain 5-HT system as a critical target for the cause and treatment of depression (aan het Rot et al., 2009; Brigitta, 2002; Charnay and Leger, 2010; Hirschfeld, 2000). Additionally, a pharmacologically induced deficiency in brain levels of the monoamine neurotransmitters (i.e. achieved by tryptophan depletion) was shown to induce a mood lowering state in both depressed patients as well as in healthy controls (Krishnan and Nestler, 2008; Oosterhof, 2016). In this respect, studies conducted on depressed patients reported a reduced neural activity in multiple brain regions innervated by 5-HT neurons including the prefrontal cortex, hippocampus, thalamus and amygdala which are all associated with depressive symptoms (Oosterhof, 2016; Pandya et al., 2012; Price and Drevets, 2010). Further evidence for the involvement of 5-HT are studies demonstrating relapse of the disease state following depletion of the 5-HT precursor tryptophan (Bremner et al., 1997; Merens et al., 2008; Nemeroff, 2002; Oosterhof, 2016) to patients undergoing remission following antidepressant drug treatment. The indole monoamine 5-HT undergoes metabolism by the monoamine oxidase enzyme (MAO) which is found in two subtypes: MAO-A and MAO-B albeit both are present in 5-HT neurons, but the latter constituting the predominant form. 5-HT is likewise NA preferentially metabolized by MAO-A, while DA is mainly metabolized by MAO-B (Oosterhof, 2016; Shih and Thompson, 1999). Following metabolism, 5-hydroxyindoleacetic acid (5-HIAA) is produced as the major 5-HT metabolite and then excreted into the cerebrospinal fluid (CSF), where it can be identified as a marker of 5-HT metabolism and neurotransmission (Oosterhof, 2016). Previous clinical and post mortem studies of depressed patients as well as CSF sampling from suicide attempters have revealed a significantly lower CSF content of 5-HIAA in these patient groups as compared to levels found in healthy controls, indicating reduced 5-HT metabolism/neurotransmission in depressed subjects (Åsberg et al., 1984; Oosterhof, 2016; Placidi et al., 2001; Roy et al., 1989). Further, another important finding that supports abnormalities in 5-HT neurotransmission in depression is the alteration in the binding affinity for some key 5-HT receptors, in particular

the pre-synaptic inhibitory 5-HT1A receptors. It was observed that the binding activity of these autoreceptors which are located on serotonergic neurons in the dorsal raphe nucleus of the midbrain is significantly increased in depression (Stockmeier et al., 1998). In contrast, the binding activity of the post-synaptic 5-HT1A receptors was found to be decreased, particularly in the prefrontal cortex of depressed patients, suggesting a reduced serotonergic transmission in these affected subjects (Oosterhof, 2016; Stockmeier et al., 1998).

Sphingolipids together with cholesterol constitute the major lipid components of the cell membranes in the brain. These lipids interact to form specific compartments in the neuronal cell membranes known as lipid rafts which are considered to be the main sites for the activation of the acid sphingomyelinase enzyme which catalyzes the degradation of sphingomyelin into ceramide and phosphorylcholine. Subsequently, the generation of ceramide results in the formation of ceramide-rich platforms in the brain cell membranes (see Chapter One, sections 1.9 and 1.10) (Dinoff et al., 2017; Müller et al., 2015; Schneider et al., 2017). Interestingly, these platforms allow clustering and binding of receptors including G-protein coupled receptors (GPCRs) such as the 5-HT1A autoreceptors. Thus, modulation of ceramide levels may affect neurochemical mechanisms including cell signaling related to 5-HT neurotransmission (see Chapter One, section 1.10.1) (Cremesti et al., 2002; Kolesnick et al., 2000; Singh et al., 2012). Importantly, it was found that this lipid-protein interaction of the cell membrane appeared to be essential in maintaining the function as well as the ligand binding activity of the 5-HT1A receptors (Singh et al., 2012).

Carmofur (1-hexacarbamoyl-5-fluorouracil) is a fluorinated pyrimidine that is converted in the body to 5-fluorouracil (a compound that inhibit DNA synthesis by inhibiting the thymidylate synthetase enzyme). Carmofur has been widely used clinically since the early eighties as an effective antineoplastic agent (Koyama et al., 1980). It was reported that this compound exerts a potent adjuvant chemotherapeutic effect with a low toxicity via mediating a synergistic action with other antitumoral agents to inhibit viability, proliferation and growth of cancer cells. In addition, it may facilitate death of cancer cells (induction of apoptosis), in particular when combined with other chemotherapeutic drugs (Sakamoto et al., 2005, 2006). Furthermore and thus of importance for the current study, carmofur is a potent inhibitor of

acid ceramidase activity leading to increased intracellular ceramide levels, an effect associated to the drug's anti-proliferative activity (Mahdy et al., 2009; Pizzirani et al., 2013; Realini et al., 2013). Acid ceramidase (AC) is a lysosomal polypeptide composed of 395 amino acids that operates optimally at a pH 4.5 to catalyze the hydrolysis of ceramide into sphingosine and fatty acid (Saied and Arenz, 2014; Shtraizent et al., 2008). Given that carmofur inhibits AC, a recent study reported that injections of carmofur (10 and 30 mg/kg i.p) to mice resulted in a significant increase of tissue ceramide levels (cerebral cortex and lung) with a concomitant reduction of sphingosine content compared to the corresponding controls (Realini et al., 2013). In this regard, a related study revealed that the anti-proliferative effect of carmofur is also dependent on its potent inhibitory activity of the acid ceramidase enzyme and not on the capability to inhibit DNA synthesis via the generation of 5-fluorouracil (Pizzirani et al., 2013). Despite the accumulated evidence suggesting that a dysregulation of the central ceramide biosynthesis could be related to depression (Dinoff et al., 2017; Müller et al., 2015; Schneider et al., 2017), to the best of our knowledge, definitive evidence regarding the link between brain ceramide and monoamine levels is still deficient. In Chapter Four of this thesis, we showed that antidepressant drugs indeed reduced brain levels of sphingolipids. In this chapter, we attempted to elucidate a link between ceramide levels and monoamine levels by investigating the action of the AC inhibitor carmofur on monoamine levels in brain regions implicated in depression.

6.1.1. Aim:

The principal aim of the present study was to investigate the effect of acute carmofur administration to rats on the levels of the principal monoamine neurotransmitters including: 5-HT, DA and NA as well as some of their metabolites namely, 5-HIAA and DOPAC in brain regions implicated in depression. Further, the central effect of carmofur treatment was evaluated by measuring levels of ceramide and its major metabolite (sphingosine) in rat brain regions by means of HPLC-UV and LC-MS techniques respectively (see Chapter Four). Specifically, the effects of acute carmofur administration or the corresponding vehicle were assessed on:

- Monoamine and metabolite levels in tissue samples from rat prefrontal cortex, hippocampus and striatum using HPLC-ECD.

- Ceramide levels in tissue samples from the prefrontal cortex, hippocampus and striatum using HPLC-UV.
- Brain sphingosine content in the same samples as above using LC-MS.

6.2. Materials and method:

6.2.1. Analysis of monoamine and metabolite levels following acute carmofur treatment by HPLC-ECD:

6.2.1.1. Carmofur treatment and sample collection:

The present study was performed to examine the effects of acute carmofur administration on the following monoamine neurotransmitters: 5-HT, DA as well as NA. In addition, levels of 5-HIAA and DOPAC, metabolites of 5-HT and dopamine respectively were measured in the three investigated brain regions (prefrontal cortex, PFC; hippocampus, HP and striatum, ST) from rats treated with carmofur or the corresponding vehicle. For this experimental set, 12 male Sprague-Dawley rats were separated into two groups (6 animals/ group/cage): The first group (control group, n = 6) received a single i.p injection (1 ml/kg) of the vehicle that carmofur was dissolved in, which consisted of 70% saline, 15% Tween-80 and 15% polyethylene glycol (Realini et al., 2013). The second group (carmofur group, n = 6) received a single i.p injection of carmofur (20 mg/kg). The rats were sacrificed one hour after the injection via the schedule one method and the whole brain was removed. Then, brain regions were rapidly dissected out on ice and snap frozen using isopentane on dry ice, weighed and stored at - 80°C to avoid enzymatic degradation until subsequent analysis by the HPLC-ECD system.

6.2.1.2. Sample preparation:

The sample preparation method and the HPLC protocol including all the mobile phases and the stationary phase used in these experiments are fully described in Chapter Two, sections 2.5.3 and 2.5.4. Following homogenization of tissues in cold 0.2 M perchloric acid (PCA) (0.1 ml per mg of tissue), the samples were centrifuged for 5 minutes and the collected clear supernatants were utilized for the measurement of 5-HT, DA, NA, 5-HIAA and DOPAC using the HPLC-ECD system. Then, the remaining sediments of the tissue homogenates were preserved at - 80°C for subsequent lipophilic extraction and further sphingosine and ceramide analysis by the LC-MS and UV-HPLC techniques respectively.

6.2.1.3. Calibration and determination of monoamine concentrations:

Fresh serial dilutions of individual monoamines and their acidic metabolite standards were prepared in 0.2 M PCA to obtain concentrations ranging from 10-500 ng/ml. The individual standards were prepared immediately before the analysis and were loaded on the column to identify the representative peaks of individual compounds. In brief, following chromatographic separation; retention times and the area under each peak were determined using Breeze 2 software (for details see Chapter Two, section 2.5.4.2). Standard calibration curves were plotted separately for each investigated group, this was done in order to calculate the concentration of the monoamines and their metabolites in each analysed brain sample (Figures 2.20 and 2.21). Validation of the method was examined by assessing the linearity of the generated standard curves and their linear coefficient of variation (R^2) values (see Chapter Two, sections 2.5.3 and 2.5.4).

6.2.1.4. Data presentation and statistical analysis:

Data from the monoaminergic HPLC study was analysed statistically by Student's t-test using Prism 5.0 Software (Graph Pad Prism Software) to determine the difference between the control and treatment groups. Values were expressed as ng/g tissue wet weight for each analysed brain sample. Datasets obtained from the sphingosine and ceramide analysis using LC-MS and HPLC-UV respectively were tested using two-way analysis of variance (two-way ANOVA with Bonferroni post-hoc test) for multiple comparison. To compare the data means, two-way ANOVA was used with testing the effect of two variables (treatment and brain region) also, observing the interaction effect between these factors or variables. All data were presented as means ± standard errors of the mean (SEM) for each group. Statistically significant difference was considered at a value of $p < 0.05$. In addition, sample content of sphingosine or ceramide was calculated as mg sphingosine or ceramide/mg protein for all the analysed samples, using the area under the peak for each integrated signal.

6.2.2. Sphingosine analysis following acute carmofur treatment by LC-MS:

6.2.2.1. Sample preparation and lipid extraction:

After completing the monoaminergic analysis and following the removal from - 80°C, the frozen tissue pellets were used to perform the lipid extraction procedure in each sample which is described in detail in Chapter Two, section 2.3.2. Then, the prepared brain samples were utilized for the subsequent sphingosine analysis in both control and treatment groups following acute carmofur administration using LC-MS. For detailed description of the LC-MS protocol used, including mobile phases, column type and LC-MS conditions see Chapter Two, section 2.3.3.

6.2.2.2. Calibrations and determination of sphingosine concentrations:

For quantification of sphingosine concentration in the brain samples, standard curves were plotted for each analysed group. Sphingosine standards were dissolved in methanol to produce stock solutions at 200 mg/L followed by storage at - 80˚C. Then immediately before the analysis, 50 mg/L working stock and subsequent fresh serial dilutions were made in methanol to provide concentrations ranging from 0.2 – 15 mg/L (Figures 2.13, 2.14 and 6.16). Validation of the method was examined by observing the linearity of the standard curves and their R^2 values (see Chapter Two, section 2.3.4).

6.2.3. Ceramide analysis following acute carmofur treatment by HPLC-UV:

6.2.3.1. Sample preparation and benzoylation of ceramide:

For the measurements of ceramide in brain lipid extracts using HPLC-UV, regional brain samples from the carmofur treated rats and their corresponding controls had to be benzoylated by a derivatization reaction using benzoyl chloride and pyridine, for detailed description of this process see Chapter Two, section 2.4.2. After reconstitution with acetonitrile, the aliquots (35 µl of the benzoylated ceramide) were injected into the HPLC-UV system for ceramide analysis. Further, the HPLC protocol including the mobile phases, the type of column and the HPLC conditions are fully described in Chapter Two, section 2.4.3.

6.2.3.2. Calibrations and determination of ceramide concentrations:

To analyse the ceramide concentration in all of the brain samples, standard curves were plotted before the analysis of each experimental group. Thus, the ceramide standard was dissolved in methanol to produce a stock solution at a concentration of 1000 mg/L which was stored at - 80˚C. For the generation of standard curves, a working stock solution of 50 mg/L and subsequent fresh serial dilutions were made up in methanol to obtain concentrations ranging from 0.5 – 40 mg/L (Figure 2.17). Validation of the method was assessed by the level of linearity of the standard curves and their R^2 values (see Chapter Two, section 2.4.3).

6.3. Results:

6.3.1. Analysis of monoamine and metabolite levels following acute carmofur treatment using HPLC-ECD:

Using the HPLC-ECD technique, a reliable detection and measurement of the following monoamine neurotransmitters was achieved: 5-HT, dopamine (DA) and noradrenaline (NA) as well as the metabolites of 5-HT and DA: 5-hydroxyindoleacetic acid (5-HIAA) and 3, 4-dihydroxyphenylacetic acid (DOPAC) respectively (Figures 6.1-6.10). Using this method, the present experiment shows that carmofur, a potent ceramidase inhibitor when administered acutely results in increases of monoamine (5-HT, DA and NA) levels in regional brain samples as compared to their levels in brain samples harvested from the corresponding vehicle injected controls (Figures 6.1, 6.8 and 6.10). This effect was however only minor for DA and NA and only significant for 5-HT (Table 6.2) and for this indole monoamine, carmofur induced a marked increase in all three brain regions analysed (Figure 6.1). Specifically, the results from this study show that a single injection of carmofur (20 mg/kg, i.p) induced a significant increase in 5-HT content in the three explored brain regions (PFC, HP and ST) compared to their corresponding controls. In the prefrontal cortex, acute carmofur treatment resulted in significantly increased 5-HT levels in comparison with the relevant controls ($p = 0.025$, $t = 2.628$, $df = 10$) (Table 6.1, Figures 6.1 and 6.3). Similarly, in tissue extracts from the hippocampus, a significant elevation of 5-HT content was detected in the treatment group compared to the corresponding vehicle-treated controls ($p = 0.032$, $t = 2.491$, $df = 10$) (Table 6.1, Figures 6.1 and 6.4). Likewise, to the prefrontal cortex and the hippocampus, in the striatum, acute carmofur administration induced significantly increased 5-HT level in the

drug-treated rats compared to their controls (p = 0.027, t = 2.585, df = 10) (Table 6.1 and Figure 6.1).

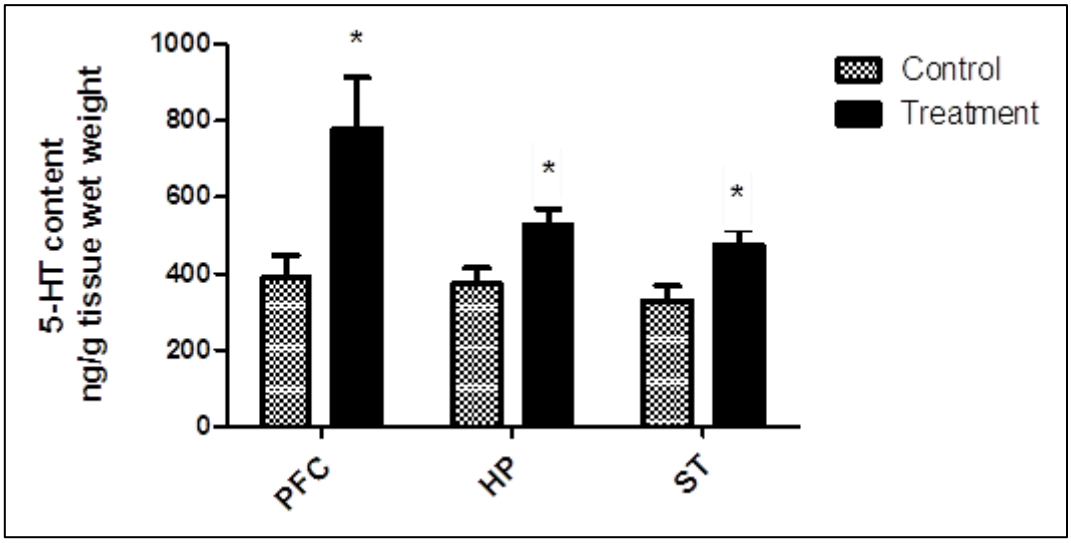

Figure 6.1: 5-HT content in (ng/g tissue wet weight) in rat brain regions following acute carmofur treatment. All values represent mean ± SEM (n = 6). Abbreviations: PFC, prefrontal cortex; HP, hippocampus and ST, striatum. * P < 0.05 (Student's t-test).

Furthermore, in the present study the effect of carmofur on the 5-HT metabolite 5-HIAA was also examined in regional brain extract. Interestingly, in contrast to whole tissue levels of the indolamine neurotransmitter 5-HT itself, levels of its acidic main metabolite 5-HIAA were consistently reduced in brain samples from carmofur treated rats compared to the corresponding control samples (Table 6.1 and Figure 6.2). Following statistical analysis and using Student's t-test, these carmofur induced reductions of 5-HIAA levels were highly significant in all three brain regions analysed; in the prefrontal cortex (p = 0.004, t = 3.687, df = 10) and striatum (p = 0.001, t = 4.554, df = 10) and in the hippocampus (p = 0.0005, t = 5.015, df = 10) see Table 6.1 and Figure 6.2. In contrast, carmofur failed to significantly alter levels of the DA metabolite DOPAC in brain regional tissue extracts from the PFC and ST but both DA and DOPAC were undetectable in the HP (Table 6.1 and Figures 6.5 and 6.8).

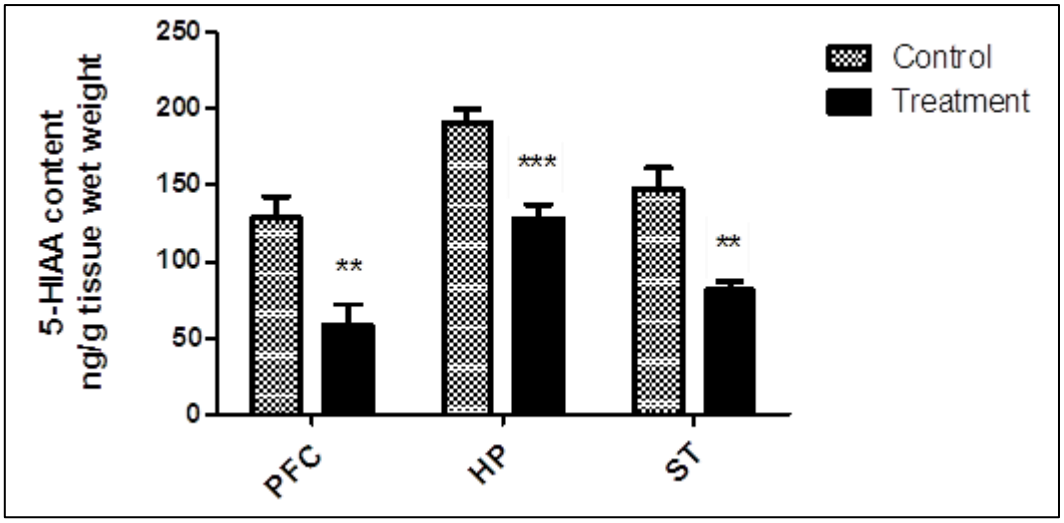

Figure 6.2: 5-HIAA content in (ng/g tissue wet weight) in rat brain regions following acute carmofur treatment. All values represent mean ± SEM (n = 6). Abbreviations: PFC, prefrontal cortex; HP, hippocampus and ST, striatum. ** P < 0.01 and *** p < 0.001 (Student's t-test).

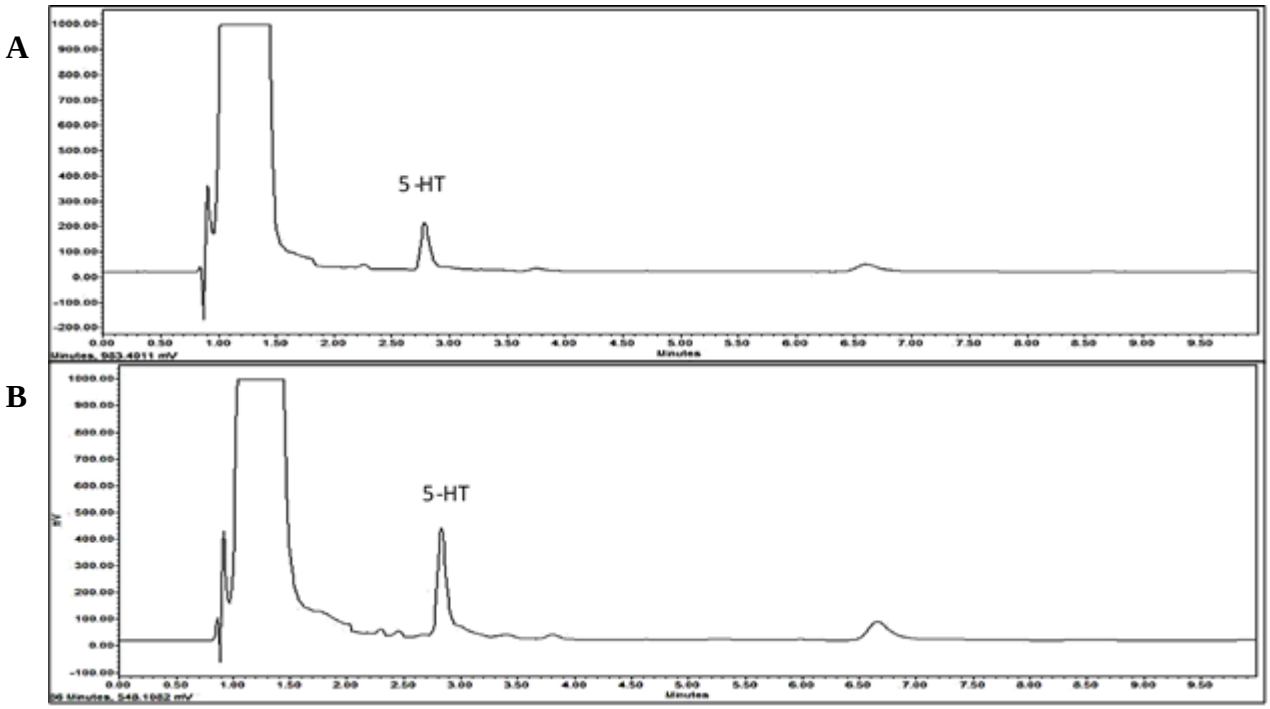

Figure 6.3: HPLC-ECD chromatogram of frontal cortical samples obtained from (A) control and (B) treated animals following acute carmofur administration showing 5-HT peak at a retention time of 2.77 and 2.82 minutes respectively.

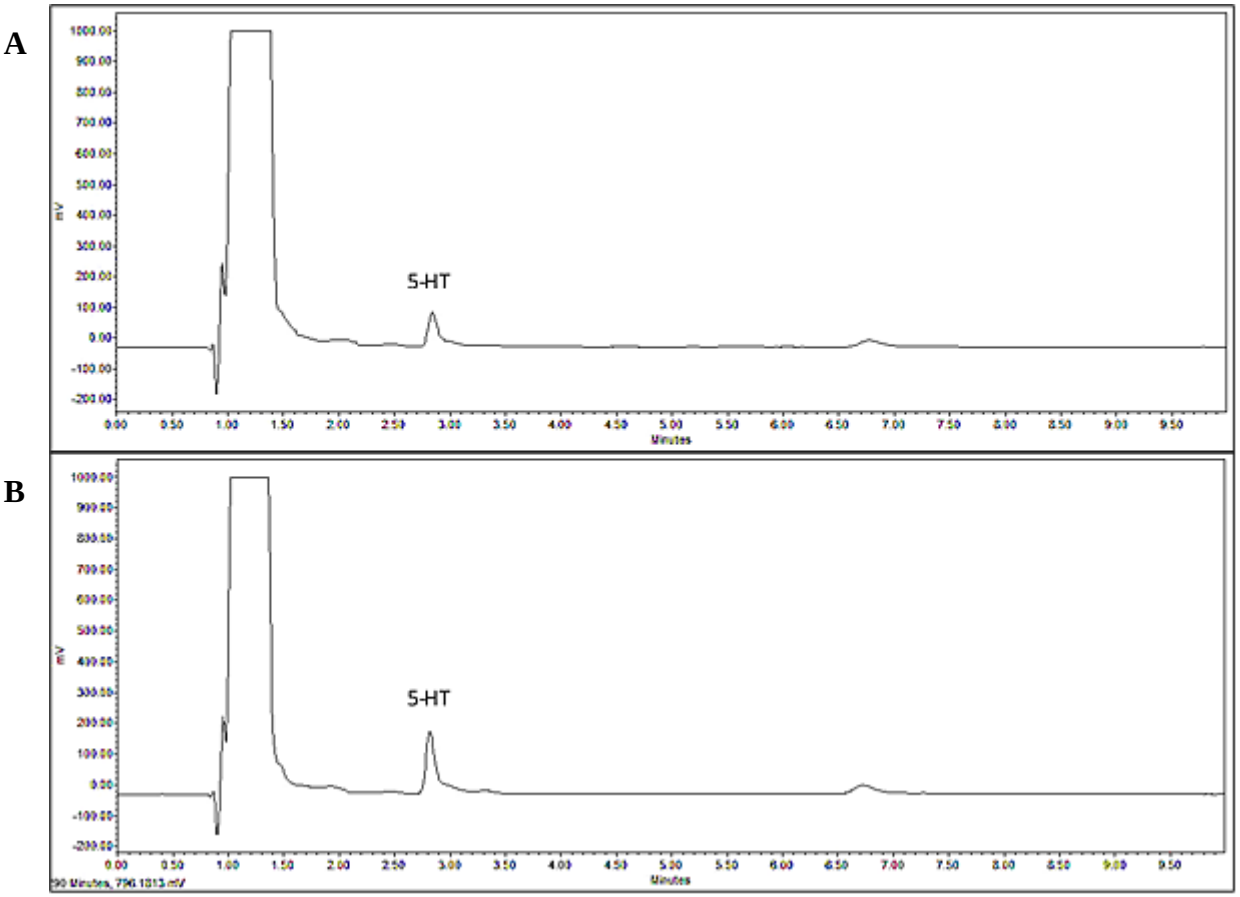

Figure 6.4: HPLC-ECD chromatogram of hippocampal samples obtained from (A) control and (B) treated animals following acute carmofur administration showing 5-HT peak at a retention time of 2.83 and 2.79 minutes respectively.

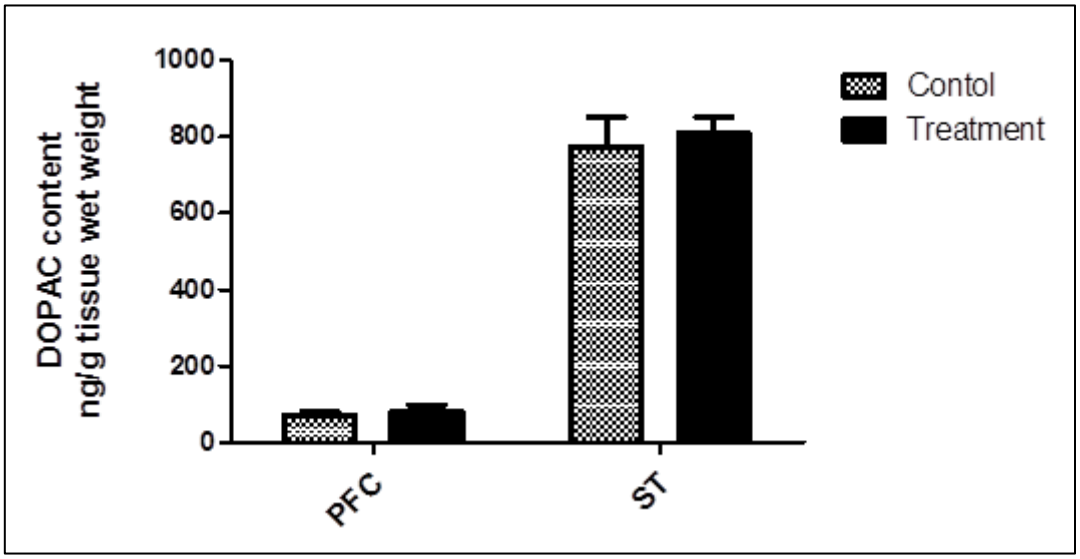

Figure 6.5: DOPAC content in (ng/g tissue wet weight) in rat brain regions (PFC and ST but DOPAC was undetectable in the HP) following acute carmofur treatment. All values represent mean ± SEM (n = 6). Abbreviations: PFC, prefrontal cortex and ST, striatum.

A

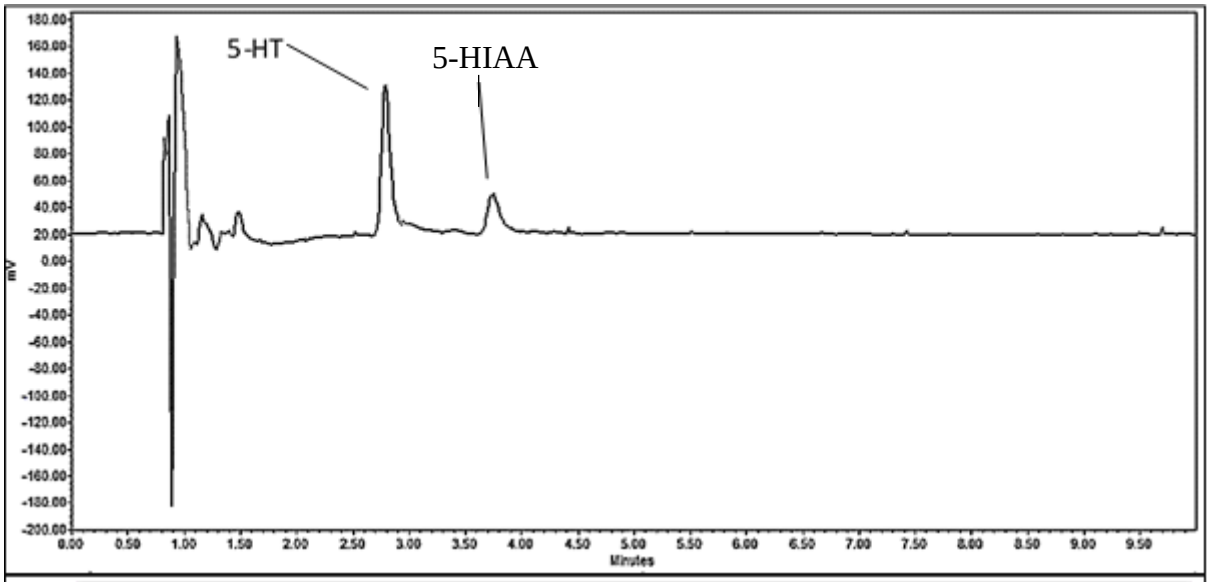

B

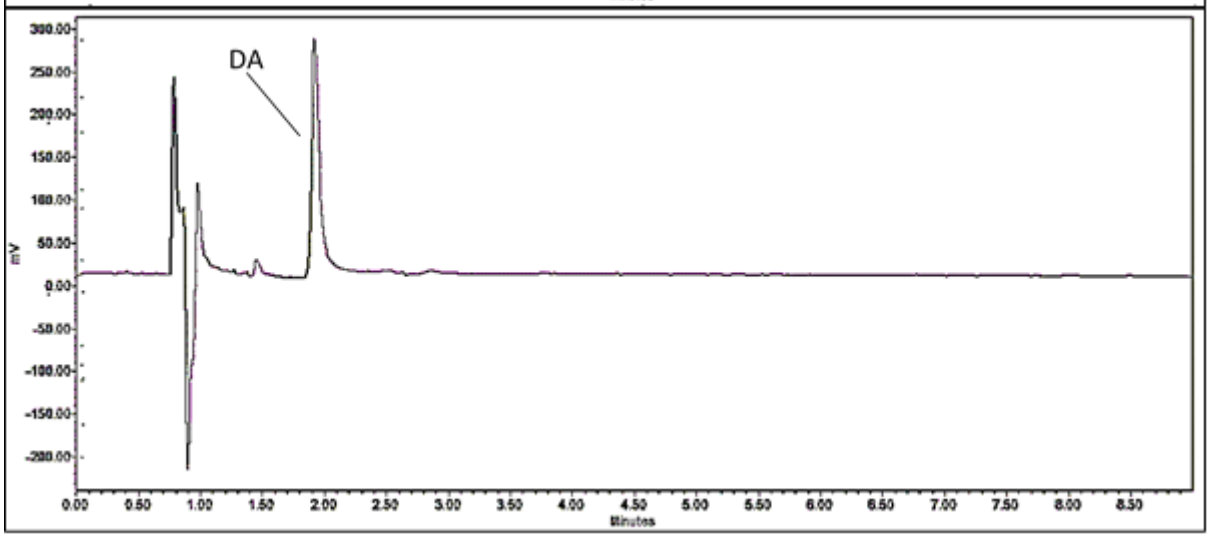

Figure 6.6: (A) HPLC-ECD chromatogram showing 5-HT and 5-hydroxyindoleacetic acid (5-HIAA) standard peaks at a concentration of 20 ng/ml and a retention time of 2.78 minute and 4 minutes respectively. (B) HPLC-ECD chromatogram showing dopamine (DA) standard peak at a concentration of 50 ng/ml and a retention time of 1.912 minute.

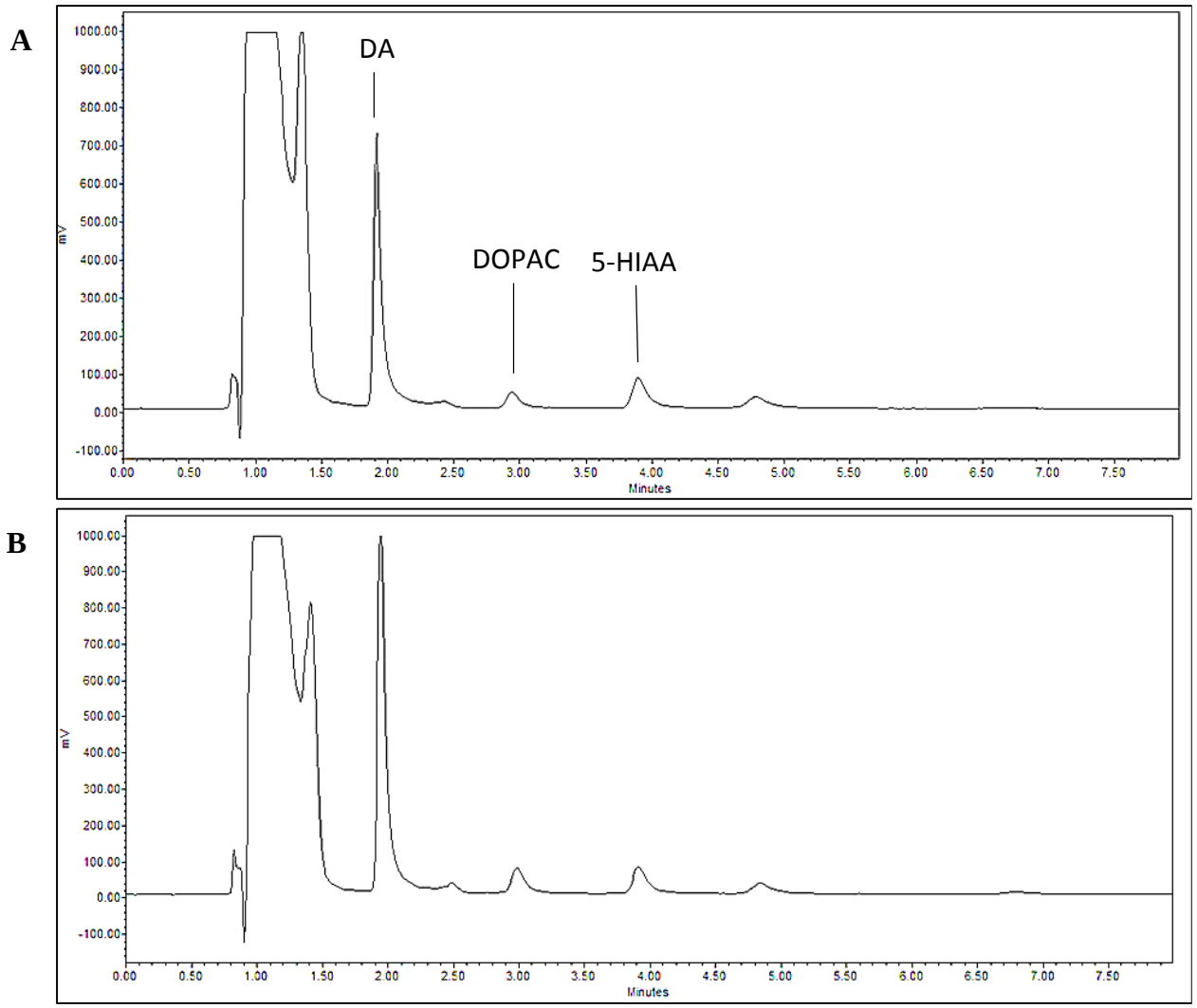

Figure 6.7: HPLC-ECD chromatogram of striatal samples obtained from (A) control and (B) treated animals following acute carmofur administration showing dopamine (DA), 3,4-dihydroxyphenylacetic acid (DOPAC) and 5-hydroxyindoleacetic acid (5-HIAA) peaks at a retention time of 1.913, 3.10 and 4.10 minutes respectively.

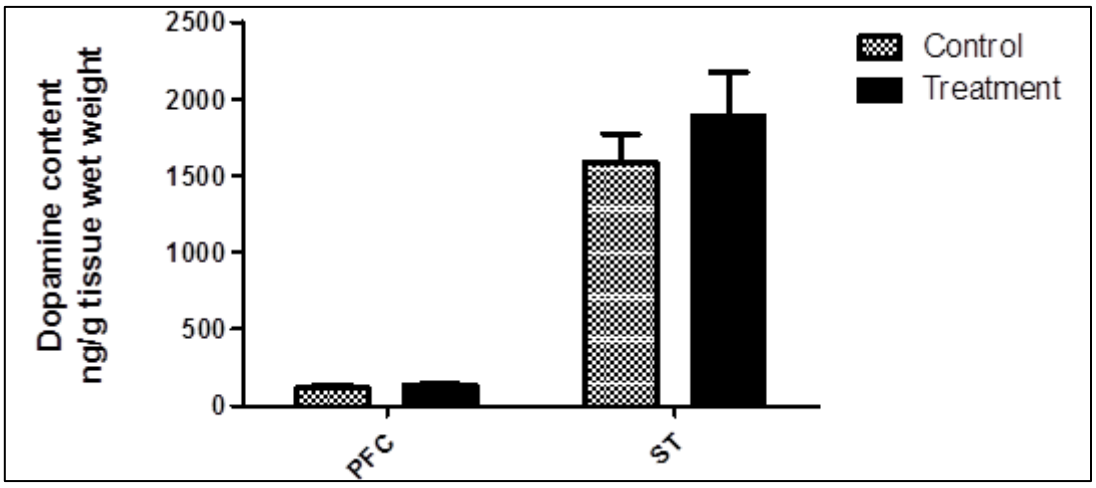

Figure 6.8: Dopamine content in (ng/g tissue wet weight) in rat brain regions (PFC and ST but DA was undetectable in the HP) following acute carmofur treatment. All values represent mean ± SEM (n = 6). Abbreviations: PFC, prefrontal cortex and ST, striatum.

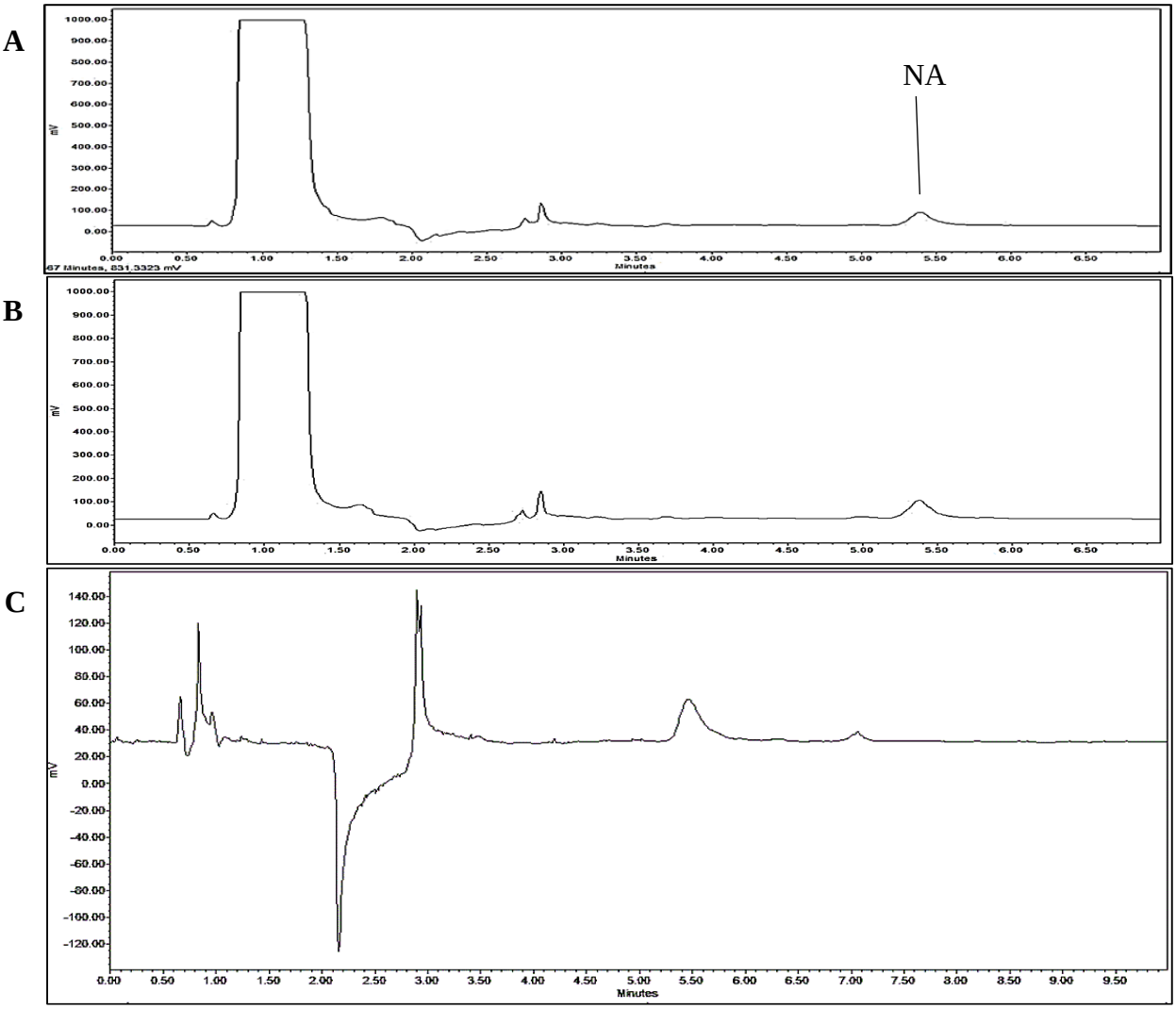

Figure 6.9: HPLC-ECD chromatogram of hippocampal samples obtained from (A) control and (B) treated animals following acute carmofur administration showing noradrenaline (NA) peak at a retention time of 5.25 minute. (C) HPLC-ECD chromatogram showing NA standard peak at a concentration of 50 ng/ml and a retention time of 5.224 minute.

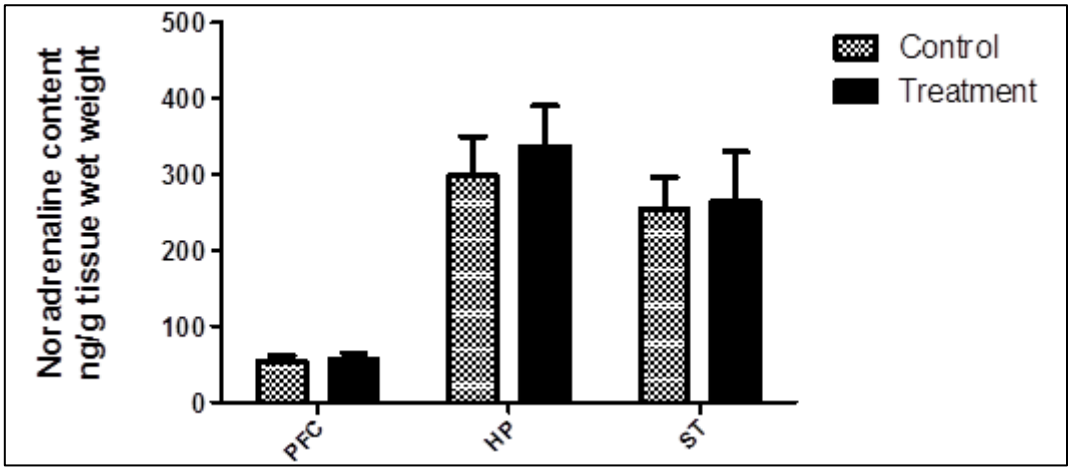

Figure 6.10: Noradrenaline content in (ng/g tissue wet weight) in rat brain regions following acute carmofur treatment. All values represent mean ± SEM (n = 6). Abbreviations: PFC, prefrontal cortex; HP, hippocampus and ST, striatum.

Table 6.1: Summary of changes in rat brain levels of monoamine neurotransmitters and their metabolites following acute carmofur treatment (20 mg/kg, i.p).

	Monoamines and metabolites	Brain region	Control group (ng/g wet weight)	Treatment group (ng/g wet weight)	P-value
1	5-HT	Prefrontal cortex	388.9 ± 59.05	777.6 ± 135.6	0.025*
		Hippocampus	373.5 ± 40.67	525.1 ± 45.22	0.032*
		Striatum	329.7 ± 39.11	474.9 ± 40.34	0.027*
2	5-HIAA	Prefrontal cortex	129.1 ± 13.53	58.32 ± 13.6	0.004**
		Hippocampus	191.2 ± 8.532	128.3 ± 9.209	0.0005***
		Striatum	147.6 ± 13.5	81.14 ± 5.581	0.001**
3	Noradrenaline	Prefrontal cortex	54.38 ± 7.475	56.18 ± 9.183	0.882
		Hippocampus	298.1 ± 52.35	337 ± 53.25	0.613
		Striatum	253.7 ± 43.26	263.5 ± 66.48	0.904
4	Dopamine	Prefrontal cortex	120.8 ± 12.64	135.5 ± 8.692	0.363
		Striatum	1588 ± 181.5	1882 ± 292.4	0.413
5	DOPAC	Prefrontal cortex	70.7 ± 11	81.43 ± 17.71	0.618
		Striatum	773.8 ± 77.19	807.5 ± 44.5	0.713

Values indicate monoamines and metabolite concentrations (ng/g tissue wet weight) as mean ± SEM (n = 6), carmofur treatment versus corresponding control group; * $p < 0.05$; ** $p < 0.01$; *** $p < 0.001$ (Student's t-test).

6.3.2. Analysis of sphingosine in rat brain following acute carmofur treatment using LC-MS:

In this chapter, carmofur has been shown to induce significant increases of 5-HT and reductions of its main metabolite 5-HIAA from brain regional whole tissue samples. Interestingly these data show that carmofur leads to increased storage of 5-HT and decreased metabolism, which indicates that inhibition of acid ceramidase (AC) decreases 5-HT neurotransmission. To confirm that carmofur indeed inhibits AC in the brain and hence increases ceramide and decreases sphingosine levels, it was deemed important to measure both of these lipids in the same brain samples that were analysed for levels of monoamines and metabolites in section 6.3.1 of the current chapter. This was achieved by means of the LC-MS and HPLC-UV techniques for the analysis of sphingosine and ceramide respectively. Statistical analysis of the generated data was performed using two-way analysis of variance (two-way ANOVA with Bonferroni post-hoc test) to assess the effect of treatment (carmofur versus vehicle administration) and brain region (PFC, HP and ST). In the present experiment, two-way ANOVA indicated a highly significant effect of brain region on the measured sphingosine level following acute carmofur treatment ($p = 0.006$, $F(2,30) = 5.996$) with a significant interaction effect between treatment and brain region ($p = 0.039$, $F(2,30) = 3.616$). A subsequent post hoc analysis using the Bonferroni t-test recorded a highly significant reduction of sphingosine content in both the prefrontal cortex (Table 6.2 and Figures 6.11, 6.12 and 6.13) and hippocampus (Table 6.2 and Figures 6.11, 6.14 and 6.15) (for both brain regions, $p < 0.001$) in the treatment group compared to the vehicle-treated controls following acute carmofur administration. However, the drug's effect on sphingosine levels in the striatum failed to reach statistical significance (Table 6.2 and Figure 6.11).

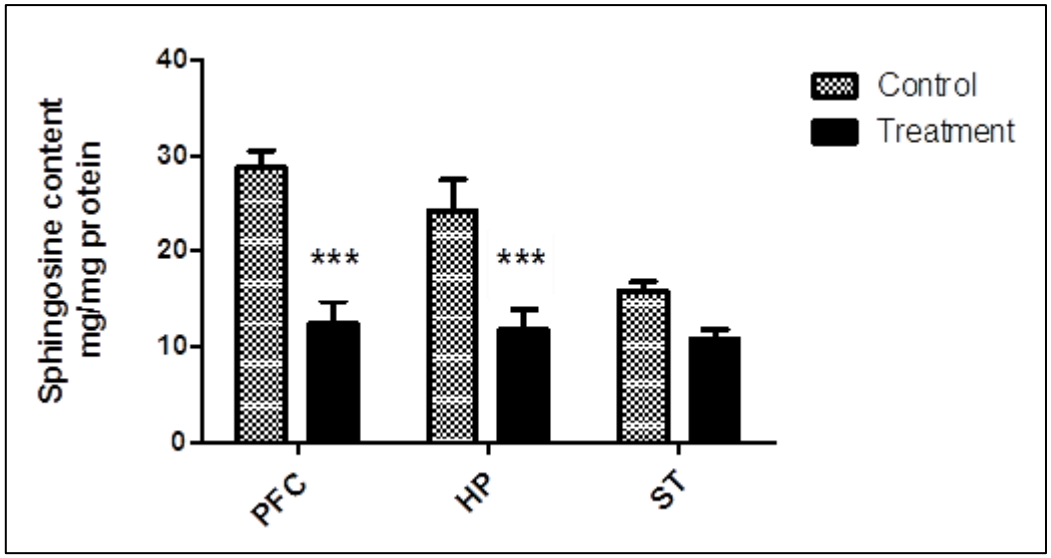

Figure 6.11: Sphingosine content in (mg/mg protein) in rat brain regions following acute carmofur treatment. All values represent mean ± SEM (n = 6). Abbreviations: PFC, prefrontal cortex; HP, hippocampus and ST, striatum. *** P < 0.001 for both the PFC and HP, but not significant for the striatum (two-way ANOVA test with Bonferroni t-test).

Table 6.2: Effect of acute carmofur treatment (20 mg/kg, i.p) on sphingosine content in rat brain regions. Abbreviations: PFC, prefrontal cortex; HP, hippocampus and ST, striatum.

	PFC (mg/mg protein)	HP (mg/mg protein)	ST (mg/mg protein)
Control	28.76 ± 1.830	24.19 ± 3.318	15.86 ± 0.972
Acute carmofur	12.43 ± 2.425 ***	11.74 ± 2.187 ***	10.79 ± 1.069

Values indicate sphingosine content (mg/mg protein) as mean ± SEM (n = 6), carmofur treatment group versus the relevant control group; *** p < 0.001 (two-way ANOVA with Bonferroni t-test).

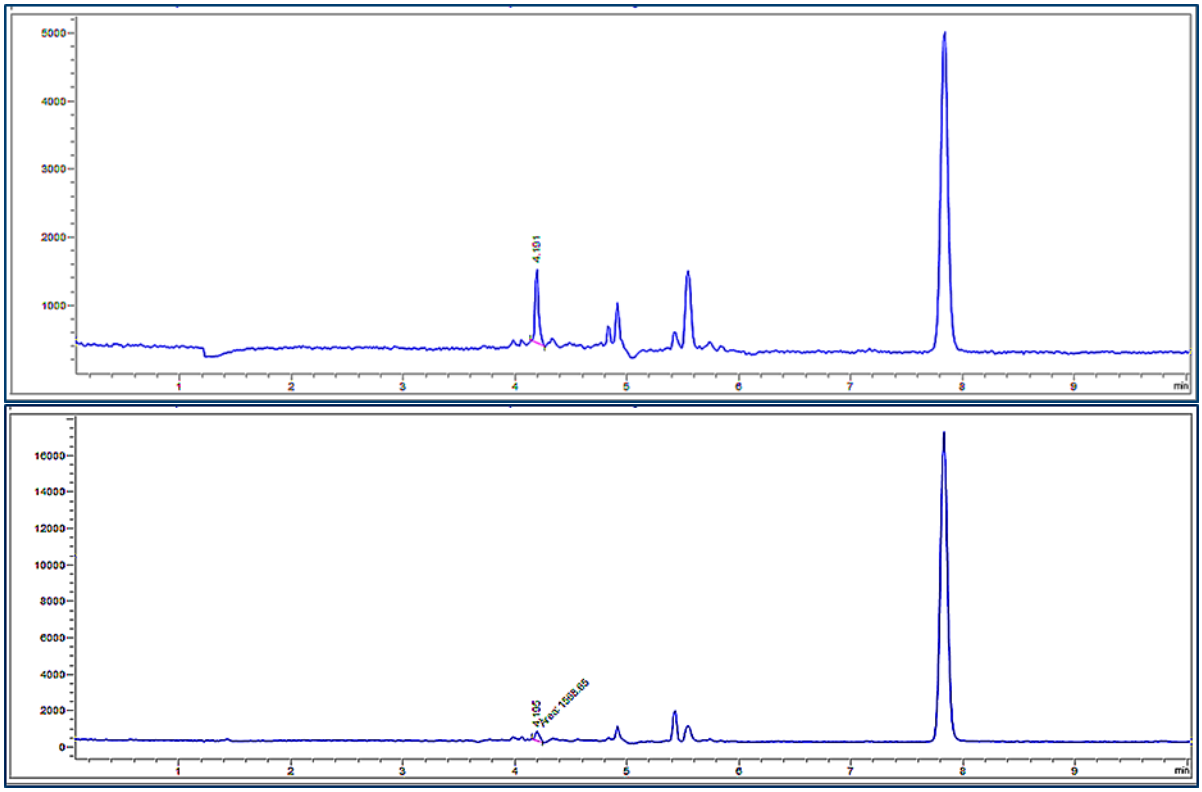

Figure 6.12: LC-MS chromatogram of frontal cortical tissue samples obtained from upper: control and lower: treated rat following acute carmofur administration showing sphingosine peak at a retention time of 4.191 and 4.195 minutes respectively.

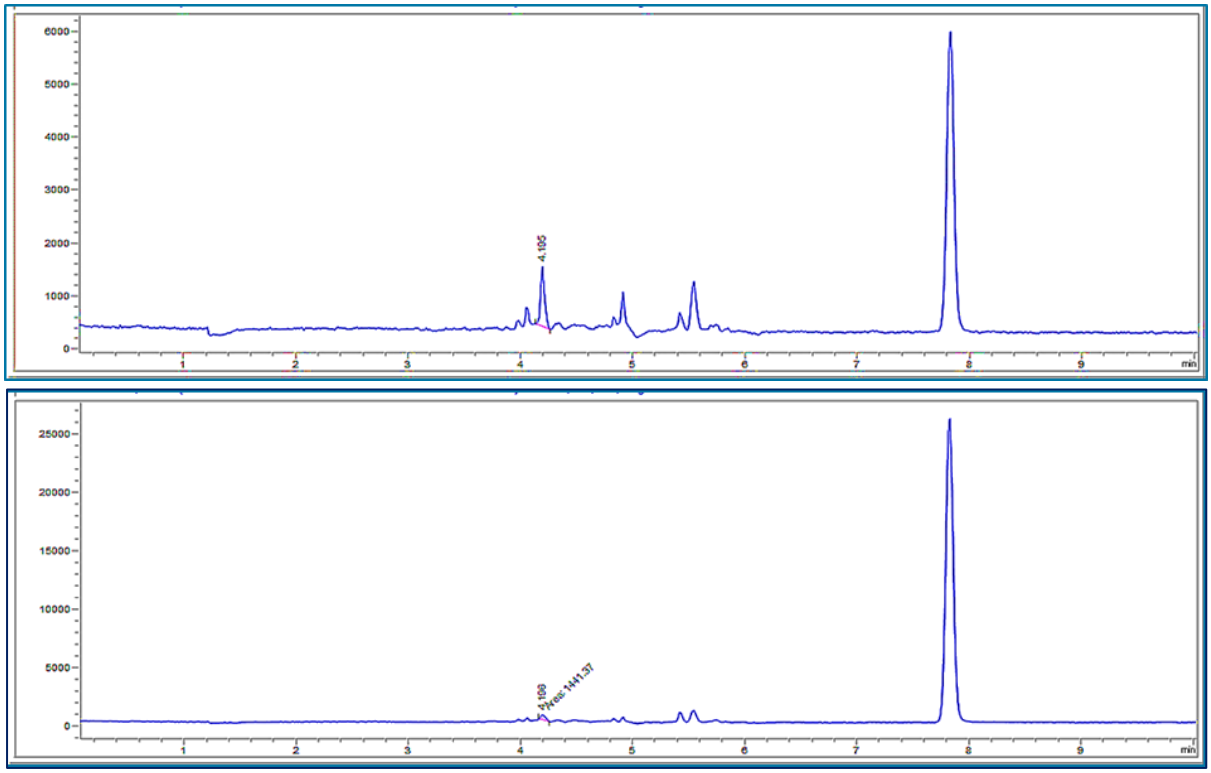

Figure 6.13: LC-MS chromatogram of frontal cortical tissue samples obtained from upper: control and lower: treated rat following acute carmofur administration showing sphingosine peak at a retention time of 4.195 and 4.196 minutes respectively.

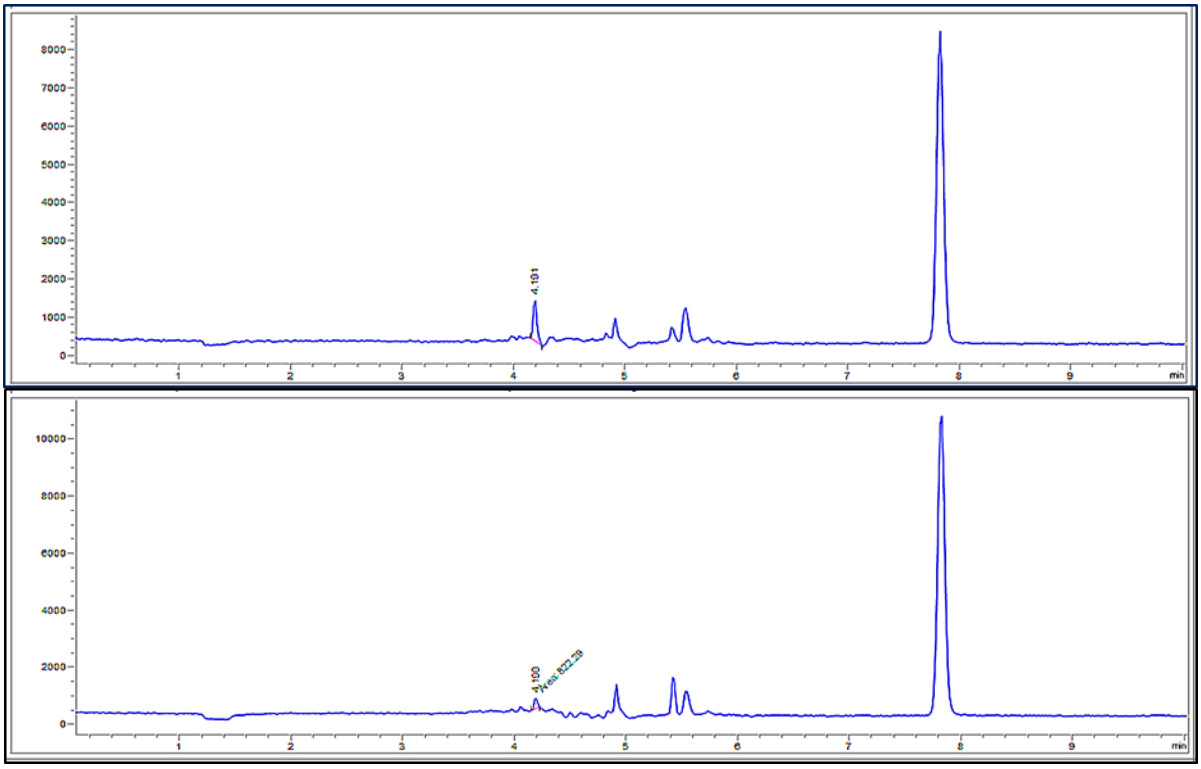

Figure 6.14: LC-MS chromatogram of hippocampal tissue samples obtained from upper: control and lower: treated rat following acute carmofur administration showing sphingosine peak at a retention time of 4.191 and 4.190 minutes respectively.

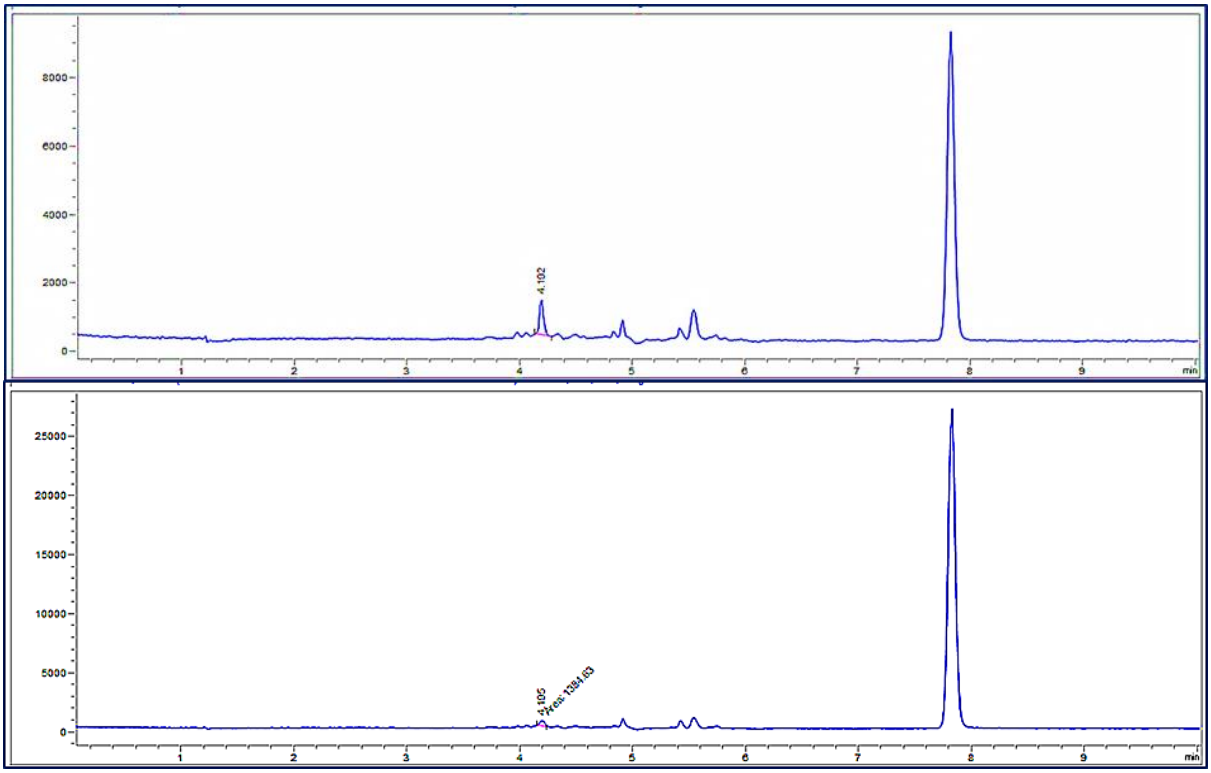

Figure 6.15: LC-MS chromatogram of hippocampal tissue samples obtained from upper: control and lower: treated rat following acute carmofur administration showing sphingosine peak at a retention time of 4.192 and 4.195 minutes respectively.

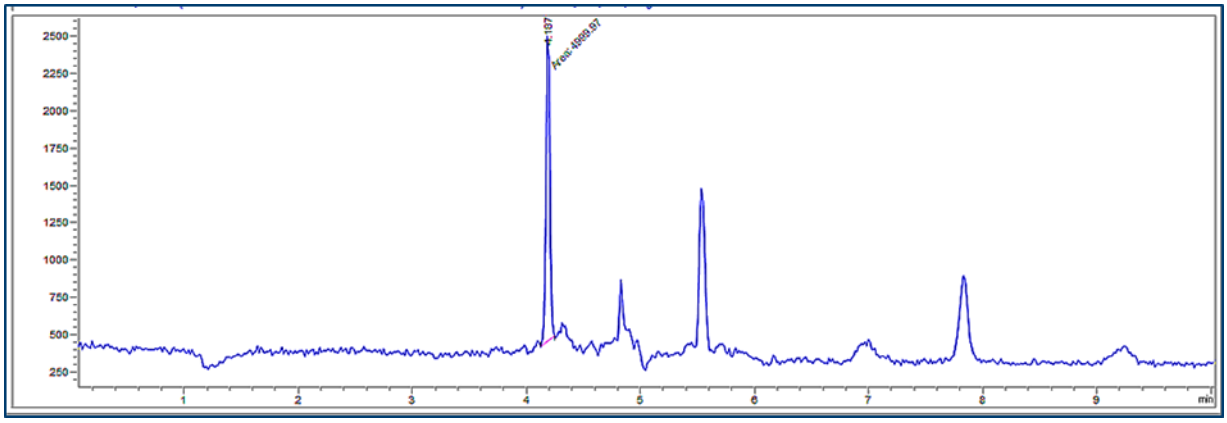

Figure 6.16: LC-MS chromatogram showing sphingosine standard peak at a concentration of 15 mg / L and a retention time of 4.187 minute.

6.3.3. Analysis of ceramide in rat brain following acute carmofur treatment using HPLC-UV:

The AC inhibition induced by carmofur is expected to be accompanied by an increase of ceramide levels (Realini et al., 2013). Therefore, in order to confirm this, a chromatographic system (HPLC-UV) was used to measure ceramide levels in our brain samples following benzoylation which indeed was successfully performed. Statistical analysis of the generated data was achieved using two-way analysis of variance (two-way ANOVA) to test for the effect of treatment (carmofur versus vehicle administration) and brain region (PFC, HP and ST). As expected, and as a further proof that carmofur indeed entered the brain of our experimental rats, acute carmofur administration (20 mg/kg, i.p) resulted in increased ceramide levels in samples from the selected brain regions. Likewise, for carmofur induced reductions of sphingosine (Figure 6.11), in the prefrontal cortex and hippocampus, these increases were highly significant. In contrast, carmofur (similarly to the reduction of sphingosine levels) failed to significantly increase ceramide levels in the striatum (Table 6.3 and Figure 6.17).

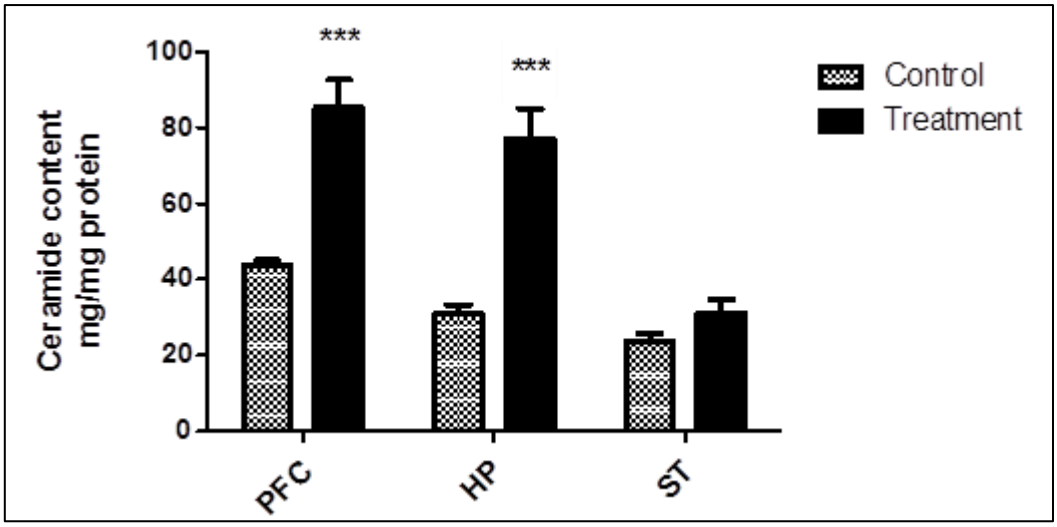

Figure 6.17: Ceramide content in (mg/mg protein) in rat brain regions following acute carmofur treatment. All values represent mean ± SEM (n = 6). Abbreviations: PFC, prefrontal cortex; HP, hippocampus and ST, striatum. *** P < 0.001 for both the PFC and HP, but not significant for the striatum (two-way ANOVA test with Bonferroni t-test).

Following acute carmofur treatment, data analysis by two-way ANOVA showed a highly significant effect of brain region ($p < 0.0001$, $F(2,36) = 31.46$) on the central ceramide content with a clearly significant interaction between treatment and brain region ($p = 0.0004$, $F(2,36) = 9.727$). The Bonferroni post hoc analysis reported a highly significant increase of ceramide level in the prefrontal cortex ($p < 0.001$) and the hippocampus ($p < 0.001$) compared to the relevant controls without any observed changes in the striatum in the carmofur-treated rats compared to their corresponding vehicle-treated animals (Table 6.3 and Figures 6.17, 6.18 and 6.19).

Table 6.3: Effect of acute carmofur treatment (20 mg/kg, i.p) on ceramide content in rat brain. Abbreviations: PFC, prefrontal cortex; HP, hippocampus and ST, striatum.

	PFC (mg/mg protein)	HP (mg/mg protein)	ST (mg/mg protein)
Control	43.76 ± 1.324	31.08 ± 2.134	23.91 ± 1.769
Acute carmofur	85.26 ± 7.356 ***	77.17 ± 7.884 ***	31.23 ± 3.449

Values indicate ceramide content (mg/mg protein) as mean ± SEM (n = 6), carmofur treatment group versus the relevant control group; *** $p < 0.001$ (two-way ANOVA with Bonferroni t-test).

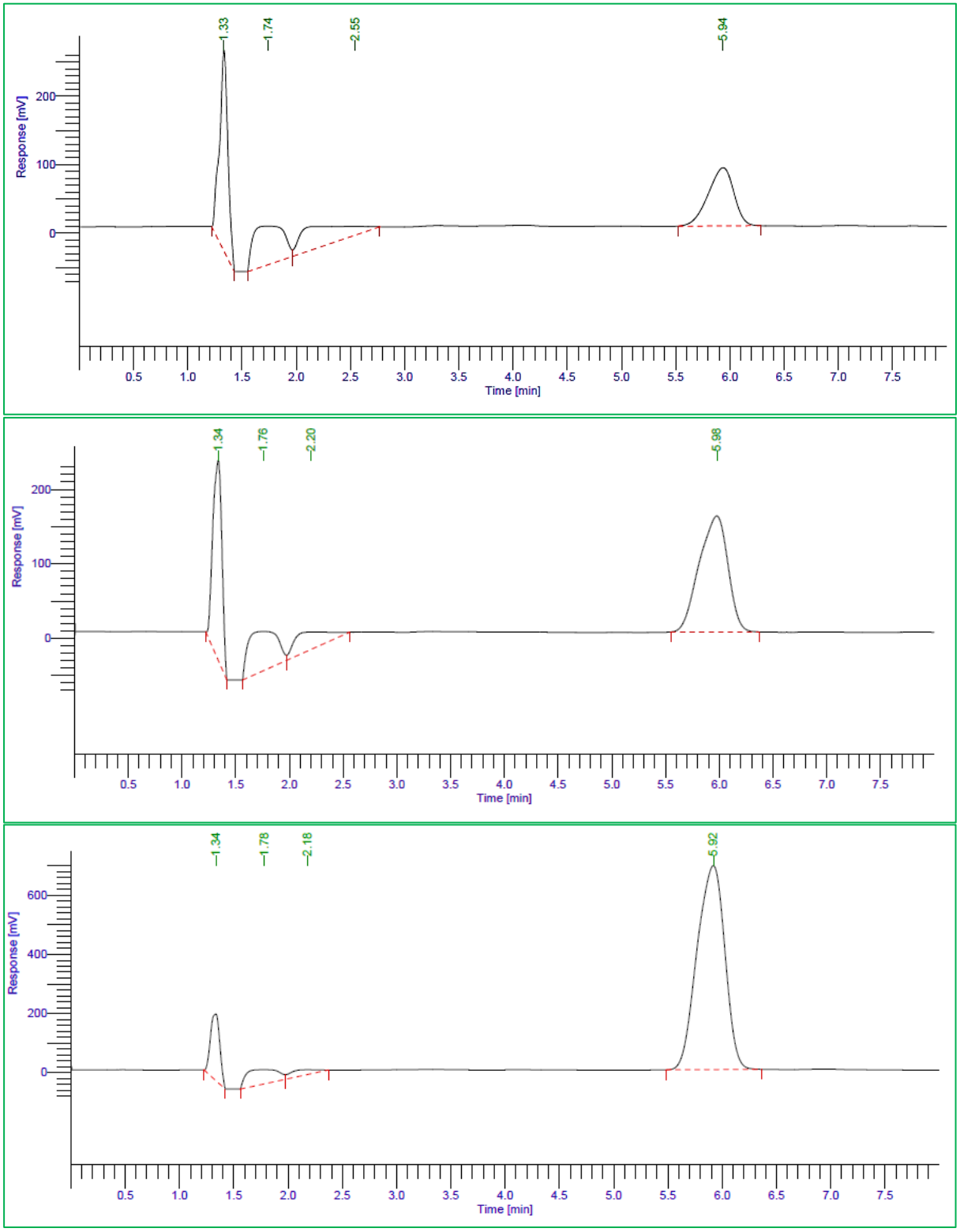

Figure 6.18: UV-HPLC chromatogram of frontal cortical samples obtained from upper: control and middle: treated animal following acute carmofur administration showing ceramide peak at a retention time of 5.94 and 5.98 minutes respectively. Lower: UV-HPLC chromatogram showing ceramide standard peak at a concentration of 40 mg/L and a retention time of 5.92 minute.

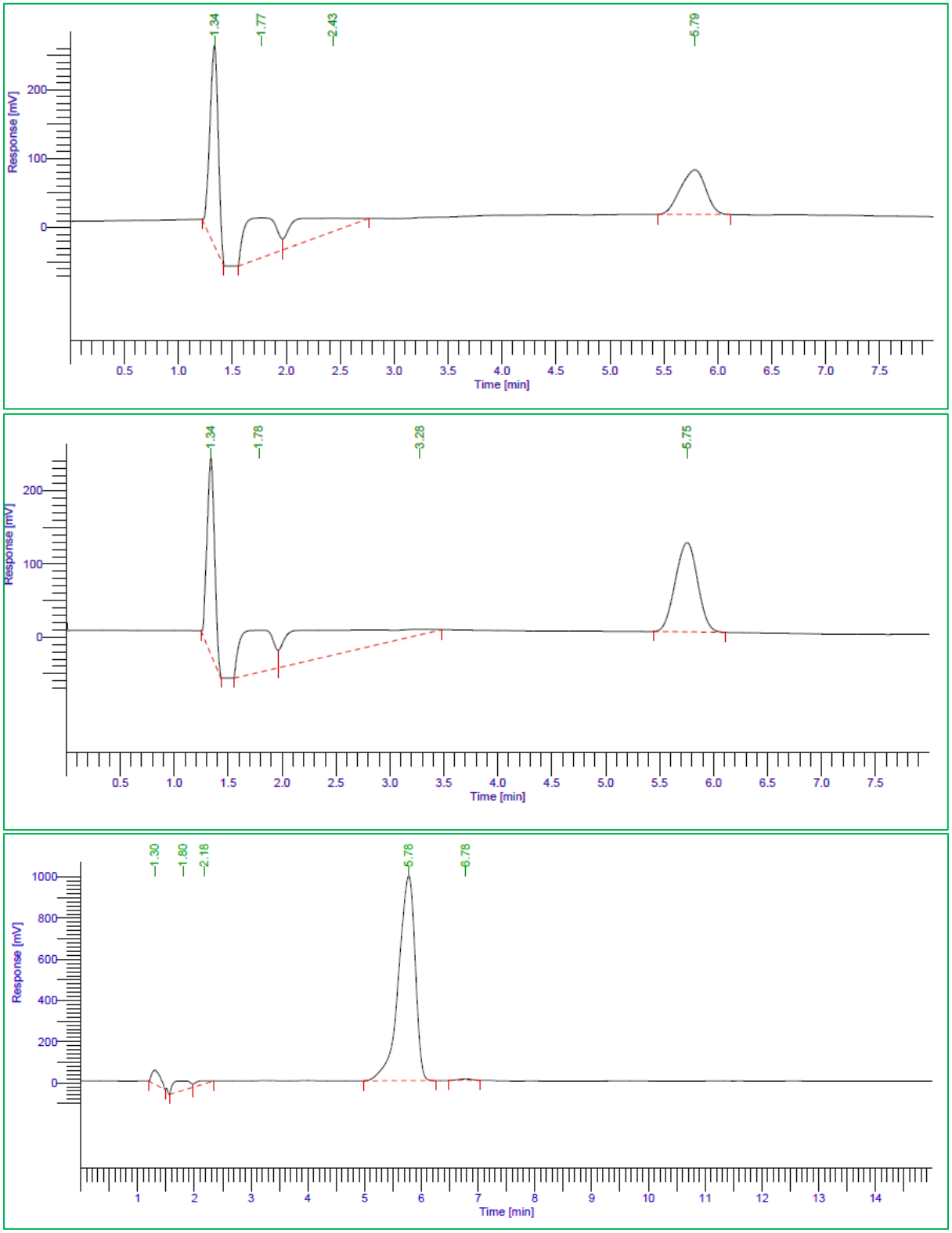

Figure 6.19: UV-HPLC chromatogram of hippocampal samples obtained from upper: control and middle: treated animal following acute carmofur administration showing ceramide peak at a retention time of 5.79 and 5.75 minutes respectively. Lower: UV-HPLC chromatogram showing ceramide standard peak at a concentration of 40 mg/L and a retention time of 5.78 minute.

6.4. Discussion:

6.4.1. Principal findings:

The key aim of this study was to investigate the effect of acute administration (20 mg/kg, i.p) of the known AC inhibitor, carmofur on central monoaminergic neurotransmission. This was performed by analysing the carmofur (20 mg/kg, i.p., one hour after the injection) induced effect on monoamine (5-HT, NA and DA) levels as well as some of their metabolites (5-HIAA and DOPAC) in regional brain samples (PFC, HP and ST) from rats treated with the drug or their corresponding vehicle treated controls using HPLC-ECD. In order to provide evidence that carmofur indeed entered the brain regions investigated and hence inhibited AC, the effect of carmofur on levels of the two sphingolipid molecules of interest for AC inhibition; ceramide and sphingosine were also investigated using the analytical techniques of HPLC-UV and LC-MS respectively. The generated data revealed that acute carmofur treatment resulted in a notable increase of 5-HT content in all of the three brain regions examined (PFC, HP and ST). In contrast, carmofur failed to significantly alter levels of the two catecholamines, DA and NA. Interestingly, the carmofur induced increase of regional whole tissue levels of 5-HT coincided with a marked reduction of the main metabolite of 5-HT, 5-HIAA in these samples (Figures 6.1 and 6.2). In comparison, the DA main metabolite DOPAC remained unaltered following carmofur administration. On the other hand, this experimental set also showed that following acute carmofur treatment levels of the two sphingolipids likely to be affected by acute inhibition of AC, namely ceramide and sphingosine were also altered by acute carmofur treatment. Thus, following carmofur injection, ceramide levels increased while sphingosine decreased in brain samples collected from carmofur treated rats compared to levels in the corresponding control samples. While these changes were highly significant in tissue samples collected from the prefrontal cortex and the hippocampus, carmofur failed to significantly alter sphingolipid levels in the striatum (Figures 6.11 and 6.17). These finding are in line with a previous albeit more limited study in mice showing that acute carmofur injection (10 mg/kg and 30 mg/kg, i.p) likewise to the current study resulted in increased levels of ceramide in one part of the brain i.e. the cerebral cortex (Realini et al., 2013).

6.4.2. Acute carmofur administration induced alterations of 5-HT and its main metabolite 5-HIAA:

The present experimental work revealed that carmofur induced increases of ceramide levels coincided with changes of brain levels of 5-HT and its main metabolite 5-HIAA indicating a decrease of 5-HT transmission (i.e. increased whole tissue levels of 5-HT and decreased 5-HIAA). In comparisons, levels of the two catecholamines: DA, NA and the DA metabolite DOPAC were unaltered following carmofur administration. In the light of depression and it's treatment, the central 5-HT system is widely suggested to play a vital role (aan het Rot et al., 2009; Elhwuegi, 2004; Krishnan and Nestler, 2008; Nemeroff, 2002). Thus, the 5-HT transporter represents the main target of many currently available antidepressant medications such as the SSRIs (Nemeroff, 2002; Oosterhof, 2016). Additionally, it has been reported that depletion of the monoamine neurotransmitters, in particular 5-HT results in a mood lowering state in both depressed patients undergoing remission as well as in the non-depressed controls (Merens et al., 2008; Oosterhof, 2016). Despite growing evidence indicating that ceramide could also play a vital role in depression and its treatment, no evidence exists regarding the direct effect of a ceramide imbalance on neurotransmission of monoamines. In this context, it was shown in Chapter Four, sections 4.3.1.2, 4.3.1.3 and 4.3.2 of this thesis that chronic but not acute treatment of two antidepressant drugs, paroxetine and desipramine decreased levels of ceramide and its metabolite sphingosine in brain areas related to the symptoms of depression.

In the central nervous system, among all of the known 5-HT receptors, the 5-HT1A receptor subtype plays a key role in signal transduction as well as its implication in various behavioural and cognitive functions including mood, sleep and learning (Marona-Lewicka and Nichols, 2011; Müller et al., 2007; Singh et al., 2012). This 5-HT receptor subtype is expressed both pre and post synaptically and belongs to the G-protein-coupled receptor family (GPCRs, that are coupled to the Gi/Go protein) (Oosterhof, 2016; Singh et al., 2012). The pre-synaptic 5-HT1A receptors are expressed predominantly on the soma and dendrites of the 5-HT neurons in the raphe nuclei of the mid brain. The somatodendritic located 5-HT1A receptors when stimulated results in an inhibitory effect on the activity of the serotonergic neurons (Oosterhof, 2016; Singh et al., 2012).

In addition, the regulation of these receptors has been implicated in the known delay in full therapeutic effect of antidepressant drugs. Thus it has been shown that following acute antidepressant drug treatment, initially there is a significant elevation of extracellular 5-HT levels in the raphe nucleus which is caused by the inhibition of somatodendritic located 5-HT transporter (Artigas, 2013; Nemeroff, 2002; Oosterhof, 2016). Concomitantly, this effect results in the activation of the inhibitory 5-HT1A autoreceptors, hence attenuating the firing activity of the serotonergic neurons temporarily. On the other hand, chronic antidepressant drug administration induces adaptive changes of the serotonergic neurons, leading to a subsequent desensitization of the 5-HT1A autoreceptors which results in decreased responsiveness of these receptors following their sustained activation. Consequently, a slow recovery of the discharging activity of the 5-HT neurons occurs, which is reflected in a gradual increase of 5-HT neurotransmission (Nemeroff, 2002; Oosterhof, 2016). Of key relevance for the present work, it has recently been reported that the essential lipid-protein interaction of cell membranes is driven by an interaction between GPCRs (as integral membrane proteins) with the surrounding membrane sphingolipids including ceramide. This process has for example been shown to have a pivotal role in modulating the interaction between the G-proteins and GPCRs and hence maintaining the structure of the receptors and their function. Interestingly, it has been postulated that these receptors via sphingolipids including ceramide undergo conformational alterations that are essential to maintain their signaling function (Singh et al., 2012; Unal and Karnik, 2012). In addition, it was observed that the indicated lipid-protein interaction is necessary for the ligand binding activity of 5-HT1A receptors. Thus, depletion of these membrane sphingolipids may result in impairment of this activity accompanied by a reduction in the expression of these autoreceptors at the level of the cell membrane (Jafurulla et al., 2008; Singh et al., 2012). Moreover, ceramide has been shown to alter the transport of monoamine neurotransmitters, particularly 5-HT either through a direct or indirect action. Directly, it acts by binding membrane ceramide enriched macrodomains to the transporter molecule (Dinoff et al., 2017; Gangoiti et al., 2010), or indirectly by activating various intracellular phosphatases and kinases (Dinoff et al., 2017; Westwick et al., 1995), thereby increasing the transport and the

reuptake of 5-HT via altering the transporter function (Dinoff et al., 2017; Kornhuber et al., 2009; Riddle et al., 2003).

In the present study, the recorded findings displayed a pronounced increase in whole tissue 5-HT content with a significantly decreased 5-HIAA level in all the analysed brain regions (PFC, HP and ST) following acute carmofur treatment. Consequently, there was a clear reduction of the 5-HIAA/5-HT ratio (the serotonin turnover ratio) (Hussain and Butt, 2008; Shannon et al., 1986), indicating a reduced concentration of the 5-HT metabolite, 5-HIAA. Therefore, reflecting a reduced 5-HT catabolic rate and possibly a decreased serotonergic activity in these brain regions. While levels of the 5-HT metabolite 5-HIAA have been found to be reduced in the cerebrospinal fluid of depressed patients (Åsberg et al., 1984). A number of studies have indicated an increase in 5-HIAA/5-HT ratio i.e. 5-HT turnover in plasma samples from patients diagnosed with depression which resulted mainly from a significant increase in the plasma concentrations of 5-HIAA (Barton et al., 2008; Shannon et al., 1986). In this context, a previous study using an animal model of depression observed that the 5-HIAA/5-HT ratio was significantly lower in a part of the brain namely, the nucleus accumbens of "depressed" rats compared to the corresponding controls. Further, this reduction of 5-HT turnover in the nucleus accumbens was found to be normalized following chronic treatment with the antidepressant desipramine (5 mg/kg/day) for 18 days (Zangen et al., 1997). Our data show that carmofur increases ceramide levels and that this effect reduces the 5-HIAA/5-HT ratio but not the DOPAC/DA ratio, hence suggesting that 5-HT neurotransmission is primarily affected by enhanced ceramide levels. The mechanism behind this effect is not fully clear, it could however, be speculated that both an effect on 5-HT transport as well as an enhanced activity of the 5-HT1A autoreceptor via enhanced ceramide concentration could be involved in the mediation of the reduced 5-HT turnover. Thus, as mentioned already ceramide has been shown to affect neuronal monoamine transport (Dinoff et al., 2017; Westwick et al., 1995). Moreover it has been demonstrated in synaptosomal preparations that ceramide decreases DA transport while it in contrast, increases 5-HT transport (Riddle et al., 2003). Further, such effect is likely to enhance whole brain tissue levels of 5-HT as detected following treatment with the ceramide enhancing drug carmofur in the present study. The 5-HT1A receptor has been

shown to be stimulated by ceramide, a lipid-protein interaction enhancing ligand binding activity of the 5-HT1A receptor. In accordance with these reported findings, it could be speculated that a carmofur induced enhancement of brain ceramide levels would enhance the activity of 5-HT1A autoreceptor function. An effect which would lead to a decreased firing of 5-HT neurons in the raphe nuclei and reduction of 5-HT release and metabolism in the forebrain. Ultimately, resulting in enhanced storage of 5-HT and reduced levels of the intracellularly produced 5-HT metabolite 5-HIAA.

6.4.3. Carmofur administration alters brain ceramide and sphingosine content:

In this study, our data demonstrated that an acute injection of the AC inhibitor carmofur at one hour after the injection resulted in a significant increase of ceramide levels in samples collected from treated animals as compared to their corresponding vehicle injected controls. This effect was accompanied by a pronounced decrease in the levels of the main ceramide metabolite sphingosine. These effects were highly significant in brain samples from the prefrontal cortex and hippocampus but in the striatum the drug only produced small and non-significant effects (Figures 6.11 and 6.17). Acid ceramidase is a lysosomal polypeptide that acts in an acidic environment (pH = 4.5) to catalyze the degradation of ceramide into sphingosine and fatty acid (Saied and Arenz, 2014; Shtraizent et al., 2008). In our study, the detected alteration in the two targeted sphingolipid molecules (ceramide and sphingosine) is likely to result from carmofur-induced inhibition of AC activity following a single intraperitoneal injection of the drug at a dose of 20 mg/kg. Consistent with our findings, a recent animal study reported a significant elevation in tissue ceramide level in the cerebral cortex and lung of mice, this together with a decreased sphingosine content two hours following acute carmofur administration (Realini et al., 2013).

6.5. Conclusion:

The current study revealed that acute carmofur treatment compared to the corresponding controls resulted in a pronounced increase of 5-HT levels which was accompanied by a significant reduction of levels for the 5-HT metabolite 5-HIAA. Importantly, this effect was seen in three brain regions (prefrontal cortex, hippocampus and striatum) implicated in depression and its treatment. In contrast, carmofur failed to induce any significant alterations in the levels of the two catecholamine neurotransmitters: DA and NA as well as for the DA metabolite DOPAC. Further, measurement of brain ceramide and sphingosine levels in the same regional tissue samples significantly showed increased ceramide levels with a concomitant reduction of the sphingosine content in the PFC and HP of the carmofur treated rats in comparison with their vehicle-treated controls. The observed carmofur-induced decrease of the 5-HIAA/5-HT ratio could indicate a reduction of 5-HT neurotransmission. This effect might be induced by an enhanced activation of the inhibitory 5-HT1A autoreceptors via increased ceramide levels and/or changes of 5-HT reuptake. However, a more detailed investigation is still necessary to provide further insight into the neurochemical relevance of the carmofur-induced increase of ceramide and how this affects 5-HT neurotransmission.

CHAPTER 7

General discussion and concluding remarks

7.1. Background:

Depression is a common psychiatric disorder with increased risk of disability and suicidal mortality. The condition further results in a considerable economic impact and the total reported number of suicidal deaths across the world is approximately 800 000 per year. Globally, it was estimated that depressive disorder affects over 300 million people worldwide which is equivalent to 4.4% of the total world's population with a higher prevalence rate among female patients compared to males (according to the WHO, 2017) (Organization, 2017). Currently, the available antidepressant medications act predominantly by facilitating 5-HT and or NA neurotransmission either via inhibiting their re-uptake back into the presynaptic nerve terminals e.g. SSRIs, SNRIs and TCAs (Cheung et al., 2006) or by inhibiting their enzymatic catabolism e.g. MAOIs (Fowler et al., 2010). However, it has been reported that more than 50% of all depressed patients do not successfully respond to multiple trials of the currently prescribed antidepressant drugs (failure to achieve remission), thus representing a well-known class of the disease termed as treatment resistant depression (Dinoff et al., 2017; McIntyre et al., 2014). Indeed, it is also well-recognised that all the currently available antidepressant medications takes an average time of 4-6 weeks to exhibit their full therapeutic effect (Tylee and Walters, 2007). In this context, the low response rate to the conventional therapy, the delayed onset of therapeutic action as well as the uncertain underlying aetiology of depression, altogether have triggered an extended investigation in the specific field of research of the present project, namely the possible involvement of sphingolipid turnover as part of the mechanism of action by antidepressant drugs. Sphingolipids, in particular ceramide has been suggested to have a role in depression (Kornhuber et al., 2009, 2014). In this context, ceramide has been linked to critical neurobiological mechanisms including cell signaling and monoamine neurotransmission (Dinoff et al., 2017; Müller et al., 2015), membrane permeability (Tsui-Pierchala et al., 2002) and apoptosis (Ruvolo, 2003). Accordingly, the primary aim of the present study was firstly to investigate the short and long-term effects of two currently used antidepressant drugs namely, the TCA desipramine and the SSRI paroxetine on water soluble brain metabolites (Chapter Three) and sphingolipid turnover (Chapter Four). Secondly, the study also sought to investigate the mechanism of action by such an effect (Chapter Five) as well as the relationship between monoamine turnover and brain ceramide levels (Chapter Six). The present

study provides further evidence in support of the possible involvement of brain sphingolipids in antidepressant drug mechanism of action.

7.2. Summary of the major findings:

7.2.1. Effects of antidepressant drugs on brain metabolites depend on treatment regime, type of drug and brain region investigated:

In Chapter Three, metabolic changes were explored in rat brain regions following acute and chronic administration of two antidepressant drugs (paroxetine and desipramine). For this purpose, 1H NMR spectroscopy was employed to investigate the effect of treatment with paroxetine and desipramine on water soluble metabolite/biomolecule levels in plasma and brain regions implicated in the pathogenesis of depression including the prefrontal cortex (PFC), hippocampus (HP) and the striatum (ST) (Drevets et al., 2008; McEwen and Morrison, 2013). In these experiments the tested drug doses of both paroxetine (5 mg/kg) and desipramine (10 mg/kg) were adopted on the bases of previously published studies (Detke et al., 1997; Hajós-Korcsok et al., 2000; Mathes and Spector, 2011). Thus, these previous studies had shown behavioural as well as biochemical changes following similar drug regimes in animal models of depression. Moreover, the doses used in the present study have be shown to reach plasma levels in rats similar to those obtained in depressed patients (Benmansour et al., 1999). More specifically, plasma levels of 30-120 ng/ml for paroxetine and 50-300 ng/ml for desipramine have been associated with therapeutic response in humans (Gillman, 2007; Hiemke et al., 2011).

Briefly, in Chapter Three of this thesis, it was shown that by using 1H NMR acute antidepressant drug administration resulted in widespread changes of several water-soluble brain metabolites. Furthermore, these changes were frequently specific to both brain region and the type of antidepressant drug used (i.e. paroxetine or desipramine). In this regard, data from this chapter indicate that acute paroxetine and desipramine treatment significantly alter the brain levels of a number of metabolites that are involved in important metabolic pathways of the brain including: energy metabolism (e.g. ATP, valine, lactate and creatine), neurotransmission (e.g. glutamate and

glutamine) as well as neuronal integrity (e.g. NAA). On the other hand, data analysis of plasma samples obtained from the acute paroxetine-treated rats revealed only significant changes for a few metabolites (i.e. creatine and succinate) compared to the corresponding controls without any significant metabolic changes in the plasma following acute desipramine administration. Other neurochemical type studies have also investigated the metabolic effects that may be associated with depression and its drug treatment using different type of imaging technologies (Brody et al., 1999; Chiappelli et al., 2015; Yüksel and Öngür, 2010; Zhao et al., 2015). In this context, a previous clinical imaging study using MRI (magnetic resonance imaging) scans revealed a decreased metabolic activity in the dorsolateral prefrontal cortex, as well as an increased metabolic activity in the ventrolateral prefrontal cortex, the orbitofrontal cortex and the inferior orbital gyrus in depressed subjects. Importantly, changes in metabolic activity in the ventrolateral prefrontal cortex and the orbitofrontal cortex were normalized following successful paroxetine treatment (40 mg/day), emphasising the potential clinical importance of brain metabolites for the symptoms of depression (Brody et al., 1999). In Chapter Three, it was also shown that in contrast to the acute treatment data which displayed significant drug-associated metabolic responses, the detected alterations were not maintained in the chronically treated rats (once daily injections for 15 days) compared to their corresponding controls in the explored brain regions and in the plasma. Taken together, this could possibly reflect the occurrence of neuroadaptive changes following repeated drug exposure.

7.2.2. Effects of acute and chronic antidepressant drug administration on sphingosine and ceramide content in rat brain regions:

Accumulated evidence suggests that sphingolipids particularly ceramide could be implicated in depression and its pharmacotherapy. Hence, an important goal of the current study was to investigate the effect of acute and chronic antidepressant drug treatment (once daily for 15 days) on brain levels of two bioactive sphingolipid molecules, namely: ceramide and its major metabolite sphingosine in regional tissue samples from treated and control rats by means of the HPLC-UV and LC-MS methods respectively. In this context, it was reported in Chapter Four that chronic but not acute antidepressant drug administration induced a brain region-specific effect

on sphingosine level. A significant reduction of sphingosine content was detected in samples from two of the explored brain regions of the rat: the prefrontal cortex and the hippocampus (a stronger effect was observed in the prefrontal cortex). In comparison, both drugs (paroxetine and desipramine) failed to significantly reduce sphingosine levels in the striatum. Further, chronic treatment with the SSRI paroxetine appeared to be more effective in comparison to chronic administration of the TCA desipramine. While chronic paroxetine administration resulted in a significant reduction of sphingosine levels in the PFC and HP, a non-significant trend for a reduced sphingosine levels was recorded following chronic desipramine treatment. Interestingly, the marked decrease in sphingosine level was recorded following chronic but not after acute treatment. A limitation of the LC-MS system used for the detection of sphingosine in our laboratory was the inability to measure molecules with a molecular weight exceeding 500 g/mol. Since the molecular weight of ceramide is 566 g/mol, the measurement of ceramide was therefore performed by the modification of a previously published HPLC-UV method (Couch et al., 1997; Ogawa et al., 2010; Tepper and Blitterswijk, 2000). This method involved extensive sample preparation and hence, was only applied for two groups of samples namely, hippocampal samples from the chronically paroxetine treated rats and their corresponding controls. Consistent with the paroxetine-induced reduction of hippocampal sphingosine levels, this drug also significantly reduced the concentration of ceramide in samples collected from the hippocampus. To confirm that the ceramide metabolite sphingosine could indeed be used as a reliable marker of ceramide, the present study found a significant correlation between hippocampal ceramide and sphingosine levels in both paroxetine-treated and control rats. Further, the observed findings from the current study are in correspondence with a previous study reporting a similar reduction of mice hippocampal ceramide level following long-term antidepressant drug therapy (Gulbins et al., 2013). This study shows however, for the first time that antidepressant drugs also reduce sphingolipid levels in the prefrontal cortex while levels in the striatum were not altered.

7.2.3. Effect of chronic antidepressant drug treatment on gene expression for two key enzymes of the brain sphingolipid pathway:

Research to date, regarding the involvement of sphingolipids in mental health related conditions have focussed on the significance of the membrane sphingolipid ceramide; its synthesis, catabolism as well as its biological correlates (e.g. monoamine neurotransmission and apoptosis) (Canals et al., 2011; Müller et al., 2015; Osherovich, 2013; Ruvolo, 2003). However, further evidence on the potential link between the dysregulation of ceramide and the related lipid-processing enzymes with depression and the mechanism of action underlying its drug treatment is still limited and hence, require more investigations. Thus, in Chapter Five, experiments were designed to investigate the effect of chronic antidepressant drug administration (once daily for 15 days) on gene expression for the two-main sphingolipid-regulating enzymes; acid sphingomyelinase (encoded by the SMPD1 gene) and acid ceramidase (encoded by the ASAH1 gene) in the three examined brain regions using the RT-qPCR technique. Our reported findings from Chapter Five revealed that chronic administration of both antidepressant drugs (i.e. paroxetine and desipramine) induced a significant reduction of the gene expression level for acid sphingomyelinase in the hippocampus of the drug-treated rats compared to the corresponding saline-injected controls. Similarly, long-term treatment with both paroxetine and desipramine resulted in a reduction of SMPD1 mRNA level in the prefrontal cortex this effect however, failed to reach significance and in the striatum both drugs had only minor effects. In Chapter Five, measurements of gene expression for the ceramide metabolising enzyme acid-ceramidase was also performed after chronic antidepressant drug treatment. The data from these experiments showed that chronic desipramine but not paroxetine treatment (non-significant reductions only) significantly reduces expression level of the ASAH1 gene in the hippocampus and the prefrontal cortex. However, likewise for the gene encoding acid sphingomyelinase, this effect was significant in the hippocampus but not in the prefrontal cortex and only minor effects were seen in the striatum.

7.2.4. Effect of acute carmofur treatment on monoamines and their metabolites in rat brain regions:

It is well known that monoaminergic neurotransmission is closely linked to depression and its therapeutic intervention (aan het Rot et al., 2009; Brigitta, 2002; Hirschfeld, 2000). A number of studies including this study suggest the involvement of the central sphingolipid system (e.g. ceramide) in the symptoms and treatment of depression as recently reviewed by Gulbins et al, 2015. Beyond doubt, the majority of currently available antidepressant drugs influences monoaminergic neurotransmission, however, little information is available regarding a potential interaction between monoamines and sphingolipids. To examine the potential relationship between these two biochemical systems, in Chapter Six, we tested the effects of the potent acid ceramidase inhibitor carmofur (a drug that has previously been used to treat some types of cancer including colorectal) on regional brain levels of monoamines and their metabolites. For this purpose, rats were injected with carmofur (20 mg/kg, i.p), sacrificed one hour later, tissue samples prepared from PFC, HP and ST and monoamine levels (5-HT, DA and NA) and some of their metabolites (5-HIAA and DOPAC) measured using HPLC-ECD. In order to confirm the brain entry of carmofur, its effect on brain levels of sphingosine and ceramide was evaluated by LC-MS and HPLC-UV respectively. As predicted, these experiments showed that carmofur by inhibiting AC significantly increased levels of ceramide and decreased levels of sphingosine. Interestingly Chapter Six appeared to demonstrate a relationship between ceramide levels and 5-HT neurotransmission. Thus, the carmofur induced enhancement of ceramide levels coincided with a significant increase of the whole tissue 5-HT content in all of the three brain regions examined (PFC, HP and ST). In contrast, carmofur failed to significantly alter levels in any of the brain regions examined of the two catecholamines, DA and NA or the DA metabolite DOPAC. Interestingly, the carmofur induced increase of regional whole tissue levels of 5-HT coincided with a marked reduction of the main 5-HT metabolite, 5-HIAA in these analysed samples. Thus, the 5-HIAA/5-HT ratio was reduced, suggesting a reduction of 5-HT neurotransmission following acute carmofur treatment. In comparison, the DA main metabolite (DOPAC) level remained unaltered after acute carmofur administration. As already mentioned briefly above, findings from Chapter Six also revealed that acute carmofur treatment altered levels of the two sphingolipids affected by the

acute inhibition of AC, namely ceramide (increased) and sphingosine (decreased) in brain samples from PFC and HP. Although carmofur also altered levels of the two sphingolipids in the striatum, these effects failed to reach statistical significance in this brain region. Moreover, in correspondence with our results, a previous animal study conducted on mice indicated that acute carmofur administration at two different doses (10 mg/kg and 30 mg/kg, i.p) resulted in increased levels of ceramide in mouse tissues including lungs as well as in one part of the brain (i.e. the cerebral cortex) (Realini et al., 2013).

7.3. General discussion and implications of the main findings:

Generally, alterations in monoaminergic functions particularly the serotonergic and noradrenergic systems have been found to be implicated in the pathogenesis of depression as well as the mechanism of antidepressant drug action (aan het Rot et al., 2009; Brigitta, 2002; Hirschfeld, 2000; Sun et al., 2017). So far, a well-recognised neurobiological mechanism underlying the disease together with the reasons behind the low response rate to the currently used antidepressant medications and their actual mechanism of action are still undetermined. Limited previous research have attempted to explore a metabolic brain profiling of depression and how this is changed following short and long-term administration of antidepressant medications. To date, however, previous neurochemical studies failed to reveal any consistent pattern of brain metabolic changes related to depression or the available drug therapy (Bai et al., 2015; Gołembiowska and Dziubina, 2000; Jia et al., 2013; Yoo et al., 2018; Zhao et al., 2015). As indicated earlier, data from Chapter Three showed that acute but not chronic antidepressant drug administration induced significant metabolic changes in a wide range of metabolites in the brain regions examined. Interestingly, the observed drug-associated metabolic responses were often both brain region (mostly decreases in hippocampus and prefrontal cortex while levels of most metabolites tended to increase in the striatum) and drug specific. These differential effects possibly reflect the fact that paroxetine and desipramine primarily block different types of transporters; SERT and NET and therefore, preferentially increase the extracellular levels of 5-HT and NA respectively. It is likely that, this initial enhancement of the synaptic monoamine levels results in the activation of the presynaptic inhibitory autoreceptors (e. g. the somatodendritic 5-

HT1A and α_2 adrenergic receptors) thus, resulting in decreased serotonergic as well as noradrenergic neurotransmission following short-term drug exposure (David et al., 2003; Hyman and Nestler, 1996). It is possible that such acute inhibition of monoamine neurotransmission is related to the acute downregulation of a number of metabolites in the hippocampus and the frontal cortex. In contrast to the acute effect, chronic antidepressant drug administration failed to show any significant metabolic alterations in the investigated brain regions, suggesting the onset of neuroadaptive changes following repeated drug administration (Lefkowitz, 1993; Sacchetti et al., 2001). Given that, the sustained activation of the 5-HT1A and α_2 autoreceptors after chronic antidepressant drug administration are well known to results in their desensitization (Artigas, 2013; Hyman and Nestler, 1996; Sacchetti et al., 2001), it is possible that such effect is related to the reversal of the metabolic effects after chronic drug treatment in the present study.

Next, the effect of acute and chronic antidepressant drug treatment was investigated on the abundance of two bioactive sphingolipid molecules namely: ceramide and its main metabolic product sphingosine in the three brain regions examined here. Results from Chapter Four demonstrate that chronic antidepressant drug administration induced a significant reduction of the ceramide metabolite sphingosine in the prefrontal cortex and hippocampus but not in the striatum (a region-specific effect). Importantly, the decrease of sphingosine levels was detected following chronic but not after acute treatment. In addition, and based on the generated data of this thesis, sphingosine was proven to be a reliable indicator of ceramide in the analysed brain extracts. In correspondence with the sphingosine data, chronic paroxetine administration resulted in a significant reduction of hippocampal ceramide level, a finding consistent with a recent animal study reporting a decreased ceramide content in mice hippocampus following long-term antidepressant drug therapy (Gulbins et al., 2013). The recorded reduction by the antidepressant drugs of the targeted sphingolipids namely; ceramide and sphingosine could partly be explained by a dysregulation of the main sphingolipid-regulating enzymes. Thus, in Chapter Five, it was shown that antidepressant drugs have the ability to downregulate the mRNA expression of SMPD1 and ASAH1, two genes encoding acid sphingomyelinase and acid ceramidase respectively.

Consistent with the presents results, a recent study also indicated that chronic treatment with the antidepressant drugs: fluoxetine and amitriptyline at doses similar to those which induce therapeutic plasma levels in depressed patients resulted in a reduction of ceramide abundance in the hippocampus, a decline of ASM activity and a concomitant reduction of depression-related behaviours in a mouse model of depression (Gulbins et al., 2013). In this context, various antidepressant drugs are recently identified as functional or indirect inhibitors of acid sphingomyelinase activity, which as discussed in Chapter Five, could be caused by the intra-lysosomal accumulation of the protonated (i.e. charged form of the drug molecule). Thus, resulting in a subsequent detachment and inactivation of the enzyme inside the acidic lysosomal lumen (Kornhuber et al., 2008, 2010, 2014). On the other hand, data from the gene expression study of the present project (Chapter Five) displayed significantly reduced ASAH1 mRNA levels (encodes acid ceramidase) in the hippocampus after long-term desipramine administration, whereas a non-significant trend towards a reduced expression level of this gene was observed following paroxetine treatment in this specific brain region. Also, a similar trend, albeit a non-significant reduction was detected for ASAH1 mRNA levels of the prefrontal cortex but not in the striatum after chronic administration of both antidepressant drugs. Accordingly, desipramine may induce a non-selective inhibition of the genes encoding the lysosomal enzymes, ASM and AC. This was not the case with paroxetine, which seems to mediate a preferential inhibition of the gene encoding the ASM enzyme. In this context, the ASM specific activity in the brain was reported to be higher compared to AC (Kornhuber et al., 2010). Overall, long-term antidepressant drug treatment may induce a pronounced down-regulation of acid sphingomyelinase and to a lesser extent acid ceramidase mRNA expression levels specifically in the hippocampus. In contrast, both drugs failed to alter gene expression levels for ASM and AC in the striatum, a brain region possibly less directly implicated in the symptoms of depression (Drevets et al., 2008) compared to the prefrontal cortex and hippocampus. In this context, findings from the present study that the striatum generally expresses lower levels and shows less antidepressant induced reduction of sphingosine when compared to the hippocampus and prefrontal cortex are of interest.

Further, a postulated relationship between ceramide and monoamine levels was tested by measuring the whole tissue level of monoamines (5-HT, DA and NA) and some of their metabolites (5-HIAA and DOPAC) in the investigated brain regions at one hour following a single injection of the acid ceramidase inhibitor carmofur. Interestingly, results from these experiments pointed to an inverse relationship between 5-HT neurotransmission and ceramide levels. Thus, data from Chapter Six showed that increased levels of ceramide in the brain coincided with increased whole tissue 5-HT content in the three brain regions investigated (PFC, HP and ST) and a significant reduction of the main 5-HT metabolite 5-HIAA. This together with a reduced 5-HIAA/5-HT ratio suggested an initial reduction of 5-HT neurotransmission after an acute carmofur injection. In contrast, carmofur treatment failed to significantly alter levels of DA and its main metabolite DOPAC as well as the neurotransmitter NA in all brain regions examined.

Previous studies have indicated that in the cell membrane, the interaction between the G-protein-coupled receptors (GPCRs) (e.g. 5-HT1A receptors) and the surrounding membrane sphingolipids including ceramide encompass an essential lipid-protein interaction that is important in maintaining the structure of the receptors as well as their function specifically their ligand binding affinity (Singh et al., 2012). In addition and relevant to the results of this thesis, it has been shown that ceramide may affect the transport of monoamine neurotransmitters, particularly 5-HT via activation of 5-HT transporter (SERT) function (Dinoff et al., 2017; Westwick et al., 1995). Moreover, it has previously been shown that acute carmofur administration by inhibiting the activity of acid ceramidase, primarily increases ceramide abundance of cell membrane lipid rafts (Dinoff et al., 2017; Realini et al., 2013). Thus, suggesting that the carmofur-induced enhancement of brain ceramide levels could directly result in changed activity of proteins located in the cell membrane lipid rafts including: the 5-HT1A autoreceptor and the 5-HT transporter. It is therefore possible that the carmofur induced reduction of the 5-HIAA/5-HT ratio, (an index of 5HT-neurotransmission; (Hussain and Butt, 2008) seen in the present study represents a reduction of serotonergic activity via ceramide induced increase of 5-HT transport and/or enhanced activity of the 5-HT1A autoreceptor.

7.4. Concluding remarks:

In summary, the data presented in the current thesis have shown a reduction of two functionally active sphingolipids, namely ceramide and sphingosine in rat brain following chronic but not acute antidepressant drug treatment. This effect is likely at least in part to be explained by the drugs ability to inhibit the lipid-metabolizing enzyme, acid sphingomyelinase in brain regions implicated in depression, in particular the hippocampus. In comparison, the antidepressant drugs had only minor effects on sphingolipid pathways of the striatum, a brain region possibly less associated with the symptoms of depression. Also, of importance the present thesis, by using the acid ceramidase inhibitor carmofur, show data which indicate an inverse relationship between ceramide levels and 5-HT neurotransmission. Given that, a reduced 5-HT neurotransmission and enhanced ceramide concentrations have both been implicated in the pathogenesis of depression, these data strengthen the involvement of sphingolipids in the mode of action of antidepressant drugs. Future studies will however, be necessary to further support the ceramide hypothesis of depression. In conclusion, data of the current thesis indicate that potential new drugs for the treatment of depression could be molecules targeting either acid sphingomyelinase or acid ceramidase activity.

BIBLIOGRAPHY

aan het Rot, M., Mathew, S.J., Charney, D.S., 2009. Neurobiological mechanisms in major depressive disorder. CMAJ Can. Med. Assoc. J. 180, 305–313. https://doi.org/10.1503/cmaj.080697.

Abernathy, K., Chandler, L.J., Woodward, J.J., 2010. ALCOHOL AND THE PREFRONTAL CORTEX. Int. Rev. Neurobiol. 91, 289–320. https://doi.org/10.1016/S0074-7742(10)91009-X.

Adinehzadeh, M., Reo, N.V., Jarnot, B.M., Taylor, C.A., Mattie, D.R., 1999. Dose–response hepatotoxicity of the peroxisome proliferator, perfluorodecanoic acid and the relationship to phospholipid metabolism in rats. Toxicology 134, 179–195. https://doi.org/10.1016/S0300-483X(99)00038-4.

Alberts, B., Johnson, A., Lewis, J., Raff, M., Roberts, K., Walter, P., 2002. The Lipid Bilayer.

Alekseyenko, O.V., Lee, C., Kravitz, E.A., 2010. Targeted Manipulation of Serotonergic Neurotransmission Affects the Escalation of Aggression in Adult Male Drosophila melanogaster. PLOS ONE 5, e10806. https://doi.org/10.1371/journal.pone.0010806.

Al-Harbi, K.S., 2012. Treatment-resistant depression: therapeutic trends, challenges, and future directions. Patient Prefer. Adherence 6, 369–388. https://doi.org/10.2147/PPA.S29716.

Altman, J., Das, G.D., 1965. Autoradiographic and histological evidence of postnatal hippocampal neurogenesis in rats. J. Comp. Neurol. 124, 319–335. https://doi.org/10.1002/cne.901240303.

Amaral, D.G., Witter, M.P., 1989. The three-dimensional organization of the hippocampal formation: a review of anatomical data. Neuroscience 31, 571–591.

Ambresin, G., Chondros, P., Dowrick, C., Herrman, H., Gunn, J.M., 2014. Self-rated health and long-term prognosis of depression. Ann. Fam. Med. 12, 57–65. https://doi.org/10.1370/afm.1562.

Amireault, P., Sibon, D., Côté, F., 2012. Life without Peripheral Serotonin: Insights from Tryptophan Hydroxylase 1 Knockout Mice Reveal the Existence of Paracrine/Autocrine Serotonergic Networks. ACS Chem. Neurosci. 4, 64–71. https://doi.org/10.1021/cn300154j.

Andersson, C., Hamer, R.M., Lawler, C.P., Mailman, R.B., Lieberman, J.A., 2002. Striatal Volume Changes in the Rat Following Long-term Administration of Typical and Atypical Antipsychotic Drugs. Neuropsychopharmacology 27, 143–151. https://doi.org/10.1016/S0893-133X(02)00287-7.

Andriamampandry, C., Muller, C., Schmidt-Mutter, C., Gobaille, S., Spedding, M., Aunis, D., Maitre, M., 2002. Mss4 Gene Is Up-Regulated in Rat Brain after Chronic Treatment with Antidepressant and Down-Regulated When Rats Are Anhedonic. Mol. Pharmacol. 62, 1332–1338. https://doi.org/10.1124/mol.62.6.1332.

Arenz, C., 2010. Small molecule inhibitors of acid sphingomyelinase. Cell. Physiol. Biochem. Int. J. Exp. Cell. Physiol. Biochem. Pharmacol. 26, 1–8. https://doi.org/10.1159/000315100

Artigas, F., 2013. Serotonin receptors involved in antidepressant effects. Pharmacol. Ther. 137, 119–131. https://doi.org/10.1016/j.pharmthera.2012.09.006.

Åsberg, M., Bertilsson, L., Mårtensson, B., Scalia-Tomba, G.-P., Thorén, P., Träskman-Bendz, L., 1984. CSF monoamine metabolites in melancholia. Acta Psychiatr. Scand. 69, 201–219. https://doi.org/10.1111/j.1600-0447.1984.tb02488.x.

Bai, S., Hu, Q., Chen, Z., Liang, Z., Wang, W., Shen, P., Wang, T., Wang, H., Xie, P., 2017. Brain region-specific metabolite networks regulate antidepressant effects of venlafaxine. RSC Adv. 7, 46358–46369. https://doi.org/10.1039/C7RA08726H.

Bai, S., Zhou, C., Cheng, P., Fu, Y., Fang, L., Huang, W., Yu, J., Shao, W., Wang, X., Liu, M., Zhou, J., Xie, P., 2015. 1H NMR-Based Metabolic Profiling Reveals the Effects of Fluoxetine on Lipid and Amino Acid Metabolism in Astrocytes. Int. J. Mol. Sci. 16, 8490–8504. https://doi.org/10.3390/ijms16048490.

Barton, D.A., Esler, M.D., Dawood, T., Lambert, E.A., Haikerwal, D., Brenchley, C., Socratous, F., Hastings, J., Guo, L., Wiesner, G., Kaye, D.M., Bayles, R., Schlaich, M.P., Lambert, G.W., 2008. Elevated brain serotonin turnover in patients with depression: effect of genotype and therapy. Arch. Gen. Psychiatry 65, 38–46. https://doi.org/10.1001/archgenpsychiatry.2007.11.

Baslow, M.H., 2003. N-acetylaspartate in the vertebrate brain: metabolism and function. Neurochem. Res. 28, 941–953.

Baslow, M.H., Guilfoyle, D.N., 2006. Functions Of N-Acetylaspartate and N-Acetylaspartylglutamate in Brain, in: N-Acetylaspartate, Advances in Experimental Medicine and Biology. Springer, Boston, MA, pp. 95–112. https://doi.org/10.1007/0-387-30172-0_7.

Beaulieu, J.-M., Gainetdinov, R.R., 2011. The Physiology, Signaling, and Pharmacology of Dopamine Receptors. Pharmacol. Rev. 63, 182–217. https://doi.org/10.1124/pr.110.002642.

Beckmann, N., Sharma, D., Gulbins, E., Becker, K.A., Edelmann, B., 2014. Inhibition of acid sphingomyelinase by tricyclic antidepressants and analogons. Front. Physiol. 5. https://doi.org/10.3389/fphys.2014.00331.

Belmaker, R.H., Agam, G., 2008. Major Depressive Disorder. N. Engl. J. Med. 358, 55–68. https://doi.org/10.1056/NEJMra073096.

Benmansour, S., Cecchi, M., Morilak, D.A., Gerhardt, G.A., Javors, M.A., Gould, G.G., Frazer, A., 1999. Effects of Chronic Antidepressant Treatments on Serotonin Transporter Function, Density, and mRNA Level. J. Neurosci. 19, 10494–10501.

Berger, M., Gray, J.A., Roth, B.L., 2009. The Expanded Biology of Serotonin. Annu. Rev. Med. 60, 355–366. https://doi.org/10.1146/annurev.med.60.042307.110802.

Berrios, G.E., 1988. Melancholia and depression during the 19th century: a conceptual history. Br. J. Psychiatry 153, 298–304. https://doi.org/10.1192/bjp.153.3.298.

Berton, O., Nestler, E.J., 2006. New approaches to antidepressant drug discovery: beyond monoamines. Nat. Rev. Neurosci. 7, 137–151. https://doi.org/10.1038/nrn1846.

Berumen, L.C., Rodríguez, A., Miledi, R., García-Alcocer, G., 2012. Serotonin Receptors in Hippocampus [WWW Document]. Sci. World J. https://doi.org/10.1100/2012/823493.

Bird, I.M., 1989. High performance liquid chromatography: principles and clinical applications. BMJ 299, 783–787.

Blier, P., de Montigny, C., 1994. Current advances and trends in the treatment of depression. Trends Pharmacol. Sci. 15, 220–226.

Bligh, E.G., Dyer, W.J., 1959. A Rapid Method of Total Lipid Extraction and Purification. Can. J. Biochem. Physiol. 37, 911–917. https://doi.org/10.1139/o59-099.

Boatright, K.M., Salvesen, G.S., 2003. Caspase activation. Biochem. Soc. Symp. 70, 233–242. https://doi.org/10.1042/bss0700233.

Bock, N., Koc, E., Alter, H., Roessner, V., Becker, A., Rothenberger, A., Manzke, T., 2013. Chronic Fluoxetine Treatment Changes S100B Expression During Postnatal Rat Brain Development. J. Child Adolesc. Psychopharmacol. 23, 481–489. https://doi.org/10.1089/cap.2011.0065.

Bohley, P., Seglen, P.O., 1992. Proteases and proteolysis in the lysosome. Experientia 48, 151–157. https://doi.org/10.1007/BF01923508.

Bonefeld, B.E., Elfving, B., Wegener, G., 2008. Reference genes for normalization: a study of rat brain tissue. Synap. N. Y. N 62, 302–309. https://doi.org/10.1002/syn.20496.

Bönisch, H., Brüss, M., 2006. The norepinephrine transporter in physiology and disease. Handb. Exp. Pharmacol. 485–524.

Bortolato, M., Chen, K., Shih, J.C., 2008. Monoamine oxidase inactivation: From pathophysiology to therapeutics. Adv. Drug Deliv. Rev., Mitochondrial Medicine and Mitochondrion-Based Therapeutics 60, 1527–1533. https://doi.org/10.1016/j.addr.2008.06.002.

Boundless, 2016. Selective Permeability. Boundless.

Brambilla, P., Stanley, J.A., Sassi, R.B., Nicoletti, M.A., Mallinger, A.G., Keshavan, M.S., Soares, J.C., 2004. 1H MRS study of dorsolateral prefrontal cortex in healthy individuals before and after lithium administration. Neuropsychopharmacology 29, 1918–1924. https://doi.org/10.1038/sj.npp.1300520.

Brand, A., Richter-Landsberg, C., Leibfritz, D., 1993. Multinuclear NMR studies on the energy metabolism of glial and neuronal cells. Dev. Neurosci. 15, 289–298.

Bremner, J.D., Innis, R.B., Salomon, R.M., Staib, L.H., Ng, C.K., Miller, H.L., Bronen, R.A., Krystal, J.H., Duncan, J., Rich, D., Price, L.H., Malison, R., Dey, H., Soufer, R., Charney, D.S., 1997. Positron emission tomography measurement of cerebral metabolic correlates of tryptophan depletion-induced depressive relapse. Arch. Gen. Psychiatry 54, 364–374.

Brigitta, B., 2002. Pathophysiology of depression and mechanisms of treatment. Dialogues Clin. Neurosci. 4, 7–20.

Brimberg, L., Flaisher-Grinberg, S., Schilman, E.A., Joel, D., 2007. Strain differences in "compulsive" lever-pressing. Behav. Brain Res. 179, 141–151. https://doi.org/10.1016/j.bbr.2007.01.014.

Britton, P., 2003. Mio malinchonico, o vero ... mio pazzo: Michelangelo, Vasari, and the problem of artists' melancholy in sixteenth-century Italy. Sixt. Century J. 34, 653–675.

Brody, A.L., Saxena, S., Silverman, D.H., Alborzian, S., Fairbanks, L.A., Phelps, M.E., Huang, S.C., Wu, H.M., Maidment, K., Baxter, L.R., 1999. Brain metabolic changes in major depressive disorder from pre- to post-treatment with paroxetine. Psychiatry Res. 91, 127–139.

Brookshire, B., 2017. Explainer: What is dopamine? [WWW Document]. Sci. News Stud. URL https://www.sciencenewsforstudents.org/article/explainer-what-dopamine (accessed 9.2.17).

Brunton, L., Chabner, B.A., Knollman, B., 2011. Goodman and Gilman's The Pharmacological Basis of Therapeutics, 12th edition. ed. McGraw-Hill Education / Medical, New York.

Calcagno, E., Guzzetti, S., Canetta, A., Fracasso, C., Caccia, S., Cervo, L., Invernizzi, R.W., 2009. Enhancement of cortical extracellular 5-HT by 5-HT1A and 5-HT2C receptor blockade restores the antidepressant-like effect of citalopram in non-responder mice. Int. J. Neuropsychopharmacol. 12, 793–803. https://doi.org/10.1017/S1461145708009760.

Campbell, S., MacQueen, G., 2004. The role of the hippocampus in the pathophysiology of major depression. J. Psychiatry Neurosci. 29, 417–426.

Canals, D., Perry, D.M., Jenkins, R.W., Hannun, Y.A., 2011. Drug targeting of sphingolipid metabolism: sphingomyelinases and ceramidases. Br. J. Pharmacol. 163, 694–712. https://doi.org/10.1111/j.1476-5381.2011.01279.x.

Celada, P., Puig, M.V., Amargós-Bosch, M., Adell, A., Artigas, F., 2004. The therapeutic role of 5-HT1A and 5-HT2A receptors in depression. J. Psychiatry Neurosci. 29, 252–265.

Celikyurt, I.K., Mutlu, O., Ulak, G., 2012. Serotonin Noradrenaline Reuptake Inhibitors (SNRIs). https://doi.org/10.5772/37999.

Chamberlain, L.H., Burgoyne, R.D., Gould, G.W., 2001. SNARE proteins are highly enriched in lipid rafts in PC12 cells: Implications for the spatial control of exocytosis. Proc. Natl. Acad. Sci. U. S. A. 98, 5619–5624. https://doi.org/10.1073/pnas.091502398.

Chang, K., Adleman, N.E., Dienes, K., Simeonova, D.I., Menon, V., Reiss, A., 2004. Anomalous Prefrontal-Subcortical Activation in Familial Pediatric BipolarDisorder: A Functional Magnetic Resonance Imaging Investigation. Arch. Gen. Psychiatry 61, 781–792. https://doi.org/10.1001/archpsyc.61.8.781.

Charnay, Y., Leger, L., 2010. Brain serotonergic circuitries. Dialogues Clin. Neurosci. 12, 471–487.

Cheung, A.H., Emslie, G.J., Mayes, T.L., 2006. The use of antidepressants to treat depression in children and adolescents. CMAJ Can. Med. Assoc. J. 174, 193–200. https://doi.org/10.1503/cmaj.050855.

Chiappelli, J., Rowland, L.M., Wijtenburg, S.A., Muellerklein, F., Tagamets, M., McMahon, R.P., Gaston, F., Kochunov, P., Hong, L.E., 2015. Evaluation of Myo-Inositol as a Potential Biomarker for Depression in Schizophrenia. Neuropsychopharmacology 40, npp201557. https://doi.org/10.1038/npp.2015.57.

Clapp, P., Bhave, S.V., Hoffman, P.L., 2008. How Adaptation of the Brain to Alcohol Leads to Dependence. Alcohol Res. Health 31, 310–339.

Cloarec, O., Dumas, M.-E., Craig, A., Barton, R.H., Trygg, J., Hudson, J., Blancher, C., Gauguier, D., Lindon, J.C., Holmes, E., Nicholson, J., 2005. Statistical Total Correlation Spectroscopy: An Exploratory Approach for Latent Biomarker Identification from Metabolic 1H NMR Data Sets. Anal. Chem. 77, 1282–1289. https://doi.org/10.1021/ac048630x.

Colado, M.I., O'Shea, E., Granados, R., Murray, T.K., Green, A.R., 1997. In vivo evidence for free radical involvement in the degeneration of rat brain 5-HT following administration of MDMA ('ecstasy') and p-chloroamphetamine but not the degeneration following fenfluramine. Br. J. Pharmacol. 121, 889–900. https://doi.org/10.1038/sj.bjp.0701213.

Cooper, G.M., 2000. Cell Membranes.

Couch, L.H., Churchwell, M.I., Doerge, D.R., Tolleson, W.H., Howard, P.C., 1997. Identification of Ceramides in Human Cells Using Liquid Chromatography with detection by Atmospheric Pressure Chemical Ionization-Mass Spectrometry. Rapid Commun. Mass Spectrom. 11, 504–512.https://doi.org/10.1002/(SICI)1097-0231(199703)11:5<504: AID-RCM886>3.0.CO;2-5.

Cremesti, A.E., Fischl, A.S., 2000. Current methods for the identification and quantitation of ceramides: An overview. Lipids 35, 937–945. https://doi.org/10.1007/s11745-000-0603-1.

Cremesti, A.E., Goni, F.M., Kolesnick, R., 2002. Role of sphingomyelinase and ceramide in modulating rafts: do biophysical properties determine biologic outcome? FEBS Lett. 531, 47–53. https://doi.org/10.1016/S0014-5793(02)03489-0.

Crespi, F., Martin, K.F., Marsden, C.A., 1988. Measurement of extracellular basal levels of serotonin in vivo using nafion-coated carbon fiber electrodes combined with differential pulse voltammetry. Neuroscience 27, 885–896. https://doi.org/10.1016/0306-4522(88)90191-1.

Crespo, F.S., Luque, R., Prieto, D., Sau, P., Albert, C., Leal, I., Luxan, A. de, Osuna, M.I., Ruiz, M., Galán, R., Cabaleiro, F., Molina, V., 2008. Biochemical changes in the cingulum in patients with schizophrenia and chronic bipolar disorder. Eur. Arch. Psychiatry Clin. Neurosci. 258, 394–401. https://doi.org/10.1007/s00406-008-0808-9.

Cuvillier, O., 2003. Sphingosine in apoptosis signaling. Biochim. Biophys. Acta 1585, 153–62. https://doi.org/10.1016/S1388-1981(02)00336-0.

Cuvillier, O., Nava, V.E., Murthy, S.K., Edsall, L.C., Levade, T., Milstien, S., Spiegel, S., 2001. Sphingosine generation, cytochrome c release, and activation of caspase-7 in doxorubicin-induced apoptosis of MCF7 breast adenocarcinoma cells. Cell Death Differ. 8, 162–171. https://doi.org/10.1038/sj.cdd.4400793.

Dauth, S., Maoz, B.M., Sheehy, S.P., Hemphill, M.A., Murty, T., Macedonia, M.K., Greer, A.M., Budnik, B., Parker, K.K., 2017. Neurons derived from different brain regions are inherently different in vitro: a novel multiregional brain-on-a-chip. J. Neurophysiol. 117, 1320–1341. https://doi.org/10.1152/jn.00575.2016.

David, D.J.P., Bourin, M., Jego, G., Przybylski, C., Jolliet, P., Gardier, A.M., 2003. Effects of acute treatment with paroxetine, citalopram and venlafaxine in vivo on noradrenaline and serotonin outflow: a microdialysis study in Swiss mice. Br. J. Pharmacol. 140, 1128–1136. https://doi.org/10.1038/sj.bjp.0705538.

Daws, L.C., 2009. Unfaithful neurotransmitter transporters: Focus on serotonin uptake and implications for antidepressant efficacy. Pharmacol. Ther. 121, 89–99. https://doi.org/10.1016/j.pharmthera.2008.10.004.

Demirkan, A., Isaacs, A., Ugocsai, P., Liebisch, G., Struchalin, M., Rudan, I., Wilson, J.F., Pramstaller, P.P., Gyllensten, U., Campbell, H., Schmitz, G., Oostra, B.A., van Duijn, C.M., 2013. Plasma phosphatidylcholine and sphingomyelin concentrations are associated with depression and anxiety symptoms in a Dutch family-based lipidomics study. J. Psychiatr. Res. 47, 357–362. https://doi.org/10.1016/j.jpsychires.2012.11.001.

Deprez, S., Sweatman, B.C., Connor, S.C., Haselden, J.N., Waterfield, C.J., 2002. Optimization of collection, storage and preparation of rat plasma for 1H NMR spectroscopic analysis in toxicology studies to determine inherent variation in biochemical profiles. J. Pharm. Biomed. Anal. 30, 1297–1310.

Derijks, H.J., Meyboom, R.H.B., Heerdink, E.R., De Koning, F.H.P., Janknegt, R., Lindquist, M., Egberts, A.C.G., 2008. The association between antidepressant use and disturbances in glucose homeostasis: evidence from spontaneous reports. Eur. J. Clin. Pharmacol. 64, 531–538. https://doi.org/10.1007/s00228-007-0441-y.

Detke, M.J., Johnson, J., Lucki, I., 1997. Acute and chronic antidepressant drug treatment in the rat forced swimming test model of depression. Exp. Clin. Psychopharmacol. 5, 107–112.

Dinoff, A., Herrmann, N., Lanctôt, K.L., 2017. Ceramides and depression: A systematic review. J. Affect. Disord. 213, 35–43. https://doi.org/10.1016/j.jad.2017.02.008.

Dobrowsky, R.T., 2000. Sphingolipid signalling domains floating on rafts or buried in caves? Cell. Signal. 12, 81–90.

Drevets, W.C., 2000. Functional anatomical abnormalities in limbic and prefrontal cortical structures in major depression. Prog. Brain Res. 126, 413–431. https://doi.org/10.1016/S0079-6123(00)26027-5.

Drevets, W.C., Price, J.L., Furey, M.L., 2008. Brain structural and functional abnormalities in mood disorders: implications for neurocircuitry models of depression. Brain Struct. Funct. 213, 93–118. https://doi.org/10.1007/s00429-008-0189-x.

Duan, H., Wang, J., 2010. Selective Transport of Monoamine Neurotransmitters by Human Plasma Membrane Monoamine Transporter and Organic Cation Transporter 3. J. Pharmacol. Exp. Ther. 335, 743–753. https://doi.org/10.1124/jpet.110.170142.

Duman, R.S., Li, N., 2012. A neurotrophic hypothesis of depression: role of synaptogenesis in the actions of NMDA receptor antagonists. Philos. Trans. R. Soc. B Biol. Sci. 367, 2475–2484. https://doi.org/10.1098/rstb.2011.0357.

Duval, F., Mokrani, M.-C., Monreal Ortiz, J.A., Schulz, P., Champeval, C., Macher, J.-P., 2005. Neuroendocrine predictors of the evolution of depression. Dialogues Clin. Neurosci. 7, 273–282.

Ehlert, K., Frosch, M., Fehse, N., Zander, A., Roth, J., Vormoor, J., 2007. Farber disease: clinical presentation, pathogenesis and a new approach to treatment. Pediatr. Rheumatol. Online J. 5, 15. https://doi.org/10.1186/1546-0096-5-15.

Eilat, E., Mendlovic, S., Doron, A., Zakuth, V., Spirer, Z., 1999. Increased Apoptosis in Patients with Major Depression: A Preliminary Study. J. Immunol. 163, 533–534.

Eisenhofer, G., Kopin, I.J., Goldstein, D.S., 2004. Catecholamine Metabolism: A Contemporary View with Implications for Physiology and Medicine. Pharmacol. Rev. 56, 331–349. https://doi.org/10.1124/pr.56.3.1.

Elhwuegi, A.S., 2004. Central monoamines and their role in major depression. Prog. Neuropsychopharmacol. Biol. Psychiatry 28, 435–451. https://doi.org/10.1016/j.pnpbp.2003.11.018.

Elmore, S., 2007. Apoptosis: A Review of Programmed Cell Death. Toxicol. Pathol. 35, 495–516. https://doi.org/10.1080/01926230701320337.

Elojeimy, S., Holman, D.H., Liu, X., El-Zawahry, A., Villani, M., Cheng, J.C., Mahdy, A., Zeidan, Y., Bielwaska, A., Hannun, Y.A., Norris, J.S., 2006. New insights on the use of desipramine as an inhibitor for acid ceramidase. FEBS Lett. 580, 4751–4756. https://doi.org/10.1016/j.febslet.2006.07.071.

Elsworth, J.D., Roth, R.H., 1997. Dopamine Synthesis, Uptake, Metabolism, and Receptors: Relevance to Gene Therapy of Parkinson's Disease. Exp. Neurol. 144, 4–9. https://doi.org/10.1006/exnr.1996.6379.

Erecińska, M., Silver, I.A., 1989. ATP and brain function. J. Cereb. Blood Flow Metab. Off. J. Int. Soc. Cereb. Blood Flow Metab. 9, 2–19. https://doi.org/10.1038/jcbfm.1989.2.

Ermine, C.M., Wright, J.L., Parish, C.L., Stanic, D., Thompson, L.H., 2016. Combined immunohistochemical and retrograde tracing reveals little evidence of innervation of the rat dentate gyrus by midbrain dopamine neurons. Front. Biol. 11, 246–255. https://doi.org/10.1007/s11515-016-1404-4.

Esmaeilzadeh, S., Valizadeh, H., Zakeri-Milani, P., 2016. A Simple, Fast, Low Cost, HPLC/UV Validated Method for Determination of Flutamide: Application to Protein Binding Studies. Adv. Pharm. Bull. 6, 251–256. https://doi.org/10.15171/apb.2016.034.

Euston, D.R., Gruber, A.J., McNaughton, B.L., 2012. The Role of Medial Prefrontal Cortex in Memory and Decision Making. Neuron 76, 1057–1070. https://doi.org/10.1016/j.neuron.2012.12.002.

Fagius, J., Osterman, P.O., Sidén, A., Wiholm, B.E., 1985. Guillain-Barré syndrome following zimeldine treatment. J. Neurol. Neurosurg. Psychiatry 48, 65–69.

Fahy, E., Subramaniam, S., Brown, H.A., Glass, C.K., Merrill, A.H., Murphy, R.C., Raetz, C.R.H., Russell, D.W., Seyama, Y., Shaw, W., Shimizu, T., Spener, F., van Meer, G., VanNieuwenhze, M.S., White, S.H., Witztum, J.L., Dennis, E.A., 2005. A comprehensive classification system for lipids. J. Lipid Res. 46, 839–861. https://doi.org/10.1194/jlr.E400004-JLR200.

Fantini, J., Barrantes, F.J., 2009. Sphingolipid/cholesterol regulation of neurotransmitter receptor conformation and function. Biochim. Biophys. Acta BBA - Biomembr. 1788, 2345–2361. https://doi.org/10.1016/j.bbamem.2009.08.016.

Felger, J.C., Lotrich, F.E., 2013. Inflammatory Cytokines in Depression: Neurobiological Mechanisms and Therapeutic Implications. Neuroscience 246, 199–229. https://doi.org/10.1016/j.neuroscience.2013.04.060.

Fernstrom, J.D., 1983. Role of precursor availability in control of monoamine biosynthesis in brain. Physiol. Rev. 63, 484–546.

Fiedorowicz, J.G., Swartz, K.L., 2004. The Role of Monoamine Oxidase Inhibitors in Current Psychiatric Practice. J. Psychiatr. Pract. 10, 239–248.

Fillenz, M., 2005. The role of lactate in brain metabolism. Neurochem. Int. 47, 413–417. https://doi.org/10.1016/j.neuint.2005.05.011.

Finberg, J.P.M., Rabey, J.M., 2016. Inhibitors of MAO-A and MAO-B in Psychiatry and Neurology. Front. Pharmacol. 7. https://doi.org/10.3389/fphar.2016.00340.

Fisher, S.K., Novak, J.E., Agranoff, B.W., 2002. Inositol and higher inositol phosphates in neural tissues: homeostasis, metabolism and functional significance. J. Neurochem. 82, 736–754. https://doi.org/10.1046/j.1471-4159.2002.01041.x.

Fowler, J.S., Logan, J., Azzaro, A.J., Fielding, R.M., Zhu, W., Poshusta, A.K., Burch, D., Brand, B., Free, J., Asgharnejad, M., Wang, G.-J., Telang, F., Hubbard, B., Jayne, M., King, P., Carter, P., Carter, S., Xu, Y., Shea, C., Muench, L., Alexoff, D., Shumay, E., Schueller, M., Warner, D., Apelskog-Torres, K., 2010. Reversible Inhibitors of Monoamine Oxidase-A (RIMAs): Robust, Reversible Inhibition of Human Brain MAO-A by CX157. Neuropsychopharmacology 35, 623. https://doi.org/10.1038/npp.2009.167.

Fowler, J.S., Logan, J., Azzaro, A.J., Fielding, R.M., Zhu, W., Poshusta, A.K., Burch, D., Brand, B., Free, J., Asgharnejad, M., Wang, G.-J., Telang, F., Hubbard, B., Jayne, M., King, P., Carter, P., Carter, S., Xu, Y., Shea, C., Muench, L., Alexoff, D., Shumay, E., Schueller, M., Warner, D., Apelskog-Torres, K., 2009. Reversible Inhibitors of Monoamine Oxidase-A (RIMAs): Robust, Reversible Inhibition of Human Brain MAO-A by CX157. Neuropsychopharmacology 35, 623–631. https://doi.org/10.1038/npp.2009.167.

Fox, M.E., Wightman, R.M., 2017. Contrasting Regulation of Catecholamine Neurotransmission in the Behaving Brain: Pharmacological Insights from an Electrochemical Perspective. Pharmacol. Rev. 69, 12–32. https://doi.org/10.1124/pr.116.012948.

Frazer, A., Hensler, J.G., 1999. Serotonin Receptors.

Frey, B.N., Stanley, J.A., Nery, F.G., Monkul, E.S., Nicoletti, M.A., Chen, H.-H., Hatch, J.P., Caetano, S.C., Ortiz, O., Kapczinski, F., Soares, J.C., 2007. Abnormal cellular energy and phospholipid metabolism in the left dorsolateral prefrontal cortex of medication-free individuals with bipolar disorder: an in vivo 1H MRS study. Bipolar Disord. 9 Suppl 1, 119–127. https://doi.org/10.1111/j.1399-5618.2007.00454.x.

Funk, R.S., Krise, J.P., 2012. Cationic amphiphilic drugs cause a marked expansion of apparent lysosomal volume: Implications for an intracellular distribution-based drug interaction. Mol. Pharm. 9, 1384–1395. https://doi.org/10.1021/mp200641e.

Futerman, A.H., Hannun, Y.A., 2004. The complex life of simple sphingolipids. EMBO Rep. 5, 777–782. https://doi.org/10.1038/sj.embor.7400208.

Gangoiti, P., Camacho, L., Arana, L., Ouro, A., Granado, M.H., Brizuela, L., Casas, J., Fabriás, G., Abad, J.L., Delgado, A., Gómez-Muñoz, A., 2010. Control of metabolism and signaling of simple bioactive sphingolipids: Implications in disease. Prog. Lipid Res. 49, 316–334. https://doi.org/10.1016/j.plipres.2010.02.004.

Gannon, M., Che, P., Chen, Y., Jiao, K., Roberson, E.D., Wang, Q., 2015. Noradrenergic dysfunction in Alzheimer's disease. Front. Neurosci. 9. https://doi.org/10.3389/fnins.2015.00220.

Gao, H.-C., Zhu, H., Song, C.-Y., Lin, L., Xiang, Y., Yan, Z.-H., Bai, G.-H., Ye, F.-Q., Li, X.-K., 2013. Metabolic Changes Detected by Ex Vivo High Resolution 1H NMR Spectroscopy in the Striatum of 6-OHDA-Induced Parkinson's Rat. Mol. Neurobiol. 47, 123–130. https://doi.org/10.1007/s12035-012-8336-z.

García-Álvarez, L., Busto, J.H., Peregrina, J.M., Avenoza, A., Oteo, J.A., 2016. Applications of 1H Nuclear Magnetic Resonance Spectroscopy in Clinical Microbiology. https://doi.org/10.5772/64450.

Garlick, P.J., 2005. The role of leucine in the regulation of protein metabolism. J. Nutr. 135, 1553S–6S.

Gąska, M., Kuśmider, M., Solich, J., Faron-Górecka, A., Krawczyk, M.J., Kułakowski, K., Dziedzicka-Wasylewska, M., 2012. Analysis of region-specific changes in gene expression upon treatment with citalopram and desipramine reveals temporal dynamics in response to antidepressant drugs at the transcriptome level. Psychopharmacology (Berl.) 223, 281–297. https://doi.org/10.1007/s00213-012-2714-0.

Gault, C., Obeid, L., Hannun, Y., 2010. An overview of sphingolipid metabolism: from synthesis to breakdown. Adv. Exp. Med. Biol. 688, 1–23.

Gillman, P.K., 2007. Tricyclic antidepressant pharmacology and therapeutic drug interactions updated. Br. J. Pharmacol. 151, 737–748. https://doi.org/10.1038/sj.bjp.0707253.

Giri, D., 2015. Polymerase Chain Reaction (PCR) : Principle, Procedure, Components, Types and Applications. LaboratoryInfo.com.

Gobin, V., Van Steendam, K., Denys, D., Deforce, D., 2014. Selective serotonin reuptake inhibitors as a novel class of immunosuppressants. Int. Immunopharmacol. 20, 148–156. https://doi.org/10.1016/j.intimp.2014.02.030.

Gołembiowska, K., Dziubina, A., 2000. Effect of acute and chronic administration of citalopram on glutamate and aspartate release in the rat prefrontal cortex. Pol. J. Pharmacol. 52, 441–448.

Goñi, F.M., Alonso, A., 2002. Sphingomyelinases: enzymology and membrane activity. FEBS Lett. 531, 38–46.

Govindaraju, V., Young, K., Maudsley, A.A., 2000. Proton NMR chemical shifts and coupling constants for brain metabolites. NMR Biomed. 13, 129–153.

Gracia-Garcia, P., Rao, V., Haughey, N.J., Bandaru, V.V.R., Smith, G., Rosenberg, P.B., Lobo, A., Lyketsos, C.G., Mielke, M.M., 2011. Plasma Ceramides Are Elevated in Depression. J. Neuropsychiatry Clin. Neurosci. 23, 215–218. https://doi.org/10.1176/appi.neuropsych.23.2.215.

Grassme, H., Jekle, A., Riehle, A., Schwarz, H., Berger, J., Sandhoff, K., Kolesnick, R., Gulbins, E., 2001. CD95 signaling via ceramide-rich membrane rafts. J. Biol. Chem. 276, 20589–20596. https://doi.org/10.1074/jbc.M101207200.

Grassmé, H., Jernigan, P.L., Hoehn, R.S., Wilker, B., Soddemann, M., Edwards, M.J., Müller, C.P., Kornhuber, J., Gulbins, E., 2015. Inhibition of Acid Sphingomyelinase by Antidepressants Counteracts Stress-Induced Activation of P38-Kinase in Major Depression. Neurosignals 23, 84–92. https://doi.org/10.1159/000442606.

Gruetter, R., Garwood, M., Uğurbil, K., Seaquist, E.R., 1996. Observation of resolved glucose signals in 1H NMR spectra of the human brain at 4 Tesla. Magn. Reson. Med. 36, 1–6.

Gulbins, A., Grassmé, H., Hoehn, R., Wilker, B., Soddemann, M., Kohnen, M., Edwards, M.J., Kornhuber, J., Gulbins, E., 2016. Regulation of Neuronal Stem Cell Proliferation in the Hippocampus by Endothelial Ceramide. Cell. Physiol. Biochem. 39, 790–801. https://doi.org/10.1159/000447789.

Gulbins, E., Palmada, M., Reichel, M., Lüth, A., Böhmer, C., Amato, D., Müller, C.P., Tischbirek, C.H., Groemer, T.W., Tabatabai, G., Becker, K.A., Tripal, P., Staedtler, S., Ackermann, T.F., Brederode, J. van, Alzheimer, C., Weller, M., Lang, U.E., Kleuser, B., Grassmé, H., Kornhuber, J., 2013. Acid sphingomyelinase–ceramide system mediates effects of antidepressant drugs. Nat. Med. 19, 934. https://doi.org/10.1038/nm.3214.

Gulbins, E., Szabo, I., Baltzer, K., Lang, F., 1997. Ceramide-induced inhibition of T lymphocyte voltage-gated potassium channel is mediated by tyrosine kinases. Proc. Natl. Acad. Sci. U. S. A. 94, 7661–7666.

Gulbins, E., Walter, S., Becker, K.A., Halmer, R., Liu, Y., Reichel, M., Edwards, M.J., Müller, C.P., Fassbender, K., Kornhuber, J., 2015. A central role for the acid sphingomyelinase/ceramide system in neurogenesis and major depression. J. Neurochem. 134, 183–192. https://doi.org/10.1111/jnc.13145.

Gundersen, B.B., Briand, L.A., Onksen, J.L., LeLay, J., Kaestner, K.H., Blendy, J.A., 2013. Increased Hippocampal Neurogenesis and Accelerated Response to Antidepressants in Mice with Specific Deletion of CREB in the Hippocampus: Role of cAMP Response-Element Modulator τ. J. Neurosci. 33, 13673–13685. https://doi.org/10.1523/JNEUROSCI.1669-13.2013.

Günther, H., 2013. NMR Spectroscopy: Basic Principles, Concepts and Applications in Chemistry. John Wiley & Sons.

Haase, J., Brown, E., 2015. Integrating the monoamine, neurotrophin and cytokine hypotheses of depression — A central role for the serotonin transporter? Pharmacol. Ther. 147, 1–11. https://doi.org/10.1016/j.pharmthera.2014.10.002.

Haenisch, B., Bönisch, H., 2011. Depression and antidepressants: insights from knockout of dopamine, serotonin or noradrenaline re-uptake transporters. Pharmacol. Ther. 129, 352–368. https://doi.org/10.1016/j.pharmthera.2010.12.002.

Hajós, M., Fleishaker, J.C., Filipiak-Reisner, J.K., Brown, M.T., Wong, E.H.F., 2004. The Selective Norepinephrine Reuptake Inhibitor Antidepressant Reboxetine: Pharmacological and Clinical Profile. CNS Drug Rev. 10, 23–44. https://doi.org/10.1111/j.1527-3458.2004.tb00002.x.

Hajós-Korcsok, E., McTavish, S.F., Sharp, T., 2000. Effect of a selective 5-hydroxytryptamine reuptake inhibitor on brain extracellular noradrenaline: microdialysis studies using paroxetine. Eur. J. Pharmacol. 407, 101–107. https://doi.org/10.1016/S0014-2999(00)00723-8.

Halim, N.D., Lipska, B.K., Hyde, T.M., Deep-Soboslay, A., Saylor, E.M., Herman, M.M., Thakar, J., Verma, A., Kleinman, J.E., 2008. Increased lactate levels and reduced pH in postmortem brains of schizophrenics: medication confounds. J. Neurosci. Methods 169, 208–213. https://doi.org/10.1016/j.jneumeth.2007.11.017.

Han, S., Park, H.-S., Lee, Y., Lee, B.-W., Kang, E.S., Cha, B.-S., 2016. Paroxetine-induced Hypoglycemia in Type 2 Diabetic Patient. Ewha Med. J. 39, 14. https://doi.org/10.12771/emj.2016.39.1.14.

Hanada, K., 2006. Discovery of the molecular machinery CERT for endoplasmic reticulum-to-Golgi trafficking of ceramide. Mol. Cell. Biochem. 286, 23–31. https://doi.org/10.1007/s11010-005-9044-z.

Hanada, K., 2003. Serine palmitoyltransferase, a key enzyme of sphingolipid metabolism. Biochim. Biophys. Acta BBA - Mol. Cell Biol. Lipids 1632, 16–30. https://doi.org/10.1016/S1388-1981(03)00059-3.

Hannun, Y.A., Obeid, L.M., 2008. Principles of bioactive lipid signalling: lessons from sphingolipids. Nat. Rev. Mol. Cell Biol. 9, 139–150. https://doi.org/10.1038/nrm2329.

Hardy, D.L., Norwood, T.J., 1998. Spectral Editing Technique for thein Vitroandin VivoDetection of Taurine. J. Magn. Reson. 133, 70–78. https://doi.org/10.1006/jmre.1998.1433.

Haris, M., Cai, K., Singh, A., Hariharan, H., Reddy, R., 2011. In vivo Mapping of Brain Myo-Inositol. NeuroImage 54, 2079–2085. https://doi.org/10.1016/j.neuroimage.2010.10.017.

Harvey, R.A., Champe, P.C., Finkel, R., Cubeddu, L., Clarke, M.A. (Eds.), 2008. Pharmacology, 4th Revised edition. ed. Lippincott Williams and Wilkins, Philadelphia.

He, X., Huang, Y., Li, B., Gong, C.-X., Schuchman, E.H., 2010. Deregulation of sphingolipid metabolism in Alzheimer's disease. Neurobiol. Aging 31, 398–408. https://doi.org/10.1016/j.neurobiolaging.2008.05.010.

He, X., Miranda, S.R., Xiong, X., Dagan, A., Gatt, S., Schuchman, E.H., 1999. Characterization of human acid sphingomyelinase purified from the media of overexpressing Chinese hamster ovary cells. Biochim. Biophys. Acta 1432, 251–264.

He, X., Okino, N., Dhami, R., Dagan, A., Gatt, S., Schulze, H., Sandhoff, K., Schuchman, E.H., 2003. Purification and characterization of recombinant, human acid ceramidase. Catalytic reactions and interactions with acid sphingomyelinase. J. Biol. Chem. 278, 32978–32986. https://doi.org/10.1074/jbc.M301936200.

Heinrich, M., Neumeyer, J., Jakob, M., Hallas, C., Tchikov, V., Winoto-Morbach, S., Wickel, M., Schneider-Brachert, W., Trauzold, A., Hethke, A., Schütze, S., 2004. Cathepsin D links TNF-induced acid sphingomyelinase to Bid-mediated caspase-9 and -3 activation. Cell Death Differ. 11, 550–563. https://doi.org/10.1038/sj.cdd.4401382.

Hering, H., Lin, C.-C., Sheng, M., 2003. Lipid Rafts in the Maintenance of Synapses, Dendritic Spines, and Surface AMPA Receptor Stability. J. Neurosci. 23, 3262–3271.

Herman, J.P., 2013. Neural control of chronic stress adaptation. Front. Behav. Neurosci. 7, 61. https://doi.org/10.3389/fnbeh.2013.00061.

Hiemke, C., Baumann, P., Bergemann, N., Conca, A., Dietmaier, O., Egberts, K., Fric, M., Gerlach, M., Greiner, C., Gründer, G., Haen, E., Havemann-Reinecke, U., Jaquenoud Sirot, E., Kirchherr, H., Laux, G., Lutz, U.C., Messer, T., Müller, M.J., Pfuhlmann, B., Rambeck, B., Riederer, P., Schoppek, B., Stingl, J., Uhr, M., Ulrich, S., Waschgler, R., Zernig, G., 2011. AGNP Consensus Guidelines for Therapeutic Drug Monitoring in Psychiatry: Update 2011. Pharmacopsychiatry 44, 195–235. https://doi.org/10.1055/s-0031-1286287.

Hirschfeld, R.M., 2000. History and evolution of the monoamine hypothesis of depression. J. Clin. Psychiatry 61 Suppl 6, 4–6.

Höglinger, D., Haberkant, P., Aguilera-Romero, A., Riezman, H., Porter, F.D., Platt, F.M., Galione, A., Schultz, C., 2015. Intracellular sphingosine releases calcium from lysosomes. eLife 4, e10616. https://doi.org/10.7554/eLife.10616.

Holmes, A., 2008. Genetic variation in cortico-amygdala serotonin function and risk for stress-related disease. Neurosci. Biobehav. Rev. 32, 1293–1314. https://doi.org/10.1016/j.neubiorev.2008.03.006.

Holmes, E., Tsang, T.M., Huang, J.T.-J., Leweke, F.M., Koethe, D., Gerth, C.W., Nolden, B.M., Gross, S., Schreiber, D., Nicholson, J.K., Bahn, S., 2006. Metabolic profiling of CSF: evidence that early intervention may impact on disease progression and outcome in schizophrenia. PLoS Med. 3, e327. https://doi.org/10.1371/journal.pmed.0030327.

Holsboer, F., 2000. The Corticosteroid Receptor Hypothesis of Depression. Neuropsychopharmacology 23, 477–501. https://doi.org/10.1016/S0893-133X(00)00159-7

Hornung, J.-P., 2003. The human raphe nuclei and the serotonergic system. J. Chem. Neuroanat. 26, 331–343.

Hussain, H.M., Butt, M.U.R.A., 2008. Comment on Esler et al. () "Increased brain serotonin turnover in panic disorder patients in the absence of a panic attack: Reduction by a selective serotonin reuptake inhibitor." Stress 11, 83–84. https://doi.org/10.1080/10253890801896082.

Hussein, R., 2016. 9 Functions of Dopamine That Serve You: What is it and How Does It Affect you? [WWW Document]. Blog CogniFit. URL https://blog.cognifit.com/functions-of-dopamine-serve-you/ (accessed 9.2.17).

Hyman, S.E., Nestler, E.J., 1996. Initiation and adaptation: a paradigm for understanding psychotropic drug action. Am. J. Psychiatry 153, 151–162. https://doi.org/10.1176/ajp.153.2.151.

Iglesias-Guimarais, V., Gil-Guiñon, E., Gabernet, G., García-Belinchón, M., Sánchez-Osuna, M., Casanelles, E., Comella, J.X., Yuste, V.J., 2012. Apoptotic DNA Degradation into Oligonucleosomal Fragments, but Not Apoptotic Nuclear Morphology, Relies on a Cytosolic Pool of DFF40/CAD Endonuclease. J. Biol. Chem. 287, 7766–7779. https://doi.org/10.1074/jbc.M111.290718.

Imajoh, M., Sugiura, H., Oshima, S., 2004. Morphological changes contribute to apoptotic cell death and are affected by caspase-3 and caspase-6 inhibitors during red sea bream iridovirus permissive replication. Virology 322, 220–230. https://doi.org/10.1016/j.virol.2004.02.006

Iversen, S.D., Iversen, L.L., 2007. Dopamine: 50 years in perspective. Trends Neurosci., Fifty years of dopamine research 30, 188–193. https://doi.org/10.1016/j.tins.2007.03.002.

Iwamori, M., Costello, C., Moser, H.W., 1979. Analysis and quantitation of free ceramide containing nonhydroxy and 2-hydroxy fatty acids, and phytosphingosine by high-performance liquid chromatography. J. Lipid Res. 20, 86–96.

Jackson, S.W., 1983. Melancholia and Mechanical Explanation in Eighteenth-Century Medicine. J. Hist. Med. Allied Sci. 38, 298–319. https://doi.org/10.1093/jhmas/38.3.298.

Jacobs, B.L., 2004. Depression The Brain Finally Gets Into the Act. Curr. Dir. Psychol. Sci. 13, 103–106. https://doi.org/10.1111/j.0963-7214.2004.00284.x.

Jacobs, B.L., van Praag, H., Gage, F.H., 2000. Adult brain neurogenesis and psychiatry: a novel theory of depression. Mol. Psychiatry 5, 262–269.

Jafurulla, M., Pucadyil, T.J., Chattopadhyay, A., 2008. Effect of sphingomyelinase treatment on ligand binding activity of human serotonin1A receptors. Biochim. Biophys. Acta 1778, 2022–2025. https://doi.org/10.1016/j.bbamem.2008.07.007.

Jain, M., Ngoy, S., Sheth, S.A., Swanson, R.A., Rhee, E.P., Liao, R., Clish, C.B., Mootha, V.K., Nilsson, R., 2014. A systematic survey of lipids across mouse tissues. Am. J. Physiol. Endocrinol. Metab. 306, E854-868. https://doi.org/10.1152/ajpendo.00371.2013.

Jernigan, P., Hoehn, R., Grassmé, H., J Edwards, M., P Müller, C., Kornhuber, J., Gulbins, E., 2015. Sphingolipids in Major Depression. https://doi.org/10.1159/000442603.

Jia, H., Feng, Y., Liu, Y., Chang, X., Chen, L., Zhang, H., Ding, G., Zou, Z., 2013. Integration of 1H NMR and UPLC-Q-TOF/MS for a Comprehensive Urinary Metabonomics Study on a Rat Model of Depression Induced by Chronic Unpredictable Mild Stress. PLOS ONE 8, e63624. https://doi.org/10.1371/journal.pone.0063624.

Kadioglu, M., Muci, E., Kesim, M., Ulku, C., Duman, E.N., Kalyoncu, N.I., Yaris, E., 2011. The Effect of Paroxetine, A Selective Serotonin Reuptake Inhibitor, on Blood Glucose Levels in Mice. Int. J. Pharmacol. 7, 283–290. https://doi.org/10.3923/ijp.2011.283.290.

Kang, J.-S., 2012. Principles and Applications of LC-MS/MS for the Quantitative Bioanalysis of Analytes in Various Biological Samples. https://doi.org/10.5772/32085.

Kang, Y., Huang, X., Pasyk, E.A., Ji, J., Holz, G.G., Wheeler, M.B., Tsushima, R.G., Gaisano, H.Y., 2002. Syntaxin-3 and syntaxin-1A inhibit l-type calcium channel activity, insulin biosynthesis and exocytosis in beta-cell lines. Diabetologia 45, 231–241. https://doi.org/10.1007/s00125-001-0718-0.

Kastrup, M.C., 2011. Cultural aspects of depression as a diagnostic entity: a historical perspective. Medicographia 33, 119–24.

Kaye, C.M., Haddock, R.E., Langley, P.F., Mellows, G., Tasker, T.C., Zussman, B.D., Greb, W.H., 1989. A review of the metabolism and pharmacokinetics of paroxetine in man. Acta Psychiatr. Scand. Suppl. 350, 60–75.

Kent, D., 2003. Snake Pits, Talking Cures & Magic Bullets: A History of Mental Illness. Twenty-First Century Books.

Khedr, L.H., Nassar, N.N., El-Denshary, E.S., Abdel-tawab, A.M., 2015. Paroxetine ameliorates changes in hippocampal energy metabolism in chronic mild stress-exposed rats. Neuropsychiatr. Dis. Treat. 11, 2887–2901. https://doi.org/10.2147/NDT.S87089.

Kitatani, K., Idkowiak-Baldys, J., Hannun, Y.A., 2008. The sphingolipid salvage pathway in ceramide metabolism and signaling. Cell. Signal. 20, 1010–1018. https://doi.org/10.1016/j.cellsig.2007.12.006.

Klerman, G.L., Cole, J.O., 1965. CLINICAL PHARMACOLOGY OF IMIPRAMINE AND RELATED ANTIDEPRESSANT COMPOUNDS. Pharmacol. Rev. 17, 101–141.

Klunk, W.E., Xu, C., Panchalingam, K., McClure, R.J., Pettegrew, J.W., 1996. Quantitative 1H and 31P MRS of PCA extracts of postmortem Alzheimer's disease brain. Neurobiol. Aging 17, 349–357.

Koch, J., Gärtner, S., Li, C.M., Quintern, L.E., Bernardo, K., Levran, O., Schnabel, D., Desnick, R.J., Schuchman, E.H., Sandhoff, K., 1996. Molecular cloning and characterization of a full-length complementary DNA encoding human acid ceramidase. Identification Of the first molecular lesion causing Farber disease. J. Biol. Chem. 271, 33110–33115.

Kolesnick, R.N., Goñi, F.M., Alonso, A., 2000. Compartmentalization of ceramide signaling: physical foundations and biological effects. J. Cell. Physiol. 184, 285–300. https://doi.org/10.1002/1097-4652(200009)184:3<285: AID-JCP2>3.0.CO;2-3.

Kolter, T., Sandhoff, K., 1999. Sphingolipids—Their Metabolic Pathways and the Pathobiochemistry of Neurodegenerative Diseases. Angew. Chem. Int. Ed. 38, 1532–1568. https://doi.org/10.1002/(SICI)1521-3773(19990601)38:11<1532: AID-ANIE1532>3.0.CO;2-U.

Kölzer, M., Werth, N., Sandhoff, K., 2004. Interactions of acid sphingomyelinase and lipid bilayers in the presence of the tricyclic antidepressant desipramine. FEBS Lett. 559, 96–98. https://doi.org/10.1016/S0014-5793(04)00033-X.

Kornhuber, J., Medlin, A., Bleich, S., Jendrossek, V., Henkel, A.W., Wiltfang, J., Gulbins, E., 2005. High activity of acid sphingomyelinase in major depression. J. Neural Transm. Vienna Austria 1996 112, 1583–1590. https://doi.org/10.1007/s00702-005-0374-5.

Kornhuber, J., Muehlbacher, M., Trapp, S., Pechmann, S., Friedl, A., Reichel, M., Mühle, C., Terfloth, L., Groemer, T.W., Spitzer, G.M., Liedl, K.R., Gulbins, E., Tripal, P., 2011. Identification of novel functional inhibitors of acid sphingomyelinase. PloS One 6, e23852. https://doi.org/10.1371/journal.pone.0023852.

Kornhuber, J., Müller, C.P., Becker, K.A., Reichel, M., Gulbins, E., 2014. The ceramide system as a novel antidepressant target. Trends Pharmacol. Sci. 35, 293–304. https://doi.org/10.1016/j.tips.2014.04.003.

Kornhuber, J., Reichel, M., Tripal, P., Groemer, T.W., Henkel, A.W., Mühle, C., Gulbins, E., 2009. The role of ceramide in major depressive disorder. Eur. Arch. Psychiatry Clin. Neurosci. 259 Suppl 2, S199-204. https://doi.org/10.1007/s00406-009-0061-x.

Kornhuber, J., Retz, W., Riederer, P., 1995. Slow accumulation of psychotropic substances in the human brain. Relationship to therapeutic latency of neuroleptic and antidepressant drugs? J. Neural Transm. Suppl. 46, 315–323.

Kornhuber, J., Tripal, P., Reichel, M., Mühle, C., Rhein, C., Muehlbacher, M., Groemer, T.W., Gulbins, E., 2010. Functional Inhibitors of Acid Sphingomyelinase (FIASMAs): a novel pharmacological group of drugs with broad clinical applications. Cell. Physiol. Biochem. Int. J. Exp. Cell. Physiol. Biochem. Pharmacol. 26, 9–20. https://doi.org/10.1159/000315101.

Kornhuber, J., Tripal, P., Reichel, M., Terfloth, L., Bleich, S., Wiltfang, J., Gulbins, E., 2008. Identification of new functional inhibitors of acid sphingomyelinase using a structure-property-activity relation model. J. Med. Chem. 51, 219–237. https://doi.org/10.1021/jm070524a.

Koyama, Y., Niitani, H., Maruyama, K., Okabayashi, K., Okazaki, N., Takakura, K., Sakano, T., Ise, T., Koyama, Y., Kimura, T., Imamura, Y., Nakajima, O., Umeda, N., Sakagami, R., Saito, T., Nakao, I., Kanko, T., Oh-hashi, Y., Ogawa, M., Inoue, Y., Yokoyama, M., Kusama, S., Tomiyama, J., Itoh, I., Sakai, Y., Kubo, A., Tominaga, T., Ishiwata, J., Hara, Y., Takatani, O., Ohta, K., Murakami, M., Taguchi, T., Nakano, Y., Jikuya, K., Inoguchi, K., Kumashiro, R., Tamada, R., 1980. Absorption and Excretion of a New Oral Antitumor Drug, 1-Hexylcarbamoyl-5-Fluorouracil (HCFU), in Cancer Patients. Jpn. J. Clin. Oncol. 10, 83–91. https://doi.org/10.1093/oxfordjournals.jjco.a038668.

Kozisek, M.E., Deupree, J.D., Burke, W.J., Bylund, D.B., 2007. Appropriate Dosing Regimens for Treating Juvenile Rats with Desipramine for Neuropharmacological and Behavioral Studies. J. Neurosci. Methods 163, 83–91. https://doi.org/10.1016/j.jneumeth.2007.02.015

Krishnan, V., Nestler, E.J., 2008. The molecular neurobiology of depression. Nature 455, 894–902. https://doi.org/10.1038/nature07455.

Lakraj, A.-A.D., Jabbari, B., Machado, D.G., 2014. Chapter 25 - Neuronal Networks and Therapeutics in Neurodegenerative Disorders, in: Faingold, C.L., Blumenfeld, H. (Eds.), Neuronal Networks in Brain Function, CNS Disorders, and Therapeutics. Academic Press, San Diego, pp. 335–348. https://doi.org/10.1016/B978-0-12-415804-7.00025-3.

Lambert, E., Hastings, J., Lambert, G., 2001. Noradrenaline synthesis, release and vesicular transport in the rat brain following subarachnoid hemorrhage. Brain Res. Bull. 55, 459–463.

Lan, M.J., McLoughlin, G.A., Griffin, J.L., Tsang, T.M., Huang, J.T.J., Yuan, P., Manji, H., Holmes, E., Bahn, S., 2009. Metabonomic analysis identifies molecular changes associated with the pathophysiology and drug treatment of bipolar disorder. Mol. Psychiatry 14, 269–279. https://doi.org/10.1038/sj.mp.4002130.

Lee, J.-H., Ko, E., Kim, Y.-E., Min, J.-Y., Liu, J., Kim, Y., Shin, M., Hong, M., Bae, H., 2010. Gene expression profile analysis of genes in rat hippocampus from antidepressant treated rats using DNA microarray. BMC Neurosci. 11, 152. https://doi.org/10.1186/1471-2202-11-152.

Lee, L.H.-W., Shui, G., Farooqui, A.A., Wenk, M.R., Tan, C.-H., Ong, W.-Y., 2009. Lipidomic analyses of the mouse brain after antidepressant treatment: evidence for endogenous release of long-chain fatty acids? Int. J. Neuropsychopharmacol. 12, 953–964. https://doi.org/10.1017/S146114570900995X.

Lee, M.M., Reif, A., Schmitt, A.G., 2013. Major depression: a role for hippocampal neurogenesis? Curr. Top. Behav. Neurosci. 14, 153–179. https://doi.org/10.1007/7854_2012_226

Lefkowitz, R.J., 1993. G protein—coupled receptor kinases. Cell 74, 409–412. https://doi.org/10.1016/0092-8674(93)80042-D.

Leonard, B., 2000. Clinical implications of mechanisms of action of antidepressants. Adv. Psychiatr. Treat. 6, 178–186. https://doi.org/10.1192/apt.6.3.178.

Lepple-Wienhues, A., Belka, C., Laun, T., Jekle, A., Walter, B., Wieland, U., Welz, M., Heil, L., Kun, J., Busch, G., Weller, M., Bamberg, M., Gulbins, E., Lang, F., 1999. Stimulation of CD95 (Fas) blocks T lymphocyte calcium channels through sphingomyelinase and sphingolipids. Proc. Natl. Acad. Sci. 96, 13795–13800. https://doi.org/10.1073/pnas.96.24.13795.

Lestage, J., Verrier, D., Palin, K., Dantzer, R., 2002. The enzyme indoleamine 2,3-dioxygenase is induced in the mouse brain in response to peripheral administration of lipopolysaccharide and superantigen. Brain. Behav. Immun. 16, 596–601.

Lewis, A.J., 1934. Melancholia: A Historical Review. Br. J. Psychiatry 80, 1–42. https://doi.org/10.1192/bjp.80.328.1.

Liddell, H.G., Scott, R., Jones, S.H.S., McKenzie, R., Glare, P.G.W., 1996. A Greek-English Lexicon, Ninth Edition with Revised Supplement. ed. Oxford University Press, Oxford, New York.

Linke, T., Wilkening, G., Lansmann, S., Moczall, H., Bartelsen, O., Weisgerber, J., Sandhoff, K., 2001. Stimulation of acid sphingomyelinase activity by lysosomal lipids and sphingolipid activator proteins. Biol. Chem. 382, 283–290. https://doi.org/10.1515/BC.2001.035.

Liu, G., Xiao, L., Fang, T., Cai, Y., Jia, G., Zhao, H., Wang, J., Chen, X., Wu, C., 2014. Pea Fiber and Wheat Bran Fiber Show Distinct Metabolic Profiles in Rats as Investigated by a 1H NMR-Based Metabolomic Approach. PLOS ONE 9, e115561. https://doi.org/10.1371/journal.pone.0115561.

Liu, W., Ge, T., Leng, Y., Pan, Z., Fan, J., Yang, W., Cui, R., 2017. The Role of Neural Plasticity in Depression: From Hippocampus to Prefrontal Cortex [WWW Document]. Neural Plast. https://doi.org/10.1155/2017/6871089.

Lloyd-Evans, E., Morgan, A.J., He, X., Smith, D.A., Elliot-Smith, E., Sillence, D.J., Churchill, G.C., Schuchman, E.H., Galione, A., Platt, F.M., 2008. Niemann-Pick disease type C1 is a sphingosine storage disease that causes deregulation of lysosomal calcium. Nat. Med. 14, 1247–1255. https://doi.org/10.1038/nm.1876.

Logemann, J., Schell, J., Willmitzer, L., 1987. Improved method for the isolation of RNA from plant tissues. Anal. Biochem. 163, 16–20.

Lübke, T., Lobel, P., Sleat, D., 2009. Proteomics of the Lysosome. Biochim. Biophys. Acta 1793, 625–635. https://doi.org/10.1016/j.bbamcr.2008.09.018.

Lundgren, J.D., Amsterdam, J., Newberg, A., Allison, K.C., Wintering, N., Stunkard, A.J., 2009. Differences in serotonin transporter binding affinity in patients with major depressive disorder and night eating syndrome. Eat. Weight Disord. - Stud. Anorex. Bulim. Obes. 14, 45–50. https://doi.org/10.1007/BF03327794.

Madhav, T.R., Pei, Q., Zetterström, T.S., 2001. Serotonergic cells of the rat raphe nuclei express mRNA of tyrosine kinase B (trkB), the high-affinity receptor for brain derived neurotrophic factor (BDNF). Brain Res. Mol. Brain Res. 93, 56–63.

Maes, M., 2008. The cytokine hypothesis of depression: inflammation, oxidative & nitrosative stress (IO&NS) and leaky gut as new targets for adjunctive treatments in depression. Neuro Endocrinol. Lett. 29, 287–291.

Mahdy, A.E., Cheng, J.C., Li, J., Elojeimy, S., Meacham, W.D., Turner, L.S., Bai, A., Gault, C.R., McPherson, A.S., Garcia, N., Beckham, T.H., Saad, A., Bielawska, A., Bielawski, J., Hannun, Y.A., Keane, T.E., Taha, M.I., Hammouda, H.M., Norris, J.S., Liu, X., 2009. Acid Ceramidase Upregulation in Prostate Cancer Cells Confers Resistance to Radiation: AC Inhibition, a Potential Radiosensitizer. Mol. Ther. 17, 430–438. https://doi.org/10.1038/mt.2008.281.

Malykhin, N.V., Carter, R., Seres, P., Coupland, N.J., 2010. Structural changes in the hippocampus in major depressive disorder: contributions of disease and treatment. J. Psychiatry Neurosci. JPN 35, 337–343. https://doi.org/10.1503/jpn.100002.

Marona-Lewicka, D., Nichols, D.E., 2011. POTENTIAL SEROTONIN 5-HT1A AND DOPAMINE D4 RECEPTOR MODULATION OF THE DISCRIMINATIVE STIMULUS EFFECTS OF AMPHETAMINE IN RATS. Behav. Pharmacol. 22, 508–515. https://doi.org/10.1097/FBP.0b013e328349fc31.

Mason, E., 2015. English: The Electrochemical Fatigue Crack Sensor, drawn after consulting the original patent drawings of U.S. Patent 602 6691.

Mathes, C.M., Spector, A.C., 2011. The Selective Serotonin Reuptake Inhibitor Paroxetine Does Not Alter Consummatory Concentration-Dependent Licking of Prototypical Taste Stimuli by Rats. Chem. Senses 36, 515–526. https://doi.org/10.1093/chemse/bjr011.

Mattinson, C.E., Burmeister, J.J., Quintero, J.E., Pomerleau, F., Huettl, P., Gerhardt, G.A., 2011. Tonic and Phasic Release of Glutamate and Acetylcholine Neurotransmission in Sub-regions of the Rat Prefrontal Cortex Using Enzyme-based Microelectrode Arrays. J. Neurosci. Methods 202, 199. https://doi.org/10.1016/j.jneumeth.2011.08.020.

McCorvy, J.D., Roth, B.L., 2015. Structure and Function of Serotonin G protein Coupled Receptors. Pharmacol. Ther. 150, 129–142. https://doi.org/10.1016/j.pharmthera.2015.01.009.

McEwen, B.S., Morrison, J.H., 2013. Brain On Stress: Vulnerability and Plasticity of the Prefrontal Cortex Over the Life Course. Neuron 79, 16–29. https://doi.org/10.1016/j.neuron.2013.06.028.

McEwen, B.S., Nasca, C., Gray, J.D., 2016. Stress Effects on Neuronal Structure: Hippocampus, Amygdala, and Prefrontal Cortex. Neuropsychopharmacology 41, 3–23. https://doi.org/10.1038/npp.2015.171.

McIntyre, R.S., Filteau, M.-J., Martin, L., Patry, S., Carvalho, A., Cha, D.S., Barakat, M., Miguelez, M., 2014. Treatment-resistant depression: definitions, review of the evidence, and algorithmic approach. J. Affect. Disord. 156, 1–7. https://doi.org/10.1016/j.jad.2013.10.043.

Medina, D.L., Di Paola, S., Peluso, I., Armani, A., De Stefani, D., Venditti, R., Montefusco, S., Scotto-Rosato, A., Prezioso, C., Forrester, A., Settembre, C., Wang, W., Gao, Q., Xu, H., Sandri, M., Rizzuto, R., De Matteis, M.A., Ballabio, A., 2015. Lysosomal calcium signalling regulates autophagy through calcineurin and TFEB. Nat. Cell Biol. 17, 288–299. https://doi.org/10.1038/ncb3114.

Mehler-Wex, C., Riederer, P., Gerlach, M., 2006. Dopaminergic dysbalance in distinct basal ganglia neurocircuits: implications for the pathophysiology of Parkinson's disease, schizophrenia and attention deficit hyperactivity disorder. Neurotox. Res. 10, 167–179.

Meiser, J., Weindl, D., Hiller, K., 2013. Complexity of dopamine metabolism. Cell Commun. Signal. CCS 11, 34. https://doi.org/10.1186/1478-811X-11-34.

Merens, W., Booij, L., Haffmans, P.J., van der Does, A., 2008. The effects of experimentally lowered serotonin function on emotional information processing and memory in remitted depressed patients. J. Psychopharmacol. (Oxf.) 22, 653–662. https://doi.org/10.1177/0269881107081531.

Merrill, A.H., Sullards, M.C., Allegood, J.C., Kelly, S., Wang, E., 2005. Sphingolipidomics: High-throughput, structure-specific, and quantitative analysis of sphingolipids by liquid chromatography tandem mass spectrometry. Methods, Molecular and Cell Biology of Lipids 36, 207–224. https://doi.org/10.1016/j.ymeth.2005.01.009.

Mesulam, M.M., Mufson, E.J., Wainer, B.H., Levey, A.I., 1983. Central cholinergic pathways in the rat: an overview based on an alternative nomenclature (Ch1-Ch6). Neuroscience 10, 1185–1201.

Michaelis, T., Helms, G., Merboldt, K.D., Hänicke, W., Bruhn, H., Frahm, J., 1993. Identification of Scyllo-inositol in proton NMR spectra of human brain in vivo. NMR Biomed. 6, 105–109.

Michelsen, K.A., Prickaerts, J., Steinbusch, H.W.M., 2008. The dorsal raphe nucleus and serotonin: implications for neuroplasticity linked to major depression and Alzheimer's disease. Prog. Brain Res. 172, 233–264. https://doi.org/10.1016/S0079-6123(08)00912-6

Mills, E., O'Neill, L.A.J., 2014. Succinate: a metabolic signal in inflammation. Trends Cell Biol. 24, 313–320. https://doi.org/10.1016/j.tcb.2013.11.008.

Ming, G.-L., Song, H., 2011. Adult neurogenesis in the mammalian brain: significant answers and significant questions. Neuron 70, 687–702. https://doi.org/10.1016/j.neuron.2011.05.001

Mitchell, A.J., 2006. Two-week delay in onset of action of antidepressants: new evidence. Br. J. Psychiatry 188, 105–106. https://doi.org/10.1192/bjp.bp.105.011692.

Mnie-Filali, O., Abrial, E., Lambás-Señas, L., Haddjeri, N., 2013. Long-Term Adaptive Changes Induced by Antidepressants: From Conventional to Novel Therapies. https://doi.org/10.5772/54553.

Moore, G.J., Bebchuk, J.M., Hasanat, K., Chen, G., Seraji-Bozorgzad, N., Wilds, I.B., Faulk, M.W., Koch, S., Glitz, D.A., Jolkovsky, L., Manji, H.K., 2000. Lithium increases N-acetyl-aspartate in the human brain: in vivo evidence in support of bcl-2's neurotrophic effects? Biol. Psychiatry 48, 1–8.

Moore, R.Y., Halaris, A.E., 1975. Hippocampal innervation by serotonin neurons of the midbrain raphe in the rat. J. Comp. Neurol. 164, 171–183. https://doi.org/10.1002/cne.901640203.

Morgan, L.D., Baker, H., Yeoman, M.S., Patel, B.A., 2012. Chromatographic assay to study the activity of multiple enzymes involved in the synthesis and metabolism of dopamine and serotonin. Analyst 137, 1409–1415. https://doi.org/10.1039/C2AN16227J.

Moussavi, S., Chatterji, S., Verdes, E., Tandon, A., Patel, V., Ustun, B., 2007. Depression, chronic diseases, and decrements in health: results from the World Health Surveys. Lancet Lond. Engl. 370, 851–858. https://doi.org/10.1016/S0140-6736(07)61415-9.

Mulinari, S., 2012. Monoamine Theories of Depression: Historical Impact on Biomedical Research. J. Hist. Neurosci. 21, 366–392. https://doi.org/10.1080/0964704X.2011.623917.

Müller, C.P., Carey, R.J., Huston, J.P., De Souza Silva, M.A., 2007. Serotonin and psychostimulant addiction: focus on 5-HT1A-receptors. Prog. Neurobiol. 81, 133–178. https://doi.org/10.1016/j.pneurobio.2007.01.001.

Müller, C.P., Reichel, M., Mühle, C., Rhein, C., Gulbins, E., Kornhuber, J., 2015. Brain membrane lipids in major depression and anxiety disorders. Biochim. Biophys. Acta 1851, 1052–1065. https://doi.org/10.1016/j.bbalip.2014.12.014.

Murphy, D.L., Lesch, K.-P., 2008. Targeting the murine serotonin transporter: insights into human neurobiology. Nat. Rev. Neurosci. 9, 85–96. https://doi.org/10.1038/nrn2284.

Murray, C.J., Lopez, A.D., 1997. Global mortality, disability, and the contribution of risk factors: Global Burden of Disease Study. Lancet Lond. Engl. 349, 1436–1442. https://doi.org/10.1016/S0140-6736(96)07495-8.

Nakatani, N., Aburatani, H., Nishimura, K., Semba, J., Yoshikawa, T., 2004. Comprehensive expression analysis of a rat depression model. Pharmacogenomics J. 4, 114–126. https://doi.org/10.1038/sj.tpj.6500234.

Nemeroff, C., 2002. Recent advances in the neurobiology of depression.

O'Connor, J.C., Lawson, M.A., André, C., Moreau, M., Lestage, J., Castanon, N., Kelley, K.W., Dantzer, R., 2009. Lipopolysaccharide-induced depressive-like behavior is mediated by indoleamine 2,3-dioxygenase activation in mice. Mol. Psychiatry 14, 511–522. https://doi.org/10.1038/sj.mp.4002148.

O'Donnell, T., Rotzinger, S., Ulrich, M., Hanstock, C.C., Nakashima, T.T., Silverstone, P.H., 2003. Effects of chronic lithium and sodium valproate on concentrations of brain amino acids. Eur. Neuropsychopharmacol. 13, 220–227. https://doi.org/10.1016/S0924-977X(03)00070-1.

Ogawa, S., Tachimoto, H., Kaga, T., 2010. Elevation of ceramide in Acetobacter malorum S24 by low pH stress and high temperature stress. J. Biosci. Bioeng. 109, 32–36. https://doi.org/10.1016/j.jbiosc.2009.07.007.

Ohnishi, T., Murata, T., Watanabe, A., Hida, A., Ohba, H., Iwayama, Y., Mishima, K., Gondo, Y., Yoshikawa, T., 2014. Defective Craniofacial Development and Brain Function in a Mouse Model for Depletion of Intracellular Inositol Synthesis. J. Biol. Chem. jbc.M113.536706. https://doi.org/10.1074/jbc.M113.536706.

Ohrmann, P., Siegmund, A., Suslow, T., Pedersen, A., Spitzberg, K., Kersting, A., Rothermundt, M., Arolt, V., Heindel, W., Pfleiderer, B., 2007. Cognitive impairment and in vivo metabolites in first-episode neuroleptic-naive and chronic medicated schizophrenic patients: a proton magnetic resonance spectroscopy study. J. Psychiatr. Res. 41, 625–634. https://doi.org/10.1016/j.jpsychires.2006.07.002.

Oleskevich, S., Descarries, L., Lacaille, J.C., 1989. Quantified distribution of the noradrenaline innervation in the hippocampus of adult rat. J. Neurosci. Off. J. Soc. Neurosci. 9, 3803–3815.

Oliveira, T.G., Chan, R.B., Bravo, F.V., Miranda, A., Silva, R.R., Zhou, B., Marques, F., Pinto, V., Cerqueira, J.J., Di Paolo, G., Sousa, N., 2016. The impact of chronic stress on the rat brain lipidome. Mol. Psychiatry 21, 80–88. https://doi.org/10.1038/mp.2015.14.

Oosterhof, C.A., 2016. Impact of Depressogenic-and Antidepressant-like Challenges on Monoamine System Activities: in vivo Electrophysiological Characterization Studies (Thesis). Université d'Ottawa / University of Ottawa. https://doi.org/http://dx.doi.org/10.20381/ruor-5197.

Organization, W.H., 2017. Depression and other common mental disorders: global health estimates.

Osherovich, L., 2013. Depressing sphingolipids. SciBX Sci.-Bus. Exch. 6. https://doi.org/10.1038/scibx.2013.675.

Panatier, A., Theodosis, D.T., Mothet, J.-P., Touquet, B., Pollegioni, L., Poulain, D.A., Oliet, S.H.R., 2006. Glia-derived D-serine controls NMDA receptor activity and synaptic memory. Cell 125, 775–784. https://doi.org/10.1016/j.cell.2006.02.051.

Pandya, M., Altinay, M., Malone, D.A., Anand, A., 2012. Where in the Brain Is Depression? Curr. Psychiatry Rep. 14, 634–642. https://doi.org/10.1007/s11920-012-0322-7.

Parasuraman, S., R, A., Balamurugan, S., Muralidharan, S., Kumar, K.J., Vijayan, V., 2014. An Overview of Liquid Chromatography-Mass Spectroscopy Instrumentation. Pharm. Methods 5.

Paxinos, G., Watson, C., 2006. The Rat Brain in Stereotaxic Coordinates: Hard Cover Edition. Elsevier.

Pei, Q., Leslie, R.A., Grahame-Smith, D.G., Zetterström, T.S., 1995. 5-HT efflux from rat hippocampus in vivo produced by 4-aminopyridine is increased by chronic lithium administration. Neuroreport 6, 716–720.

Pestana, E.A., Belak, S., Diallo, A., Crowther, J.R., Viljoen, G.J., 2009. Real-Time PCR – The Basic Principles, in: Early, Rapid and Sensitive Veterinary Molecular Diagnostics - Real Time PCR Applications. Springer, Dordrecht, pp. 27–46. https://doi.org/10.1007/978-90-481-3132-7_3.

Pettus, B.J., Chalfant, C.E., Hannun, Y.A., 2002. Ceramide in apoptosis: an overview and current perspectives. Biochim. Biophys. Acta BBA - Mol. Cell Biol. Lipids, Lipids in apoptosis 1585, 114–125. https://doi.org/10.1016/S1388-1981(02)00331-1.

Pewzner-Jung, Y., Ben-Dor, S., Futerman, A.H., 2006. When Do Lasses (Longevity Assurance Genes) Become CerS (Ceramide Synthases)? INSIGHTS INTO THE REGULATION OF CERAMIDE SYNTHESIS. J. Biol. Chem. 281, 25001–25005. https://doi.org/10.1074/jbc.R600010200.

Philipp, M., Brede, M., Hein, L., 2002. Physiological significance of α2-adrenergic receptor subtype diversity: one receptor is not enough. Am. J. Physiol. - Regul. Integr. Comp. Physiol. 283, R287–R295. https://doi.org/10.1152/ajpregu.00123.2002.

Pieczenik, S.R., Neustadt, J., 2007. Mitochondrial dysfunction and molecular pathways of disease. Exp. Mol. Pathol. 83, 84–92. https://doi.org/10.1016/j.yexmp.2006.09.008.

Pies, R., 2010. Antidepressants work, sort of--our system of care does not. J. Clin. Psychopharmacol. 30, 101–104. https://doi.org/10.1097/JCP.0b013e3181d52dea.

Pirot, S., Jay, T.M., Glowinski, J., Thierry, A.-M., 1994. Anatomical and Electrophysiological Evidence for an Excitatory Amino Acid Pathway from the Thalamic Mediodorsal Nucleus to the Prefrontal Cortex in the Rat. Eur. J. Neurosci. 6, 1225–1234. https://doi.org/10.1111/j.1460-9568.1994.tb00621.x.

Pitt, J.J., 2009. Principles and Applications of Liquid Chromatography-Mass Spectrometry in Clinical Biochemistry. Clin. Biochem. Rev. 30, 19–34.

Pizzirani, D., Pagliuca, C., Realini, N., Branduardi, D., Bottegoni, G., Mor, M., Bertozzi, F., Scarpelli, R., Piomelli, D., Bandiera, T., 2013. Discovery of a new class of highly potent inhibitors of acid ceramidase: synthesis and structure-activity relationship (SAR). J. Med. Chem. 56, 3518–3530. https://doi.org/10.1021/jm301879g.

Placidi, G.P.A., Oquendo, M.A., Malone, K.M., Huang, Y.-Y., Ellis, S.P., Mann, J.J., 2001. Aggressivity, suicide attempts, and depression: relationship to cerebrospinal fluid monoamine metabolite levels. Biol. Psychiatry 50, 783–791. https://doi.org/10.1016/S0006-3223(01)01170-2.

Pouwels, P.J., Frahm, J., 1998. Regional metabolite concentrations in human brain as determined by quantitative localized proton MRS. Magn. Reson. Med. 39, 53–60.

Pouwels, P.J., Frahm, J., 1997. Differential distribution of NAA and NAAG in human brain as determined by quantitative localized proton MRS. NMR Biomed. 10, 73–78.

Powell, T., Fernandes, C., Schalkwyk, L., 2012. Depression-Related Behavioral Tests. Curr. Protoc. Mouse Biol. 2. https://doi.org/10.1002/9780470942390.mo110176.

Powers, R., 2009. NMR metabolomics and drug discovery. Magn. Reson. Chem. MRC 47 Suppl 1, S2-11. https://doi.org/10.1002/mrc.2461.

Price, J.L., Drevets, W.C., 2010. Neurocircuitry of Mood Disorders. Neuropsychopharmacology 35, 192–216. https://doi.org/10.1038/npp.2009.104.

Prince, M., Patel, V., Saxena, S., Maj, M., Maselko, J., Phillips, M.R., Rahman, A., 2007. No health without mental health. The Lancet 370, 859–877. https://doi.org/10.1016/S0140-6736(07)61238-0.

Pryor, R.J., Wittwer, C.T., 2006. Real-time polymerase chain reaction and melting curve analysis. Methods Mol. Biol. Clifton NJ 336, 19–32. https://doi.org/10.1385/1-59745-074-X:19.

Puig, M.V., Gulledge, A.T., 2011. Serotonin and Prefrontal Cortex Function: Neurons, Networks, and Circuits. Mol. Neurobiol. 44, 449–464. https://doi.org/10.1007/s12035-011-8214-0.

Quansah, E., 2017. Molecular and Neurochemical Effects of Methylphenidate on the Developing Brain.

Rajkumar, R., Mahesh, R., 2008. Assessing the Neuronal Serotonergic Target-based Antidepressant Stratagem: Impact of In Vivo Interaction Studies and Knockout Models. Curr. Neuropharmacol. 6, 215–234. https://doi.org/10.2174/157015908785777256.

Ramachandraih, C.T., Subramanyam, N., Bar, K.J., Baker, G., Yeragani, V.K., 2011. Antidepressants: From MAOIs to SSRIs and more. Indian J. Psychiatry 53, 180–182. https://doi.org/10.4103/0019-5545.82567.

Ramamoorthy, S., Shippenberg, T.S., Jayanthi, L.D., 2011. Regulation of monoamine transporters: Role of transporter phosphorylation. Pharmacol. Ther. 129, 220–238. https://doi.org/10.1016/j.pharmthera.2010.09.009.

Rango, M., Cogiamanian, F., Marceglia, S., Barberis, B., Arighi, A., Biondetti, P., Priori, A., 2008. Myoinositol content in the human brain is modified by transcranial direct current stimulation in a matter of minutes: A 1H-MRS study. Magn. Reson. Med. 60, 782–789. https://doi.org/10.1002/mrm.21709.

Rapport, M.M., Green, A.A., Page, I.H., 1948. Serum vasoconstrictor, serotonin; isolation and characterization. J. Biol. Chem. 176, 1243–1251.

Realini, N., Solorzano, C., Pagliuca, C., Pizzirani, D., Armirotti, A., Luciani, R., Costi, M.P., Bandiera, T., Piomelli, D., 2013. Discovery of highly potent acid ceramidase inhibitors with in vitro tumor chemosensitizing activity. Sci. Rep. 3, 1035. https://doi.org/10.1038/srep01035.

Reed, J.C., 2000. Mechanisms of Apoptosis. Am. J. Pathol. 157, 1415–1430.

Reichel, M., Richter-Schmidinger, T., Mühle, C., Rhein, C., Alexopoulos, P., Schwab, S.G., Gulbins, E., Kornhuber, J., 2014. The Common Acid Sphingomyelinase Polymorphism p.G508R is Associated with Self-Reported Allergy. Cell. Physiol. Biochem. 34, 82–91. https://doi.org/10.1159/000362986.

Rhein, C., Reichel, M., Kramer, M., Rotter, A., Lenz, B., Mühle, C., Gulbins, E., Kornhuber, J., 2017. Alternative splicing of SMPD1 coding for acid sphingomyelinase in major depression. J. Affect. Disord. 209, 10–15. https://doi.org/10.1016/j.jad.2016.09.019.

Riddle, E.L., Rau, K.S., Topham, M.K., Hanson, G.R., Fleckenstein, A.E., 2003. Ceramide-induced alterations in dopamine transporter function. Eur. J. Pharmacol. 458, 31–36.

Rot, M. aan het, Mathew, S.J., Charney, D.S., 2009. Neurobiological mechanisms in major depressive disorder. Can. Med. Assoc. J. 180, 305–313. https://doi.org/10.1503/cmaj.080697.

Rother, J., van Echten, G., Schwarzmann, G., Sandhoff, K., 1992. Biosynthesis of sphingolipids: dihydroceramide and not sphinganine is desaturated by cultured cells. Biochem. Biophys. Res. Commun. 189, 14–20.

Roy, A., Jong, J.D., Linnoila, M., 1989. Cerebrospinal Fluid Monoamine Metabolites and Suicidal Behavior in Depressed Patients: A 5-Year Follow-up Study. Arch. Gen. Psychiatry 46, 609–612. https://doi.org/10.1001/archpsyc.1989.01810070035005.

Rudnick, G., 2006. Serotonin transporters--structure and function. J. Membr. Biol. 213, 101–110. https://doi.org/10.1007/s00232-006-0878-4.

Rush, A.J., Trivedi, M.H., Wisniewski, S.R., Nierenberg, A.A., Stewart, J.W., Warden, D., Niederehe, G., Thase, M.E., Lavori, P.W., Lebowitz, B.D., McGrath, P.J., Rosenbaum, J.F., Sackeim, H.A., Kupfer, D.J., Luther, J., Fava, M., 2006. Acute and Longer-Term Outcomes in Depressed Outpatients Requiring One or Several Treatment Steps: A STAR*D Report. Am. J. Psychiatry 163, 1905–1917. https://doi.org/10.1176/ajp.2006.163.11.1905.

Ruvolo, P.P., 2003. Intracellular signal transduction pathways activated by ceramide and its metabolites. Pharmacol. Res., Pharmacology of Ceramide and Sphingolipids 47, 383–392. https://doi.org/10.1016/S1043-6618(03)00050-1.

Sacchetti, G., Bernini, M., Gobbi, M., Parini, S., Pirona, L., Mennini, T., Samanin, R., 2001. Chronic treatment with desipramine facilitates its effect on extracellular noradrenaline in the rat hippocampus: studies on the role of presynaptic alpha2-adrenoceptors. Naunyn. Schmiedebergs Arch. Pharmacol. 363, 66–72.

Sahay, A., Hen, R., 2007. Adult hippocampal neurogenesis in depression. Nat. Neurosci. 10, 1110–1115. https://doi.org/10.1038/nn1969.

Saied, E.M., Arenz, C., 2014. Small molecule inhibitors of ceramidases. Cell. Physiol. Biochem. Int. J. Exp. Cell. Physiol. Biochem. Pharmacol. 34, 197–212. https://doi.org/10.1159/000362995.

Sakamoto, J., Hamada, C., Rahman, M., Kodaira, S., Ito, K., Nakazato, H., Ohashi, Y., Yasutomi, M., 2005. An Individual Patient Data Meta-analysis of Adjuvant Therapy with Carmofur in Patients with Curatively Resected Colon Cancer. Jpn. J. Clin. Oncol. 35, 536–544. https://doi.org/10.1093/jjco/hyi147.

Sakamoto, J., Oba, K., Matsui, T., Kobayashi, M., 2006. Efficacy of Oral Anticancer Agents for Colorectal Cancer. Dis. Colon Rectum 49, S82. https://doi.org/10.1007/s10350-006-0601-7.

Sapolsky, R.M., 2001. Depression, antidepressants, and the shrinking hippocampus. Proc. Natl. Acad. Sci. U. S. A. 98, 12320–12322. https://doi.org/10.1073/pnas.231475998.

Schiepers, O.J.G., Wichers, M.C., Maes, M., 2005. Cytokines and major depression. Prog. Neuropsychopharmacol. Biol. Psychiatry 29, 201–217. https://doi.org/10.1016/j.pnpbp.2004.11.003.

Schildkraut, J.J., 1965. The catecholamine hypothesis of affective disorders: a review of supporting evidence. Am. J. Psychiatry 122, 509–522. https://doi.org/10.1176/ajp.122.5.509.

Schneider, M., Levant, B., Reichel, M., Gulbins, E., Kornhuber, J., Müller, C.P., 2017. Lipids in psychiatric disorders and preventive medicine. Neurosci. Biobehav. Rev. 76, 336–362. https://doi.org/10.1016/j.neubiorev.2016.06.002.

Schousboe, A., Bak, L.K., Sickmann, H.M., Sonnewald, U., Waagepetersen, H.S., 2007. Energy substrates to support glutamatergic and GABAergic synaptic function: Role of glycogen, glucose and lactate. Neurotox. Res. 12, 263–268. https://doi.org/10.1007/BF03033909.

Schultz, J.E., Siggins, G.R., Schocker, F.W., Türck, M., Bloom, F.E., 1981. Effects of prolonged treatment with lithium and tricyclic antidepressants on discharge frequency, norepinephrine responses and beta receptor binding in rat cerebellum: electrophysiological and biochemical comparison. J. Pharmacol. Exp. Ther. 216, 28–38.

Sekar, S., Verhoye, M., Van Audekerke, J., Vanhoutte, G., Lowe, A.S., Blamire, A.M., Steckler, T., Van der Linden, A., Shoaib, M., 2011. Neuroadaptive responses to citalopram in rats using pharmacological magnetic resonance imaging. Psychopharmacology (Berl.) 213, 521–531. https://doi.org/10.1007/s00213-010-2084-4.

Shaner, R.L., Allegood, J.C., Park, H., Wang, E., Kelly, S., Haynes, C.A., Sullards, M.C., Merrill, A.H., 2009. Quantitative analysis of sphingolipids for lipidomics using triple quadrupole and quadrupole linear ion trap mass spectrometers. J. Lipid Res. 50, 1692–1707. https://doi.org/10.1194/jlr.D800051-JLR200.

Shannon, N.J., Gunnet, J.W., Moore, K.E., 1986. A comparison of biochemical indices of 5-hydroxytryptaminergic neuronal activity following electrical stimulation of the dorsal raphe nucleus. J. Neurochem. 47, 958–965.

Sheline, Y.I., 2011. Depression and the Hippocampus: Cause or Effect? Biol. Psychiatry 70, 308–309. https://doi.org/10.1016/j.biopsych.2011.06.006.

Shenoy, A.R., Dehmel, T., Stettner, M., Kremer, D., Kieseier, B.C., Hartung, H.P., Hofstetter, H.H., 2013. Citalopram suppresses thymocyte cytokine production. J. Neuroimmunol. 262, 46–52. https://doi.org/10.1016/j.jneuroim.2013.06.006.

Shi, C., Wu, C., Cao, A., Sheng, H.-Z., Yan, X., Liao, M., 2007. NMR-spectroscopy-based metabonomic approach to the analysis of Bay41-4109, a novel anti-HBV compound, induced hepatotoxicity in rats. Toxicol. Lett. 173, 161–167. https://doi.org/10.1016/j.toxlet.2007.07.010.

Shih, J.C., Thompson, R.F., 1999. Monoamine oxidase in neuropsychiatry and behavior. Am. J. Hum. Genet. 65, 593–598.

Shneker, B.F., Cios, J.S., Elliott, J.O., 2009. Suicidality, depression screening, and antiepileptic drugs Reaction to the FDA alert. Neurology 72, 987–991. https://doi.org/10.1212/01.wnl.0000344403.13815.8d.

Shtraizent, N., Eliyahu, E., Park, J.-H., He, X., Shalgi, R., Schuchman, E.H., 2008. Autoproteolytic cleavage and activation of human acid ceramidase. J. Biol. Chem. 283, 11253–11259. https://doi.org/10.1074/jbc.M709166200.

Siegel, A., Sapru, H.N., 2010. Essential Neuroscience, 2nd Revised edition. ed. Lippincott Williams and Wilkins, Philadelphia, Pa.

Siegel, G.J., Agranoff, B.W., Albers, R.W., Molinoff, P.B., 1989. Basic neurochemistry: molecular, cellular, and medical aspects. Raven Press, New York.

Singh, P., Paila, Y.D., Chattopadhyay, A., 2012. Role of glycosphingolipids in the function of human serotonin1A receptors. J. Neurochem. 123, 716–724. https://doi.org/10.1111/jnc.12008.
Siskind, L.J., 2005. Mitochondrial Ceramide and the Induction of Apoptosis. J. Bioenerg. Biomembr. 37, 143–153. https://doi.org/10.1007/s10863-005-6567-7.
Smith, R.N., Agharkar, A.S., Gonzales, E.B., 2014. A review of creatine supplementation in age-related diseases: more than a supplement for athletes. F1000Research 3. https://doi.org/10.12688/f1000research.5218.1.
Smith, S.M., Vale, W.W., 2006. The role of the hypothalamic-pituitary-adrenal axis in neuroendocrine responses to stress. Dialogues Clin. Neurosci. 8, 383–395.
Snyder, J.S., Soumier, A., Brewer, M., Pickel, J., Cameron, H.A., 2011. Adult hippocampal neurogenesis buffers stress responses and depressive behavior. Nature 476, 458–461. https://doi.org/10.1038/nature10287.
Sofuoglu, M., Sewell, R.A., 2009. Norepinephrine and Stimulant Addiction. Addict. Biol. 14, 119–129. https://doi.org/10.1111/j.1369-1600.2008.00138.x.
Sousa, N., Almeida, O.F.X., 2012. Disconnection and reconnection: the morphological basis of (mal)adaptation to stress. Trends Neurosci. 35, 742–751. https://doi.org/10.1016/j.tins.2012.08.006.
Speed, N.K., 2010. The Role of Insulin Signaling on Dopamine Transporter Trafficking [WWW Document]. URL http://etd.library.vanderbilt.edu/available/etd-07212010-144350/ (accessed 6.15.17).
Spiegel, S., 1999. Sphingosine 1-phosphate: a prototype of a new class of second messengers. J. Leukoc. Biol. 65, 341–344.
Ss, S., Rm, S., Grd, P., Rao, T.P., Be, K.S., 2015. Electrochemical Detection of Dopamine in Presence of Serotonin and Ascorbic acid at Tetraoctyl ammonium bromide Modified Carbon Paste Electrode: A Voltammetric Study. J. Biosens. Bioelectron. 6, 1–7. https://doi.org/10.4172/2155-6210.1000168.
Staněk, L., 2013. [Polymerase chain reaction: basic principles and applications in molecular pathology]. Cesk. Patol. 49, 119–121.
Stockmeier, C.A., Shapiro, L.A., Dilley, G.E., Kolli, T.N., Friedman, L., Rajkowska, G., 1998. Increase in serotonin-1A autoreceptors in the midbrain of suicide victims with major depression-postmortem evidence for decreased serotonin activity. J. Neurosci. Off. J. Soc. Neurosci. 18, 7394–7401.
Stork, C., Renshaw, P.F., 2005. Mitochondrial dysfunction in bipolar disorder: evidence from magnetic resonance spectroscopy research. Mol. Psychiatry 10, 900–919. https://doi.org/10.1038/sj.mp.4001711.
Stoscheck, C.M., 1990. Quantitation of protein. Methods Enzymol. 182, 50–68.
Strakowski, S.M., Delbello, M.P., Adler, C.M., 2005. The functional neuroanatomy of bipolar disorder: a review of neuroimaging findings. Mol. Psychiatry 10, 105–116. https://doi.org/10.1038/sj.mp.4001585.
Strelow, A., Bernardo, K., Adam-Klages, S., Linke, T., Sandhoff, K., Krönke, M., Adam, D., 2000. Overexpression of Acid Ceramidase Protects from Tumor Necrosis Factor–Induced Cell Death. J. Exp. Med. 192, 601–612.
Suchard, J.R., 2008. Fluoxetine Overdose-Induced Seizure. West. J. Emerg. Med. 9, 154–156.

Sullards, M.C., Liu, Y., Chen, Y., Merrill, A.H., 2011. Analysis of mammalian sphingolipids by liquid chromatography tandem mass spectrometry (LC-MS/MS) and tissue imaging mass spectrometry (TIMS). Biochim. Biophys. Acta 1811, 838–853. https://doi.org/10.1016/j.bbalip.2011.06.027.

Sulser, F., Vetulani, J., Mobley, P.L., 1978. Mode of action of antidepressant drugs. Biochem. Pharmacol. 27, 257–261. https://doi.org/10.1016/0006-2952(78)90226-5.

Sun, L., Fang, L., Lian, B., Xia, J.-J., Zhou, C., Wang, L., Mao, Q., Wang, X.-F., Gong, X., Liang, Z.-H., Bai, S.-J., Liao, L., Wu, Y., Xie, P., 2017. Biochemical effects of venlafaxine on astrocytes as revealed by 1H NMR-based metabolic profiling. Mol. Biosyst. 13, 338–349. https://doi.org/10.1039/C6MB00651E.

Sun, W., Xu, R., Hu, W., Jin, J., Crellin, H.A., Bielawski, J., Szulc, Z.M., Thiers, B.H., Obeid, L.M., Mao, C., 2008. Upregulation of the human alkaline ceramidase 1 and acid ceramidase mediates calcium-induced differentiation of epidermal keratinocytes. J. Invest. Dermatol. 128, 389–397. https://doi.org/10.1038/sj.jid.5701025.

Suzuki, E., Handa, K., Toledo, M.S., Hakomori, S., 2004. Sphingosine-dependent apoptosis: a unified concept based on multiple mechanisms operating in concert. Proc. Natl. Acad. Sci. U. S. A. 101, 14788–14793. https://doi.org/10.1073/pnas.0406536101.

Swijsen, A., Nelissen, K., Janssen, D., Rigo, J.-M., Hoogland, G., 2012. Validation of reference genes for quantitative real-time PCR studies in the dentate gyrus after experimental febrile seizures. BMC Res. Notes 5, 685. https://doi.org/10.1186/1756-0500-5-685.

Tafesse, F.G., Ternes, P., Holthuis, J.C.M., 2006. The Multigenic Sphingomyelin Synthase Family. J. Biol. Chem. 281, 29421–29425. https://doi.org/10.1074/jbc.R600021200.

Taha, T.A., Mullen, T.D., Obeid, L.M., 2006. A house divided: ceramide, sphingosine, and sphingosine-1-phosphate in programmed cell death. Biochim. Biophys. Acta 1758, 2027–2036. https://doi.org/10.1016/j.bbamem.2006.10.018.

Taverna, E., Saba, E., Rowe, J., Francolini, M., Clementi, F., Rosa, P., 2004. Role of Lipid Microdomains in P/Q-type Calcium Channel (Cav2.1) Clustering and Function in Presynaptic Membranes. J. Biol. Chem. 279, 5127–5134. https://doi.org/10.1074/jbc.M308798200.

Taylor, C., Fricker, A.D., Devi, L.A., Gomes, I., 2005. Mechanisms of action of antidepressants: from neurotransmitter systems to signaling pathways. Cell. Signal. 17, 549–557. https://doi.org/10.1016/j.cellsig.2004.12.007.

te Vruchte, D., Lloyd-Evans, E., Veldman, R.J., Neville, D.C.A., Dwek, R.A., Platt, F.M., van Blitterswijk, W.J., Sillence, D.J., 2004. Accumulation of glycosphingolipids in Niemann-Pick C disease disrupts endosomal transport. J. Biol. Chem. 279, 26167–26175. https://doi.org/10.1074/jbc.M311591200.

Tepper, A.D., Van Blitterswijk, W.J.V., 2000. Ceramide mass analysis by normal-phase high-performance liquid chromatography. Methods Enzymol. 312, 16–22.

Tettamanti, G., 2004. Ganglioside/glycosphingolipid turnover: new concepts. Glycoconj. J. 20, 301–317. https://doi.org/10.1023/B:GLYC.0000033627.02765.cc.

Torres, G.E., Gainetdinov, R.R., Caron, M.G., 2003. Plasma membrane monoamine transporters: structure, regulation and function. Nat. Rev. Neurosci. 4, 13–25. https://doi.org/10.1038/nrn1008.

Trivedi, M.H., Rush, A.J., Wisniewski, S.R., Nierenberg, A.A., Warden, D., Ritz, L., Norquist, G., Howland, R.H., Lebowitz, B., McGrath, P.J., Shores-Wilson, K., Biggs, M.M., Balasubramani, G.K., Fava, M., STAR*D Study Team, 2006. Evaluation of outcomes with citalopram for depression using measurement-based care in STAR*D: implications for clinical practice. Am. J. Psychiatry 163, 28–40. https://doi.org/10.1176/appi.ajp.163.1.28.

Tsang, T.M., Griffin, J.L., Haselden, J., Fish, C., Holmes, E., 2005. Metabolic characterization of distinct neuroanatomical regions in rats by magic angle spinning 1H nuclear magnetic resonance spectroscopy. Magn. Reson. Med. 53, 1018–1024. https://doi.org/10.1002/mrm.20447.

Tsang, T.M., Woodman, B., McLoughlin, G.A., Griffin, J.L., Tabrizi, S.J., Bates, G.P., Holmes, E., 2006. Metabolic characterization of the R6/2 transgenic mouse model of Huntington's disease by high-resolution MAS 1H NMR spectroscopy. J. Proteome Res. 5, 483–492. https://doi.org/10.1021/pr050244o.

Tsui-Pierchala, B.A., Encinas, M., Milbrandt, J., Johnson, E.M., 2002. Lipid rafts in neuronal signaling and function. Trends Neurosci. 25, 412–417.

Tylee, A., Walters, P., 2007. Onset of action of antidepressants. BMJ 334, 911–912. https://doi.org/10.1136/bmj.39197.619190.80.

Ueda, N., 2015. Ceramide-Induced Apoptosis in Renal Tubular Cells: A Role of Mitochondria and Sphingosine-1-Phoshate. Int. J. Mol. Sci. 16, 5076–5124. https://doi.org/10.3390/ijms16035076.

Unal, H., Karnik, S.S., 2012. Domain coupling in GPCRs: the engine for induced conformational changes. Trends Pharmacol. Sci. 33, 79–88. https://doi.org/10.1016/j.tips.2011.09.007.

Vallone, D., Picetti, R., Borrelli, E., 2000. Structure and function of dopamine receptors. Neurosci. Biobehav. Rev. 24, 125–132.

Van Zijl, P.C., Barker, P.B., 1997. Magnetic resonance spectroscopy and spectroscopic imaging for the study of brain metabolism. Ann. N. Y. Acad. Sci. 820, 75–96.

Veiga, M.P., Arrondo, J.L., Goñi, F.M., Alonso, A., Marsh, D., 2001. Interaction of cholesterol with sphingomyelin in mixed membranes containing phosphatidylcholine, studied by spin-label ESR and IR spectroscopies. A possible stabilization of gel-phase sphingolipid domains by cholesterol. Biochemistry (Mosc.) 40, 2614–2622.

Videbech, P., Ravnkilde, B., 2004. Hippocampal volume and depression: a meta-analysis of MRI studies. Am. J. Psychiatry 161, 1957–1966. https://doi.org/10.1176/appi.ajp.161.11.1957.

Vieira-Coelho, M., Serrão, M., Afonso, J., Pinto, C., Moura, E., 2009. Catecholamine synthesis and metabolism in the central nervous system of mice lacking α2-adrenoceptor subtypes. Br. J. Pharmacol. 158, 726–737. https://doi.org/10.1111/j.1476-5381.2009.00375.x.

Walther, D.J., Bader, M., 2003. A unique central tryptophan hydroxylase isoform. Biochem. Pharmacol. 66, 1673–1680.

Wang, G., Dinkins, M., He, Q., Zhu, G., Poirier, C., Campbell, A., Mayer-Proschel, M., Bieberich, E., 2012. Astrocytes Secrete Exosomes Enriched with Proapoptotic Ceramide and Prostate Apoptosis Response 4 (PAR-4) POTENTIAL MECHANISM OF APOPTOSIS INDUCTION IN ALZHEIMER DISEASE (AD). J. Biol. Chem. 287, 21384–21395. https://doi.org/10.1074/jbc.M112.340513.

Watson, J., Collin, L., Ho, M., Riley, G., Scott, C., Selkirk, J.V., Price, G.W., 2000. 5-HT1A receptor agonist-antagonist binding affinity difference as a measure of intrinsic activity in recombinant and native tissue systems. Br. J. Pharmacol. 130, 1108–1114. https://doi.org/10.1038/sj.bjp.0703394.

Welford, R.W.D., Vercauteren, M., Trébaul, A., Cattaneo, C., Eckert, D., Garzotti, M., Sieber, P., Segrestaa, J., Studer, R., Groenen, P.M.A., Nayler, O., 2016. Serotonin biosynthesis as a predictive marker of serotonin pharmacodynamics and disease-induced dysregulation. Sci. Rep. 6, srep30059. https://doi.org/10.1038/srep30059.

Westwick, J.K., Bielawska, A.E., Dbaibo, G., Hannun, Y.A., Brenner, D.A., 1995. Ceramide activates the stress-activated protein kinases. J. Biol. Chem. 270, 22689–22692.

Wible, C.G., 2013. Hippocampal Physiology, Structure and Function and the Neuroscience of Schizophrenia: A Unified Account of Declarative Memory Deficits, Working Memory Deficits and Schizophrenic Symptoms. Behav. Sci. 3, 298–315. https://doi.org/10.3390/bs3020298.

Windahl, M.S., 2009. English: Catecholamine biosynthesis.

Wiser, O., Bennett, M.K., Atlas, D., 1996. Functional interaction of syntaxin and SNAP-25 with voltage-sensitive L- and N-type Ca2+ channels. EMBO J. 15, 4100–4110.

Wong, K.C., 2014. Review of NMR Spectroscopy: Basic Principles, Concepts and Applications in Chemistry. J. Chem. Educ. 91, 1103–1104. https://doi.org/10.1021/ed500324w.

Wong, R.S., 2011. Apoptosis in cancer: from pathogenesis to treatment. J. Exp. Clin. Cancer Res. 30, 87. https://doi.org/10.1186/1756-9966-30-87.

Woodcock, J., 2006. Sphingosine and ceramide signalling in apoptosis. IUBMB Life 58, 462–466. https://doi.org/10.1080/15216540600871118.

Wrona, M.Z., Lemordant, D., Lin, L., Blank, C.L., Dryhurst, G., 1986. Oxidation of 5-hydroxytryptamine and 5,7-dihydroxytryptamine. A new oxidation pathway and formation of a novel neurotoxin. J. Med. Chem. 29, 499–505. https://doi.org/10.1021/jm00154a013.

Xia, J., Sinelnikov, I.V., Han, B., Wishart, D.S., 2015. MetaboAnalyst 3.0--making metabolomics more meaningful. Nucleic Acids Res. 43, W251-257. https://doi.org/10.1093/nar/gkv380.

Xia, J., Wishart, D.S., 2016. Using MetaboAnalyst 3.0 for Comprehensive Metabolomics Data Analysis. Curr. Protoc. Bioinforma. 55, 14.10.1-14.10.91. https://doi.org/10.1002/cpbi.11.

Xia, J., Wishart, D.S., 2002. Using MetaboAnalyst 3.0 for Comprehensive Metabolomics Data Analysis, in: Current Protocols in Bioinformatics. John Wiley & Sons, Inc. https://doi.org/10.1002/cpbi.11.

Yamada, M., Takahashi, K., Tsunoda, M., Nishioka, G., Kudo, K., Ohata, H., Kamijima, K., Higuchi, T., Momose, K., Yamada, M., 2003. Differential expression of VAMP2/synaptobrevin-2 after antidepressant and electroconvulsive treatment in rat frontal cortex. Pharmacogenomics J. 2, 6500135. https://doi.org/10.1038/sj.tpj.6500135.

Yamada, M., Takahashi, K., Tsunoda, M., Nishioka, G., Kudo, K., Ohata, H., Kamijima, K., Higuchi, T., Momose, K., Yamada, M., 2002. Differential expression of VAMP2/synaptobrevin-2 after antidepressant and electroconvulsive treatment in rat frontal cortex. Pharmacogenomics J. 2, 377. https://doi.org/10.1038/sj.tpj.6500135.

Yang, L., Beal, M.F., 2011. Determination of neurotransmitter levels in models of Parkinson's disease by HPLC-ECD. Methods Mol. Biol. Clifton NJ 793, 401–415. https://doi.org/10.1007/978-1-61779-328-8_27.

YassineMrabet, C.| D.| C.|, 2017. English: Simple functional diagram of an LCMS system with increased clarity.

Yildiz-Yesiloglu, A., Ankerst, D.P., 2006. Neurochemical alterations of the brain in bipolar disorder and their implications for pathophysiology: a systematic review of the in vivo proton magnetic resonance spectroscopy findings. Prog. Neuropsychopharmacol. Biol. Psychiatry 30, 969–995. https://doi.org/10.1016/j.pnpbp.2006.03.012.

Yoo, C.-H., Song, K.-H., Lim, S.-I., Woo, D.-C., Choe, B.-Y., 2018. Metabolic effects of light deprivation in the prefrontal cortex of rats with depression-like behavior: In vivo proton magnetic resonance spectroscopy at 7T. Brain Res. https://doi.org/10.1016/j.brainres.2018.02.047.

Yüksel, C., Öngür, D., 2010. Magnetic Resonance Spectroscopy Studies of Glutamate-Related Abnormalities in Mood Disorders. Biol. Psychiatry 68, 785–794. https://doi.org/10.1016/j.biopsych.2010.06.016.

Zangen, A., Overstreet, D.H., Yadid, G., 1997. High serotonin and 5-hydroxyindoleacetic acid levels in limbic brain regions in a rat model of depression: normalization by chronic antidepressant treatment. J. Neurochem. 69, 2477–2483.

Zeidan, Y.H., Jenkins, R.W., Korman, J.B., Liu, X., Obeid, L.M., Norris, J.S., Hannun, Y.A., 2008. Molecular targeting of acid ceramidase: implications to cancer therapy. Curr. Drug Targets 9, 653–661.

Zetterström, T., Sharp, T., Collin, A.K., Ungerstedt, U., 1988. In vivo measurement of extracellular dopamine and DOPAC in rat striatum after various dopamine-releasing drugs; implications for the origin of extracellular DOPAC. Eur. J. Pharmacol. 148, 327–334. https://doi.org/10.1016/0014-2999(88)90110-0.

Zhao, J., Jung, Y.-H., Jang, C.-G., Chun, K.-H., Kwon, S.W., Lee, J., 2015. Metabolomic identification of biochemical changes induced by fluoxetine and imipramine in a chronic mild stress mouse model of depression. Sci. Rep. 5, 8890. https://doi.org/10.1038/srep08890.

Zhou, W., Yoshioka, M., Yokogoshi, H., 2009. Sub-chronic effects of s-limonene on brain neurotransmitter levels and behavior of rats. J. Nutr. Sci. Vitaminol. (Tokyo) 55, 367–373.

Zira, A., Kostidis, S., Theocharis, S., Sigala, F., Engelsen, S.B., Andreadou, I., Mikros, E., 2013. 1H NMR-based metabonomics approach in a rat model of acute liver injury and regeneration induced by CCl4 administration. Toxicology 303, 115–124. https://doi.org/10.1016/j.tox.2012.10.015.